Molecular mechanism of the kinetochore-microtubule attachment in fission yeast

Kuo-Shun Hsu

University College London

and

Cancer Research UK London Research Institute

PhD Supervisor: Takashi Toda

A thesis submitted for the degree of

Doctor of Philosophy

University College London

September 2011

Declaration

I, Kuo-Shun Hsu, confirm that the work presented in this thesis is my own. Where information has been derived from other sources, I confirm that this has been indicated in the thesis.

Abstract

Kinetochore capture by the spindle microtubule is a crucial step required for chromosome biorientation. Any errors in this process would result in production of aneuploid progenies, a hallmark of human cancer. The Ndc80 complex, a conserved outer kinetochore complex, comprising four components, Ndc80/Hec1, Nuf2, Spc24 and Spc25, constitutes one of the core microtubule-binding sites within the kinetochore. Despite this knowledge, molecular mechanism by which this complex contributes to establishment of correct bipolar attachment of the kinetochore to the spindle microtubule remains largely elusive. Here I show that the conserved internal loop of fission yeast Ndc80 directly binds the Dis1/TOG microtubule-associated protein, thereby coupling spindle microtubule dynamics with kinetochore capture. Ndc80 loop mutant proteins fail to recruit Dis1 to kinetochores, imposing unstable attachment and frequent spindle collapse. In these mutants, mitotic progression is halted attributable to spindle assembly checkpoint activation, and chromosomes remain in the vicinity of the spindle poles without congression. *dis1* deletion precisely phenocopies the loop mutants. Furthermore, forced targeting of Dis1 to the Ndc80 complex rescues loop mutant's defects. I propose that Ndc80 comprises two microtubule-interacting interfaces; the N-terminal region directly binds the microtubule lattice, whilst the internal loop interacts with the plus end of microtubules via Dis1/TOG. Therefore, my results provide a crucial insight into how the Ndc80 complex establishes stable bipolar attachment to the spindle microtubule.

In addition, integrity of the Ndc80 complex is also required for the kinetochore tethering to the SPB during interphase. Loss of Ndc80 results in kinetochore declustering in the nucleus, and those scattered kinetochores are found to colocalise with cytoplasmic microtubules and the tubulin nucleation factor γ-TuC. Further investigation will be needed to understand how Ndc80 affects the γ-TuC distribution and/or how Ndc80 and the γ-TuC participate in the SPB-kinetochore anchorage in interphase.

Acknowledgement

I would express my sincere gratitude to my PhD supervisor, Takashi Toda, for his tireless support, supervision, inspiration and patience to me and to my project. I also thank my closest colleagues, Chii-Shyang and Hiro, for their initial instruments to my project in the early stage. Thanks to all my lab members: Hiro, Chii-Shyang, Chiho, Nathalie, Amy, Kathleen, Susheela, Isabelle, Risa, Akiko, Ngang-Heok, and Hirofumi, for sharing experiences about the lab, experiments, living, and the fun in London. All of you mean to me for the kindness, encouragement, and friendships, and you make my time in London colourful and memorable. I also thank the Yeast group in the 3rd floor: Frank's lab, Julie's lab, Jacky's lab, and Martin's lab, for their reagent sharing, kind help, useful discussion, and encouragement. All those events (lab retreat, birthday party, karaoke, bowling, Friday drink, etc.) really make me feel "we are family".

I would like to specially thank again to Chii-Shyang, my closest friend, for his all-the-time accompany in any aspect through my first two years and half. I would pass my deepest thanks to Peggy, the most important supporter in these ten years, for her 24hr/day unlimited support, carefulness, and encouragement. Last, my families are one of the most important supporting forces behind me. Without any part of you, I mean ALL OF YOU, I could not have made it through!

Scientifically, for our paper to be accepted, I would like to thank Fred Chang, Ursula Fleig, Silke Hauf, Yasushi Hiraoka, Jonathan Millar, Kayoko Tanaka and Yoshinori Watanabe, Ayumu Yamamoto, and Mitsuhiro Yanagida for the generous gift of reagents/strains for this study; Martin Singleton's laboratory for kind help and for critical reading of our manuscript and inspiring discussion; Nicola O'Reilly and the Peptide Synthesis unit for preparations of the peptide arrays; Tomoyuki Tanaka for informing us of his results on budding yeast Ndc80 and Dam1 prior to publication.

Table of Contents

Table of figures

List of tables

Abbreviations

Δ	gene deletion
5-FOA	5-fluoroorotic acid
aa	amino acid
APC/C	anaphase-promoting complex/cyclosome
CBB	coomassie brilliant blue
CCAN	constitutive centromere-associated network
CFP	cyan fluorescent protein
DAPI	4',6-diamidino-2-phenylindole
dNTP	deoxynucleosine triphosphate
DTT	dithiothreitol
EMM	Edinburgh minimal medium
eMTOC	equatorial microtubule organising centre
GDP	guanosine diphosphate
GFP	green fluorescent protein
GST	glutathione *S*-transferase
GTP	guanosine triphosphate
hph^r	hygromycin B resistance
HPLC	high performance liquid chromatography
HU	hydroxyurea
iMTOC	interphase microtubule organising centre
IP	immunoprecipitation
IPTG	isopropyl β-D-1-thiogalactopyranoside

kan^r	kanamycin resistance
KT	kinetochore
LB	Luria-Bertani
mCherry	monomeric Cherry
mRFP	monomeric red fluorescent protein
MT	microtubule
MTOC	microtubule organising centre
nat^r	nourseothricin resistance
NE	nuclear envelope
PAA	post-anaphase array
PEG	polyethylene glycol
PMSF	phenylmethylsulphonyl fluoride
PNPP	*p*-nitrophenyl phosphate
PVDF	polyvinylidene Difluoride
SAC	spindle assembly checkpoint
SDS-PAGE	sodium dodecyl sulfate polyacrylamide gel electrophoresis
SPB	spindle pole body
TBZ	thiabendazole
WCE	whole cell extract
YE5S	yeast extract with supplements
YFP	yellow fluorescence protein
γ-TuC	γ-tubulin complex

Chapter 1. Introduction

"We have seen that all organisms are composed of essentially like parts, namely, of cells; that these cells are formed and grow in accordance with essentially the same laws; hence, that these processes must everywhere result from the operation of the same forces." --- Schwann 1839

(Quoted by Sr. Paul Nurse during his Nobel speech, 2001)

1.1 Cell division cycle in general

The cell division cycle is a repeating process that leads a cell to duplicate its chromosomes and to divide them into two identical daughter cells. The process of the cell cycle needs to be tightly regulated, as otherwise the abnormal division will cause cell death. Another extreme case for abnormal cell proliferation is to cause the uncontrolled tissue growth, such as tumour formation, in which the cell cycle is no longer normally regulated (Hanahan and Weinberg, 2011).

A typical cell cycle consists of four continuous phases, i.e. the G1 (Gap1), S (DNA synthesis), G2 (Gap2), and M (Mitosis) phase. In G1, the cell increases its size and synthesises all the proteins required for DNA replication in the following S phase. In G2, the cell continues to grow until it is ready for the next step, mitosis, the duration when the replicated chromosomes equally separate into two daughter cells. The newborns are now entering next G1 phase and repeating the cell cycle again to proliferate. Nevertheless, depending on the environmental conditions, the daughters may enter a quiescent phase (G0), in which cells are not propagating but metabolically active.

Fission yeast spends about 70% of the time in G2 phase, and 10% each in M, G1, and S phase. Longitudinal polar growth of fission yeast in different cell cycle stages makes it distinct from other fungi including budding yeast. Cells are in a rod shape and have a rigid cell wall. Cell growth exclusively occurs at the cell tip. The average width of a haploid cell is constantly ~4 μm; in contrast,

the length of the cell varies at different cell cycle stages: ~ 7 μm in early G2, continuing to increase the cell size in G2 until the maximum length reaches ~ 14 μm before entering mitosis, and back to ~7 μm after cytokinesis and septation-dependent division. This feature renders a unique opportunity to easily monitor the cell cycle stage in this organism. Under rich nutritional conditions, G1 and S phase are very short, periods of which are almost indistinguishable from those of preceding cytokinesis. When two daughter cells are physically separated by fission, they are already in early G2 phase, containing the duplicated chromosomes (2N) in the nucleus. Fission yeast spends about three-quarters of the time in a long G2 phase. During this period, cells must grow to a certain size until again entering mitosis to separate its duplicated DNA (Figure 1.1).

1.2 Mitosis in general

During the cell cycle, mitosis is the shortest phase but with most stunning cytological events that can be visualised under microscopy. In higher eukaryotes, mitosis can be further divided into several distinct phases with different characteristics: **Prophase** --- a stage when the chromatin starts to condense into a compact chromosome, and the centrosome pair moves to the opposite pole, followed by nuclear envelope break down; **Prometaphase** --- centrosomes emanate spindle microtubules to search and capture the sister chromatids through association with kinetochores; **Metaphase** --- all the sister chromatids are bioriented (bipolar attachment) and congressed to the metaphase plate in the cell centre; **Anaphase** --- the kinetochore microtubules abruptly shorten to pull the sister chromatids apart to the opposite spindle poles (Anaphase A), and the interpolar (pole-to-pole) microtubules progressively extend to push two spindle poles further away from each other (Anaphase B); **Telophase** --- chromatids decondense, and the nuclear envelopes of the daughter cells reappear. The contractile ring is formed; **Cytokinesis** --- the

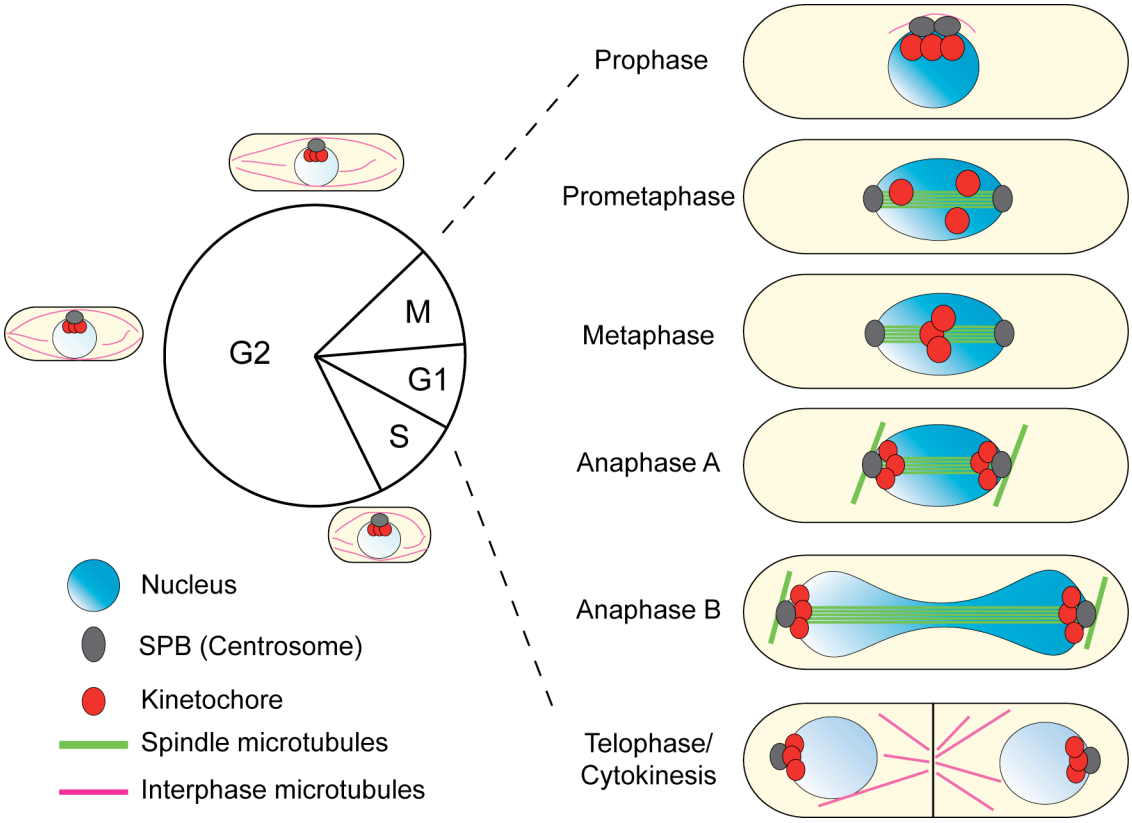

Figure 1.1 Fission yeast cell cycle and mitosis.

medial contractile ring constricts to form a cleavage furrow, which then ingresses, followed by abscission that physically cleaves the midbody into two.

The mitotic phases in fission yeast largely follow the way as described above, but the nuclear envelope does not break down (see Figure 1.1). This is the most striking difference between the open (higher eukaryotes) and closed (yeasts) mitosis. Upon mitotic entry, the nuclear envelope may become locally permeable (Tallada et al., 2009). This allows the spindle pole body (SPB, the centrosome equivalent in yeasts) to be able to be inserted into the nuclear envelope for the mitotic function (Ding et al., 1997). This process requires the SPB components such as Cut11 and Pcp1 (West et al., 1998, Fong et al., 2010). Furthermore, based on the length of the pole-to-pole distance, anaphase in fission yeast can be further divided into anaphase A and anaphase B. During anaphase A, the pole-to-pole distance keeps constant as in metaphase, whereas the distance dramatically increases during anaphase B due to the sliding forces from interpolar spindle microtubules (Hagan and Hyams, 1996).

1.3 Microtubules

1.3.1 Dynamic behaviour of microtubules

Microtubules (MTs) are one of the most important cytoskeletons that have been involved in many vital cellular activities, such as mitosis, cell division, trafficking, signalling, migration, polarised growth, nucleus positioning, organelles distribution and the maintenance of cell shape (La Carbona et al., 2006) (Akhmanova and Steinmetz, 2008). The microtubule wall comprises 13 protofilaments that are assembled into a cylindrically hollow with a diameter of about 25 nm. These protofilaments are composed of $\alpha\beta$-tubulin heterodimers that are aligned in a uniform head-to-tail fashion (Figure 1.2).

Microtubules can elongate by incorporating extra $\alpha\beta$-tubulin subunits to their polymer ends (polymerisation or assembly); conversely, they can shorten the

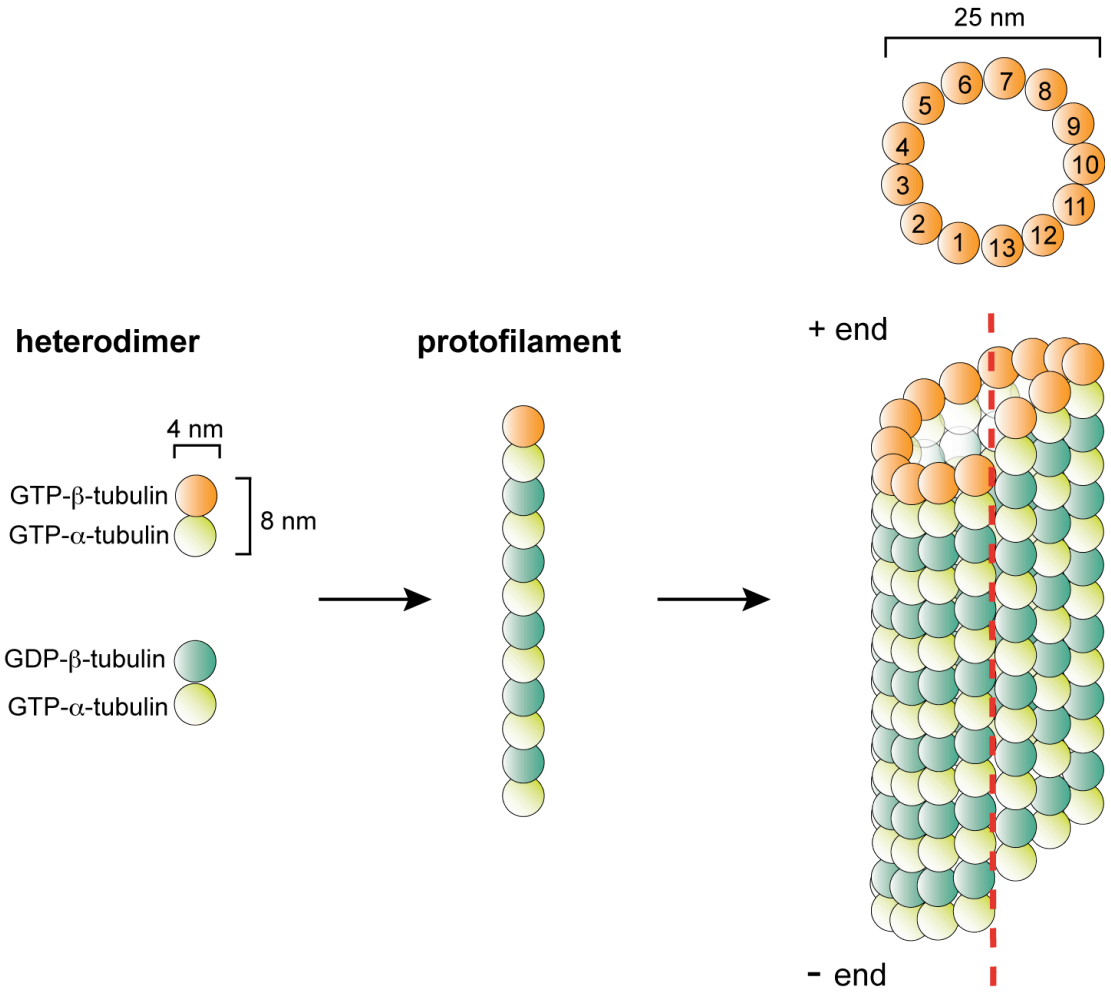

Figure 1.2 Microtubule structure and assembly.

Both α- and β-tubulin monomer bind GTP, but only the one on β-tubulin is exchangeable. A tubulin heterodimer is 4nm in width, and 8 nm in length. When these tubulin dimers assemble, a liner protofilament is formed. One microtubule contains 13 protofilaments that associate with each other laterally. The nature of the GTP-capped microtubule exhibits polarity where the GTP-capped end is dynamic plus end; in contrast, the minus end contains the GTP-nonexchangable-α-tubulin.

length by dissociating the αβ-tubulin dimers from the polymer ends (depolymerisation or disassembly). The assembly/disassembly of microtubules are driven by the binding, hydrolysis and exchange of GTP on the tubulin subunits. While both the α-tubulin and the β-tubulin monomer contain GTP, only the one in β-tubulin is exchangeable and is able to be hydrolysed (Nogales et al., 1998). This differentiated features of two tubulin monomers confers on the microtubule an intrinsic polarity, by which α-tubulin faces to the less-dynamic end (minus end) and β-tubulin to the more-dynamic end (plus end) (Mitchison, 1993, Nogales et al., 1999).

Once incorporated into the microtubule polymer, the GTP-bound form of a tubulin dimer is converted to the GDP-bound form (Nogales et al., 1998), which tends to facilitate depolymerisation. When the rate of tubulin dimer incorporation exceeds the rate of GTP hydrolysis, the microtubule plus end is stabilised by a GTP-tubulin 'cap', which protects the plus end from rapid shrinkage (Drechsel and Kirschner, 1994). In contrast, when the GTP hydrolysis is faster than tubulin dimer incorporation, the 'cap' protection will be lost, and consequently microtubules rapidly depolymerise.

Microtubules are highly dynamic, and constantly switch between stages of polymerisation and depolymerisation. From polymerisation to depolymerisation, the transition point is called 'catastrophe'; on the other hand, the switching from depolymerisation to polymerisation is named 'rescue'. These dynamic behaviours together are referred to as microtubule "dynamic instability" (Mitchison and Kirschner, 1984). This dynamic feature enables microtubules to rapidly explore the cellular interior to 'search and capture' their targets, such as kinetochores during mitosis (Kirschner and Mitchison, 1986).

In theory, both plus and minus ends of the microtubule are capable of being dynamic. However, the minus end of microtubules is often sheltered by other cellular organelles *in vivo*, thus blocking the minus end dynamics. In many organisms including fission yeast, spindle microtubules emanating from the centrosome/SPB are highly dynamic in their plus ends, but the minus ends near

the centrosome/SPB are rather very steady. Indeed under EM observation of the cellular microtubules, structures of the plus end appear to be open, blunt, sheets, flared, or ram-horn (multiple dynamic structures); in contrast, the minus ends near the centrosome are pointed and closed, and only very few are blunt and slightly flared (O'Toole et al., 2003, Zovko et al., 2008).

1.3.2 Microtubule nucleation and organisation in fission yeast

In vivo, the sites where microtubules are nucleated and polymerised are named 'MTOCs' (microtubule organising centres). In most organisms, the major MTOC is the centrosome, a structure composed of two perpendicular centrioles that is enriched with γ-tubulin, and surrounded by pericentriolar materials (PCMs) (Bettencourt-Dias and Glover, 2007). In fission yeast, the SPB is one of the MTOCs to nucleate microtubules in both interphase and mitosis. One of the key factors for MT nucleation is the γ-TuC (γ-tubulin complex), which consists of Gtb1/γ-tubulins (GCP1), Alp4/GCP2, Alp6/GCP3, Gfh1/GCP4, Mod21/GCP5, and Alp16/GCP16 (Stearns et al., 1991, Vardy and Toda, 2000, Fujita et al., 2002, Venkatram et al., 2004, Anders et al., 2006). The γ-TuC is proposed to assemble a ring structure with 13-fold microtubule-like symmetry, on which αβ-tubulin dimers can incorporate to polymerise MTs (Keating and Borisy, 2000, Moritz et al., 2000, Kollman et al., 2010). Mto1/Mod20, Mto2, Msd1 and Pcp1 have been implicated in the recruitment of γ-TuC to the SPB (Sawin et al., 2004, Samejima et al., 2005, Venkatram et al., 2005, Janson et al., 2005, Zimmerman and Chang, 2005, Toya et al., 2007, Fong et al., 2010).

In interphase, the SPB resides at the cytoplasmic face of the nuclear envelope, where it organises cytoplasmic MTs (Hoog et al., 2007). In addition, there are other non-SPB sites to nucleate microtubules, called iMTOCs (interphase MTOCs) (Figure 1.3). iMTOCs can locate near the nuclear periphery, in the cytoplasm, or on the existing microtubules (Janson et al., 2005). Mto1 and Mto2 play a key role to create these iMTOCs by recruiting the γ-TuC (Zimmerman and Chang, 2005, Samejima et al., 2005). The crosslinker Ase1 and the motor

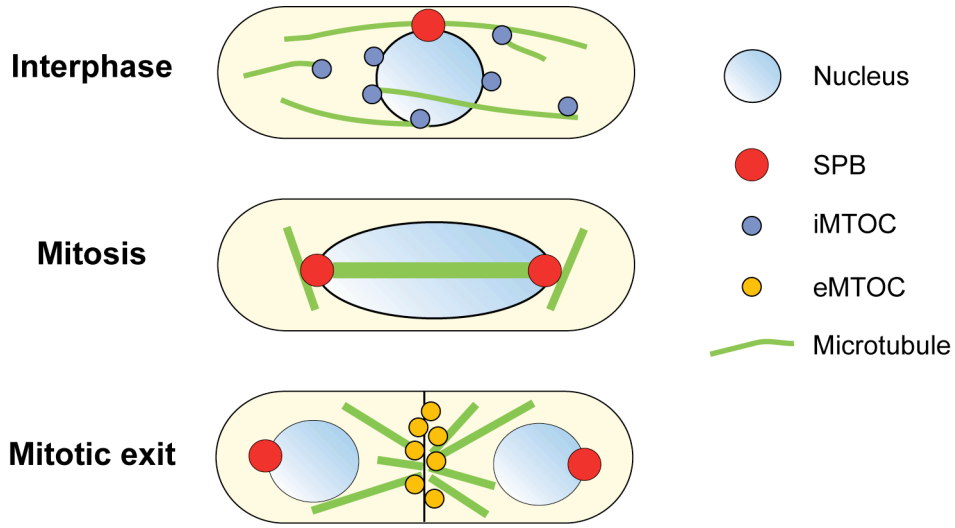

Figure 1.3 Fission yeast MTOCs.

In fission yeast, the SPB and other iMTOCs organise and emanate microtubules in interphase. iMTOCs can nucleate cytoplasmic microtubules from the pre-existing microtubules, the nuclear periphery, or the cytoplasm. During cytokinesis, right after the disassembly of spindle microtubules, the post-anaphase array microtubules are assembled from eMTOCs in the cell centre.

Klp2 (Kinesin-14) mediate the bundling of the newly synthesised MTs with the pre-existing microtubule bundles (Carazo-Salas and Nurse, 2006, Daga et al., 2006, Janson et al., 2007). There are on average 3-5 bundles of cytoplasmic microtubules in the interphase cells, and each bundle contains 2-3 parallel microtubules (Sagolla et al., 2003, Carazo-Salas et al., 2005). These microtubule bundles are oriented along the longitudinal axis of the cell, with the dynamic plus ends extending toward the cell tips, and with the steady minus ends converging close to the nuclear envelope (Drummond and Cross, 2000, Hoog and Antony, 2007).

Upon mitotic entry, the interphase microtubules deform, and the duplicated SPBs are inserted into the nuclear envelope to activate the spindle nucleation (Ding et al., 1997). A classic EM observation revealed that during early prometa/metaphase, there are averagely 12-14 microtubules nucleated from each pole, and about 18-24 microtubules are attached to the six kinetochores of three chromosomes, named kinetochore microtubules or K-fibres (3-4 K-fibres/kinetochore) (Ding et al., 1993). Furthermore, there are about 4 pole-to-pole microtubules interdigitated, a process that requires Cut7 (kinesin-5) (Hagan and Yanagida, 1992, Ding et al., 1993). The SPBs also nucleate astral microtubules, and it was proposed that the spindle orientation checkpoints (SOC) are mediated by these astral microtubules that extend toward the cytoplasmic cortex (Gachet et al., 2001, Oliferenko and Balasubramanian, 2002, Gachet et al., 2004, Tournier et al., 2004). However this hypothesis has been under scrutiny in that these astral microtubules in early mitosis are indeed in the nucleus, not in the cytoplasm (Zimmerman et al., 2004). Recent studies show that the initial spindle orientation is determined by the orientation of interphase microtubules in the previous G2 phase, which is in turn determined by the position of the SPB (Vogel et al., 2007, Daga and Nurse, 2008), again disputing the SOC proposal.

During anaphase A, the kinetochore microtubules directionally depolymerise to pull the attached sister kinetochores to opposite poles. In anaphase B, the pole-to-pole microtubules start to elongate and push two poles further to the cell tips.

After anaphase, the spindles disassemble from the SPBs, and the post anaphase array (PAA) starts to nucleate from the eMTOCs (equatorial MTOCs) in the cell centre, which is followed by cytokinesis and the reestablishment of cytoplasmic microtubule bundles in two daughters (Hagan and Hyams, 1988).

1.3.3 MAPs for chromosome segregation

In vitro, microtubules can self-assemble from purified αβ-tubulin dimers, but it is very slow. *In vivo*, many microtubule-associated proteins (MAPs) are involved in microtubule formation and microtubule dynamics regulation, including many kinesin family motor proteins and +TIPs (microtubule plus-end tracking proteins) (Akhmanova and Steinmetz, 2008). There have been over 45 proteins in mammals classified into 14 kinesin sub-families based on sequence homology within their motor domains (from the *Greek*, '*Kinein*', to move.) (Lawrence et al., 2004). Here I only focus on fission yeast MAPs that have been implicated in mitotic chromosome segregation, as required for the understanding of my thesis work.

1.3.3.1 Mal3 (EB1, end-binding 1)

EB1 is perhaps the best-known +TIP, which promotes both the rescue and catastrophe of microtubules (depends on the testing systems and conditions) (Akhmanova and Steinmetz, 2010). Structurally EB1 contains the microtubule-binding calponin-homology (CH) domain in its N-terminus, followed by a flexible linker that connects the coiled-coil EBH domain in the middle and the EEY motif in the very end of C-terminus. EB1 can interact with many other MAPs that bear the 'SXIP motif' or 'GKNDG' CAP-Gly motif, and bring them to the microtubule plus ends (Akhmanova and Steinmetz, 2008). In fission yeast, Mal3 (EB1) is required for both microtubule loading and plus end tracking of Tip1 (CLIP-170 family) and Tea2 (Kinesin 7) (Browning et al., 2003, Bieling et al., 2007). Structural studies indicate that Mal3 may stabilise microtubules by preferentially binding to the microtubule seam (Sandblad et al., 2006), or it changes the microtubule lattice structure from 'B form' to 'A form' (des Georges et al., 2008). Recent high-resolution fluorescence research reveals that both human EB1 and

fission yeast Mal3 specifically bind to the GTP-form-mimicking tubulin on the microtubule lattice, suggesting that these proteins preferentially recognise the growing microtubule ends (Maurer et al., 2011).

In vivo, Mal3 was first identified from a screen for minichromosome loss and sensitivity to TBZ (a tubulin poison). The *mal3*$^{+}$ gene can be deleted (non-essential), and the *mal3* deletion mutant exhibits defects in cell shape, despite that the mitotic spindle appears largely normal. Overexpression of Mal3 reveals its localisation along the whole cytoplasmic and spindle microtubules (Beinhauer et al., 1997). Furthermore, a genetic interaction between Mal3 and Moe1 (another MAP that negatively regulates microtubule assembly) has been reported, and the double deletion results in cold-sensitivity, which causes severe defects in microtubule morphologies. Investigating phenotypes of this double mutant reveals that these two proteins are together required for proper microtubule integrity/dynamics and distribution of γ-tubulin to the SPBs during mitosis (Chen et al., 2000). In addition, phenotypes of the *mal3* deletion mutant are suppressed by overproducing Spc7 (KNL1 homologue, a kinetochore component). It thus suggests a close relationship of Mal3 and kinetochore function (Kerres et al., 2004, Kerres et al., 2007). Mal3 is also linked to prevention of monopolar attachment by cooperation with Bub1-mediated spindle checkpoint in fission yeast (Asakawa et al., 2005b, Asakawa et al., 2006).

1.3.3.2 Klp5 and Klp6 (Kinesin 8)

Among those kinesin families are kinesin-8 and kinesin-13 (previously named Kin1) that have primarily contributed to the microtubule destabilisation in various organisms (Wordeman, 2010). So far there is no kinesin-13 homologue identified in fission yeast. Nevertheless, fission yeast contains two non-essential kinesin-8 motors, Klp5 and Klp6, which share about 50% identity with each other.

They were first described to localise to the interphase microtubule, spindle microtubules, and spindle midzone, and both of them fostered microtubule

disassembly as the *klp* deletion mutants exhibit a long, curl cytoplasmic microtubules and more resistant to TBZ (West et al., 2001). Subsequent studies show that Klp5 and Klp6 form heterocomplexes to localise and function at the kinetochore-microtubule interface (West et al., 2002, Garcia et al., 2002b). Chromosomes in either deletion mutant move back and forth between two poles and do not align properly, suggesting Klp5 and Klp6 function to promote the normal chromosome movement (West et al., 2002). Another study shows that when either gene of these two is deleted, kinetochore-microtubule attachment is impaired in some population of cells, which activates the Mad2-dependent checkpoints; other cells present defects that only trigger Bub1-dependent arrest, followed by the lagging chromosome phenotypes, suggesting that Klp5 and Klp6 are required for efficient capturing in prometaphase, and/or tension generation in metaphase (Garcia et al., 2002b).

The kinetochore localisation of Klp5 depends on Alp14 (another MAP, see below). Double deletion of either two of Klp5, Klp6, Dis1 and Alp14 is lethal, and phenotypes of either double deletion mutant are similar, suggesting these MAPs play a collaborative role in the establishment of bipolar attachment by regulating microtubule dynamics at the kinetochore-microtubule interface (Garcia et al., 2002a). It is also synthetic lethal between the *klp5/klp6* deletion mutant and the *dam1* deletion mutant. These proteins are together required for the formation of bipolar attachment in a parallel way: Dam1 is required for syntelic attachment correction and Klp5/Klp6 may be involved in merotelic attachment (Sanchez-Perez et al., 2005).

Klp5 and Klp6 may also cooperate with Ras1-Scd1 pathway to promote contractile ring formation in cytokinesis (Li and Chang, 2003). In addition, recent study indicates that Klp5 and Klp6 are mutually dependent on each other for their nuclear mitotic localisation (Unsworth et al., 2008).

1.3.3.3 Ase1 (MAP65/PRC1)

Ase1 is a microtubule bundling factor, and is conserved from yeasts to humans (PRC1) with similarity about 40% (Yamashita et al., 2005). In interphase, fission

yeast Ase1 localises to the overlapping area of cytoplasmic microtubules; in early mitosis it reduces the spindle localisation, and reappears to the spindle midzone during anaphase. Ase1 is non-essential, and both deletion and overexpression of Ase1 result in anaphase spindle collapse. Deletion of Ase1 causes nuclear and septum mis-positioning and cytokinesis defects, which brings about diploidisation and chromosome loss (Yamashita et al., 2005). Furthermore, when treating with Latrunculin A (an actin polymerisation inhibitor), the *ase1* deletion mutant cells encounter an exacerbated Mph1/Mad3/Bub1-dependent mitotic delay, suggesting that both Ase1 and the intact actin cytoskeleton are required for preanaphase spindle stability (Meadows and Millar, 2008).

The coordination between Ase1 and the motor Klp2 (Kinesin-14) is crucial for the bundling reaction of the cytoplasmic microtubules (Carazo-Salas and Nurse, 2006, Daga et al., 2006). The subsequent investigation demonstrates that Ase1 not only crosslinks the anti-parallel microtubules, but also regulates the sliding force of Klp2 based on polarity and overlap length (Janson et al., 2007).

Recent data suggests Ase1 acts as a regulatory platform to recruit, and cooperates with, the Klp9 tetramer (kinesin-6) in anaphase B spindle midzone. The interaction between Ase1 and Klp9 is controlled by Cdc2 kinase and the opposing phosphatase Clp1, as such that in mitosis both Ase1 and Klp9 are phosphorylated by Cdc2, thus prohibiting the binding of these two proteins; while upon anaphase B onset, Clp1 dephosphorylates both proteins and promote their interaction and midzone localisation, thereby triggering the anaphase B spindle elongation (Fu et al., 2009).

1.3.3.4 Dis1 and Alp14 (chTOG/XMAP215) and Peg1/Cls1 (CLASP)

The XMAP215/Dis1 proteins, one of the most evolutionarily ancient MAPs in all major kingdoms of eukaryotes, are found in yeasts (Dis1 and Alp14 in fission yeast, and Stu2 in budding yeast), *Dictyostelium* (DdCP224), plants (Mor1 in *A. thaliana*), and animals (Zyg9 in *C. elegans*, Msps in *Drosophila*, XMAP215 in *Xenopus* and ch-TOG in humans) (Gard et al., 2004). All of them contain 2-5

core TOG domains, each of which is composed of several HEAT repeats. The C-terminal regions are diverse in their sequences. During the cell cycle and organism development, the family proteins can dramatically change their cellular localisations. These include cytoplasmic microtubules, endoplasmic reticulum, centrosome/acentrosomal poles/SPB, mitotic spindles and the kinetochores, suggesting a multi-role nature of Dis1/XMAP215 *in vivo* (Ohkura et al., 2001).

The founding member, XMAP215, was first identified from *Xenopus* extracts as a potent assembly-promoting factor for microtubule plus-ends, in which it increased microtubule growth rate by ~10-fold (Gard and Kirschner, 1987). Nevertheless, the protein family also increases the shortening rate and suppresses the rescue frequency (Vasquez et al., 1994). Consistent with this, the later identified human homologue, ch-TOG (colonic and hepatic Tumour Overexpressing Gene), was shown to localise at the centrosome, spindles, and near chromosomes in mitosis, with similar ability to promote the microtubule polymerisation at both ends (Charrasse et al., 1998). Cellular depletion of chTOG by RNAi results in a failure of chromosome congression and the induction of spindle assembly checkpoint-dependent arrest (Meraldi et al., 2004). Further *in vivo* examinations corroborate the microtubule-growth-promoting activity of XMAP215 such that interfering with XMAP215/TOG function decreases microtubule growth rates and results in shorter spindles and spindle morphological defects (Tournebize et al., 2000, Goshima et al., 2005). However, the microtubule 'destabilising' activity of XMAP215 (and Stu2) is also reported (Shirasu-Hiza et al., 2003, van Breugel et al., 2003). In addition, XMAP215 is phosphorylated in a cell cycle-dependent manner *in vivo*, and from an *in vitro* assessment it is suggested that Cdk1-dependent phosphorylation might negatively regulate the stabilisation activity of XMAP215 (Gard and Kirschner, 1987, Vasquez et al., 1999).

By using an *in vitro* optical trap experimental system, Kerssemakers *et al.* have proposed that XMAP215 speeds up microtubule growth by facilitating the addition of long oligomers (6-8 tubulin dimers) (Kerssemakers et al., 2006).

Crystal structures of the TOG domains from Msps, Zyg9, and Stu2, have been recently solved, and reveal a flat, paddle-like structural feature of the TOG domain, in which several intra-repeat linking loops at the narrow side of the paddle are important for direct tubulin binding (Al-Bassam et al., 2007, Slep and Vale, 2007). More recently, it has been shown by Tony Hyman's group that Dis1/XMAP215 can track the microtubule plus end, where it acts as a processive polymerase that directly catalyses the loading of up to 25 αβ-tubulin dimers to the growing plus end once at a time (Brouhard et al., 2008). Unlike budding yeast Stu2, which forms a dimer to bind an αβ-tubulin subunit (Al-Bassam et al., 2006), an XMAP215 monomer suffices to wrap around one αβ-tubulin dimer by its 5 tandem TOG motifs (Brouhard et al., 2008). Lastly, a region rich in basic amino acids that resides in between the last two TOG domains of XMAP215 has been recently shown to directly bind the microtubule lattice (Widlund et al., 2011).

There are two TOG proteins in fission yeast: Dis1 and Alp14. Dis1 was originally identified in fission yeast by a mutant screening that was defective in sister chromatid disjoining. The *dis1* mutants are cold sensitive with phenotypes that condensed sister chromosomes anomalously move to the spindle pole without segregation, followed by breakage of the elongated anaphase spindle (Ohkura et al., 1988, Nabeshima et al., 1995). Domain analysis by overexpressing Dis1 fragments demonstrates that the N-terminal region of Dis1 is required for cell-cycle dependent localisation, the middle region (containing the basic-rich area) is essential for microtubule association, and the C-terminal region is necessary for SPB and nuclear localisation (Nakaseko et al., 1996). When live-image and chromatin immunoprecipitation (CHIP) are applied, Dis1 is found to localise to the kinetochore specifically in mitosis, where the function of Dis1 is required for proper bipolar spindle formation (Nabeshima et al., 1998, Nakaseko et al., 2001). Like XMAP215, Dis1 is phosphorylated by Cdc2 upon mitotic entry (Nabeshima et al., 1995), and the phosphorylation is required for Dis1 translocation from cytoplasmic microtubules to the kinetochores in mitosis, which in turn ensures accurate chromosome segregation (Aoki et al., 2006).

Alp14 was identified as a cell shape mutant with altered polarity (Radcliffe et al., 1998). Unlike *dis1* mutants, the *alp14* deletion mutant is temperature-sensitive, and under the restrictive condition it exhibits anomalously short cytoplasmic microtubules that are unable to reach the cell tips, thereby bringing about bent or branched cells. In addition to functioning on cytoplasmic microtubules, Alp14 also plays a crucial role in proper attachment between spindle microtubules and the kinetochores, as well as in the spindle assembly checkpoint in mitosis (Garcia et al., 2001). Another difference from Dis1 is that Alp14 has a binding partner Alp7 (a TACC homologue), which delivers Alp14 from the SPB to the microtubule-kinetochore interface through spindle microtubules (Sato et al., 2004). Although both TOGs are non-essential in fission yeast, *dis1 alp14* double deletion mutant is synthetic lethal, and overexpressing one protein can compensate for defects of the other, suggesting a closely overlapping role between these TOGs (Garcia et al., 2001, Garcia et al., 2002a).

Fission yeast Peg1 (also named as Cls1) is a homologue of human CLASP, containing a TOG-like domain in its N-terminus (Al-Bassam et al., 2010). Peg1 was originally identified in a mutant screening of spindle formation defects and a screen for molecules that antagonised Mal3 function (Grallert et al., 2006). In this study, the authors demonstrated that Peg1 was required for spindles and astral microtubule formation but yet destabilised interphase cytoplasmic microtubules; the latter was proposed to be achieved by slowing down the microtubule polymerisation rate at cell tips in a way independent of Mal3 or Tip1, though these three proteins indeed interacted. Instead the authors proposed dynein was required for the destabilising activity of Peg1.

However, another group disputed this finding by showing that Cls1/Peg1 localised to overlapping microtubules within the mitotic spindles and interphase bundles, but not to microtubule plus ends. Ase1 mediated the localisation of Peg1/Cls1 to the antiparallel microtubule overlapping zones, where Peg1 prevented disassembly of the entire microtubule (Bratman and Chang, 2007). A following study reveals that Cls1 forms a homodimer to bind an $\alpha\beta$-tubulin dimer through conserved TOG-like domains, in a way that is similar to Stu2. By doing

so, Cls1 acts as a local stabiliser to promote microtubule rescue (Al-Bassam et al., 2010). Another study reports that Peg1 associates with mitochondria and is involved in mitochondrial distribution (Chiron et al., 2008), though another recent study has questioned this notion (Fu et al., 2011).

1.3.3.5 The Dam1/DASH complex

In budding yeast, the essential Dam1 complex consists of 10 subunits (Dam1, Duo1, Ask1, Hsk3, Spc34, Spc19, and Dad1-4). The first identified component was Duo1 (Death Upon Overproduction), which contributes to the mitotic spindle function that is sensed by the spindle assembly checkpoint (Hofmann et al., 1998). Dam1 (Duo1 and Mps1 interacting factor) was next identified and shown to localise on spindle microtubules and likely the kinetochores, and was implicated in spindle integrity (Jones et al., 1999). After that, all other components were subsequently discovered and large amounts of studies in budding yeast established the indispensability of the Dam1 complex in the microtubule-kinetochore interaction and bi-orientation, as well as the functional interaction with Ipl1/Aurora B (Enquist-Newman et al., 2001, Cheeseman et al., 2001a, Cheeseman et al., 2001b, Kang et al., 2001, Janke et al., 2002, Cheeseman et al., 2002). It has also been shown that Dam1 contributes to the end-on attachment of spindle microtubules to chromosome in an Mps1-dependent manner (Shimogawa et al., 2006, Tanaka et al., 2007).

The major breakthrough came from the successful reconstitution of 10 subunits *in vitro*, and 16 repeating units of this recombinant protein complex was surprisingly found to form a ring (or a paired helix) surrounding the microtubule wall, which can processively move along the microtubule depolymerising end (Miranda et al., 2005, Westermann et al., 2005, Westermann et al., 2006, Wang et al., 2007, Grishchuk et al., 2008a). This ring model fits well to the 'Hill theory', a classical hypothesis that the microtubule end is inserted into kinetochore through a channel or sleeve structure, which couples chromosome movement to the energy release from microtubule depolymerisation (Hill, 1985). However, the ring conformation is quickly challenged by the observation that individual

non-ring Dam1 complex is sufficient to diffuse along the microtubule lattice in fission yeast cells (Grishchuk et al., 2008b, Gestaut et al., 2008). More recently, the Dam1 complex is found to not only continuously track the depolymerising microtubule, but also the growing end to serve as a processivity factor for Ndc80 (Asbury et al., 2006, Tien et al., 2010, Lampert et al., 2010).

In fission yeast, two independent studies identified the Dam1 complex, one by a biochemical affinity approach (Liu et al., 2005) and the other from a genetic suppressor screen of TBZ sensitivity of the *cdc13-117* (cyclin B) and *mal3-1* (EB1) mutant (Sanchez-Perez et al., 2005). It was shown by both groups that the kinetochore localisation of the Dam1 complex depends on Mal2, Sim4 and Mis6 (the Mis6 complex), not the Mis12, Nuf2, or Cnp1 kinetochore component. Furthermore, Dam1 functionally coordinates with Klp5/Klp6 for bipolar chromosome attachment, as the non-essential *dam1* deletion mutant is lethal with both the *klp5* and *klp6* deletion mutant (Sanchez-Perez et al., 2005). In addition, the *dam1* deletion is also lethal with *dis1* deletion, but not *alp14* deletion mutant (Karen Griffiths and Takashi Toda, unpublished data). A following study isolates *dam1* temperature-sensitive mutants in a *klp5*-null background, and find that defects of the *dam1-A8 klp5* double mutant was rescued by adding the tubulin drug TBZ, suggesting that the hyper-stabilised attachment between microtubule and kinetochore is the primary defect in this mutant (Griffiths et al., 2008). In addition, it has been shown that the Dam1 complex and the kinesin motor Klp2 are required for the retrieval of the unattached kinetochores to the SPB (Franco et al., 2007, Gachet et al., 2008). Although the whole complex is conserved, the fission yeast Dam1 complex is non-essential, and the protein copy number is too low to form a ring (Joglekar et al., 2008). It has also been recently demonstrated that this non-ring Dam1 complex is able to modulate the dynamics of interphase cytoplasmic microtubules (Gao et al., 2010).

So far, no clear Dam1 homologue or any of the other 9 components comprising the Dam1 complex has been found in higher eukaryotes. However, the newly identified Ska complex (containing Ska1, Ska2 and Ska3/Rama1) is arguably

proposed to be a functional equivalent of vertebrate Dam1 complex. The Ska complex is functionally implicated in microtubule-kinetochore attachment, maintenance of metaphase plate, and checkpoint silencing (Hanisch et al., 2006, Gaitanos et al., 2009, Theis et al., 2009, Welburn et al., 2009, Raaijmakers et al., 2009, Daum et al., 2009).

1.4 Kinetochore

1.4.1 Structure overview

60-80 proteins have been identified from yeasts to humans to constitute the whole kinetochore, a rapidly evolved but functionally conserved supercomplex assembled on centromeric DNA (Meraldi et al., 2006, Cheeseman and Desai, 2008). It consists of several subcomplexes that are delicately associated with each other (Westermann et al., 2003, De Wulf et al., 2003, Obuse et al., 2004a, Okada et al., 2006, Foltz et al., 2006) (Table 1.1).

Under an electron microscopy, the kinetochore in vertebrate cells was initially visualised as a tri-laminated structure on the centromeric region of mitotic chromosomes (Brinkley and Stubblefield, 1966, Jokelainen, 1967, Rieder and Salmon, 1998). The inner kinetochore layer forms the interface with centromeric chromatin; the outer layer is about 60 nm thick and forms the interface for spindle microtubules. These two regions are electron dense, whereas the central layer is less clear under this observation. Since then, a general concept to divide the kinetochore broadly into two entities has been naturally formed among the kinetochore research community. When microtubules are removed by adding the microtubule depolymerising agent, a structure called ‘fibrous corona’ is seen protruding out from the outer kinetochore.

Recently, electron tomography of the vertebrate kinetochore reveals that microtubule ends are embedded in a radial mesh at the outer kinetochore; no precisely repeated unit of binding sites are observed, suggesting the

Table 1.1 Kinetochore components are conserved from yeasts to humans. (updated from (Santaguida and Musacchio, 2009)).

Complex	*H. sapiens*	*S. cerevisiae*	*S. pombe*
CENP-A nucleosome			
CENP-A nucleosome	CENP-A	Cse4	Cnp1
	CENP-B		Abp1, Cbh1, Cbh2
		Cbf1	
CBF3 complex		Skp1	
		Ctf13	
		Cep3	
		Ndc10	
CCAN/Ctf19/Mis6 complex			
CCAN (*H. sapiens*) Ctf19 or COMA complex (*S. cerevisiae*) Mis6 or Sim4 complex (*S. pombe*)	CENP-C	Mif2	Cnp3
	CENP-H	Mcm16	Fta3
	CENP-I	Ctf3	Mis6
	CENP-K	Mcm22	Sim4
	CENP-L	Mcm19	Fta1
	CENP-M		
	CENP-N	Chl4	Mis15
	CENP-O	Mcm21	Mal2
	CENP-P	Ctf19	Fta2
	CENP-Q	Okp1	Fta7
	CENP-R		
	CENP-U	Amc1	Mis17
	CENP-S	YOL086W-A	SPBC2D10.16/Mhf1
	CENP-X	YDL160C-A	SPCC576.12C/Mhf2
	CENP-T	Cnn1	SPBC800.13/Cnp20
	CENP-W	YDR374W-A	SPAC17G8.15/New1
		Ame1	
		Nkp1	
		Nkp2	
			Fta4
			Fta5
			Fta6
KMN network			
Knl1 complex	KNL1/Blinkin	Spc105	Spc7
	Zwint	YDR532c	Sos7
Mis12 complex	MIS12	Mtw1	Mis12
	DSN1	Dsn1	Mis13
	NNF1	Nnf1	Nnf1
	NSL1	Nsl1	Mis14
Ndc80 complex	NDC80	Ndc80	Ndc80
	NUF2	Nuf2	Nuf2
	SPC24	Spc24	Spc24
	SPC25	Spc25	Spc25
Spindle assembly checkpoint			
SAC	MAD1	Mad1	Mad1
	MAD2	Mad2	Mad2
	BUBR1	Mad3	Mad3
	BUB1	Bub1	Bub1
	BUB3	Bub3	Bub3
	CDC20	Cdc20	Slp1
	MPS1	Mps1	Mph1
Chromosome passenger complex			
CPC	Aurora B	Ipl1	Ark1
	INCENP	Sli15	Pic1
	Survivin	Bir1	Bir1/Cut7
	Borealin	Nbl1	Nbl1

kinetochore encounters a drastic spatial rearrangement when binding to microtubules (Dong et al., 2007). This study challenges the view that in organisms with a regional centromere, the molecular architecture of the kinetochore-microtubule attachment sites are simply multi-repeating units from that of a single unit of budding yeast outer kinetochore, which only interacts with one microtubule (Joglekar et al., 2006, Joglekar et al., 2008, McEwen and Dong, 2010). An important progress in the kinetochore field is the super-resolutional constitution of the whole kinetochore architecture, which illustrates the spatial relationship between several key kinetochore components in a digital-nanometre scale. (Schittenhelm et al., 2007, Joglekar and DeLuca, 2009, Wan et al., 2009, Schittenhelm et al., 2009).

1.4.2 Functional classification of kinetochore modules

The overall kinetochore architecture can be functionally classified into four modules: (1) **CCAN** (constitutive centromere-associated network) --- functions at the centromere-kinetochore interface and important for the loading of CENP-A nucleosomes (histone H3 variants) onto the centromere region; (2) **KMN network** (KNL-1/Mis12 complex/Ndc80 complex) --- constitutes the core kinetochore-microtubule interacting surface, also acts as a platform for recruiting other components; (3) **Spindle assembly checkpoint (SAC)** --- monitors the status of attachment/tension and generates a “wait” signal to delay mitotic progression if necessary; (4) **Chromosome passenger complex (CPC)** --- sensitises and regulates the stable kinetochore-microtubule attachment by correcting the inappropriate interaction into the bi-orientated fashion. These modules dynamically and tightly cooperate as a nanodevice to promote faithful chromosome segregation.

1.4.3 Constitutive centromere-associated network (CCAN)

As named, proteins in this class constitutively localise to the centromere-kinetochore interface throughout the cell cycle (Cheeseman and Desai, 2008). Initial studies on the kinetochore began with identifying the first three canonical centromeric proteins: CENP-A, CENP-B and CENP-C (Earnshaw and Rothfield,

1985). CENP-A is a variant of histone-H3, and is able to specifically incorporate into centromeric chromatin. This epigenetic mark specifies a site for kinetochore assembly (Perpelescu and Fukagawa, 2011). CENP-B recognises an α-satellite DNA sequence, but elimination of CENP-B has no adverse effect on kinetochore function (Masumoto et al., 1989, Amor and Choo, 2002).

Systematic approaches have led to identification of more authentic CCAN components in vertebrates (Sugata et al., 1999, Nishihashi et al., 2002, Obuse et al., 2004b, Okada et al., 2006, Foltz et al., 2006, Izuta et al., 2006, Hori et al., 2008). Based on genetic and biochemical analysis, Fukagawa's group further classifies those 16 authentic CCANs into six subgroups: CENP-C, CENP-H/I/K, CENP-L/M/N, CENP-O/P/Q/R/U(50), CENP-T/W, and CENP-S/X (Perpelescu and Fukagawa, 2011).

In higher eukaryotes, CENP-C acts as a major connecting point to bridge the inner centromere to the outer kinetochore by directly interacting with Nnf1, a component of the Mis12 complex (Screpanti et al., 2011, Przewloka et al., 2011). A super-resolution map reveals that CENP-C and CENP-H localise within CENP-A–rich subdomains presumably on H3-containing nucleosomes, whereas CENP-T localises exclusively in interspersed H3-rich blocks (Ribeiro et al., 2010). In contrast, CENP-N locates spatially closest to CENP-A at the centromere, whose function may be involved in decoding information carried by CENP-A, thereby promoting the kinetochore assembly (Carroll et al., 2009). Furthermore, artificial targeting of CENP-C or CENP-T onto the chromosome arm is found to be sufficient to recruit the KMN component (such as Mis12 and Ndc80) to the ectopic site (Gascoigne et al., 2011). In line with this finding, CENP-T is found to be elastic, by which the C-terminus binds to chromatin DNA and the N-terminus can be extended out about 30-40 nm, the length likely being able to reach the outer kinetochore (Suzuki et al., 2011). Collectively these findings imply that in vertebrates, CENP-C and CENP-T/W act as two major linkers to connect the centromeric chromatin platform with the outer kinetochore components KMN, and the linkage between CENP-T and Spc24-Spc25 (the Ndc80 complex) is likely conserved in budding yeast (Takashi Toda, personal

communication). Another intriguing work shows that CENP-H and CENP-I can quickly translocate within the sister kinetochore pair of the oscillated chromosome; and with CENP-Q, which has an intrinsic microtubule-binding activity, these three proteins modulate the turnover of the bound microtubule and promote the chromosome alignment at the metaphase plate (Amaro et al., 2010).

Most of the CCAN proteins are conserved in yeasts (see Table 1.1). Cnp3 is the fission yeast orthologue of CENP-C (Holland et al., 2005). The Mis6 complex corresponds to the CENP-H/I/K subgroup (Saitoh et al., 1997), and the Fta2-Mal2 complex is similar to the CENP-O/P/Q/R/U subcomplex (Kerres et al., 2006).

In fission yeast, Cnp3 is found to act as a multiplatform, mediating the binding of Fta1, Moa1, and the Pcs1-Mde4 complex, to promote faithful chromosome segregation in both mitosis and meiosis (Tanaka et al., 2009). The Mis6 complex has been implicated in mitotic spindle length control, faithful chromosome segregation, Cnp1 (CENP-A) loading, and spindle checkpoint signaling (Saitoh et al., 1997, Goshima et al., 1999, Takahashi et al., 2000, Saitoh et al., 2005). The activity of Mis6 for Cnp1 localisation is likely conserved in vertebrates but not budding yeast (Measday et al., 2002, Okada et al., 2006). The close association between the Mis6 complex and the Fta2-Mal2 complex has been demonstrated, and thus these two complexes are also regarded as the same complex (Liu et al., 2005). Recently, the module linker between the Mis6 complex and the Fta2-Mal2 complex has been mapped to Mis17 (Shiroiwa et al., 2011). Like human CENP-N, fission yeast Mis15 is able to interact with Cnp1 (CENP-A) with Mis6 and Mis17. Consistently, mutation of Mis15 reduces Cnp1 localisation to the centromere (Hayashi et al., 2004).

Although named as CENP proteins, CENP-E, CENP-V and CENP-F are not truly CCAN as they transit this region only in mitosis. CENP-E and CENP-F localise in the fibrous corona in G2/M phase and translocate to midzone afterward (Yen et al., 1991, Rattner et al., 1993, Liao et al., 1995, Yao et al.,

1997). The role of CENP-E includes facilitating the sliding movement of chromosomes close to a spindle pole towards the spindle equator (Alexander and Rieder, 1991, Schaar et al., 1997, Weaver et al., 2003). CENP-V is required for centromere organization, chromosome alignment and cytokinesis (Tadeu et al., 2008).

1.4.4 The KMN (KNL1-Mis12 complex-Ndc80 complex) network

'The KMN network' is named after the finding that in *C. elegans*, these protein complexes act together to constitute the major interface for microtubule binding at the outer kinetochore (Cheeseman et al., 2006), though the prototype of yeast KMN had been recognised previously (Nekrasov et al., 2003, Liu et al., 2005) (Figure 1.4). Many proteins in the KMN were originally identified through purification and identification of spindle pole body from budding yeast, or by the genetic component mutant screening from fission yeast (Rout and Kilmartin, 1990, Takahashi et al., 1994, Osborne et al., 1994, Saitoh et al., 1997, Wigge et al., 1998). When their functions were discovered to associate with nuclear division, studies of the KMN started to thrive.

1.4.4.1 KNL1/Spc7/Spc105

In *C. elegans*, KNL1 was identified from an RNAi screening of embryos with a 'kinetochore-null' phenotype, which the kinetochore assembly is abolished and chromosomes are unable to distribute to the metaphase plate (Desai et al., 2003). In this organism, KNL1 is a core component to link the inner kinetochore (CENP-C and CENP-A) with other KMN proteins at the outer kinetochore (Cheeseman et al., 2004). From the *in vitro* microtubule binding experiment, it is demonstrated that in addition to Ndc80, KNL1 also contributes to direct microtubule binding (Cheeseman et al., 2006).

Human KNL1 is also named Blinkin, for its direct interaction with the checkpoint proteins Bub1 and BubR1, and the RZZ-related component Zwint1 (Kiyomitsu et al., 2007). The interactions with Bub1 and BubR1 are through the KI motif found in the KNL1 N-terminus (aa 150-250), a domain that is functionally crucial

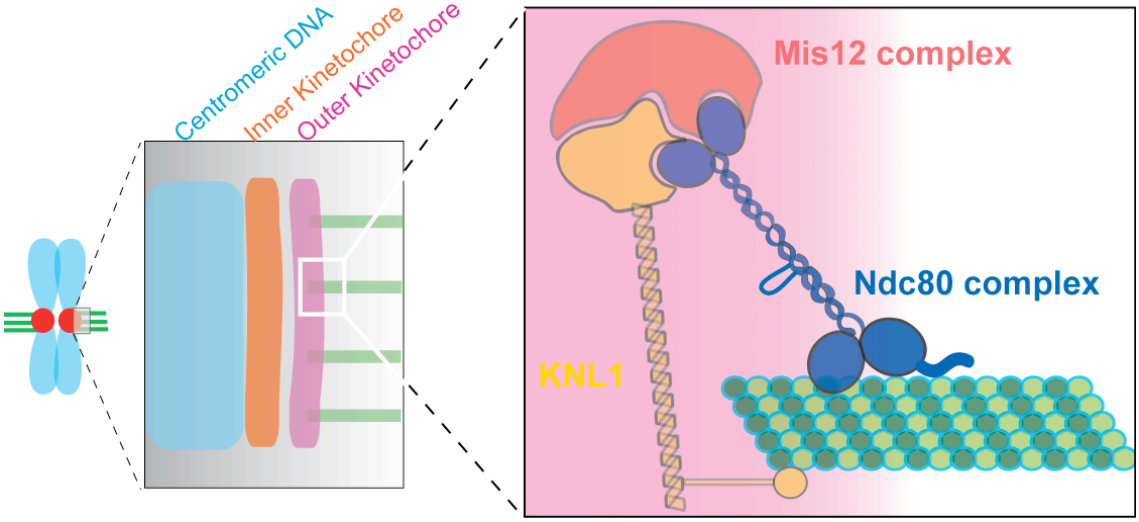

Figure 1.4 The KMN network constitutes the microtubule-interaction interface.

Under electron microscopy, the kinetochore architecture can be divided into two electron-dense layers: the inner kinetochore that bridges centromere with other kinetochore components, and the outer kinetochore in which the KMN network (KNL1-Mis12 complex-Ndc80 complex) is the major protein complex that directly interacts with microtubules.

for chromosome alignment and segregation. Furthermore, binding sites for Mis14 (the Mis12 complex) and Zwint1 are distinct but close in the C-terminal coiled-coil domain of KNL1 (Kiyomitsu et al., 2011). It has also been found that KNL1 can directly recruit the PP1 phosphatase by its very N-terminal end, and the interaction seems to be regulated by Aurora B phosphorylation, by which KNL1 reduces the binding to PP1 (Welburn et al., 2010, Liu et al., 2010). This study suggests a positive feedback loop such that Aurora B activity at kinetochores not only targets substrates directly, but also prevents its opponent PP1 from kinetochore loading. More detailed descriptions are given in section 1.5.5.

Budding yeast Spc105 was the first member identified for this protein family (Wigge et al., 1998). Chromosome segregation defects are seen in the *spc105* mutant (Nekrasov et al., 2003). It was thought Spc105 functions alone before the discovery of its binding partner Kre28 (Pagliuca et al., 2009). Whether or not Kre28 is functionally equivalent to Zwint1 remains to be determined, but the Spc105-Kre28 complex together is required for kinetochore binding of microtubule-associated proteins (Bim1, Bik1 and Slk1), kinesin motors (Cin8, Kar3), and checkpoint proteins (Mad2 and Bub1). Inactivation of Spc105 affects sister kinetochore biorientation, despite that the microtubule binding *per se* is not severely abolished (Pagliuca et al., 2009).

In fission yeast, Spc7 was identified as a multicopy suppressor of the *mal3* (EB1) deletion mutant (Kerres et al., 2004). Genetic and biochemical data indicate that the N-terminus of Spc7 is required for kinetochore localisation of Mal3 through direct binding. Spc7 temperature-sensitive mutants exhibit chromosome mis-segregation, delocalisation of the Mis12 complex and Fta2 from the kinetochores, and unstable spindle phenotypes (Kerres et al., 2004, Kerres et al., 2007). These studies together suggest an intriguing possibility that KMN is not only responsible for microtubule binding, but also involved in the spindle integrity maintenance and dynamics regulation. Sos7, the binding partner of Spc7, is recently discovered (Takashi Toda, personal communication). Sos7 is functionally related to Zwint1, as spSos7 and hZwint1

interact in a two-hybrid analysis. Temperature-sensitive *sos7* alleles lead to severe chromosome mis-segregation, which is due to the compromised kinetochore-microtubule interaction. Interestingly, despite the unknown significance, Sos7 appears to affect the subcellular localisation of Clp1/Flp1, a Cdc14-like phosphatase (Takashi Toda, personal communication). Spc7 also binds PP1 in fission yeast (Meadows et al., 2011). Importance of this finding is discussed in section1.5.5.

1.4.4.2 The Mis12/Mtw1/MIND complex

Work done in budding yeast first depicted that the Mtw1 complex (also named MIND) consists of four subunits: Mtw1/Mis12, Dsn1/Mis13, Nsl1/Mis14 and Nnf1 (Euskirchen, 2002, Nekrasov et al., 2003). It constitutes a core linker between inner kinetochore (Mif2) and the outer microtubule-binding interface (the Ndc80 complex) (Westermann et al., 2003). The Mtw1 complex promotes chromosome biorientation through the monitoring by Ipl1 (Aurora B in budding yeast) (Pinsky et al., 2003). Recently, Dsn1, together with Mif2/CENP-C, is proposed to recruit the monopolin complex component Csm1 to the kinetochore. By doing so, Csm1 helps to clamp and crosslink kinetochore components to enforce sister chromatids co-orientation in budding yeast meiosis 1 and to suppress merotelic attachment in fission yeast mitosis (Corbett et al., 2010).

The founding member in this category is fission yeast Mis12, identified from a mutant screen with a high rate of minichromosome loss (Takahashi et al., 1994). Following studies in both fission yeast and budding yeast establish a role of Mis12 in faithful chromosome segregation (Goshima et al., 1999). The phosphorylation seems to be involved in regulation of Mis12 function, by which the Ppe1/PP6 phosphatase negatively regulates Mis12 and the counteracting Gsk3 kinase likely reverses the regulation (Goshima et al., 2003). Soon after, four components of the fission yeast Mis12 complex are identified, and it is found that the complex is highly conserved from yeast to humans (Obuse et al., 2004a).

In humans, the Mis12 complex is found to interact with the centromeric heterochromatin component HP1 (Obuse et al., 2004a). Mis14 is reported to contribute to the chromosome recruitment of HP1, which is required for the centromeric loading of Shugoshin and Aurora B (Kiyomitsu et al., 2010). Depletion of the Mis12 complex causes a mitotic delay and chromosome misalignment, accompanied with reduced levels of Ndc80, BubR1, CENP-E, CENP-A, and CENP-H at the centromere/kinetochore (Kline et al., 2006). Aurora B phosphorylation of hMis13 is required for its kinetochore recruitment, which in turn determines the localisation of Nuf2 (an Ndc80 complex component) and CENP-E to the outer kinetochore (Yang et al., 2008). The Mis12 complex is also shown to bring the Hsp90-Sgt1 chaperone to the kinetochore, which in turn ensures the fidelity of multiprotein assembly during chromosome segregation (Davies and Kaplan, 2010).

In fly, the Mis12 complex is proposed to contain only three subunits without Dsn1, and the fly KNL1 is speculated to perform a dual role for both KNL1 and Dsn1 in *Drosophila* kinetochore (Przewloka et al., 2009). Different from other organisms, the *mis12* and *nsl1* mutants in fly are defective in chromosomal anaphase movement, rather than the congression, despite the severe kinetochore delocalisation of Ndc80 (Venkei et al., 2011). It is of note that no CENP-T homologue has been identified in *Drosophila*.

Recently, three independent structural studies reveal a linear conformation of the Mis12 complex (Maskell et al., 2010, Petrovic et al., 2010, Hornung et al., 2011). It is all agreed that overall topology of the Mis12 complex is similar between budding yeast and humans, though the way this complex binds to KNL1/Spc105 and Spc24-Spc25 (the Ndc80 complex) may differ. One implication from these studies is that the Mis12 complex behaves as a hub for outer kinetochore assembly. Indeed, it is reported that almost all of the budding yeast kinetochore components, from inner centromere Cse4 (CENP-A) to the outer KMN, can be affinity-purified with the Dsn1-Flag beads (Akiyoshi et al., 2010).

1.4.4.3 The Ndc80/HEC1 complex

Ndc80 and Nuf2 were originally identified in budding yeast as apparent spindle pole body components (Rout and Kilmartin, 1990, Osborne et al., 1994, Wigge et al., 1998). Nevertheless, the first evidence for Ndc80 kinetochore function comes from a study for Hec1 (highly expressed in cancer), the human homologue of Ndc80, which demonstrates that the proteins localise to the kinetochores and play a role in mitotic chromosome movements (Chen et al., 1997). Two instrumental yeast studies subsequently describe that this four-subunit complex consists of Ndc80, Nuf2, Spc24 and Spc25, and is responsible for chromosome segregation and the checkpoint response (Janke et al., 2001, Wigge and Kilmartin, 2001). Studies in other organisms soon reveal Ndc80 as an evolutionarily conserved protein (Howe et al., 2001, Nabetani et al., 2001, McCleland et al., 2003, Williams et al., 2007). Since then, extensive investigations into the Ndc80 complex pervade the kinetochore field.

In every organism, when the function of the Ndc80 protein is interfered either by mutation, RNAi knockdown, or antibody depletion, the kinetochore-microtubule attachment is severely affected and results in failure of chromosome congression and mis-segregation (Chen et al., 1997, Wigge and Kilmartin, 2001, Howe et al., 2001, Nabetani et al., 2001, He et al., 2001, DeLuca et al., 2002, Hori et al., 2003, McCleland et al., 2003, De Wulf et al., 2003, Westermann et al., 2003, Desai et al., 2003, Bharadwaj et al., 2004, McCleland et al., 2004, Cheeseman et al., 2004, DeLuca et al., 2006, Cheeseman et al., 2006, Williams et al., 2007). It is thus established that the role of Ndc80 in kinetochore-microtubule attachment is conserved in all species. The involvement of Ndc80 in SAC signalling is also conserved, likely through the direct interaction with Mad1 (Nabetani et al., 2001, Martin-Lluesma et al., 2002, DeLuca et al., 2003, Meraldi et al., 2004, Guimaraes et al., 2008). Studies for localisation dependency reveal that the Ndc80 complex is indeed required for the kinetochore localisation of the Ska and RanGAP/RanBP2 complex, Mad1, Mad2, and Mps1, budding yeast Dam1 complex, Stu2, and the motor proteins Cin8 and Kip1 (He et al., 2001, Martin-Lluesma et al., 2002, Joseph et al., 2004,

Tytell and Sorger, 2006, Hanisch et al., 2006, Ohta et al., 2010).

Structural determination leads our understanding of the Ndc80 complex to the next era. The complex has a long dumbbell-like structure (about 57 nm), with two globular domains at either end, which are separated by long coiled-coil regions in between. One globular end consists of the Spc24-Spc25 subdomain, as a receptor facing to the Mis12 complex, whilst the other end comprises the Ndc80-Nuf2 CH dimer (calponin homology domain), which faces directly to the microtubule lattice (Wei et al., 2005, Ciferri et al., 2005, Wei et al., 2006, Wei et al., 2007, Maiolica et al., 2007, Ciferri et al., 2008, Maskell et al., 2010, Petrovic et al., 2010, Hornung et al., 2011) (Figure 1.5). Ndc80 contains a flexible tail in its N-terminus, and an internal loop within the coiled-coil region. The latter is predicted to act as a kink to bent the whole protein complex *in vivo*, though the exact function remains unclear (Maiolica et al., 2007, Wang et al., 2008, Wan et al., 2009).

Microtubule binding activity resides in the dual CH domains of the Ndc80-Nuf2 head, which bind to microtubule via electrostatic interactions. The CH domains in both Ndc80 and Nuf2 contain several positive residues, which are responsible for direct interaction with the negatively charged E-hook in tubulin C-terminus on the microtubule lattice (Wei et al., 2007, Ciferri et al., 2008). However, new evidence shows that the CH domain of Nuf2 may play a structurally supportive role, rather than direct binding to microtubule lattice (Wilson-Kubalek et al., 2008, Alushin et al., 2010, Sundin et al., 2011).

Containing positive charges, Ndc80 N-tail itself is also able to bind microtubules directly (Guimaraes et al., 2008, Miller et al., 2008, Tooley et al., 2011), and may somehow trigger the oligomerisation of neighboring Ndc80 complexes to cooperatively enhance the overall binding affinity (Cheeseman et al., 2006, Wei et al., 2007, Alushin et al., 2010). Furthermore, this N-tail contains several Aurora B sites and the phosphorylation has been demonstrated *in vitro* and *in vivo*. The phosphorylation adds extra negative charges on the N-tail and results

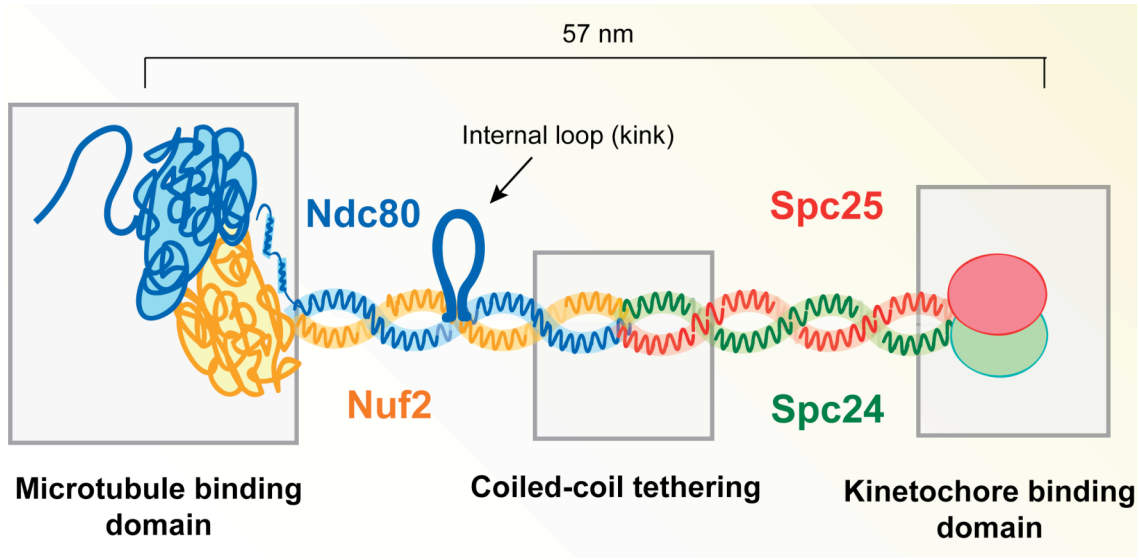

Figure 1.5 The structure of the conserved Ndc80 complex.

The Ndc80 complex forms a long rod-like structure with the globular domains at both ends. The overall length is 57 nm (Wei et al., 2005). The N-terminal of both Ndc80 and Nuf2 form the calponin-homology (CH) domain dimer, which are similar to the EB1 CH dimer, and confer the microtubule-binding activity. Ndc80 N-tail also binds to microtubule lattice directly. These four proteins tether together within the middle coiled-coil domains. However, there is an internal flexible loop structure within the Ndc80 coiled-coil shaft, the function of which is currently uncertain. The other end consists of the Spc24-Spc25 subcomplex dimer, which directly faces other kinetochore components, such as the Mis12 complex.

in the reduced affinity of microtubule binding. This modification is regarded as an important regulatory mechanism for Aurora B-dependent error-correction of the spindle-kinetochore attachment in early mitosis (Cheeseman et al., 2004, DeLuca et al., 2006, Ciferri et al., 2008) (more details in section 1.5.5). However, in budding yeast, the N-tail can be deleted without viability loss, suggesting a non-essential role of this N-tail in budding yeast. Thus the mechanism in which this N-tail is involved might be different between budding yeast and higher eukaryotes (Kemmler et al., 2009, Akiyoshi et al., 2009a).

As mentioned, Aurora B phosphorylation is an important pathway to regulate the Ndc80-microtubule interaction. Other reports show that Nek2 kinase also targets human Ndc80, which phosphorylation in this case increases microtubule-binding activity of Ndc80 (Chen et al., 2002, Du et al., 2008). The Nek2 phosphorylation site of Ndc80 (S165) is next to K166, a residue that has been shown to directly bind to microtubule lattice as a ‘toe’ (Alushin et al., 2010, Sundin et al., 2011).

When the function of endogenous Ndc80 is blocked by injection of an anti-Ndc80 antibody, which acts in a dominant-negative fashion, the plus end of the kinetochore microtubule loses its dynamics and becomes very stable, resulting in the hyperstretch of sister kinetochores (DeLuca et al., 2006). This study thus raises the interesting question as to how Ndc80 couples the microtubule binding activity to the regulatory ability of microtubule dynamics.

Recently, a fibril structure connected to the flared microtubule protofilaments has been proposed as a new model to couple the chromosome movement to microtubule depolymerisation, and Ndc80 is believed to be the best candidate for this linear structure (McIntosh et al., 2008). Another group uses a bead-coupling technique applied onto the Ndc80 complex, and find that Ndc80 complex-coated beads can move along the microtubule lattice, and track the depolymerising microtubule end by biased-diffusion. These data argue that Ndc80 is able to act as a kinetochore coupler to move a cargo (chromosome) in either a polymerising or depolymerising stage of microtubules (Powers et al.,

2009). Whether or not this is the case *in vivo* remains to be further examined. *In vitro*, the Dam1 complex can enhance the microtubule binding of the Ndc80 complex, suggesting that in budding yeast, Dam1 may be the coupler to coordinate Ndc80 activity to move the chromosomes (Lampert et al., 2010, Tien et al., 2010).

The whole KMN network, including the Ndc80 complex, has been found detached from outer kinetochore during early meiotic phase in fission yeast, and this detachment is correlated with centromere-SPB dissociation and is required for the following horse-tail movement (when telomeres are associated with the SPB) (Nabetani et al., 2001, Asakawa et al., 2005a, Hayashi et al., 2006). While vertebrate Ndc80 only assembles to the outer kinetochore during mitosis, yeast Ndc80 is always there throughout the whole mitotic cell cycle. It is suggested that Ndc80 may be required for kinetochore clustering around the interphase SPB (Appelgren et al., 2003), and recently being involved in maintenance of nuclear organisations in fission yeast (King et al., 2008). However, the function of Ndc80 in interphase is still largely elusive.

1.5 Spindle assembly checkpoint

1.5.1 The kinetochore-microtubule attachment

In mitosis, the most important task for spindle microtubules is to properly attach to the kinetochores in a bipolar manner, generating driving forces required for faithful chromosome segregation. The initial microtubule-kinetochore attachment is thought to be stochastic, and several possible attachments may happen during the course of 'search and capture' (Figure 1.6). The correct attachment is '**bipolar**' attachment (or amphitelic attachment), by which each kinetochore of sister chromatids is attached to each pole; when two kinetochores are both attached to the same pole, it is called '**syntelic**' attachment; when only one kinetochore of the sister is attached to one pole, it is termed '**monotelic**' attachment; when two kinetochores become attached to

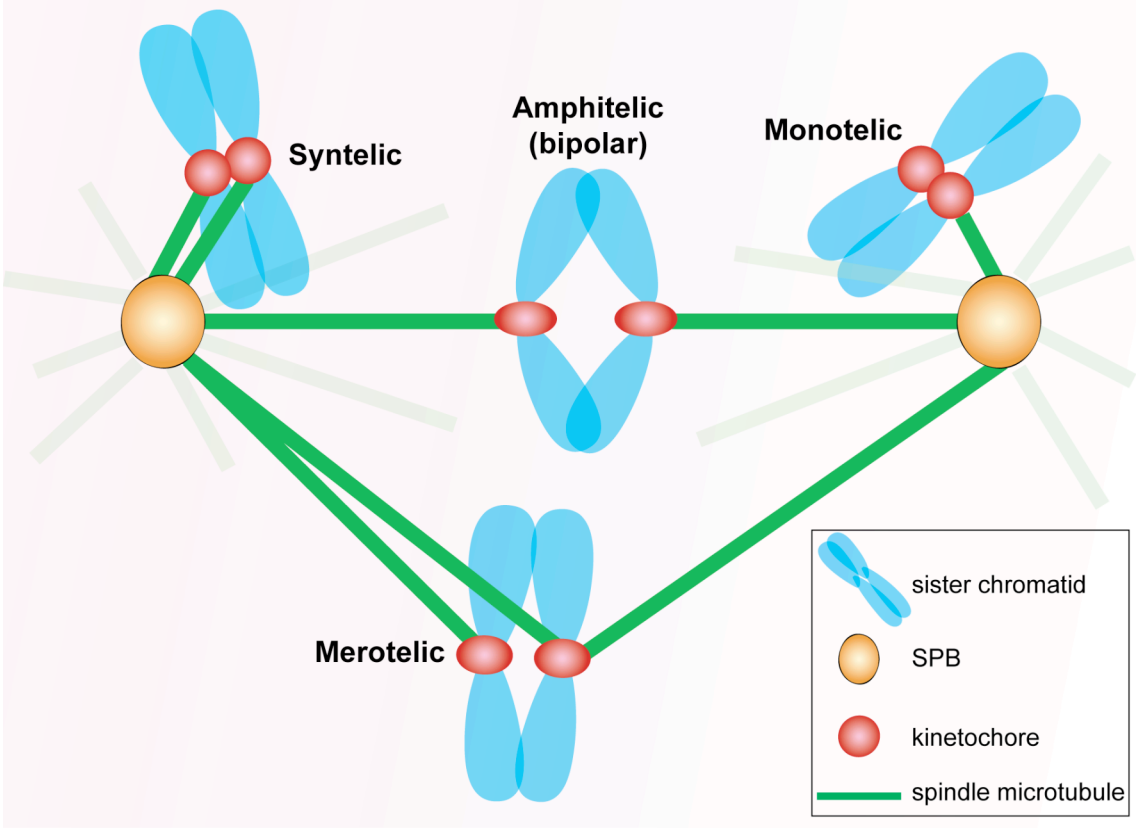

Figure 1.6 Different types of kinetochore-microtubule attachments.
Amphitelic attachment, by which each kinetochore of the sister chromosome is attached to each pole, is the ultimate goal for the chromosome biorientation; when two kinetochores of the sister are attached simultaneously to one pole, it is called syntelic attachment; when only one kinetochore is attached, it is named monotelic attachment; merotelic attachment is the situation where both kinetochores are attached, but at least one kinetochore is also attached to the other pole.

opposite poles rather than just one pole, it is referred to as '**merotelic**' attachment. Furthermore, under some conditions, for example when the kinetochore is severely impaired, the attachment will become weak and unstable, and thus the kinetochore is lost from microtubule attachment. A surveillance mechanism exists in the cells to monitor the attachment, block the premature chromosome segregation, and correct the wrongly attached kinetochores, ultimately ensuring that all chromosomes are correctly biooriented at the cell equator. This is named the spindle assembly checkpoint (SAC).

1.5.2 The SAC components

Twenty years ago, two pioneering studies described isolation of genes, mutation of which failed to arrest the budding yeast cells in mitosis in the presence of tubulin poisons (Li and Murray, 1991, Hoyt et al., 1991). Two classes of "spindle assembly checkpoint (SAC)" genes were identified: the *MAD* (mitotic-arrest deficient) genes, including *MAD1, MAD2, and MAD3* (homologue of human *BUBR1*), and the *BUB* (budding uninhibited by benzimidazole) genes, including *BUB1* and *BUB3*. Since then researches have been extensively carried out to decipher the molecular mechanisms of SAC surveillance coupling to the progression of chromosome segregation. SAC signalling negatively regulates Cdc20, an activator of the APC/C (the E3 ubiquitin ligase anaphase promoting complex/cyclosome), by triggering the formation of the MCC (mitotic checkpoint complex), which consists of Mad2, Mad3, Bub3, and Cdc20. Assembly of this complex sequesters Cdc20 from binding to APC/C and thus prevents the ubiqutination of two key substrates Cyclin B and sercurin, whose degradation by the 26S proteasome in turn triggers anaphase onset (Hwang et al., 1998, Kim et al., 1998, Vanoosthuyse and Hardwick, 2009b, Sudakin et al., 2001, Fraschini et al., 2001, Millband et al., 2002, Peters, 2006).

Other core SAC components include Aurora B (Ipl1 in *S. cerevisiae* and Ark1 in *S. pombe*) and MPS1 (multipolar spindle-1, named Mph1 in *S. pombe*), which are involved in the amplification of SAC signalling, namely the promotion of MCC formation and the error-correction process of kinetochore-microtubule

attachment (Weiss and Winey, 1996, Hardwick et al., 1996, Abrieu et al., 2001, Tanaka et al., 2002, Hauf et al., 2003, Petersen and Hagan, 2003, Morrow et al., 2005). Additionally SAC function in higher eukaryotes requires the RZZ complex (ROD-ZW10-ZWILCH); p31^{comet} (CMT2); protein kinases such as MAPK, CDK1-Cyclin B, NEK2 and PLK1 (Polo); microtubule motor kinetochore proteins CENP-E (Kinesin-7), dynein and dynactin (Musacchio and Salmon, 2007).

1.5.3 The Mad2-template model

Function of the SAC is closely linked to the kinetochore, as many SAC components are found dynamically associated with the kinetochore during prometaphase. The current mainstream thought as to how the kinetochore is involved in SAC amplification is summarised in the “Mad2-template model” (De Antoni et al., 2005) (Figure 1.7). In this model, the Mad1 homodimer is stably bound to the unattached kinetochore and is required for the kinetochore localisation of Mad2 (Sironi et al., 2002). Mad2 exists as two different conformations, O-Mad2 (the ‘open’ form) and C-Mad2 (the ‘close’ form), where only C-Mad2 is favourable of binding Cdc20 (Sironi et al., 2001, Shah et al., 2004, Luo et al., 2004). Mad2 binding to Mad1 likely induces a conformational switch to C-Mad2 (Luo et al., 2002). Once located, the immobile Mad1-C-Mad2 complex at the kinetochore subsequently acts as a template to convert the rapidly cycling O-Mad2 to C-Mad2, a conformer required to bind Cdc20 (Mapelli et al., 2007, Yang et al., 2007). Now each free C-Mad2 likely promotes conformational switch of more cytosolic O-Mad2, triggering a global firing of the checkpoint response.

An important implication of this model lies in the autocatalytic prion-like reaction from the Mad1-C-Mad2 ‘seed’ at the unattached kinetochore, followed by the positive-feedback loop amplification of SAC signalling (Musacchio and Salmon, 2007). It well explains why a single unattached kinetochore is sufficient to activate the robust checkpoint signalling (Rieder et al., 1995). Indeed, this model is supported by recent studies showing that immobilised Mad1/Mad2 at

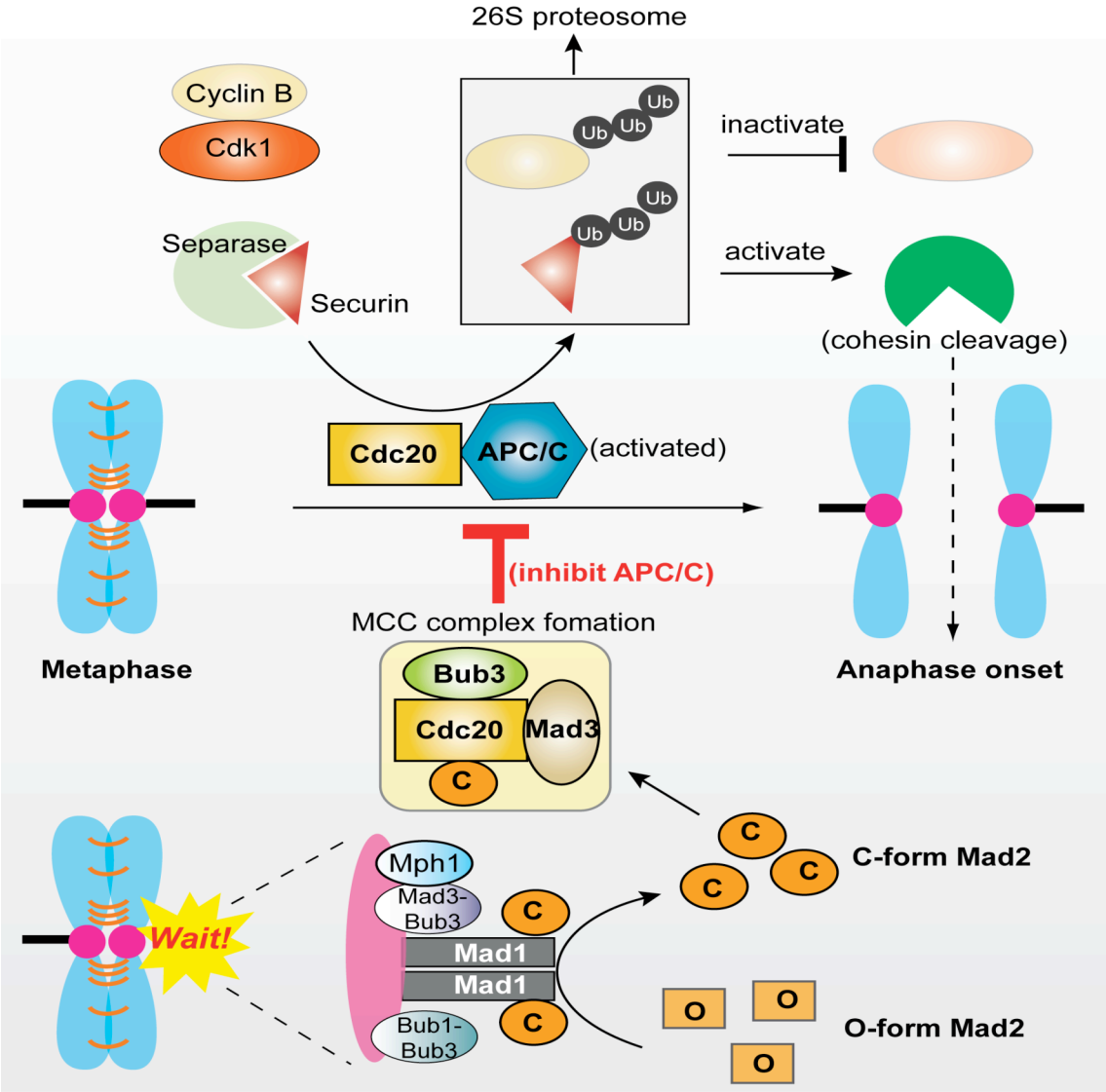

Figure 1.7 Mechanism of spindle checkpoint activation.

When correct bipolar attachments are established, Cdc20 activates the APC/C, which in turn promotes the degradation of securin (the separase inhibitor) and cyclin B (the Cdk1 cyclin). Degradations of these two key substrates trigger the separase activation and Cdk1 inactivation. These two events coordinately result in the cleavage of cohesin and subsequent anaphase onset. When the kinetochore is unattached (or without tension), the kinetochore-localised Mad1-Mad2 plays a key role to transform the cytosolic open-Mad2 into the active close-form. The increased close-Mad2 promotes the formation of the MCC complex and therefore blocks the activity of Cdc20 that is required for APC/C activation.

the unattached kinetochores catalyses production of cytosolic MCC (Kulukian et al., 2009), which in turn as an entity associates and blocks the APC/C (Herzog et al., 2009). Furthermore, constitutive Mad1-Mad2 targeting to the kinetochore is reported to be sufficient for metaphase arrest even without a primary attachment error signal (Maldonado and Kapoor, 2011).

1.5.4 Attachment vs. Tension: the debate

What have been proposed to be sensed by checkpoint signalling are (1) lack of kinetochore-microtubule attachment (kinetochores remain unattached), and/or (2) lack of tension in the centromere-kinetochore region between sister chromatids.

The ‘attachment’ hypothesis is first raised from the live-image observation that a single unattached kinetochore is sufficient to block anaphase onset. When this unattached kinetochore is laser-ablated, the opposite kinetochore remains attached but without tension, and the cell enters anaphase, suggesting that the unattached kinetochore, not tension, is the source of the checkpoint signal (Rieder et al., 1995). Another line of evidence lies in the fact that when Aurora B is inhibited to block its error correction activity (see below), the SAC becomes satisfied regardless of the correct or wrong attachments (Ditchfield et al., 2003, Hauf et al., 2003).

The ‘tension’ theory stems from the micromanipulation on a syntelically-attached or an unpaired chromosome, in which an anti-poleward force from the microneedle leads to the stabilisation of the incorrect attachment and releases the cell from checkpoint arrest (Nicklas and Koch, 1969, Li and Nicklas, 1995). These classic experiments strongly suggest that tension across the sister kinetochore (inter-kinetochore) directly satisfies the SAC. Underpinning the ‘tension’ theory, cells are found to be arrested in mitosis when treated with an Eg5 (Kinesin-5) inhibitor, Monastrol, which causes the monotelic or syntelic attachment (Kapoor et al., 2000). Another evidence is that cells receiving low doses of vinblastine (a tubulin depolymerising drug) become arrested in mitosis with bioriented chromosomes and low tension (Skoufias et al., 2001).

In some situations, for example, the *cdc6* (blocks DNA replication) or the cohesin mutant in budding yeast and of HeLa cells with unreplicated genomes (MUG), the formation of sister kinetochore is prevented and therefore no tension is applied to the attached kinetochore. Interestingly, only short delay is observed under these conditions, degree of which is much less than that caused by the MT-depolymerising agent, which entirely destroys the attachment, suggesting that 'lack of tension' is sufficient to trigger SAC signalling, but 'lack of attachment' seems to be the major determinant for the SAC response (Shonn et al., 2000, Stern and Murray, 2001, Biggins and Murray, 2001, O'Connell et al., 2008).

These two primary defects are naturally intertwined, as in the absence of external forces from bound microtubules, there is inevitably no tension formed between sister kinetochores. How to tease these two sources apart is still technically challenging. Thus "what checkpoint exactly senses" is nonetheless the most controversial issue in the checkpoint field to date.

1.5.5 Aurora B: the link between tension sensing and error correction

The chromosomal passenger complex (CPC) contains the core Aurora B kinase and three non-enzymatic subunits: INCENP, Survivin, and Borealin, which are universally conserved (Ruchaud et al., 2007, Nakajima et al., 2009, Bohnert et al., 2009). During mitosis, CPC locates to the inner centromere site until anaphase onset, and relocates to the midzone of anaphase spindles and the equatorial cell cortex. As described below, Aurora B is important in the establishment of proper KT-MT attachment. In budding yeast, Ipl1/Aurora B has been shown to promote turnover of kinetochore-spindle pole body attachments (Tanaka et al., 2002). This study reflects an important implication that Aurora B may sense the tension status and response to correct the wrong attachment, pathway of which is proposed for more than 40 years (Nicklas and Koch, 1969). Indeed, inhibition of Aurora B leads to accumulation of syntelic attachments (Kallio et al., 2002, Ditchfield et al., 2003, Hauf et al., 2003), while reactivating Aurora B in the same condition reverses these errors by selectively

destabilising incorrect attachments (Lampson et al., 2004). In this scenario, Aurora B indirectly activates the SAC by creating the unattached kinetochore, which is the targeting site for Mad1/Mad2 checkpoint (Pinsky et al., 2006).

It is generally believed that Aurora B corrects the wrong attachments by phosphorylating its targets at the outer kinetochores. Mechanisms as to how the inner centromeric Aurora B is able to physically 'touch' to the components at the outer kinetochore may require a structural extension of INCENP and/or molecular diffusion of Aurora B (Sandall et al., 2006, Wang et al., 2011). In budding yeast, it has been shown that phosphorylation of Dam1 may reduce its binding to Ndc80, thus resulting in the detachment of microtubule from the kinetochore (Cheeseman et al., 2002, Shang et al., 2003). In metazoans, one major target of Aurora B is MCAK (mitotic centromere-associated kinesin, Kinesin-13), a microtubule depolymerising factor. Phosphorylation of MCAK by Aurora B affects its kinetochore localisation, as well as downregulates its depolymerising activity toward microtubules (Andrews et al., 2004, Lan et al., 2004). Likely, Aurora B also corrects some tension-less merotelic attachments by regulating MCAK (Knowlton et al., 2006, Cimini et al., 2006).

Ndc80 also emerges as another key target for Aurora B phosphorylation. Phosphorylation sites of Ndc80 have been mapped onto the flexible N-terminal tail (DeLuca et al., 2006, Cheeseman et al., 2006, Ciferri et al., 2008). This N-tail is positively charged and required for direct binding toward microtubule lattice via interaction with the tubulin E-hook (Guimaraes et al., 2008, Miller et al., 2008). Furthermore, prevention of Aurora B phosphorylation of Ndc80 results in kinetochore hyperstretch and increases frequencies of merotelic attachments *in vivo* (Ciferri et al., 2005, Cimini et al., 2006, DeLuca et al., 2006); on the other hand, phosphorylation of Ndc80 *in vitro* causes the reduction of MT binding of this protein (Cheeseman et al., 2006). Recently, it is also found that the whole KMN network, including Ndc80, KNL1 and Mis13/Dsn1 (the Mis12 complex), is spatially and differentially phosphorylated by Aurora B. A key concept from this study is that the combinational phosphorylation of the KMN network generates graded levels of microtubule-

binding activities; as such the binding is severely compromised when KMN is fully phosphorylated (Welburn et al., 2010). These studies together strongly implicate the KMN network as the key substrate that is central to Aurora B-mediated error correction.

There are several ways to regulate Aurora B activity at the inner centromere, such as the autophosphorylation of INCENP and Aurora B itself (positive feedback) (Ruchaud et al., 2007); a conformational change of CPC by INCENP extension which results in a physical association of Aurora B with the outer kinetochore substrates (Sandall et al., 2006); translocation to the midzone spindle, which is dependent on the kinesin motor Klp2 and dephosphorylation of INCENP (Pereira and Schiebel, 2003, Gruneberg et al., 2004); interactions with the protein TD-60; binding of the CPC to microtubules; activation by other kinases like Chk1; TLK-1 (Tousled-like kinase) and Mps1, or inactivation by phosphatases including PP1 and PP2A (Lampson and Cheeseman, 2011).

Recently, major progress in understanding of the role for Aurora B in the SAC machinery was achieved by an elegant experiment set with FRET sensor sensitive to Aurora B phosphorylation (Liu et al., 2009). Important insight from this study posits that Aurora B may continuously exert the kinase activity, where the efficacy decreases as a function of the distance from its substrates. Another two papers measuring the “inter-kinetochore“ and “intra-kinetochore” stretching in HeLa and fly S2 cells are also thought-provoking (Maresca and Salmon, 2009, Uchida et al., 2009). The crucial message from these studies is that inter-kinetochore stretching, a traditionally credible marker for detecting tension, is not a reliable parameter for tension monitoring and SAC response prediction; rather, the “intra-kinetochore” stretching” is the relevant readout for tension and SAC satisfaction. Together, these studies suggest that rather than change in intrinsic kinase activity, the ability of Aurora B to sense tension relies on the spatial separation of Aurora B relative to its substrates at the outer kinetochore.

1.5.6 Checkpoint silencing

Several mechanisms have been proposed to turn the checkpoint off after all the

chromosomes are bi-oriented at the metaphase plate. In metazoans, dynein is the key to 'strip' the SAC proteins off from microtubule-attached kinetochores (Howell et al., 2001). CENP-E has been shown to be required for enhancing the recruitment of BubR1 to unattached kinetochores (Weaver et al., 2003); conversely, BubR1-dependent checkpoint signalling is silenced by CENP-E upon the microtubule attachment (Mao et al., 2005). Another way to silence the SAC includes $P31^{comet}$-mediated structural mimicry-based inhibition of C-Mad2, by which $P31^{comet}$ competes with O-Mad2 to interact with C-Mad2 that is bound either to Mad1 or to Cdc20 (Habu et al., 2002, Xia et al., 2004, Yang et al., 2007). However, how the local environment near the kinetochore regulates $P31^{comet}$ activity remains unknown. The posttranslational modification of checkpoint proteins, such as ubiquitylation and/or phosphorylation of Cdc20, also contributes to checkpoint silencing (Wassmann et al., 2003, Chung and Chen, 2003, Reddy et al., 2007, Kim et al., 2010b). In addition, the inactivation of Cdk1, which is due to the destruction of cyclin B at anaphase onset, plays a role in SAC response (D'Angiolella et al., 2003, Potapova et al., 2006).

Interestingly, several mechanisms described above for SAC silencing seem not essential or nonexistent in yeasts, suggesting other universal pathways might still await discovery. In budding yeast, degradation of Mps1 by the APC/C, so as the translocation of chromosome passenger complex (CPC) from centromere, incapacitates the SAC engagement after anaphase onset (Palframan et al., 2006, Mirchenko and Uhlmann, 2010). Both mechanisms are likely conserved in higher eukaryotes (Jelluma et al., 2010, Vazquez-Novelle and Petronczki, 2010).

Another avenue leading to checkpoint inactivation lies in the PP1 phosphatase (Dis2 in fission yeast and Glc7 in budding yeast), which is recently demonstrated in both yeasts to be crucial for checkpoint silencing by opposing Aurora B, activity of which is required to maintain the SAC response (Pinsky et al., 2009, Vanoosthuyse and Hardwick, 2009a, Akiyoshi et al., 2009b). How the checkpoint-silencing function of PP1-Aurora B separates from that of kinetochore disassembly or kinetochore-microtubule re-attachment is unclear

(Emanuele et al., 2008, Liu et al., 2010). However, further studies reveal that interaction between PP1 and KNL1/Spc7/Spc105 is important for the checkpoint silencing activity at the kinetochore, and the concentration of PP1 at the kinetochore needs to be finely tuned for cell viability (Rosenberg et al., 2011, Meadows et al., 2011). Nevertheless, in addition to the kinetochore pool of PP1, the kinesin motor proteins Klp5 and Klp6 (Kinesin-8) are also involved in PP1-dependent SAC silencing in fission yeast, where the motor domains of these kinesins are dispensable for function. This suggests that there might be two independent pools of PP1 that together are needed to completely switch the SAC off (Meadows et al., 2011)

1.6 Fission yeast as a model

I use the fission yeast *Schizosaccharomyces pombe* as a model. Fission yeast is a unicellular *Ascomycete* fungus, containing three chromosomes of 5.7, 4.7, and 3.5 Mb in size with 5144 genes in the whole genome (Wood et al., 2002, Rhind et al., 2011, Bitton et al., 2011). This model is economically amenable, and many important genes involved in various cell cycle processes, including chromosome segregation during mitosis, are highly conserved (for example, Table 1.1). Other advantages for using this model organism are:

(1) Amenable genetic manipulation. Due to the high frequency of homologous recombination in fission yeast, it is readily feasible to integrate a desired DNA fragment into genome at the specific locus for endogenous gene tagging, fusion, deletion, disruption, or modification. In the case of gene deletion, fission yeast definitely offers a much cleaner background compared to mammalian siRNA knockdown. Furthermore, there are various vectors available for transformation and episomal gene expression at different expression levels.

(2) A clear life cycle. As fission yeast is heterothallic, under nutrient-limited conditions, cells with opposite mating types (h^- and h^+) will conjugate to form a diploid zygote, which proceeds through meiosis to produce four spores. While

under rich media conditions, cells can switch to the vegetative growth (mitotic cycle). The clear life cycle allows *pombe* researchers to obtain a desired genetic background simply by strain crossing and marker selection. In addition, it makes possible the genetic mapping and gene dosage studies, such as the 'haplo-insufficiency". The fast growth rate also facilitates the experimentation (the doubling time is ~130 min under optimal conditions).

(3) Comprehensive database. The genome sequence of fission yeast has been completed (Wood et al., 2002). Following genome-wide studies have built up several valuable database sets for the *pombe* research community. These include the ORFeome to determine the cellular localisation of 4431 proteins (Matsuyama et al., 2006, Hayashi et al., 2009), a high-density and quantitatic genetic interaction map (Roguev et al., 2008), a comprehensive deletion library developed to cover 99% of the genome (Kim et al., 2010a, Spirek et al., 2010), and the comparative functional genomics across the *Schizosaccharomyces* clade (Rhind et al., 2011). Recently, a brand new, comprehensive, on-line resource called 'PomBase' is also on the way (Valerie Wood, 6th pombe meeting, Boston 2011).

1.7 Motivation of this study

During mitosis, cells need to separate chromosomes accurately to avoid aneuploidy, which is the most common characteristic of human solid tumours (Kops et al., 2005). Upon mitotic entry, spindle microtubules are reorganized and emanated from two centrosomes to catch kinetochores on chromosomes. During this "search and capture" stage, microtubules dynamically polymerise and/or depolymerise to enhance the chance to grab the kinetochores. When all sister chromatids are attached in a bipolar fashion, microtubules stay stable in the balance of polymerisation and depolymerisation. When cells enter anaphase, kinetochore microtubules depolymerise to pull the sister chromosomes apart from each other to the opposite poles. To avoid

chromosome mis-segregation, it is thus important for cells to tightly regulate the dynamic microtubule behavior during mitosis.

Studies in mammalian cells reveal that Ndc80/Hec1 is specifically overexpressed in human cancers (Highly Expressed in Cancer) (Chen et al., 1997). Animal models also demonstrate the oncogenic nature of Ndc80 because the overexpression of Ndc80 results in mitotic checkpoint hyperactivation, which in turn increases the frequency of aneuploidy and tumorigenesis (Hayama et al., 2006, Diaz-Rodriguez et al., 2008). The expression level of Ndc80 has been linked to tumour grade and poor prognosis of the lung and breast cancer patients (Hayama et al., 2006, Bieche et al., 2011). These results not only mark the potential of Ndc80 as a diagnostic or prognostic marker, and a promising target for developing new anti-cancer drugs (Gurzov and Izquierdo, 2006, Li et al., 2007, Numnum et al., 2008, Momeny et al., 2008, Wu et al., 2008), but also spotlight the importance of more detailed basic research on the cellular function of the Ndc80 proteins.

Despite the extensive characterisation of the kinetochore architecture mentioned above, the detailed mechanism of kinetochore-microtubule attachment, especially the regulation of microtubule dynamics via the kinetochore components, remains largely elusive. Furthermore, although the knowledge about Ndc80 has been improved by biochemical and structural approaches, many questions remain to be clarified, especially in the molecular mechanism of controlling microtubule dynamics. First, how does the Ndc80 complex modulate the activity of other microtubule-binding proteins? Second, how does it interact with the inner layer of the kinetochore? Third, how do spindle checkpoints exert their activity through Ndc80? How do these proteins together affect microtubule dynamics and how are these interactions regulated? It would be crucial to answer these questions, which will lead to hints for developing new therapeutic targets of human cancers.

It is also worthy to mention that in mammalian cells, the outer kinetochore components can be observed on the duplicated chromosomes from prophase

to late anaphase of every cell cycle (Cheeseman and Desai, 2008). In yeasts, however, the outer kinetochore, such as Ndc80, is found to steadily locate at the centromeric region throughout the whole vegetative division cycle (Nabetani et al., 2001). The physiological meaning for this is currently elusive.

In the present thesis, I study the kinetochore component Ndc80 in fission yeast, and focus on its role in microtubule dynamics control and the kinetochore-microtubule attachment during the course of chromosome segregation, as well as its potential role beyond mitosis. Starting from temperature-sensitive mutant isolation, I characterise the mutant defects in depth. I will describe my results in the following four chapters, with the discussion in the end of each chapter. In the end, I will provide general concluding remarks and potential future directions deviated from my thesis work.

Chapter 2. Isolation of the *ndc80* mutants

2.1 *ndc80*$^+$ is essential for viability

In the beginning of my Ndc80 project, I first assessed whether *ndc80*$^+$ is an essential gene for cell viability. I replaced one copy of the *ndc80*$^+$ genes with kanamycin-resistant cassette (*kan*^{r}) in wild type diploid cells. The *kan*^{r} marker fragment was PCR amplified from pFA6a-kanMX6 plasmid with the primer pair that reversely complements the 80 base pair (bp) of *5'*- and *3'*-untranslated regions (UTR) of *ndc80*$^+$ right next to the start and the stop codon, respectively. The PCR products were then transformed into a wild type diploid strain. Thanks to the relatively high frequency nature of homologous recombination in yeast cells, the amplified fragments can be incorporated into genome at the *ndc80*$^+$ locus. Transformants were selected on rich (yeast extract with supplements, YE5S) plates containing kanamycin. The desired clones were confirmed by colony PCR, to make sure that the recombination occurred at the right position and the genotype was in a heterozygous manner, which means only one copy of *ndc80*$^+$ is intact, but the other replaced by the *kan*^{r} marker.

Tetrad dissection was performed in the heterozygous diploids cells. Only two spores of each tetrad could grow to form colonies, which were sensitive to kanamycin drug (Figure 2.1A and B), where the other two spores died at the germination stage, indicating that *ndc80*$^+$ is essential for viability.

2.2 Rationale for isolation of specific *ndc80* temperature-sensitive mutants

Since *ndc80*$^+$ is essential, I am not able to start the experiment with making a haploid deletion strain. I then sought to isolate *ndc80* temperature-sensitive (ts) mutants. The temperature sensitive mutant is a conditional mutant, for it

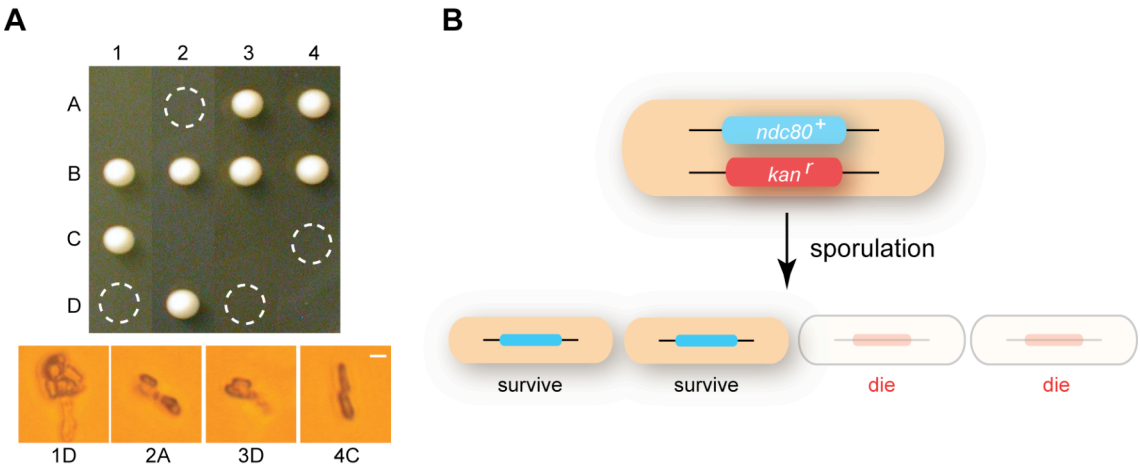

Figure 2.1 *ndc80*$^{+}$ is essential.

(A) Tetrad dissection of *ndc80* deletion heterozygous diploid. In the diploid cells, a kanamycin-resistance marker cassette replaced one copy of the *ndc80*$^{+}$ genes. Two out of four spores were non-viable on the YE5S plate, and died after germination. Scale bar, 5 μm.

(B) The viable spores were kanamycin-sensitive (not shown).

behaves normally as the wild type cells at the permissive temperature, but the defective phenotypes appear when the mutant cells are grown at the restrictive temperature.

As in many cases one protein may bear multiple functions, complete deletion or shut-off of the entire gene may result in numerous defective phenotypes that make dissection of a specific function difficult. ts mutant isolation takes the advantage in that it makes possible to isolate separation-of-function mutants when the gene-of-interest plays more than one role in the cells. Ndc80 for example, the protein's integrity at outer kinetochores has been reportedly involved in not only kinetochore assembly, but also spindle assembly checkpoint signaling and microtubule capturing (Martin-Lluesma et al., 2002, McCleland et al., 2003, DeLuca et al., 2006, Cheeseman et al., 2006). It can be envisioned if the Ndc80 functions were completely abolished by heat-inactivation, Ndc80 complex would be no longer able to localise at the kinetochores. As a result, cells would exhibit multiple defective phenotypes. Such completely loss-of-function mutants would consequently obstruct the delineation of specific spindle phenotypes. For this reason, I intended to focus on the mutants that preserve the Ndc80 complex signals at the kinetochores.

In order to assess whether isolated *ndc80* mutants retained capability of the kinetochore localisation, each mutant was tagged with *nuf2*$^{+}$-YFP-*ura4*$^{+}$ or *spc25*$^{+}$-YFP-*nat*^{r} (nourseothricin-resistance), and the YFP signals were observed at the restrictive temperature. If the overall structure of the Ndc80 complex is disrupted by mutations, no YFP signals will be detected at the kinetochores. However if YFP signals are detected at the kinetochores, I assume that activities of complex formation and the kinetochore localisation remain intact in mutants (Figure 2.2).

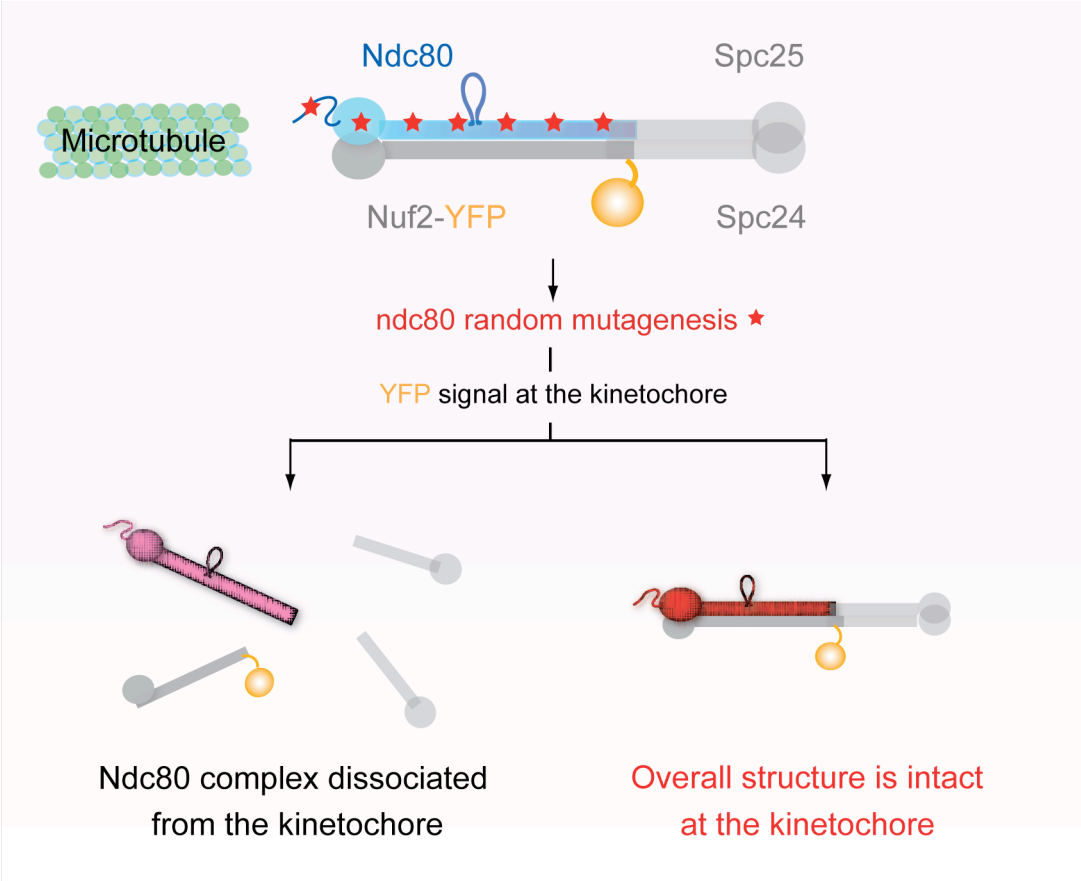

Figure 2.2 Isolating *ndc80* mutants that retain kinetochore localising activities.

To examine whether isolated ts mutants retain capability of kinetochore localisation, NUf2-YFP and/or Spc25-YPF signals were observed in each mutant at the restrictive temperature. If the Ndc80 complex fails to assemble due to the mutations, no YFP signals would be detected at the kinetochore (left). However if YFP signals were detected at the kinetochore, it was assumed that activities of complex formation and kinetochore localisation are intact in the mutant (right).

2.3 Experimental procedures of *ndc80* ts mutant screening and isolation

For the ts mutant isolation, my colleague had constructed a strain in which the endogenous *ndc80*$^{+}$ gene was tagged with a *kan*^{r} marker at its 3' UTR. I extracted the genomic DNA from this strain. The *ndc80*$^{+}$-*kan*^{r} fragment was amplified by PCR with a primer set that annealed to 500 bp upstream and 330 bp downstream of the *ndc80*$^{+}$ locus. This PCR fragment with larger homologous regions has two advantages: (1) possibly allow higher occurrence of homologous recombination to obtain more transformants; (2) increase the probability of isolating mutants with mutations in the close proximity of N-terminus of *ndc80*$^{+}$ coding region, at which the frequency of recombination is expected to be lower than other regions.

The amplified *ndc80*$^{+}$-*kan*^{r} fragment then served as a template for the following error-prone PCR. The amount (2.5 mM) of deoxyguanosine triphosphate (dGTP) used in error-prone PCR was 10 times higher than that of the other three dNTPs (250 μM each). The concentration imbalance may contribute to biased nucleotide incorporation. As a result, mutations may be randomly introduced during PCR reaction. Several DNA polymerases were tested to optimise the PCR reaction efficiency prior to experiments, including CRUK in-house polymerase, LA polymerase (Takara), Z polymerase (Takara), and Vent polymerase (NEB). In my hands, both Z and Vent polymerase could be used to produce a clear single band of the predicted size. However, the yield could be maximised by using Vent polymerase with additional magnesium supplied. I thus used the same condition to amplify the random mutagenic fragments.

The error-prone PCR fragments were transformed into the wild type strains tagged with either *nuf2*$^{+}$-*yfp*$^{+}$-*ura4*$^{+}$ or *spc25*$^{+}$-*yfp*$^{+}$-*nat*^{r}. The transformants were spread on YE5S plates at 27℃ for 1 day, allowing the homologous recombination to occur more completely. The plates were then replica plated onto YE5S+kanamycin plates for marker selection at 27℃. After 4 days incubation, the YE5S+kanamycin plates were further replica plated on three

identical YE5S plates containing Phloxin B dye that stains dead cells as dark pink colours. These plates were incubated separately: one at 27℃, another at 36℃ and the other at 20℃ for 1 to 3 days. Temperature-sensitive mutants were identified when comparing their ability of colony formation at different temperatures. Colonies that can grow at 27℃ but not at 36℃ are namely ts mutants, while those that grow at 27℃ but not at 20℃ are cold-sensitive (cs) mutants (Figure 2.3).

From two independent experiment sets, in total about 8,000 colonies were screened, and 22 ts and 10 cs mutants were isolated. To rule out the possibility of additional extragenic mutation(s) in the genome that also contribute to the temperature-sensitive phenotypes, I backcrossed all the *ndc80* mutants with a wild type strain. Segregants from most *ndc80* mutants showed 100% cosegregation of the ts phenotype and kanamycin resistance, indicating the intragenic mutation(s) within the *ndc80* locus are responsible for the ts phenotype. But one mutant, ts*13*, was ruled out after the backcrossing because the ts phenotype and kanamycin resistance was not correlated, suggesting responsible mutation(s) other than those in *ndc80* might exist extragenically in this mutant.

2.4 Initial characterisation and classification of isolated *ndc80* mutants

To aid the further classification and selection from my mutant list, I set up several characterisation criteria to examine those mutants, including the cellular morphology, the serial dilution spot assay of temperature-sensitivity and TBZ-sensitivity (thiabendazole, a microtubule poison), the growth curve and, most importantly, the kinetochore localisation of the Ndc80 complex at the restrictive temperature. The results are summarised in Table 2.1. For clarity, only the sequenced alleles were included in the table.

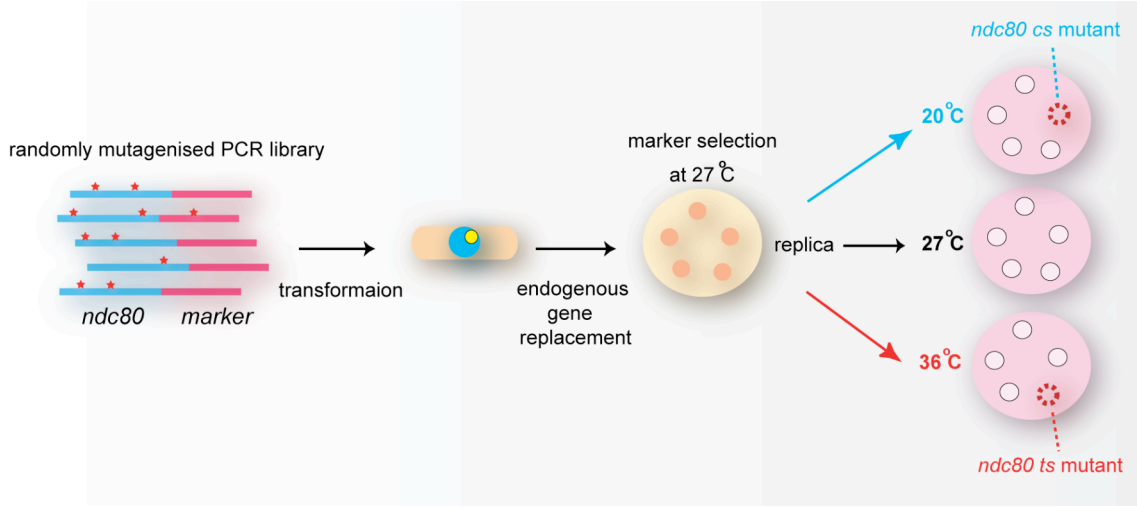

Figure 2.3 The procedure of temperature-sensitive mutant isolation.

The randomly mutagenised PCR pools were transformed into a strain tagged with either Nuf2-YFP or Spc25-YFP. The transformants were grown on the YE5S plate for 1 day at 27℃ to allow the homologous recombination occur more completely. The plate was then replica plated onto a YE5S plate containing the selection drug (kanamycin in my screening), and left growth for 4 days at 27℃. After the colonies formed at 27℃, the transformants were replica plated again onto three identical YE5S plates containing Phloxin B. These three plates were incubated at different temperatures as indicated. When a colony could grow at 27℃ but not at 36℃, it was assigned as the ts mutant; on the other hand, when the colony could not grow at 20℃, this transformant was assigned as a cs mutant.

Table 2.1 Summary of initial assessments for the *ndc80* mutants

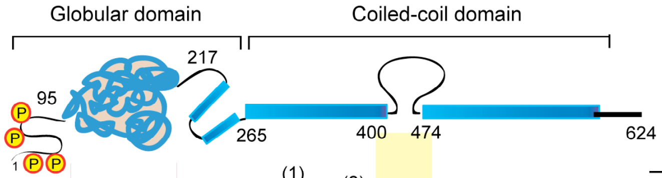

Mutant	Mutations [(1), (2)]	Morphology (3)	Sensitivity (spot test): Temperature (4)	Sensitivity (spot test): TBZ (5)	Growth Curve (6)	YFP signal (wt as 100%): Spc25-YFP	YFP signal (wt as 100%): Nuf2-YFP
ts-03	**L336P* (green)	L/c	–	S	±	83%	
ts-20	***T23I* (Aurora B site?), *M308T*	N/L	±	S	±	88%	
ts-21	*T307A*, **E379G*, *L405P*	L/B/c	–	S	–	>95%	
ts-24	***A424D*, *Q560R*	L/C	±	N	+	>95%	
ts-26	*L485P*, ***L605S*	L/B/c	–	S	±		59%
ts-31	*F132L*, ***N281D* (Nuf2 binding), *N421H*	L	±	R	+	>95%	
ts-34	*S317P* (green), *I406V*	L/B/C	–	S	±		86%
ts-36	*V79A*, *R137G* (MT binding), *K416E*, **S517P* (green)	N	±	S	±	84%	
ts-102	*K459R*, ***L591P*	L/B/C	–	N	±		25%
cs-01	*L556P*	L/B	–	S	±	>95%	
cs-05	*L599Q*	N/L/B	±	R	±	>95%	

(1) * or ** marks the conserved residues among different speices.

(2) The green color marks the residues that interrupt the coiled-coil score for more than 50%.

(3) Morphology: L, longer; N, normal; B, branch; C, curve; c: cut.

(4) Temperature sensitivity: -, strong; ±, modest.

(5) TBZ sensitivity: S, sensitive; N, normal; R, resistant.

(6) Growth curve: +, >2 doublings; ±, >1 doubling; -, <1 doubling.

2.4.1 Cellular morphology

I first observed their cellular morphologies after grown on the YE5S+Phloxin B plates at 36℃ for 1 day. Like many other mitotic mutants, most of the *ndc80* mutants showed severe morphological defects. For example, cells appeared longer, branched, and curved or banana shape (Table 2.1). The cut phenotype, in which cytokinesis happened in the absence of normal nuclear division, was also often seen. However, some mutants (*ts-20*, *ts-36*, *ts-101 cs-05*) looked generally normal under a conventional light microscope, indicating the temperature sensitivity was modest and the defect might be relatively mild. This is nevertheless reminiscent of some of the *mis* mutants, another class of mitotic mutants that cause minichromosome instability (Takahashi et al., 1994).

2.4.2 Temperature and TBZ sensitivity

To reveal the differences between *ndc80* mutants regarding the degree of temperature sensitivity, a serial dilution spot assay was performed on YE5S+Phloxin B plates. 5 x 10^4 cells were spotted on the first line and ten-fold dilutions were applied serially. Based on the spot assay result, I classified the *ndc80* mutants into three categories: Normal (+): *ts-35*; Moderate (±): *ts-10, 20, 22, 24, 31, 36, 125* and *cs-05, 10, 108, 119*; Strong (-): *ts-02, 03, 21, 26, 27, 29, 34, 101, 102, 129, 133, 138, 139* and *cs-01, 02, 12, 125, 130, 137* (Figure 2.4 and Table 2.1).

As the Ndc80 complex has been shown to be involved in microtubule capture during mitosis, I utilised the same method to assess the sensitivity of the *ndc80* mutants against a microtubule depolymerising agent, TBZ (thiabendazole). This assessment is informative because many mutants that interfere with microtubule function are either sensitive or resistant to TBZ. The spot assay was conducted on YE5S plates containing 5, 10, 15, or 20 μg/ml of TBZ at 27℃. *ndc80* mutants exhibited different growth rates upon TBZ treatment. Like other kinetochore mutants or mutants of several important microtubule-associated proteins that comprise the kinetochore-microtubule

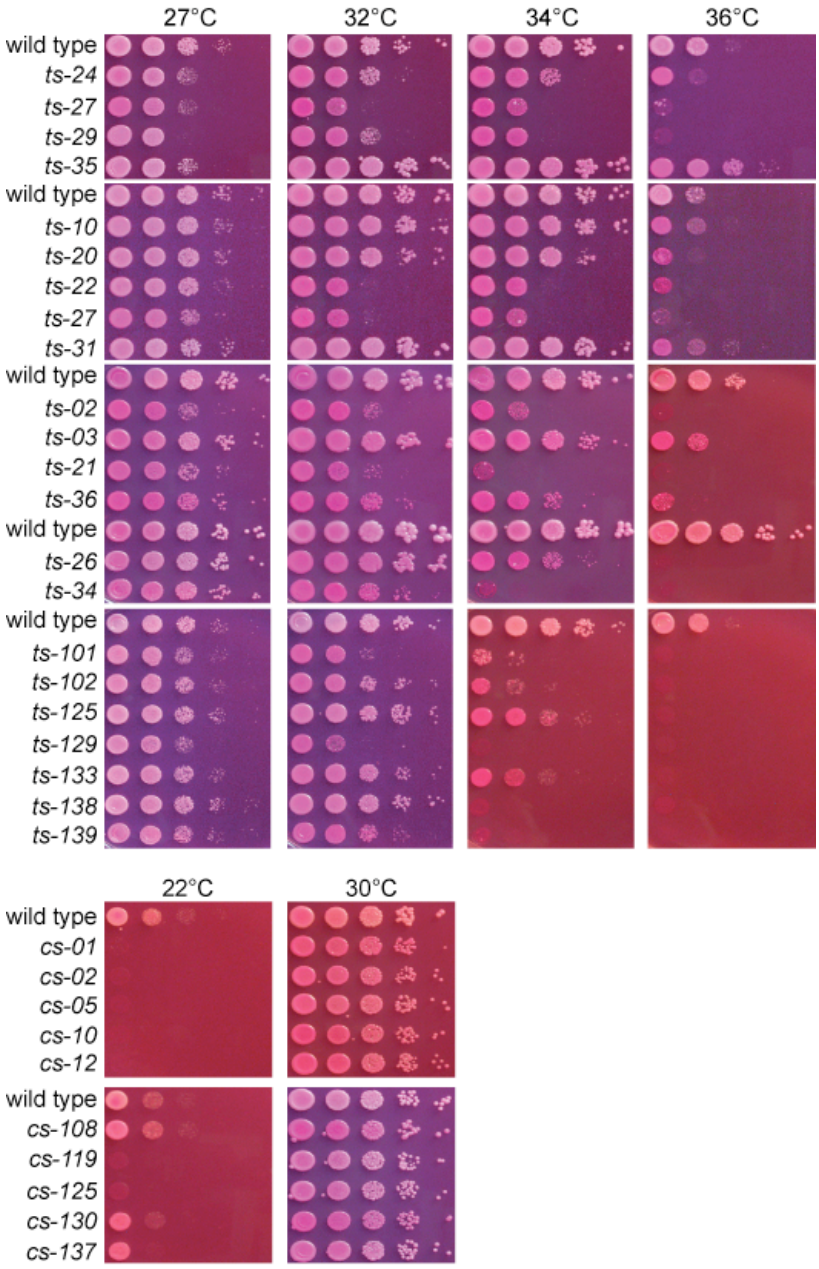

Figure 2.4 Temperature sensitivity of the *ndc80* mutants.

Serially ten-fold diluted cells (5 x 10^4 cells in the first line) were spotted on YE5S plates containing Phloxin B dye. The plates were incubated 3 or 4 days at the indicated temperatures.

interphase (e.g. Δ*mal3*, Δ*dis1,* Δ*alp14*, or Δ*dam1*) (Ohkura et al., 1988, Garcia et al., 2002a, Beinhauer et al., 1997, Aoki et al., 2006, Sanchez-Perez et al., 2005), many *ndc80* mutants exhibited TBZ sensitivity phenotype. With respect to TBZ sensitivity, the *ndc80* mutants were classified into three categories: Normal (N): *ts-10, 24, 27, 29, 35, 101, 102, 125, 133* and cs-*119, 125, 137*; Resistant (R): *ts-31, 138* and *cs-05*; Sensitive (S): *ts-02, 03, 20, 21, 22, 26, 34, 36, 129, 139* and *cs-01, 02, 10, 12, 108, 130* (Figure 2.5 and Table 2.1). Compared to wild type, some mutants were rather resistant to TBZ; nevertheless, it is also not unreasonable to obtain such "gain of function" mutants in my screening, by which the *ndc80* mutations may keep the kinetochore microtubules hyper-stable. Consistent with this assumption, a special case has been reported that microinjection of anti-Ndc80 N-terminal antibody (9G3) into PtK1 cells stabilises kinetochore microtubules (DeLuca et al., 2006). Furthermore, mutants of other microtubule-associated proteins, like Δ*klp5*, Δ*klp6*, or Δ*dam1-A8*, also show similar TBZ-resistant phenotypes (West et al., 2001, Griffiths et al., 2008). These data reinforce the important role of Ndc80 in kinetochore-microtubule attachments, and perhaps potentially link Ndc80 with other microtubule-associated proteins in a coordinated network that modulates microtubule attachment and dynamics.

2.4.3 The growth curve

To confirm the molecular defects of *ndc80* mutants on cell cycle progression, I determined their growth curves at both permissive and restrictive temperatures. Cells were grown in YE5S liquid cultures overnight at 27℃ for the ts mutants and 32℃ for the cs mutants (permissive temperatures). The cultures were diluted into 2 x 10^6 cells/ml to allow the cells to grow from early exponential phase, as time 0. Soon after the dilution, the cultures were split equally into two flasks; one was continuously incubated at the permissive temperature, and the other immediately shifted to the restrictive temperature (36℃ for the ts mutants and 19℃ for the cs mutants). The cell concentration was monitored over time. In the wild type cells, there were almost three doublings within 8 hr at 36℃, and

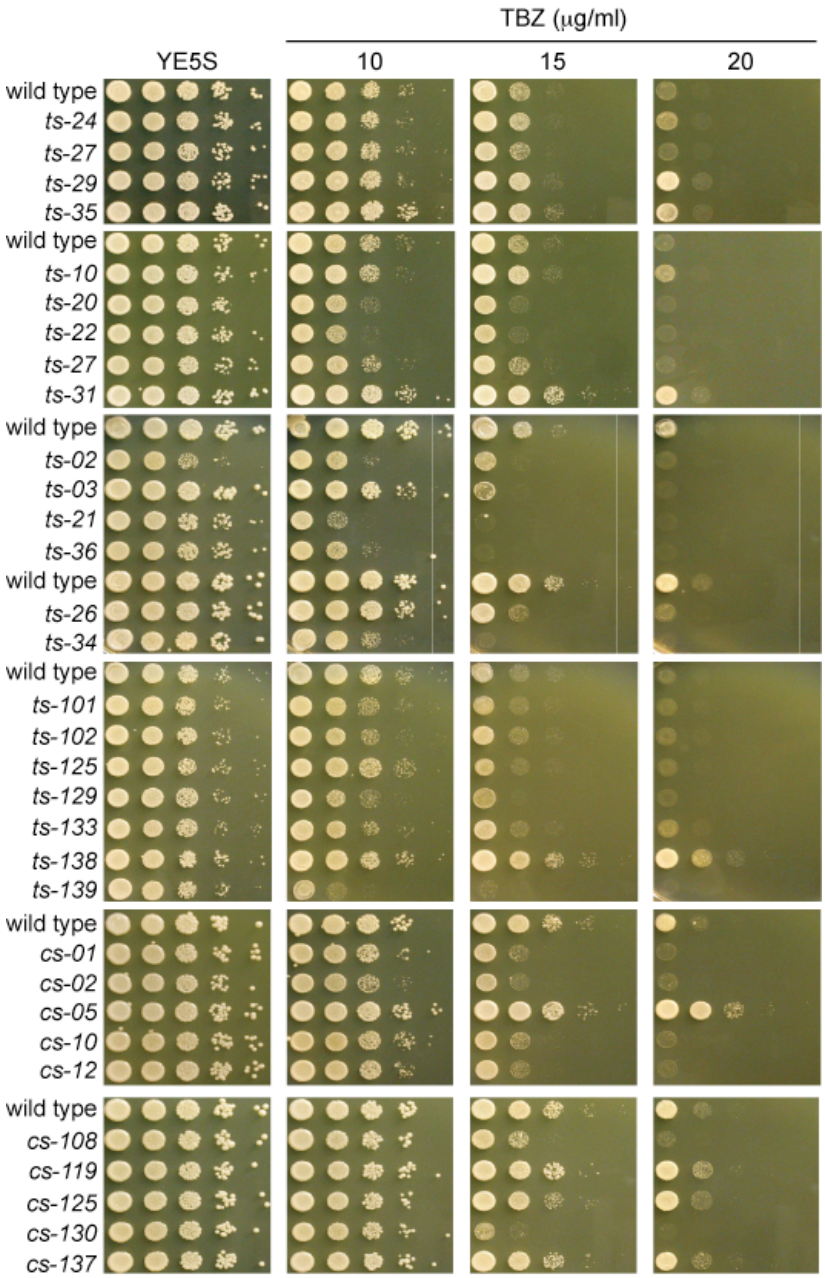

Figure 2.5 TBZ sensitivity of the *ndc80* mutants.

Serially ten-fold diluted cells (5 x 10^4 cells in the first spot) were spotted on the YE5S plates with various concentrations of TBZ (0, 10, 15, and 20 μg/ml). The plates were incubated 3 days at 27℃ for the ts mutants and at 30℃ for the cs mutants.

four doublings within 24 hr at 19℃. In contrast, most *ndc80* mutants showed different degrees of growth defects at restrictive temperatures. Compared to the wild type cells, most of the ts mutants only passed one or two rounds of the division cycle (one to four rounds for the cs mutants) at end point of the measurement, suggesting the essential role(s) of *ndc80*$^{+}$ in cell cycle progression. I classified these mutants by the number of cycle passages within 8 hr at 36℃ (ts) or shift-down for 24 hr at 19℃ (cs): Mild (+, >2 cycles): *ts-10, 22, 24, 29, 31* and *cs-108, 119, 125, 130, 137*; Moderate (±, >1 cycle): *ts-02, 03, 20, 26, 27, 34, 35, 36, 101, 102, 125, 129, 133, 138, 139* and *cs-01, 02, 05,12*; Strong (-, <1 cycle): *ts-21* and *cs-10* (Table 2.1). The representative growth curves from each category are shown in Figure 2.6.

2.4.4 Signals of the Ndc80 complex at the kinetochores

Last, as the Ndc80 protein forms a complex with other three proteins largely by coiled tethering, it is important to know whether mutation(s) in *ndc80* mutants interfere with the overall Ndc80 complex formation and the complex localisation at the kinetochore. To address this question, the mutant cell tagged with Nuf2-YFP or Spc25-YFP was collected after temperature shift-up for 6 hr (for the ts mutants) or 24 hr (for the cs mutants). The sample cells were immediately fixed with 1.6 % paraformaladehyde, followed by washing with phosphate buffered saline (PBS). The Nuf2-YFP or Spc25-YFP signal was then observed with the stained DNA (by DAPI) under a fluorescence microscope (Volocity, Improvision Co.). Indeed, mutants exhibited various degrees of the signal retention at the kinetochore dots. Some of them kept the signals in almost all the cells, and some dramatically lost their YFP signals. Based on the percentage of YFP signal-positive cells in the whole population, I classified the *ndc80* mutants into three categories: +, signal remained (>75% of the cells remained clear YFP signals at the kinetochore): *ts-03, 20, 21, 22, 24, 25, 31, 34, 35, 36, 125* and all the *cs* mutants; ±, in-between (25-75% of the cells remained clear YFP signals at the kinetochore): *ts-02, 10, 26, 27, 129, 133, 138, 139*; −, signal lost (<25% of the cells remained clear YFP signals at the kinetochore): *ts-101, 102* (Table 2.1) (Figure 2.7).

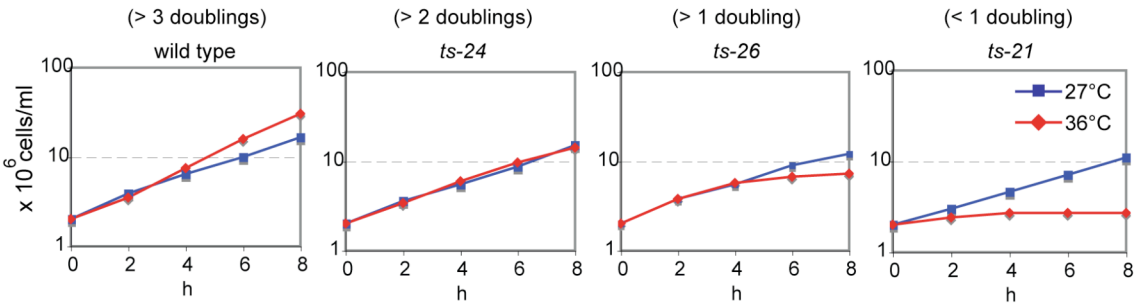

Figure 2.6 Representative growth curves of the *ndc80* mutants.

Overnight grown cultures in the YE5S liquid media were diluted into two identical flasks to the final volume of 20 ml (2 x 10^6 cells/ml). One of them immediately shifted the temperature up to 36℃; another one kept growth at 27℃. The cell concentration was monitored every two hours.

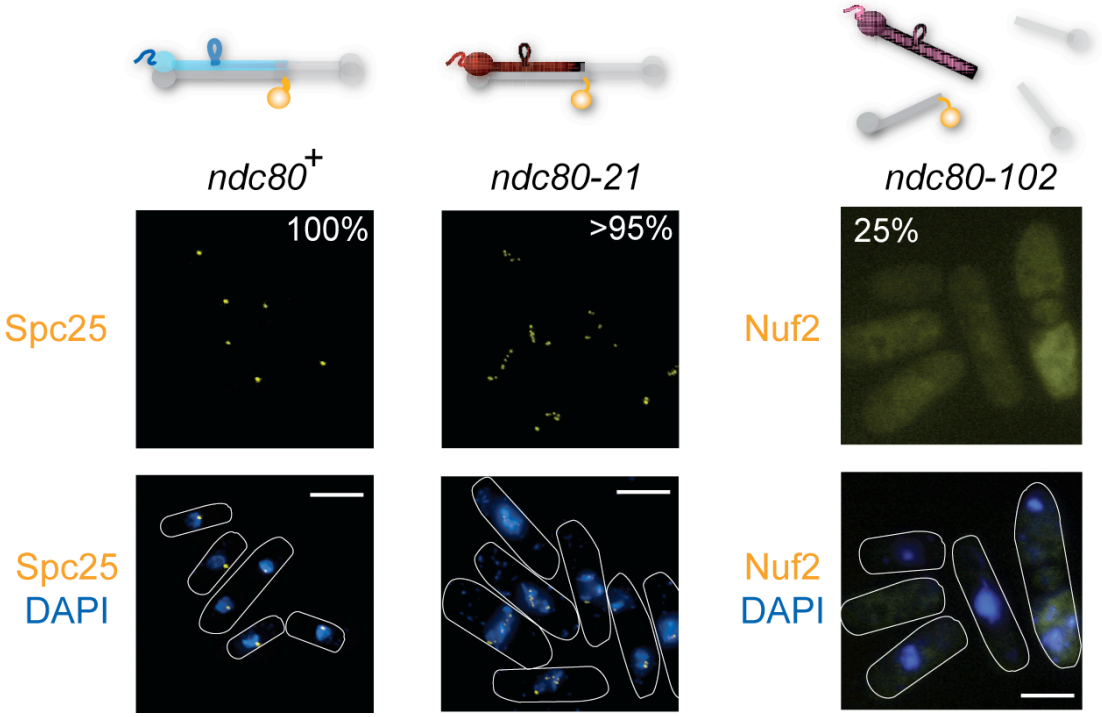

Figure 2.7 Nuf2-YFP or Spc25-YFP signals in the *ndc80* mutants.

After 6 hr incubation at 36℃, the cells were fixed with 1.6% paraformaldehyde for 10 min at room temperature, followed by 2 x PBS wash. The samples were stained with DAPI and observed under an immunofluorescence microscopy (Volocity, Improvision Co.). Scale bar, 5 μm.

Judged from several parameters that had been assessed on my mutant list, I decided to pick up the alleles that showed relatively strong temperature-sensitivity and kinetochore retention of the Ndc80 complex, for further sequencing analysis of the mutation sites. That is, *ts-03, 20, 21, 24, 31, 34, 36,* and cs-*01, 05*. I also picked up mutant alleles that lose Ndc80 complex integrity moderately (*ts-26*) and severely (*ts-102*).

2.5 Sequencing of *ndc80* mutants

To get a better understanding of which domain is malfunctioning in each *ndc80* mutant, I sequenced these eleven mutant alleles. Results are also summarised in Table 2.1. Three mutant alleles contained only one mutation: L336P (leucine mutated into proline) in *ts-03*, L556P in *cs-01*, and L599Q (leucine mutated into glutamine) in *cs-05*. Another three mutants contained mutation(s) in the N-terminal globular domain, by which Ndc80 directly interacts with microtubules. T23I (threonine mutated into isoleucine) in *ts-20* allele is a highly conserved residue that has been predicted as a potential Aurora B phosphorylation site. R137G (arginine mutated into glycine) in *ts-36* is parallel to human Ndc80 K123 (lysine), which has been demonstrated as a physical interacting point toward the acidic C-terminal tail of tubulins (Ciferri et al., 2008). I postulate this mutation may directly affect the microtubule binding in these mutants.

ts-26 and *ts-102* that moderately and extensively lost the Nuf2-YFP signals each contained two mutations in the C-terminal region. Mutations in the very end of Ndc80 (L605S in ts-*26* and L591P in *ts-102*) presumably affected the whole heterotetramer intra-connection in this region (Wei et al., 2005, Ciferri et al., 2005, Maiolica et al., 2007). However, many mutants also contained mutations in the coiled-coil domain. Since the mutants I selected were largely based on the kinetochore retention of the Ndc80 complex, this finding was unexpected. Although many of the C-terminal mutations do not alter the coiled-coil configuration dramatically (judged by the coil scoring, not shown), some did

severely abolish the coiled-coil structure (residues that affect the coil score more than 50% are considered “severe” and labeled in green in Table 2.1). This would probably be the case for *ts-03*, *34*, and *36*. Furthermore, in the *ts-31* allele, N281D (asparagine mutated into aspartic acid) is highly conserved and the corresponding residue in human Ndc80 has been implicated into direct interaction with human Nuf2 protein (Ciferri et al., 2008), suggesting formation of the Ndc80-Nuf2 subcomplex might be interfered in this mutant. Nevertheless, It is not unreasonable to postulate that in addition to the structural role in tethering with Nuf2, Spc24, and Spc25, there may be some undiscovered function(s) of Ndc80 relying upon the long coiled-coil region. Very interestingly, when I compared the mutation sites in different alleles, I found that many of them resided within an uncharacterised internal loop (aa 400-474) between the two coiled-coil regions. Mutations within this loop apparently do not interrupt the coiled-coil score prediction (not shown), suggesting that these mutations do not affect the complex tethering. Although two putative models have been proposed to illustrate the internal loop function, namely the fine-tuning mode and the tension traducing/sensing model (Wang et al., 2008, Wan et al., 2009), detailed examinations for these hypotheses are lacking, and so far no physiological or functional evidence is available to delineate the molecular role of this internal loop *in vivo*. However, many mutants contain at least two mutations, and it remains to be further verified which mutation is the most crucial one in a given mutant allele.

From the sequencing result, I identified several interesting mutation sites that might be directly involved in microtubule binding, and presumably Aurora B regulation, and most interestingly, I noticed that the uncharacterised internal loop is a hot spot where mutations frequently occur, and the *in vivo* function of this loop remains elusive.

2.6 Snap shot images of *ndc80* mutant phenotypes

To further characterise the defective phenotypes, I tagged the *ndc80* mutants with GFP-Atb2 (α2-tubulin), Mis6-2mRFP (a kinetochore marker) and Cut12-CFP (an SPB marker), and observed microtubule morphologies and localisation of the kinetochore and SPB components. Since the cold-sensitive mutants require longer incubation time for the phenotype appearance, I decided to analyse only the ts mutants. The mutant cells were exponentially grown in YE5S liquid cultures at 36℃ for 4 hr. While cells were collected, they were immediately fixed with 3.2% paraformaldehyde and 0.3% glutaldehyde for 10 min at room temperature. After washing in PBS, the samples were observed under a DeltaVision high-resolution microscope (Applied Precision).

As predicted, all the tested *ndc80* mutants showed massive defects in mitotic chromosome segregation (Figure 2.8). Many kinetochore dots were unevenly distributed to the two poles and some of them were far away from the spindles or the SPBs in mid-mitosis. Lagging chromosomes were also seen in late anaphase in some mutants. All the patterns were ascribable to its established role in proper kinetochore-microtubule attachments. However, I noticed that in *ndc80-21*, cells exhibited a very severe spindle defect such that the mitotic spindle became extremely short around the spindle pole body. Apparently the integrity of spindle microtubules could not even be maintained, indicating that microtubule stability was disrupted in this mutant. This observation was in agreement with the TBZ sensitivity profile, in which *ndc80-21* was hypersensitive to the microtubule depolymerising agent. This spindle defect was attributed to the malfunction of the Ndc80 protein rather than its delocalisation, since 95% of Spc25-YFP signal was still retained at the kinetochore under the same condition (Table 2.1 and Figure 2.7).

Among those *ndc80* mutants is *ndc80-21* that shows the strong defects in temperature and TBZ sensitivity, the cell growth, and the unstable spindle phenotype without losing Ndc80 complex integrity from the kinetochores. This mutant allele contains three mutations: *T307A*, *E379G*, and *L405P*, where the

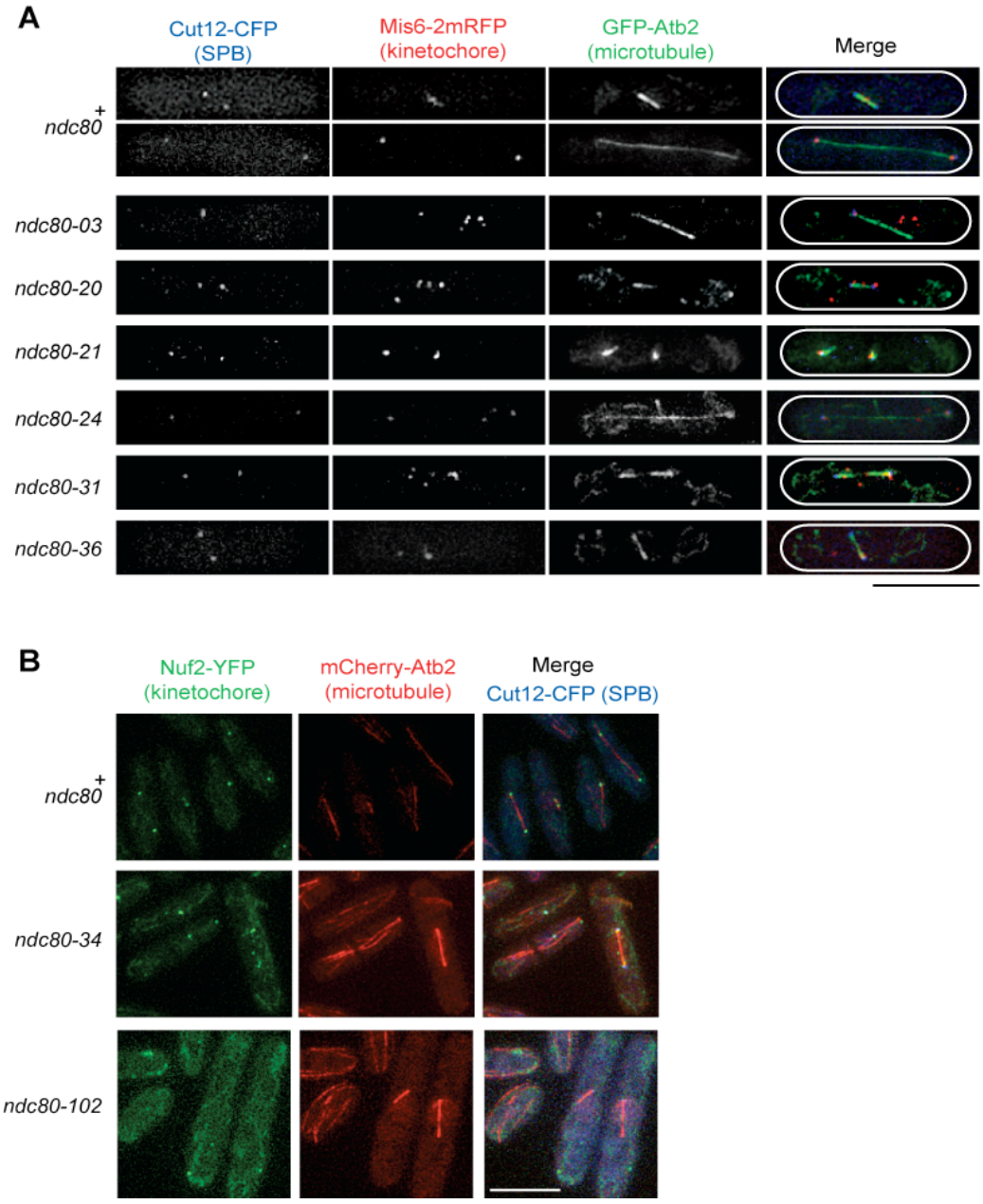

Figure 2.8 Fixed images of the *ndc80* mutants.

Cells were tagged with Cut12-CFP, Mis6-2mRFP, and GFP-Atb2 in (A) or Cut12-CFP, Nuf2-YFP, and mCherry-Atb2 in (B) as an SPB marker, a kinetochore marker, and a tubulin marker, respectively. Cells were incubated at 36℃ for 4 hr before fixation with 3.2% paraformaldehyde plus 0.3% glutaldehyde for 10 min at the room temperature. Images were taken with the DeltaVision high-resolution microscope (Applied Precision). Scale bars, 5 μm.

T307A resides in the first coiled-coil shaft, and *E379* and *L405* locate in the vicinity of and within the mysterious internal loop, respectively. I thus from now on mainly focused on this mutant for most of the time of my PhD study. Nevertheless, I also spent some efforts on another allele showing distinct phenotypes. I will introduce the work done on *ndc80-26* in chapter 5.

2.7 Episomally overexpressing Ndc80 rescues *ndc80-21*

The fact that the ts phenotype and the mutated *ndc80* gene can genetically cosegregate during crossing suggests that the *ndc80* gene is responsible for the defective phenotype. Another way to confirm whether the defective phenotype is exclusively from the mutated gene rather than other mutations hidden in the genome is to reintroduce the wild type gene directly into the mutant. I thus cloned the *ndc80*$^{+}$ gene into an overexpression vector (pREP1) bearing the *nmt1* (no message in thiamine) promoter, namely, the gene expression driven under *nmt1* is induced or repressed in the absence or presence of thiamine, respectively (Maundrell, 1993). The pREP1-*ndc80*$^{+}$ plasmid or empty vector was introduced into a wild type strain and an *ndc80-21* mutant. The resulting clones were plated onto YE5S or selective medium plates with or without thiamine, and incubated for 2 to 3 days at 27℃ or 36℃. As expected, episomally expressing Ndc80 wild type proteins fully suppressed the temperature sensitivity of *ndc80-21* either in the presence of thiamine (YE5S) or without thiamine (EMM-T) (Figure 2.9). Taken together, these two pieces of evidence strongly indicate the mutated *ndc80* gene in *ndc80-21* is the sole cause for temperature sensitivity.

2.8 The mutant Ndc80 protein is not significantly reduced in *ndc80-21*

It can be envisioned that when the proteins are not properly folded into the

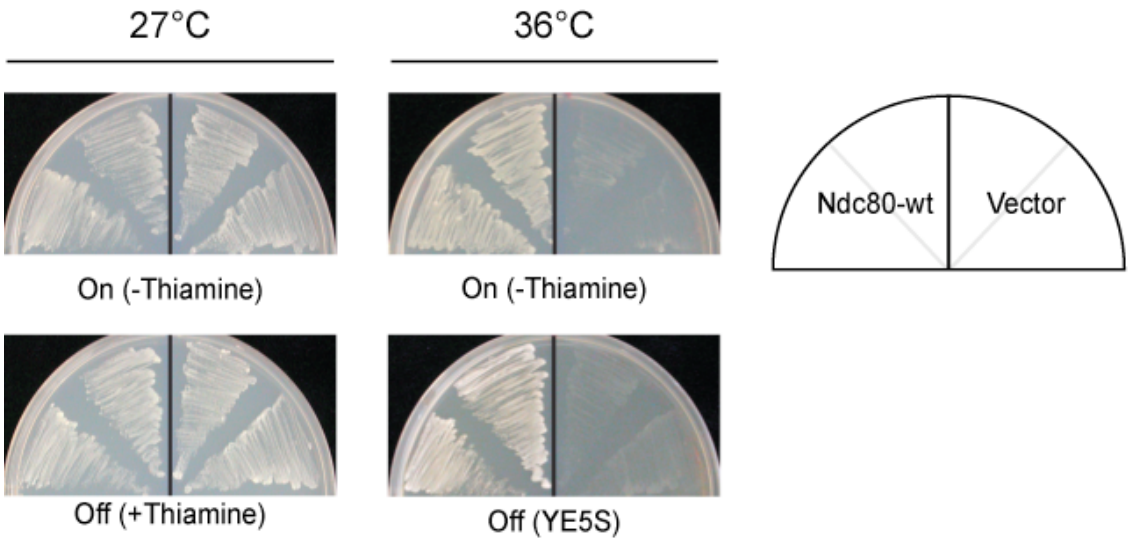

Figure 2.9 pREP1-Ndc80 suppresses *ndc80-21*.

The pREP1 plasmid bearing a wild type Ndc80 or the vector alone was episomally introduced into an *ndc80-21* strain. Two independent resulting transformants were streaked out on YE5S medium plates or Edinburgh minimal medium (EMM) plates with or without thiamine. These plates were grown at different temperatures as indicated.

native conformation, for a quality control reason they may be quickly destroyed by proteasome-mediated degradation. In order to check whether mutant Ndc80 proteins in *ndc80-21* are down regulated at the restrictive temperature, I then sought to produce an anti-Ndc80 polyclonal antibody, both for the current usage and for its potential applications in the future.

To achieve this, I cloned and expressed the Ndc80 proteins in *E. coli* FB810. The *ndc80*$^{+}$ fragments were PCR amplified from the wild type cDNA library, and then cloned into the pET-14b vector, in which the construct is designed to be N-terminally His-tagged. The expression of the full-length construct could be appreciated under 2hr incubation with 1 mM IPTG at 37℃ (not shown). However, when the construct plasmid was sent to the Protein Isolation Laboratory at Cancer Research UK London Research Institute, the large-scale production of Ndc80 protein was not successful.

A polyclonal antibody was then produced externally by Eurogentec. Two oligopeptides, corresponding to ^{94}IKDPRPLSDRRYQQEC^{109} and ^{523}RETASEEKNAFDAE^{536}, were synthesised and mixed together as an antigen pool to immunise two rabbits at the same time. The resulting sera from these two rabbits were merged and purified through different affinity columns that coupled either oligopeptide. To test the antibody specificity and at the same time to examine the protein level in different strains, I collected the cell extracts from the Ndc80 wild type cells, the Ndc80-GFP tagging cells, and the *ndc80-21* mutant cells. All these cells were incubated at 36℃ for 4h before harvest. The cell extracts were separated by SDS-PAGE and transferred onto a PVDF membrane, followed by immunoblotting with either purified antibody. Only one antibody (EP081971), which recognises ^{523}RETASEEKNAFDAE^{536}, could faintly detect the endogenous Ndc80 band, although the antibody titre seemed to be low and the specificity was not as great as wished. Importantly, compared to the wild type cells, the amounts of the mutant Ndc80 proteins in *ndc80-21* did not significantly reduce, even after 4hr incubation at the restrictive temperature (Figure 2.10). These data suggest mutations in *ndc80-21* do not trigger the protein degradation, and this is consistent with the previous fluorescent

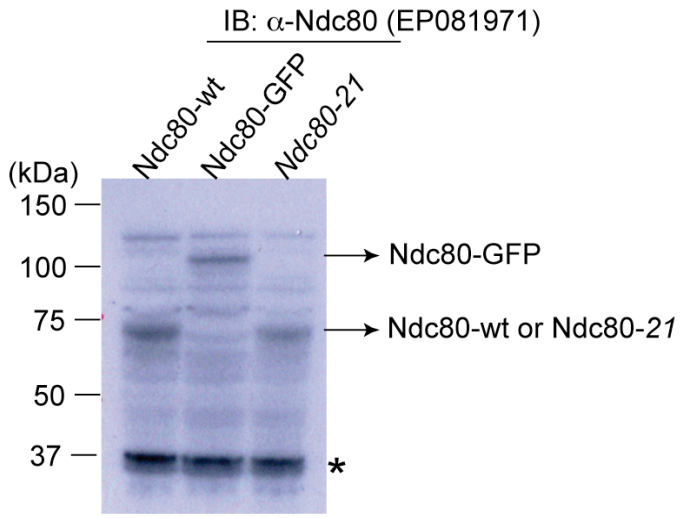

Figure 2.10 The mutant protein is not significantly reduced in *ndc80-21*.
20 ml of exponentially grown cultures were incubated at 36℃ for 4h. The proteins were extracted by a quick alkaline method. Briefly, the cells were treated with 0.3N NaOH at RT for 10 min. The pellets were dissolved in 1x sample buffer and boiled for 5 min before separating by SDS-PAGE. After transferring to a PVDF membrane, the proteins were immunoblotted with a polyclonal anti-Ndc80 antibody (EP081971) at 1:100 dilution. Asterisk labelled non-specific bands acted as loading controls.

counting that >95% of the *ndc80-21* cells remain the Spc25-YFP signals at their kinetochores (Table 2.1).

2.9 Overall integrity of the Ndc80 complex in *ndc80-21*

The Ndc80-Nuf2 subcomplex interacts with Spc24-Spc25 subcomplex in their coiled-coil domains and exposes the Ndc80 N-terminus to the outward space for microtubule binding (Wei et al., 2007, Maiolica et al., 2007, Ciferri et al., 2008). However, it is not clear how exactly these four proteins localise to the outer kinetochore, *i.e.* either the four subunits assemble all together as a unit then load on to the kinetochore, or Ndc80-Nuf2 conjoins sequentially after Spc24-Spc25 hitches the Spc7/Mis12 complex.

I have shown that Spc25-YFP signals in *ndc80-21* remained at the kinetochore. From these data I postulate the whole heterotetramer of Ndc80 complex in this mutant stays at the kinetochores as stably as in wild type cells. However, if sequential assembly were the case, it would be less convincing to argue overall complex integrity only by observing Spc25-YFP at the kinetochores.

To address this point, I tagged the *ndc80-21* strain with Nuf2-YFP. The same experimental procedure was conducted to evaluate the kinetochore YFP signals. From this observation I found that Nuf2-YFP was also intact, as >95% of the cells retained the Nuf2-YFP signals at the kinetochore dots (Figure 2.11A). In a parallel experiment, I observed a strain previously exhibiting low Nuf2-YFP signals, *ndc80-102*, which was then double-tagged with Nuf2-YFP and Spc25-YFP. Compared to the strain with a single tagging (Nuf2-YFP alone), I found the double-tagging (Nuf2-YFP & Spc25-YFP) strain exhibited a similar degree of the signal loss from the kinetochores (Figure 2.11B), suggesting that the whole Ndc80 complex simultaneously disassembles from its niche.

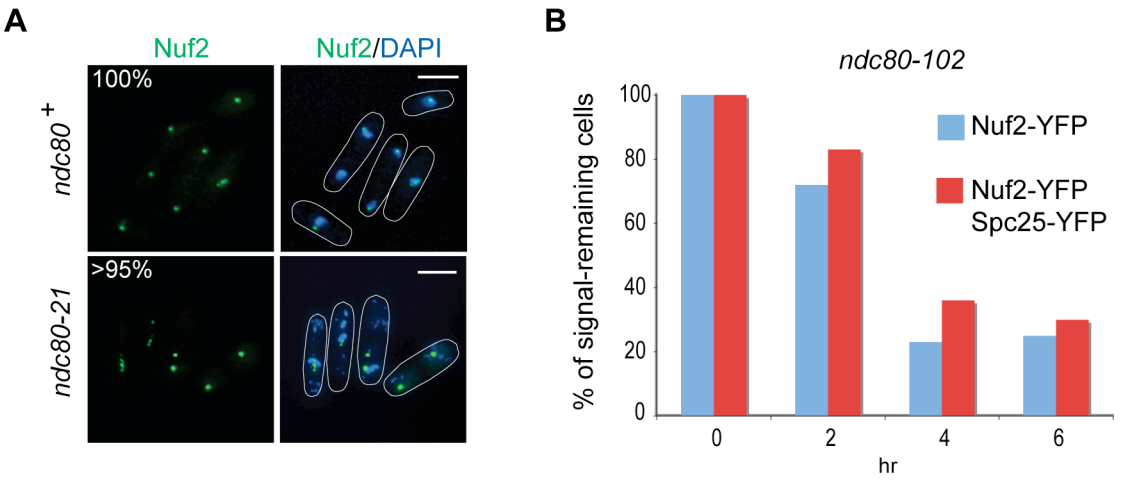

Figure 2.11 The whole Ndc80 complex assembles onto the kinetochores in *ndc80-21*, but entirely disassembles in *ndc80-102*.

(A) The fluorescent signals were observed and counted after incubation at 36℃ for 4 hr in wild type and in *ndc80-21*, and (B) for 0, 2, 4, and 6 hr in *ndc80-102* with different backgrounds. Scale bar, 5 μm.

Collectively, these data indicate the whole Ndc80 complex is maintained at the kinetochores in *ndc80-21*. These also argue that the four Ndc80 complex subunits form a complex at once to load onto the kinetochores, and also disperse at the same time from the KMN network in the *ndc80-102* mutant.

2.10 Summary

In this chapter I first describe the essentiality of the *ndc80*$^{+}$ gene, followed by a temperature-sensitive mutant screening and isolation. From two sets of independent screenings, I have isolated 22 ts and 10 cs mutants. Initial assessments done in those mutants include the cell morphology observation, the degree of temperature sensitivity and sensitivity against TBZ, patterns of the growth curve, and the Ndc80 complex localisation at the kinetochores. Sequencing analysis reveals that each mutant contains either single or multiple point mutations in various domains (i.e. N-terminal region, coiled-coil regions). Notably I have also found the internal loop as a hot spot area where the mutations have been frequently identified, implying an important yet unclear role for this loop for Ndc80 function. The fixed image examination confirms the mitotic role of Ndc80 in chromosome segregation, and importantly, reveals a strong mutant allele (*ndc80-21*) that is severely defective in spindle microtubule stability. Based on these parameters, I decided to focus on *ndc80-21* for further analysis. This mutant allele can be fully complemented by episomally expressing Ndc80, suggesting the intragenic mutation(s) in the *ndc80* locus is responsible for the defect. Furthermore, a polyclonal anti-Ndc80 antibody was produced, and amounts of the mutant Ndc80 proteins detected by this antibody are not reduced in *ndc80-21*, consistent with the conclusion that the overall integrity of the Ndc80 complex is intact at the kinetochores.

2.11 Discussion

As predicted, *ndc80*$^{+}$ is essential in fission yeast, and most likely essential in all living organisms. Despite its extensive studies in other organisms, close investigation of the *ndc80*$^{+}$ function is somehow lacking in the *S. pombe* cells. In budding yeast, several ts mutants of the Ndc80 complex were isolated, and all of them exhibited chromosome mis-segregation during mitosis (Osborne et al., 1994, Wigge et al., 1998, Janke et al., 2001, Wigge and Kilmartin, 2001, Le Masson et al., 2002, Montpetit et al., 2005). However, integrity of the whole complex was not examined (at least never been shown) for these alleles, imposing the concern that some of them may be complete loss-of-function.

Given the potential multiple roles of Ndc80, I specifically focus on the mutant that retains the ability for its complex formation at the kinetochores. To dissect the Ndc80 function specifically on microtubule dynamics, I expected to obtain many mutants that bear N-terminal mutations, the region of which is known for direct microtubule binding but not for the whole complex integrity (Cheeseman et al., 2006, Ciferri et al., 2008). The sequencing results are surprising to some extent, for only few N-terminal mutations are identified within those mutants sequenced. One possibility is that during the introduction of the random mutagenic PCR pools into the cells, the probability of the homologous replacement in the N-terminal region is principally lower than the rest of the gene. Alternatively, despite its crucial role in microtubule direct binding, the N-terminal mutations may not cause the temperature sensitivity, by which the judgment of my mutant isolation is made. Screening by the TBZ sensitivity may be an alternative way to isolate certain desired mutants. On the other hand, since the mutants I selected for sequencing are largely retaining the kinetochore localisation, many mutations are unexpectedly locating within the C-terminal part of the Ndc80 protein. At this stage it was difficult for me to firmly rule out the possibility that some of the mutations might slightly loosen the stiffness of the whole Ndc80 complex structure by interfering with the coiled-coil conformation without losing its kinetochore localisation activity. It is likely the case in *ts-03, 34,* and *36*, in which the Ndc80 complex structure may be locally

compromised, although it does not entirely interrupt the whole complex at the kinetochores.

Another unexpected result from sequencing is the hot spot internal loop, for which defined mechanistic roles have been suggested during the course of my project (Wang et al., 2008, Wan et al., 2009). However, the *in vivo* significance has not been carefully delineated. It is interesting that *ndc80-21*, a promising mutant allele that exhibits dramatic unstable spindle phenotypes also contains mutations within or close to the loop. This coincidence thus potentially links the uncharacterised loop to microtubule dynamic regulation.

The formation of stable Ndc80-Nuf2 subcomplexes precludes the purification of Ndc80 protein alone in *E. coli*. Coexpression seems to be required for the *in vitro* reconstitution. Indeed, when I coexpressed the short version of Ndc80 (aa 1-370) and Nuf2 (aa 1-254), this “mini” subcomplex could be copurified even after several purification steps, including the affinity column, ionic exchange column, and gel filtration, implying a very tight interaction between these two proteins (not shown) (Wei et al., 2007). *In vivo*, it is unknown how the Ndc80 heterotetramer loads onto the kinetochores. It can be perceived either two subcomplexes sequentially assemble, or heterotetramer forms before localising at the kinetochores. My data seem to favour the latter hypothesis (Figure 2.7 and 2.11). Consistent with this, a structural study of the whole Ndc80 complex by cross-linking and mass spectrometry analysis reveals these two subcomplexes extensively entangle with each other in the connecting area (Maiolica et al., 2007). Therefore when the outer Ndc80-Nuf2 subcomplex is disturbed, the inner Spc24-Spc25 subcomplex may also be affected.

Work done in human cancers and the mouse model has found that Ndc80/Hec1 are overproduced in several cancers from patients, and expression levels of this protein seem to correlate with the tumour grade and prognosis (Hayama et al., 2006, Bieche et al., 2011). Overexpression of Ndc80 in mouse even increases the frequency of certain cancer occurrence, imposing its oncogenic and tumourigenic feature (Diaz-Rodriguez et al., 2008). However, I notice that

overexpression of wild type Ndc80 proteins is not toxic to the fission yeast cells, and no conspicuous aberrance is found on the cell growth. The cellular morphology also appears normal under microscopic examination. Whether or not cells proceed the division cycle with a faster rate remains to be seen. Currently I do not look into this further.

Chapter 3. Detailed characterisation of *ndc80-21* reveals a crucial role of the internal loop in microtubule dynamics and stability

3.1 Synchronous Culture analysis of *ndc80-21*

To precisely pinpoint the cell cycle stage at which *ndc80-21* is defective, I synchronised *ndc80-21* cell cultures by using centrifugal elutriation. This method relies solely on a physical separation, without otherwise chemical or genetic interferences introduced to the cells. It thus provides a more natural way to obtain a synchronous cell population that mimics the physiological conditions. This technique is based on manipulation of the balance between a pumping-pushing force and the opposing centrifugal force, both of which are exerted simultaneously on the cells in a centrifugal chamber. Another key factor that makes synchronisation possible is the distinct nature of *pombe* cell size, which varies at different cell cycle stages.

3 litres of exponential cell cultures incubated at 27℃ were pumped into the centrifugal chamber and a stronger centrifugal force was applied. Under this condition, larger sized cells tended to move away from the centre of the spinning rotor, while small early G2 cells with slow sedimentation would accumulate in the front line population close to the exit of the centrifugal chamber. After the partition of early G2 cells from other cell populations, the counteracting pumping force was increased to push out the small early G2 cells from the centrifugal chamber. The collected early G2 cells were then filter concentrated to 150 ml of 4 x 10^6 cells/ml, and the culture was immediately shifted up to 36℃, as time 0. Cell cycle progression was monitored by Calcofluor staining (which stains septa). Cell viability was monitored accordingly at each time point as the synchronous growth proceeded, and meanwhile, chromosome segregation was also observed by DAPI staining.

During 6 hr incubation, wild type cells could proceed through nearly three rounds of the cell cycle without any viability loss (Figure 3.1). In *ndc80-21*, no significant loss of viability was observed within the first 60 min, when the cells stayed in the interphase (G2). However, viability dramatically dropped in the first mitotic division, concomitant with the increase of chromosome mis-segregation. This result clearly demonstrates the indispensability of Ndc80 in chromosome segregation during mitosis, and its non-essential role in interphase.

3.2 Live image analysis of *ndc80-21*

To look into details of the mitotic behaviour of *ndc80-21*, apart from the observation of fixed cells, I carried out time-lapse live image analysis. Exponentially growing cells at 27℃were transferred onto a lectin-coated culture dish and incubated at 36℃ for 30 min in a Deltavision live microscope equipped with a temperature-controlling system. Two key characteristic features of *ndc80-21* were observed from the live image recording: unstable spindle microtubule morphologies and abnormal kinetochore movements.

3.2.1 Unstable spindle microtubule morphologies

In fission yeast, mitosis can be defined into three phases by different spindle lengths: Phase I (<2μm), bipolar spindles start to form (corresponding to prophase and prometaphase); Phase II (~2μm), spindle length keeps constant (prometaphase to anaphase A); Phase III (>2μm), interpolar spindles elongate to push two poles away from each other to the cell tip (anaphase B) (Nabeshima et al., 1998). As shown in Figure 3.2A (the upper panel), the wild type cells formed normal bipolar spindles from two separated poles when they proceeded through mitotic entry. These cells progressed into three distinct phases within 20 min, in which they spent about 2 to 3 min in Phase I, ~8 min in

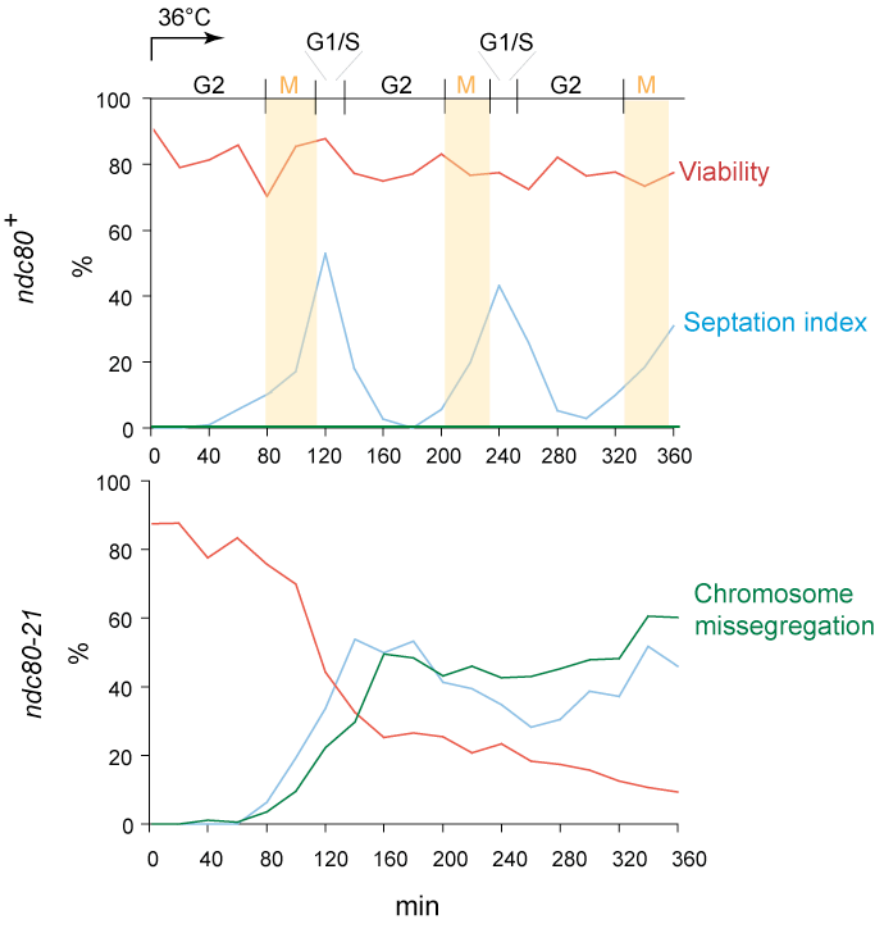

Figure 3.1 Synchronous culture analysis of *ndc80-21*.

Early G2 cells collected from centrifugal elutriation were shifted to 36℃ immediately at time 0. The septation index was used to monitor cell cycle progression. At each time point, the cells were counted and plated onto YE5S plates and incubated at 27℃ for 4 days. Viability was accordingly calculated by the number of colonies formed on the plate divided by the number of cells originally plated.

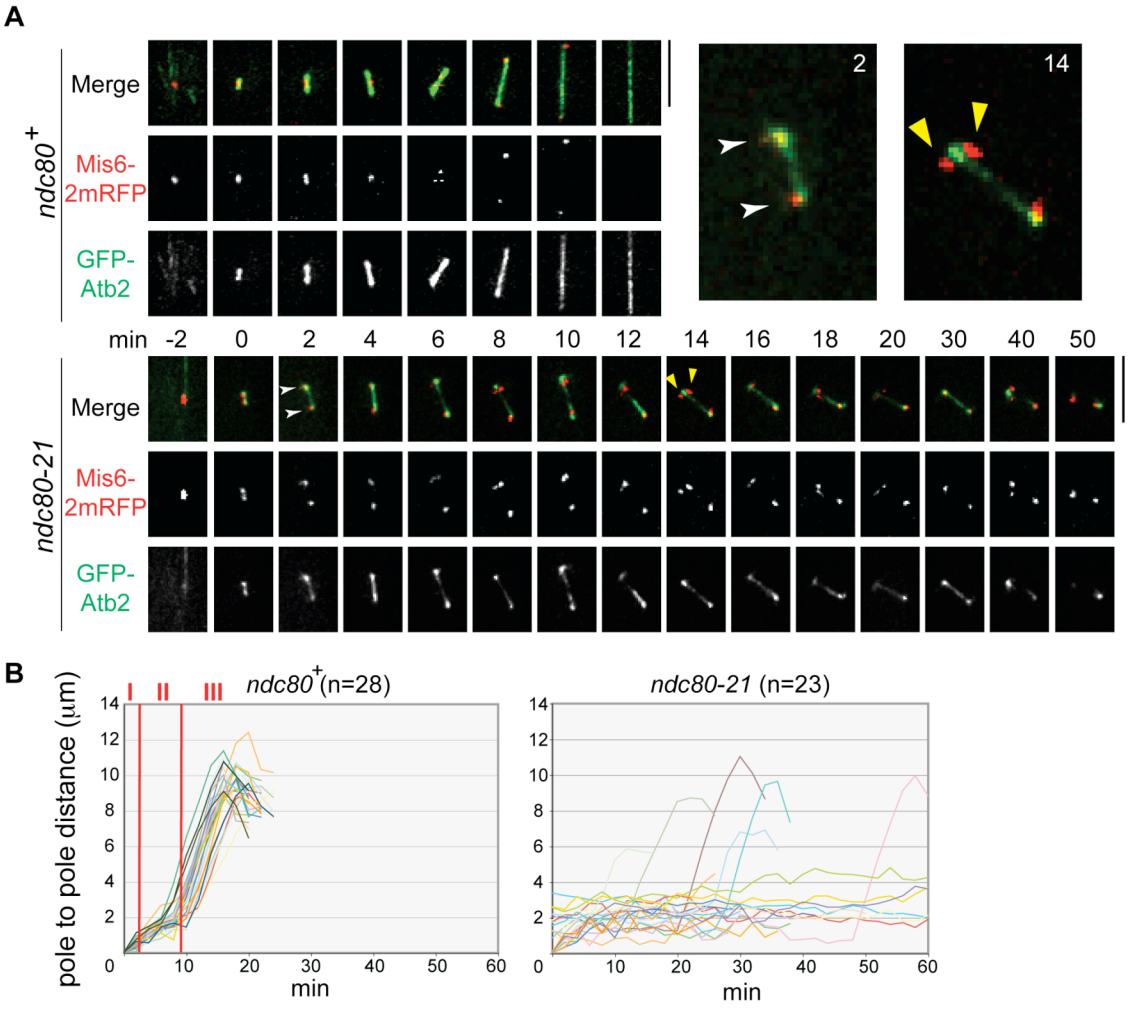

Figure 3.2 Unstable preanaphase spindles and abnormal kinetochore movements in *ndc80-21*.

(A) Time-lapse images of spindle microtubules (GFP-Atb2, α2-tubulin, green) and kinetochores (Mis6-2mRFP, a kinetochore component Mis6 tagged with two copies of monomeric RFP, red) are shown (wild type, top, and *ndc80-21*, bottom, cultured at 36℃ for 30 min). Merged images of two time points (2 min and 14 min) were enlarged in the top right corner. White arrowheads indicate the colocalised kinetochore with spindle poles; yellow arrowheads point out the lost kinetochore from spindle poles. Bars, 5 μm. (B) Profiles of mitotic progression. Changes of the inter-SPB distance are plotted against time in wild type (left, n=28) or *ndc80-21* (right, n=23). A prolonged phase II- mitotic delay was evident in *ndc80-21*.

Phase II, and 6 to 8 min in Phase III (100%, n=28, Figure 3.2B, left). In striking contrast, *ndc80-21* showed a persistently short spindle for more than 50 minutes (74%, 17 out of 23 mitotic cells observed, Figure 3.2A, the lower panel). The spindle length reflects the prolonged mitotic delay, corresponding to the period between prometaphase and anaphase A (Phase II) (Figure 3.2B, right). The microtubule intensity also looked dimmer in this mutant, and the spindle integrity was not constantly maintained. Instead the spindles seemed to collapse (or became very faint in the middle) and reformed several times during the movie period. This result is consistent with my previous observation of fixed images (Figure 2.8), and confirms that the mitotic spindles are extremely unstable in *ndc80-21*. Furthermore, compared to wild type, in which the pole-to-pole distance remained within 2 μm during phase II, the distance in *ndc80-21* appeared longer (Figure 3.2B, right). The distance increment strongly indicates that spindle-kinetochore force is too weak to counteract the interpolar pushing force (Goshima et al., 1999, Appelgren et al., 2003).

3.2.2 Kinetochore movements

In the wild type cells, the kinetochores appeared close to the spindle poles during early prophase/prometaphase, congressed and aligned to the nuclear centre in metaphase, and separated equally towards the opposite poles in anaphase A (Figure 3.2A, the upper panel). In contrast, kinetochore dots in *ndc80-21* seemed to locate in close vicinity of two separated poles during the whole period of the movie (Figure 3.2A, the lower panel). The congression movement was hardly seen in this mutant. I envision that the *ndc80-21* mutation results in destabilisation and shortening of spindle microtubules, thereby kinetochores only weakly attach to spindle microtubules and thus remain localised closely to the spindle poles. Monotelic attachment or even loss of attachment is also evident from the increment of the interpolar distance as mentioned above.

Furthermore, when taking a closer inspection of individual time frames, I found that the kinetochore signals were not always associated with the spindle poles;

instead they often detached from the poles and microtubules (compare time frame 2 min and 14 min in Figure 3.2A). In some extreme cases, they even wandered in space further away from the spindle poles (not shown). This strongly argues that an interaction between the kinetochores and microtubules was highly unstable, resulting in alternating the physical configurations between attached and detached states. Therefore chromosomes were hardly congressed to the metaphase plate, and consequently the mutant cells arrested at prometaphase triggered by activation of the spindle assembly checkpoint (see below).

3.3 Sister chromatids are not separated in *ndc80-21*

Fission yeast contains three chromosomes. When the wild type cells are tagged with a kinetochore maker (e.g. Mis6-2mRFP), it can be occasionally captured the moment of six kinetochore dots moving toward the opposite poles within a narrow time window between metaphase and anaphase A. This renders strong evidence of the sister chromatid separation, as it demonstrates the resolution of tension applied between sister kinetochores. However, it becomes difficult to judge the segregation of sister chromatids when all the kinetochore signals are close to the spindle poles, which is exactly the case in *ndc80-21*. Another uncertainty of using a kinetochore marker is the difficulty to distinguish which two kinetochores belong to the sister chromatids.

To examine the pattern of sister chromatid segregation precisely, I tagged cells with *cen2*-GFP to visualise the movement of chromosome II. The visualisation was achieved by utilising the *lac* operon system (Robinett et al., 1996). First, the array of the *lac* operator (*lacO*) repeat sequences was integrated into the genome, which is 5 kb away from the centromere of chromosome II (*cen2*). A fusion gene encoding GFP-Lac repressor (GFP-LacI) flanked with a nuclear localisation sequence (NLS) was then integrated into a second site in the genome (*his7*$^{+}$ loci). By doing so, the expressed GFP-LacI-NLS fusion proteins

could transport into the nucleus, and then tether specifically to the *lacO* tandem repeats as a fluorescent mark of the centromeric DNA (the strain was made by Yanagida's lab). Sad1-dsRed, which is a constitutive spindle pole body component, was also introduced into the same strain to label the SPB.

Cells were filmed after being incubated at 36℃ for 30 min. As the kymograph image shows in Figure 3.3, in the wild type cells, *cen2*-GFPs initially oscillated between the two poles during prophase/prometaphase and aligned at the equator in metaphase when tension is applied onto the sister chromatid. The *cen2*-GFP pair then equally separated to the opposite poles in anaphase A (100%, n=12). Similar to wild type, *ndc80-21* also moved *cen2*-GFPs back-and-forth between two poles in early stage of prophase or prometaphase, suggesting the initial binding of the kinetochores to spindle microtubules may still happen in this mutant. However, instead of separating to two SPBs, the paired *cen2*-GFPs stayed close to one SPB for more than 40 minutes, confirming that the sister chromatid was not segregated in the *ndc80-21* mutant (74%, 17 out of 23 cells) (Figure 3.3, the lower panel).

Nevertheless, the *cen2*-GFP signals occasionally split and appeared distinguishable when they dissociated apart from the pole (see time point after 30 min in Figure 3.3). This centromere movement coincided with shortening of the pole-to-pole distance, implying a counteracting force against the interpolar pushing force was temporarily generated. It is conceivable that each sister kinetochore was attached by the microtubules from the opposite poles. Nevertheless, this bipolar attachment failed to maintain for a long period, and the *cen2*-GFP pair moved back toward the same pole very quickly and became indistinguishable again. This movement indicates that the *ndc80-21* mutant tried very hard to separate its sister chromatids, but the stable kinetochore-microtubule attachments were barely established.

Taken together, I conclude that malfunction of Ndc80 affects the dynamics of the microtubules, abolishes the stable interaction between microtubules and the kinetochores, and fails to separate the sister chromatids.

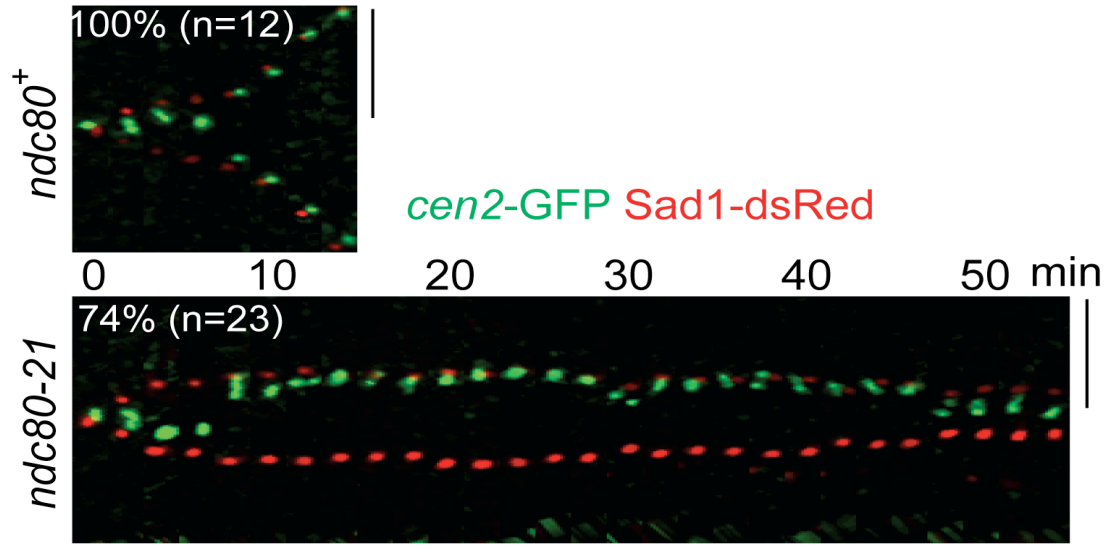

Figure 3.3 Sister centromere behaviour in *ndc80-21*.

Wild type (top, n=12) or *ndc80-21* (bottom, n=23) cells containing *cen2*-GFP (green) and Sad1-dsRed (red, an SPB marker) cultured at 36℃ for 30 min were recorded (2 min intervals) and converted to kymograph. Bars, 5 μm.

3.4 Spindle assembly checkpoint surveillance in *ndc80-21*

3.4.1 Mad2 checkpoint protein is recruited to the kinetochores

The spindle assembly checkpoint (SAC) is a surveillance machinery to prevent premature chromosome segregation by sensing and/or correcting the wrongly attached kinetochores that cannot generate tension (Musacchio and Salmon, 2007). Having seen the prolonged mitotic delay in *ndc80-21*, I then examined whether it was due to the activation of SAC. Using the cells bearing Mad2-GFP (a core SAC component), Cut12-CFP (SPB), and Mis6-2mRFP (kinetochore), I first confirmed that in the wild type cells, the Mad2 checkpoint protein transiently accumulated at the kinetochores during early prometaphase, suggesting some of the centromere/kinetochores were not properly attached (Figure 3.4, the upper panel). However, when all the attachments were in a bipolar fashion, Mad2-GFP disappeared prior to the onset of anaphase. The *ndc80-21* mutant, in striking contrast, exhibited a persistent accumulation of Mad2 signal at the kinetochores for over 50 minutes (Figure 3.4, the lower panel), suggesting that the kinetochore-microtubule interaction was aberrant, in the way of mono-orientation either monotelically or syntelically, or even lost the attachment completely, all of which were unable to generate tension.

3.4.2 Aurora B kinase is required for Mad2-dependent SAC activation

Aurora B kinase is a universal component of the SAC, arguably a tension sensor at the centromere/kinetochore (Lampson and Cheeseman, 2011). The function of Ark1 (Aurora kinase in fission yeast) is reportedly required for the association of Mad2 with kinetochores (Petersen and Hagan, 2003). By switching off Ark1's activity, I next asked whether Mad2 recruitment to the kinetochores is a prerequisite event for the mitotic arrest in *ndc80-21*. In order to inactivate Ark1 specifically in the middle of mitotic block, I introduced an ATP analogue-sensitive mutant allele of *ark1* (*ark1-as3*) into *ndc80-21*, which was a kind gift from Dr. Silke Hauf (Hauf et al., 2007). The analogue-sensitive mutant conditionally inactivates the functions of a specific protein by adding a small molecule, which is structurally similar to the original cofactor required for the

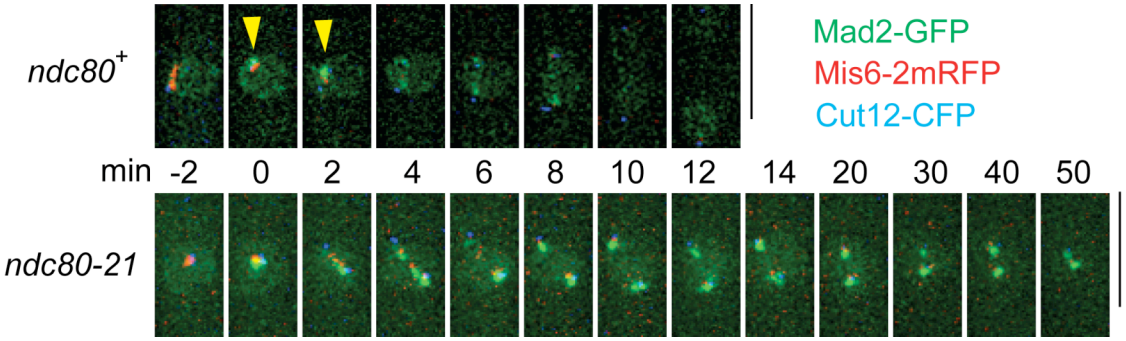

Figure 3.4 The SAC component is constitutively activated in *ndc80-21*.
Wild type (top) or *ndc80-21* (bottom) cells containing Mad2-GFP (green), Mis6-2mRFP (kinetochore, red), and Cut12-CFP (SPB) was shifted up to 36℃ for 40 min and mitotic images were recorded. Arrowheads indicate transient kinetochore localisation (about 2 min) of Mad2 in wild type. Bars, 5 μm.

protein's function. In the case of protein kinase, ATP is a cofactor as the phosphate donor for kinase activity. One can mutate the ATP-binding pocket of kinase-of-interest to create a docking site for an ATP analogue, 1NM-PP1, which chemically does not contain any transferable phosphate (Bishop et al., 2000). The analogue inhibitor thus specifically binds to this mutated kinase, inactivates its kinase activity without affecting any other kinases in the cells. Another advantage of using an analogue-sensitive mutant is that one can inactivate the protein activity by adding the inhibitory analogue at any desired time point or temperature, which makes temporal-separation-of-function possible.

The Mad2-GFP signals were observed in the *ndc80-21* strain and the *ndc80-21 ark1-as3* double mutant. Under normal conditions, especially when the spindle assembly checkpoint is not engaged, the percentage of the mitotic population is only about 5~10%. In order to synchronise the cells, hydroxyurea (HU)-induced S phase arrest and release was applied in this experiment. Both cell cultures were treated with 12 mM HU at 25℃ for 4 h, washed out by filtration and incubated in HU-free media at 36℃. 5 μM 1NM-PP1 or DMSO alone was added 30 min later after temperature shift-up. Upon further 60 min incubation, cells were observed under a fluorescence microscope. As shown in (Figure 3.5), DMSO alone had no effect on Mad2 signalling, as the percentage of the GFP positive cells remained at ~75% in both strains. In sharp contrast, addition of the analogue inhibitor indeed drastically reduced the Mad2-GFP signals at the kinetochores in the *ndc80-21 ark1-as3* double mutant, but not in *ndc80-21* alone. This observation strongly suggests that the mitotic arrest in *ndc80-21* requires the kinetochore retention of the Mad2 checkpoint proteins, which is dependent on Aurora B kinase activity.

3.4.3 *ndc80-21* is defective in forming stable preanaphase spindles

Extending this notion, I further asked what happens to the spindle microtubules in *ndc80-21* when Mad2 is detached from the kinetochores. To this end, I

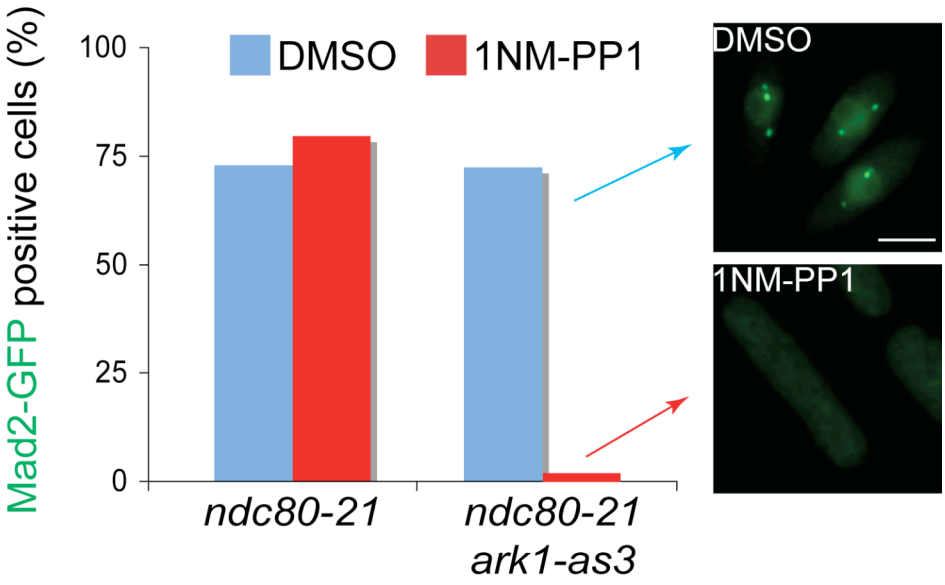

Figure 3.5 Aurora B kinase mediates the SAC in *ndc80-21*.

ndc80-21 and analogue-sensitive *ndc80-21 ark1-as3* cells containing Mad2-GFP were shifted to 36℃ after HU-arrest release. 1NM-PP1 (5 μM) or solvent DMSO was added to each culture 30 min after temperature shift up. These cultures were left for another 60 min and observed under fluorescence microscope. Mad2-GFP kinetochore dots were no longer retained in the absence of Ark1 function (see images on the right). Scale bar, 5 μm.

introduced GFP-Atb2 (α2-tubulin) and Sid4-mRFP (another SPB marker) into the *ndc80-21 ark1-as3* double mutant. The same procedure was carried out and the analogue (1NM-PP1) or the solvent alone (DMSO) was added. Cells receiving DMSO still arrested in mitosis and exhibited similar spindle defects as described earlier (two lumps of the short spindle signals close to the spindle poles with much dimmer signals in the middle region). In contrast, normal elongated anaphase spindles were present in the cells treated with 1NM-PP1 (Figure 3.6). I thus conclude that *ndc80-21* is specifically defective in forming stable prometaphase/metaphase spindles, but this mutant is capable of organising anaphase B spindles when SAC is inactivated. In other words, Ndc80 is required for forming only stable spindle-kinetochore microtubules prior to anaphase onset, but not pole-to-pole microtubules during anaphase B.

3.4.4 Does Aurora B inactivation fully silence the checkpoint?

Interestingly, when the mitotic cells were counted in the same experiment, I found that upon the 1NM-PP1 treatment, about 70% of the mitotic cells were able to release from the prometaphase arrest, but the rest still remained at the pre-anaphase stage (Figure 3.7A). This implies that some of these cells might still receive an arresting signal even though they lacked significant amounts of Mad2-GFP associated with kinetochores (Figure 3.5). To address this notion, I compared the cell viability of *ndc80-21* strains in Δ*mad2* and *ark1-as3* backgrounds. As seen in Figure 3.7B, the viability curve of *ndc80-21* alone (blue line) was indistinguishable from that of *ndc80-21 ark1-as3* receiving DMSO (yellow line), validating the reliability of this assay system. While compared to *ndc80-21 ark1-as3* treated with 1NM-PP1 (green line), *ndc80-21* Δ*mad2* (red line) dropped its viability faster within the first two hours. This indicates that inhibiting Aurora B kinase activity in the mutant is not equivalent to Mad2 checkpoint deletion. Nevertheless, at this stage I could not rule out the possibility that the analogue inhibitor does not 100% kill Aurora B function in the experimental condition. As a result, residual remaining kinase activity might be sufficient to arrest cell cycle progression.

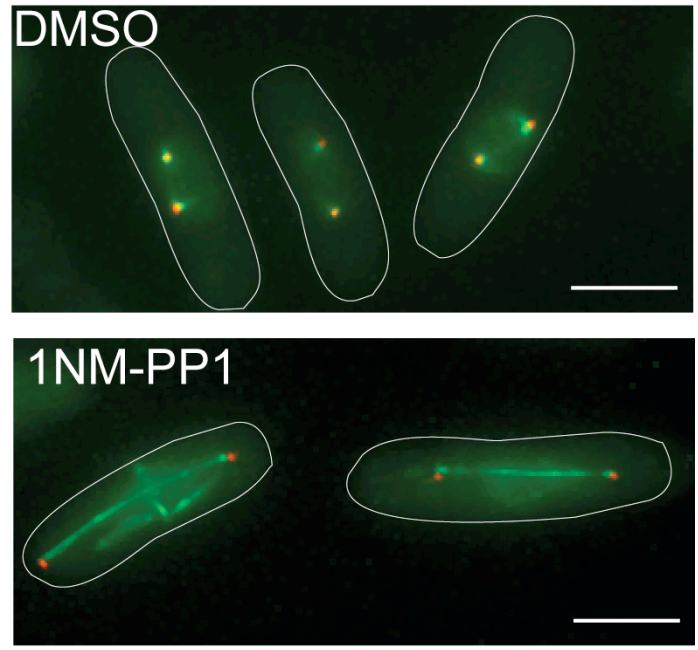

Figure 3.6 Normal elongated spindle morphology in *ndc80-21 ark1-as3*.
ndc80-21 ark1-as3 double mutant cells were tagged with GFP-Atb2 (α2-tubulin) and Sid4-mRFP (an SPB marker). After HU-arrest release, the cultures were shifted to 36℃. 1NM-PP1 (5 μM) or solvent DMSO was added 30 min after the temperature shift-up. These cultures were left for another 60 min and observed under a fluorescence microscope. Scale bars, 5 μm.

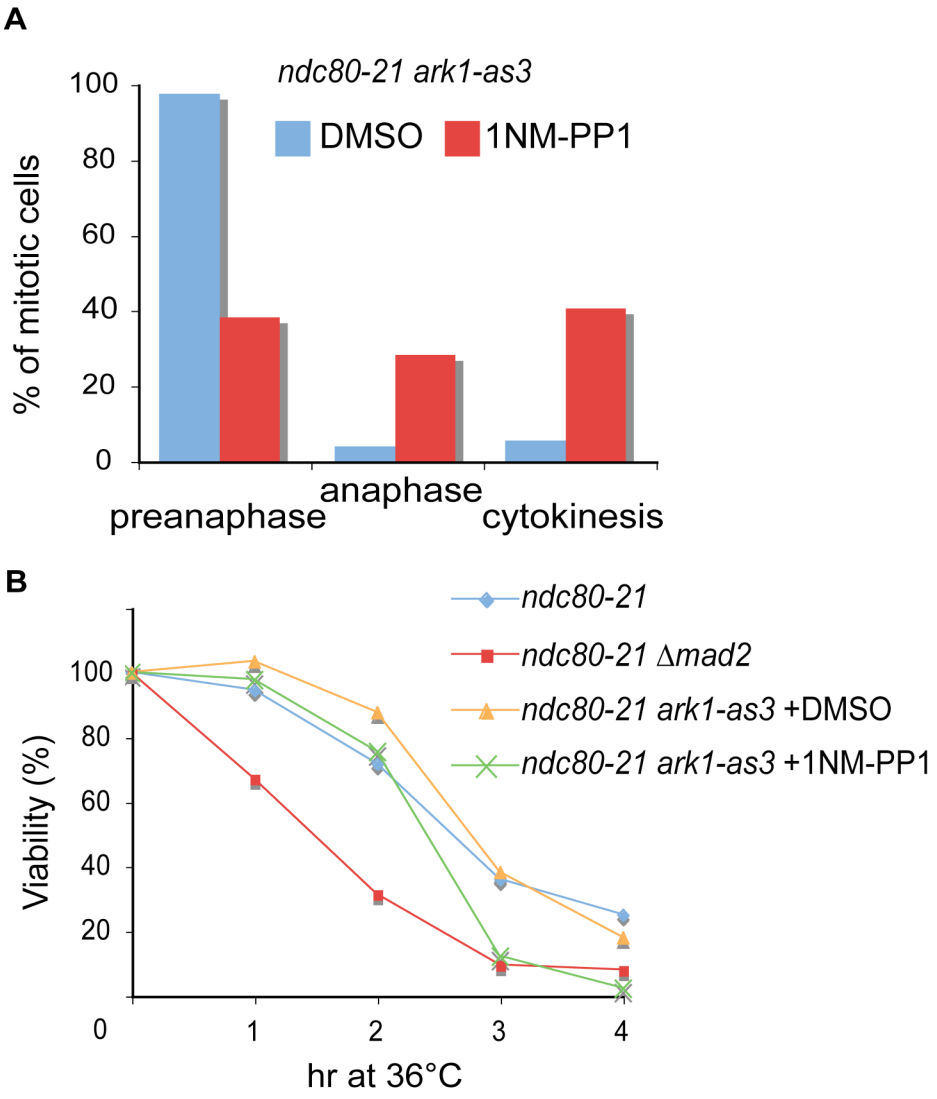

Figure 3.7 Consequence of Aurora B and Mad2 inactivation in *ndc80-21*.

(A) The same procedure as in Figure 3.5 and 3.6 was carried out in *ndc80-21 ark1-as3*. Percentages of cells corresponding to preanaphase, anaphase and cytokinetic stages were counted. n>200.

(B) In order to measure viability drop, cultures of indicated *ndc80-21* strains were shifted from 27℃ to 36℃ at time 0 and aliquots were spread on rich plates and incubated at 27℃. DMSO or 1NM-PP1 was added 30 min after temperature shift up.

3.5 *ndc80-21* is defective in the internal loop

In *ndc80-21*, one mutation (T307A) locates in the first coiled-coil domain, while the other two mutations (E379G and L405P) situate very close and within the internal loop, of which the *in vivo* function remains elusive (Figure 3.8A). To determine the crucial mutation(s) responsible for the temperature sensitivity phenotype, I constructed plasmids that contain *ndc80* genes with single or double of those mutations. Site-directed mutagenesis was used to introduce the desired mutation(s), and the amplified fragments were cloned into pREP1 vector (*nmt1* promoter). Sequencing was performed to verify all the mutation sites. Stoichiometrically there are 8 copies of the Ndc80 complexes surrounding one microtubule at the outer kinetochore (Joglekar et al., 2006, Joglekar et al., 2008, McEwen and Dong, 2010). Ectopic expression of extra copies of Ndc80 proteins can compete with the endogenous mutant proteins and assemble onto the outer kinetochores. In this scenario, a plasmid that bears a mutation that is not responsible for the temperature sensitivity will thus rescue the temperature sensitivity phenotype; on the other hand, the plasmid containing the same mutation responsible for *ndc80-21* defect will not be able to compensate the ts phenotype of this mutant.

Plasmid complementation was done in YE5S plate (with thiamine in the ingredients) using the serial dilution spot assay. The ectopically expressed wild type Ndc80 and Ndc80-T307A and Ndc80-E379G rescued *ndc80-21*, whereas Ndc80-L405P failed to fully compensate for the temperature sensitivity. The double mutant Ndc80-T307A/E379G proteins also complemented *ndc80-21* to the same degree as wild type Ndc80. In contrast, when combined with E379G, which was silent on its own, the double mutant Ndc80-L405P/E379G proteins recapitulated the robust ts phenotype of *ndc80-21* (Figure 3.8B). Although E379G might have some contribution to Ndc80 malfunction, this result strongly indicates that L405P, the residue situated within the internal loop, is the most crucial mutation among the three responsible for the *ndc80-21* defective phenotypes. This therefore surprisingly links the internal loop with the defects of unstable kinetochore-microtubule attachments, and

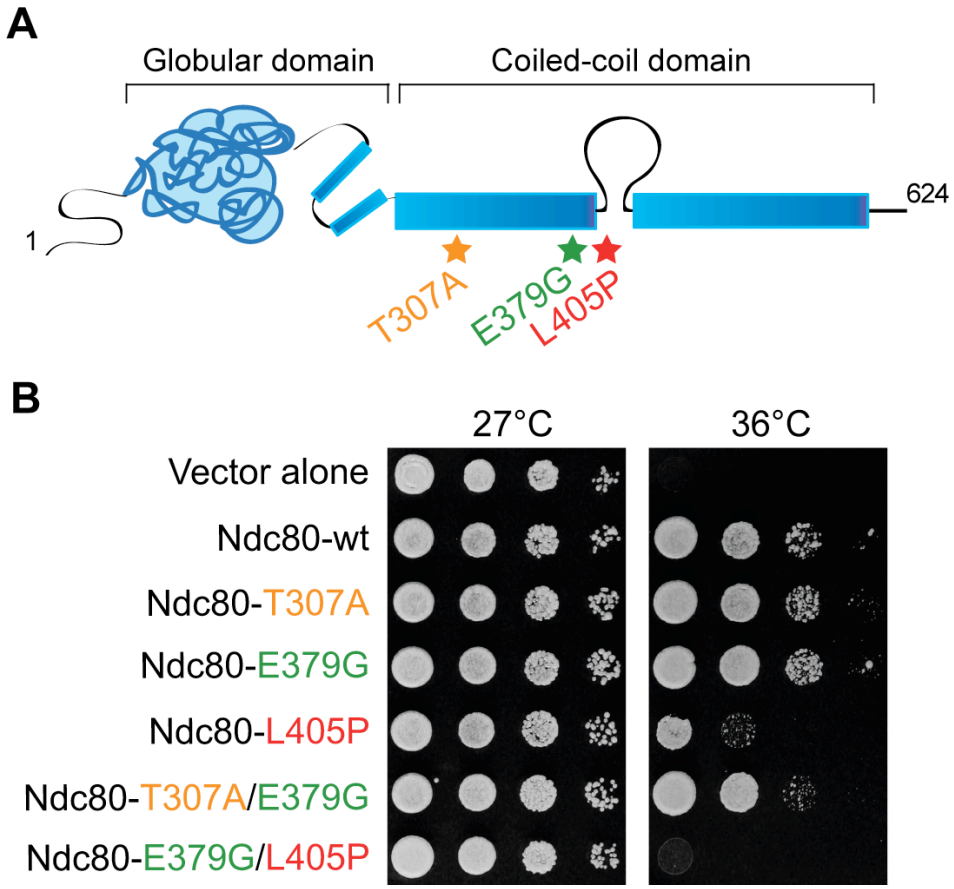

Figure 3.8 L405P is the most crucial mutation responsible for *ndc80-21* phenotypes.

(A) A schematic view of Ndc80 with three mutation sites (asterisks) in *ndc80-21*. (B) The ndc80 gene containing indicated mutation(s) were introduced into an *ndc80-21* strain as episomal plasmids. 10-fold serial dilution ($5x10^4$ cells in the first spot) was applied on rich media, followed by incubation at 27℃ or 36℃ for 3 days.

possibly implying a direct or indirect role of this loop in regulating microtubule dynamics. Very interestingly, sequences around L405 among different species show a considerable homology, although the residue itself is not highly conserved (Figure 3.9). Furthermore, within the loop it may exist a predicted secondary structure (β-sheet), potentially implying that this loop may exert its function(s) through protein-protein interaction (Wang et al., 2008).

Since the molecular functions of the internal loop remained mysterious, identification of L405P as the key mutation causing unstable kinetochore-microtubule attachments motivated me to scrutinise the loop's *in vivo* significance in more detail.

3.6 The internal loop and the N-tail are both essential for Ndc80 function

First, I asked whether this internal loop on its own is essential for cell viability. I made two constructs in which the internal loop was deleted. One construct (Ndc80Δ*400-476*) lacked only the loop region, while in the other construct (Ndc80Δ*371-476*) a further 30 amino acid residues proximal to the N-terminus were also removed. The N terminal tail of Ndc80 has been demonstrated to be crucial for microtubule binding and Aurora B targeting in higher eukaryotes, but non-essential in budding yeast (Guimaraes et al., 2008, Miller et al., 2008, Kemmler et al., 2009, Akiyoshi et al., 2009a). Accordingly a third construct that deleted the N-terminal 94 amino acid extension (Ndc80Δ*2-94*) was created. Expressions of these mutants were again driven under the *nmt1* promoter (pREP1 vector). Plasmids (with the budding yeast *LEU2* gene that complements the fission yeast *leu1* mutation) were episomally introduced into the heterogeneous diploid cells, in which one copy of the endogenous *ndc80*$^{+}$ genes was replaced with an *ura4*$^{+}$ cassette (Figure 3.10A). Diploid cells containing the plasmid were allowed to sporulate, and the sporulated haploid cells were selected against the auxotrophic markers. Based on Mendel's

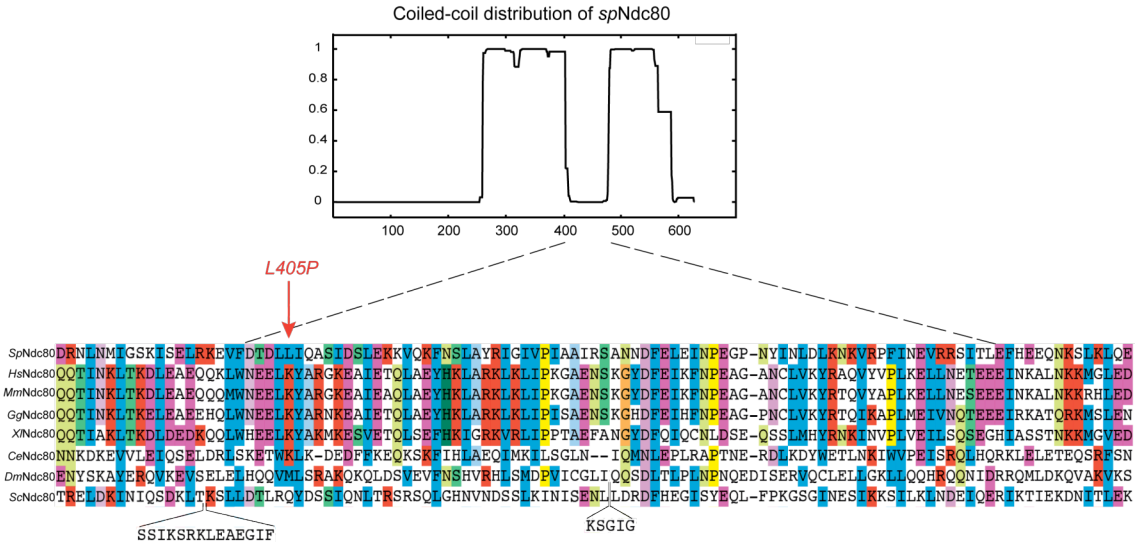

Figure 3.9 Sequence homology of Ndc80 internal loop among species.

The coiled-coil profile of fission yeast Ndc80 is presented in the upper panel. In the lower panel, amino acid residues corresponding to the internal loop of Ndc80 from different species are aligned. L405 (leucine), which is mutated to P (proline) in *ndc80-21*, is marked with an arrow. *Sp, Schizosaccharomyces pombe; Hs, Homo sapiens; Mm, Mus musculus; Gg, Gallus gallus; Xl, Xenopus laevis; Ce, Caenorhabditis elegans; Dm, Drosophila melanogaster; Sc, Saccharomyces cerevisiae.*

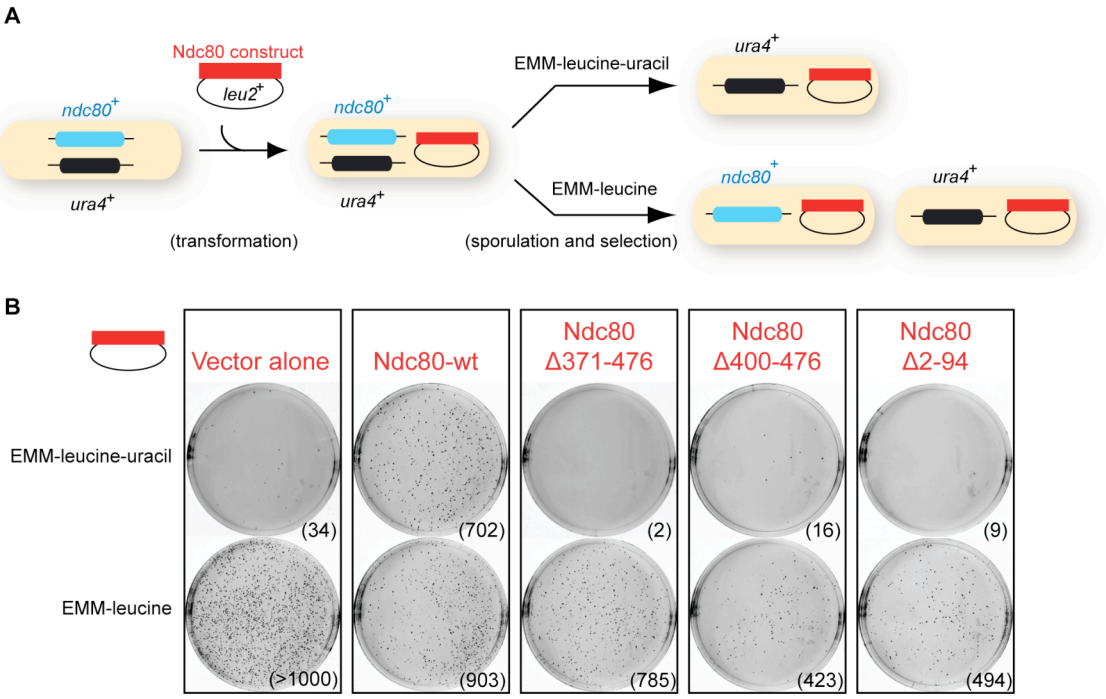

Figure 3.10 The N-tail and internal loop of Ndc80 are both essential for viability.

(A) A schematic illustration of the experimental procedure. pREP1-plasmids (with a *LEU2* marker) bearing various Ndc80 constructs were introduced into diploid cells, in which one copy of the endogenous *ndc80*$^+$ was replaced with an *ura4*$^+$ marker. The transformed cells were allowed to sporulate. Equal amounts of the resulting cell solutions were plated onto two indicated EMM plates for marker selection. Note that thiamine was added at all times to repress the *nmt* promoter.

(B) The selection plates were allowed to grow at 30℃ for 5 days. Numbers of the grown colonies were counted and presented at the right corner within the parentheses.

principle, one should expect that the number of the resulting segregants onto the [EMM minus leucine] plate would be twice as that onto the [EMM minus leucine minus uracil] plate. This was the case in the plasmid bearing the wild type Ndc80 (Figure 3.10B). However, almost no colonies could grow on the [EMM minus leucine minus uracil] plate in plasmids bearing Ndc80Δ2-94, Ndc80Δ371-476, or Ndc80Δ400-476, indicating these mutant proteins could not complement the *ndc80* deleted haploid cells (Figure 3.10B). From these data, I conclude that both the N-terminal tail and the internal loop are essential for cell viability and required for Ndc80 function.

3.7 The N-tail and the internal loop act independently

Having seen the crucial mutation (L405P) of *ndc80-21* is within the internal loop, and it is this loop that is required for the essential function of Ndc80 for cell viability, I then sought to transform these Ndc80 plasmids with or without the N-tail or the internal loop into *ndc80-21*, to ask whether these constructs are able to complement the ts phenotype. As predicted, both Ndc80 loop-less constructs (Ndc80Δ371-476 and Ndc80Δ400-476) failed to suppress the temperature sensitivity phenotype of *ndc80-21* (Figure 3.11). But very interestingly, I found that another construct Ndc80Δ2-94 indeed rescued *ndc80-21*, albeit partially. This is unexpected, because if the major function of the internal loop is to modulate the binding of N-terminal tail toward the microtubule lattice (the fine-tuning model), one would expect no difference in terms of the ts complementarities between Ndc80Δloop and Ndc80ΔN-tail. However, the effects of these two regions on *ndc80-21* are clearly different, implying the fine-tuning activity may not be the sole function of the internal loop *in vivo*. This result illustrates a functional separation between the N-terminal tail and the internal loop, and further suggests that the internal loop may more actively be involved in microtubule dynamics control and kinetochore-microtubule attachment.

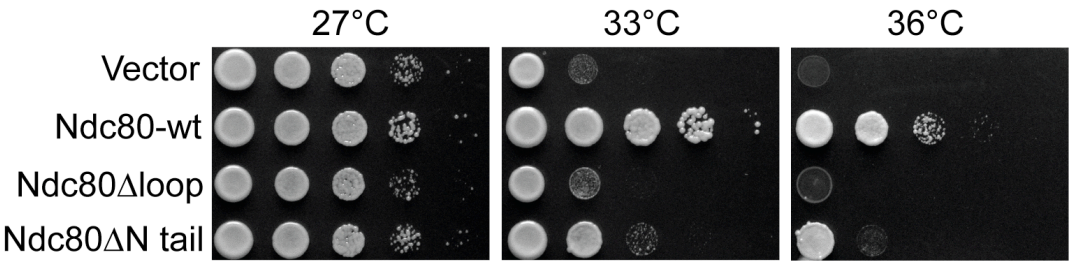

Figure 3.11 Nonfunctionality of loop-less Ndc80.

Plasmids producing wild type, loop-less (Ndc80Δ400-476), or N-terminally truncated (Ndc80Δ2-94) Ndc80 were introduced into an *ndc80-21* strain. Spot test ($5x10^4$ cells in the first spot) was performed on rich media, and the plates were incubated at the indicated temperatures for 3 days.

3.8 Ndc80 loop-less mutants behave dominant-negatively in wild type cells

3.8.1 Ndc80 loop-less mutants are unable to correctly separate chromosomes and arrest in mitosis

To extend the knowledge about how the internal loop of Ndc80 is required for the protein function, I introduced these Ndc80 loop-less constructs into the haploid wild type cells tagged with GFP-Atb2 (α2-tubulin), Mis6-2mRFP (kinetochore marker) and Cut12-CFP (SPB marker). Although the endogenous copy of the *ndc80*$^{+}$ gene was present, the overproduced Ndc80 loop-less proteins clearly acted in a dominant-negative fashion to cause severe toxicity and result in cell death (Figure 3.12A).

To further illuminate the underlying reason of the above lethality, I measured the mitotic index and observed the pattern of chromosome segregation by fixing the cells after 14 to 18 hr incubation at 30℃ in a thiamine-free condition (note that the *nmt* promoter needs more than 12 hr to induce the gene expression). Cells overproducing the wild type Ndc80 proceeded the cell division cycle normally as the mitotic index was compatible with that of cells bearing vector alone. In contrast, however, cells overexpressing Ndc80Δ371-476 or Ndc80Δ400-476 clearly increased their mitotic population up to ~50% in a time-dependent fashion (Figure 3.12B). Furthermore, the frequency of aberrant chromosome segregation was concomitantly increased in these two populations (Figure 3.12C). This result indicates that overproducing the Ndc80 loop-less mutant proteins causes a severe mitotic defect, by which the chromosomes are mis-segregated. The accumulation of mitotic cells is presumably due to the surveillance of SAC, which is activated to aim in the correction of the segregation error.

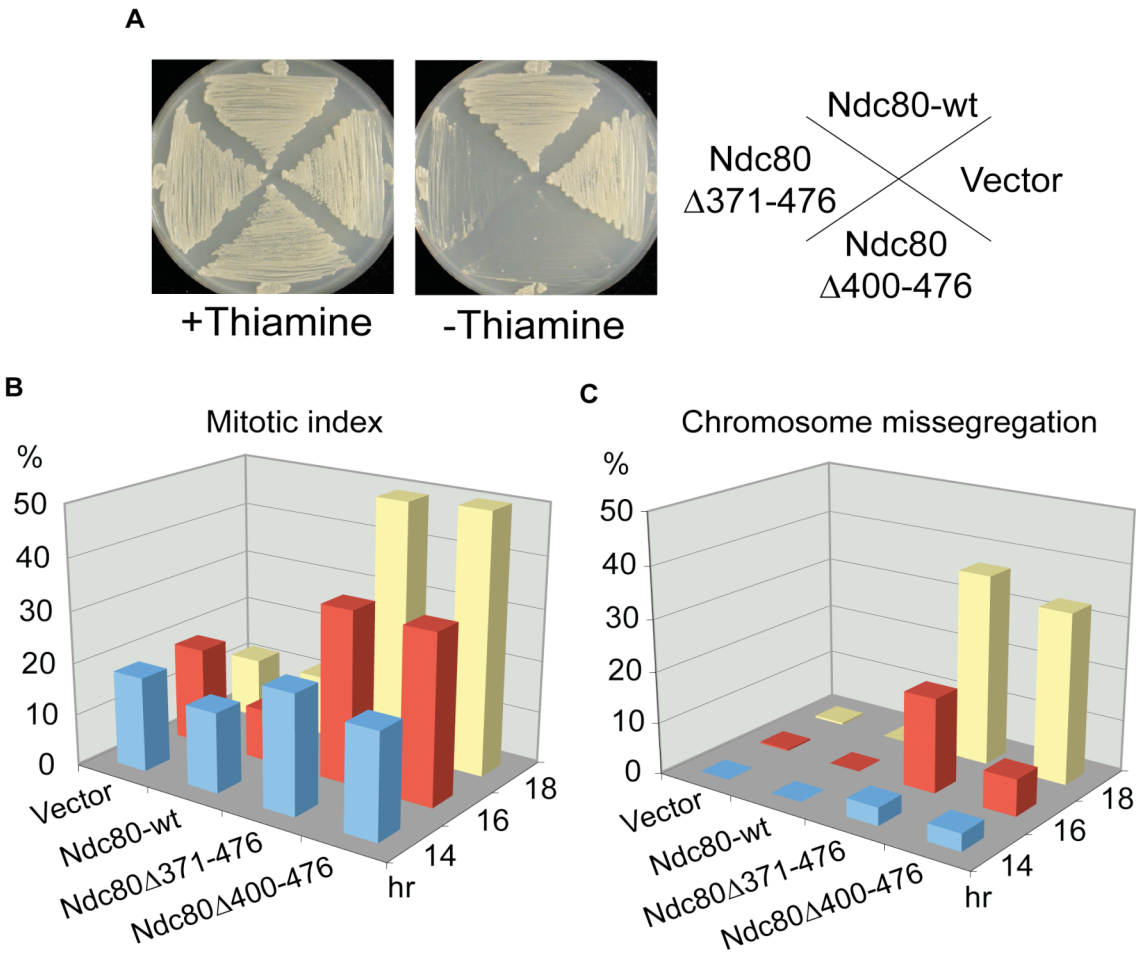

Figure 3.12 Dominant-negative effects of overproduced loop-less Ndc80.
(A) Cells containing plasmids expressing wild type Ndc80 or two types of loop-less Ndc80 (Ndc80Δ400-476 and Ndc80Δ371-476) under the thiamine-repressible *nmt1* promoter were streaked on EMM plates in the presence (left, repressed) or absence of thiamine (right, derepressed) and incubated at 30℃ for 3 days. (B and C) Defective mitosis in cells overproducing loop-less Ndc80. Cells were grown in EMM liquid media in the absence of thiamine at 30℃ for 14-18 hr, and the percentage of mitotic cells (B, microtubule morphology and the number of SPBs) and patterns of chromosome segregation (C, kinetochores and DAPI) were observed (n > 200).

3.8.2 Ndc80 loop-less proteins are able to incorporate into the Ndc80 complex and localise at outer kinetochores

To confirm whether the dominant negative effect described above is due to the expression of the truncated Ndc80 construct, I verified the protein expression levels by immunoblotting. The result shows that Ndc80 loop-less proteins were indeed overproduced under the thiamine-free condition (Figure 3.13A).

Another uncertainty for overexpressing deletion proteins is their localisation. These loop-less Ndc80 proteins may be able to localise at the authentic place, or simply accumulate in the cells and titrate their endogenous binding partner(s) from the canonical loci. Therefore, phenotypes that cells exhibit might arise from loss of function of the binding partners, rather than loop-less protein itself. To address this point, I subcloned these constructs into a vector with the *nmt41-gfp*$^{+}$ cassette, by which the desired protein can be N-terminally tagged with GFP under control of the *nmt41* promoter. The obtained plasmids were introduced into a wild type strain containing Nuf2-mCherry.

nmt41 is also a multi-copy promoter subject to the transcriptional repression by thiamine. Although its relative promoter activity is about 6~7 times less than that of *nmt1* (Basi et al., 1993), the protein expression level driven by *nmt41* is still over 10 times higher than the average endogenous promoters in most cases. Indeed, overproducing GFP-Ndc80Δloop under *nmt41* caused the cell death, too (Figure 3.13B). I thus envision GFP-Ndc80Δloop proteins also behave dominant-negatively in the same way as *nmt1*-Ndc80Δloop when overproduced.

Cells bearing plasmids were cultured in liquid minimal media without thiamine at 30℃ for 16 h and fluorescence images were taken. Some cells showed non-specific uniform background GFP signals, validating the overproduction of Ndc80 from the *nmt* promoter (Figure 3.13C). Importantly, Nuf2-mCherry signals could be seen clearly at the kinetochores, and colocalised with the GFP-Ndc80 loop-less proteins. These data strongly indicate the loop deletion constructs are indeed able to tether other three proteins to constitute the whole

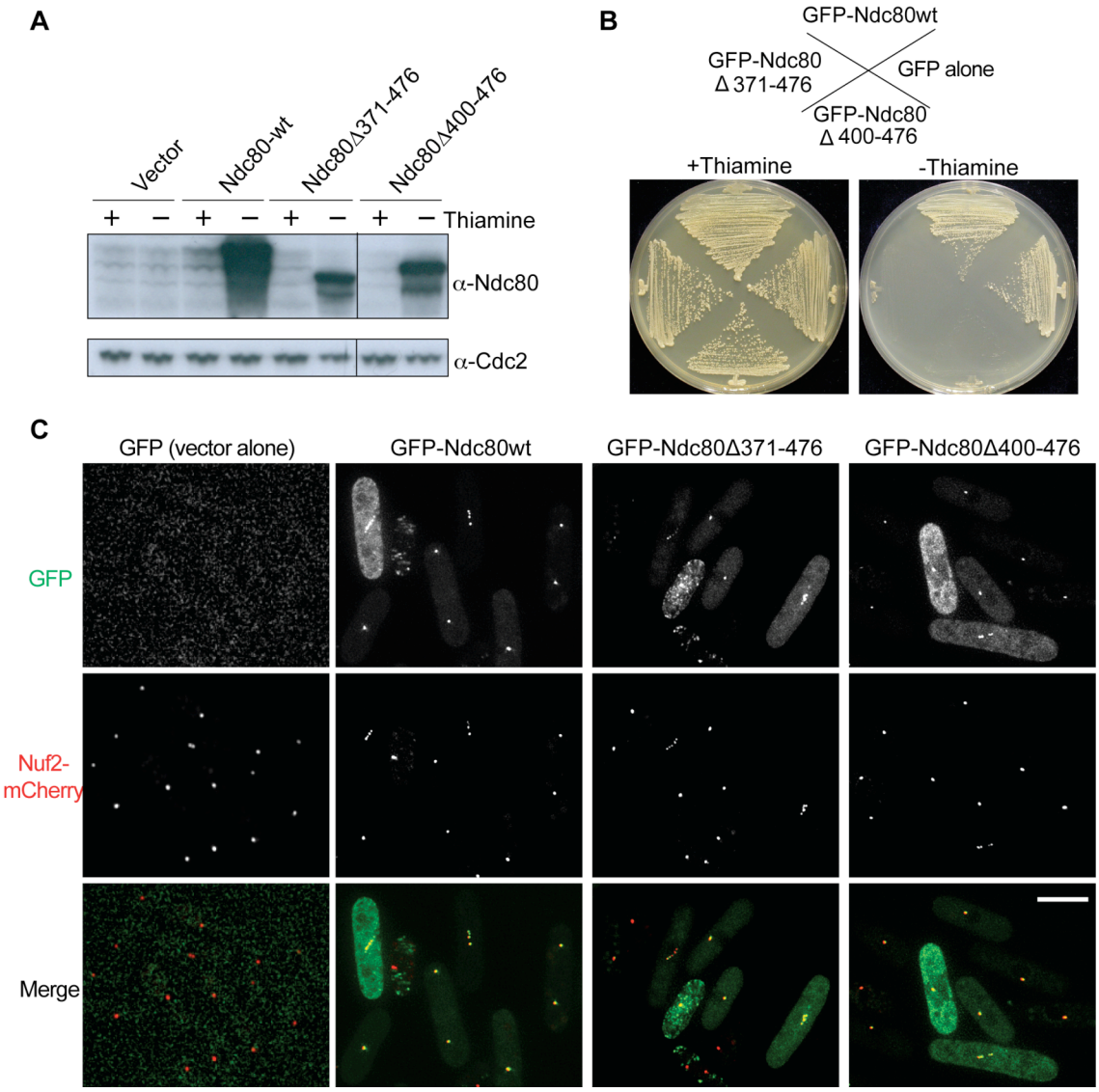

Figure 3.13 Expression and incorporation of Ndc80 loop-less mutant proteins at the kinetochore.

(A) Cells were cultured in liquid EMM with or without thiamine at 30℃ for 16 hr. 30 μg protein extracts were run on the gel for immunoblotting. The Ndc80 protein was detected with anti-Ndc80 antibody, and amounts of Cdc2 were used as the internal control. (B and C) Cells carrying indicated plasmids (*nmt41*-GFP) were streaked on EMM plates with (left, repressed) or without (right, derepressed) thiamine. The same strains (containing Nuf2-mCherry) were cultured in liquid EMM (without thiamine) at 30℃ for 16 hr before imaging. Scale bar, 5 μm.

Ndc80 complex and locate onto the kinetochores. Therefore, I conclude that the internal loop plays no roles in the assembly of the Ndc80 complex.

3.8.3 Ndc80 loop-less mutants exhibit the same unstable spindle phenotype as the *ndc80-21* mutant

The mitotic defect and the delay in cells overproducing Ndc80 loop-less proteins are reminiscent of those observed in the *ndc80-21* mutant. To reconcile how this internal loop could directly or actively be involved in microtubule dynamics, live image analysis was applied to visualise the mitotic events when the Ndc80 loop-less mutant proteins were overproduced. Spindle microtubules of these overproducing cells exhibited fragile morphologies: spindle collapse with two blobs around the opposite spindle poles, to which kinetochores were associated in close proximity (Figure 3.14). These phenotypes are the same as those observed in *ndc80-21*, in which the spindle microtubules are extremely unstable and the stable kinetochore-microtubule attachment is hardly established. The dominant-negative behaviour of Ndc80 loop-less mutants strengthens my previous conclusion that the defect of *ndc80-21* is originated from the malfunction of the internal loop. Taken together, my data argue that the internal loop of Ndc80 plays an essential role in assembling and stabilising bipolar spindle microtubules and thus promotes establishment of proper kinetochore-microtubule attachment.

3.9 Summary

In this chapter, I first examined the essential role of Ndc80 in mitosis by synchronous culture analysis. The time-lapse live imaging of *ndc80-21* reveals a prolonged phase II mitotic delay. The spindle microtubules are extremely unstable and often break/collapse in the middle. The kinetochores are in close proximity to two spindle poles, but often lost from the poles, suggesting the kinetochore-microtubule attachments are too fragile for chromosome

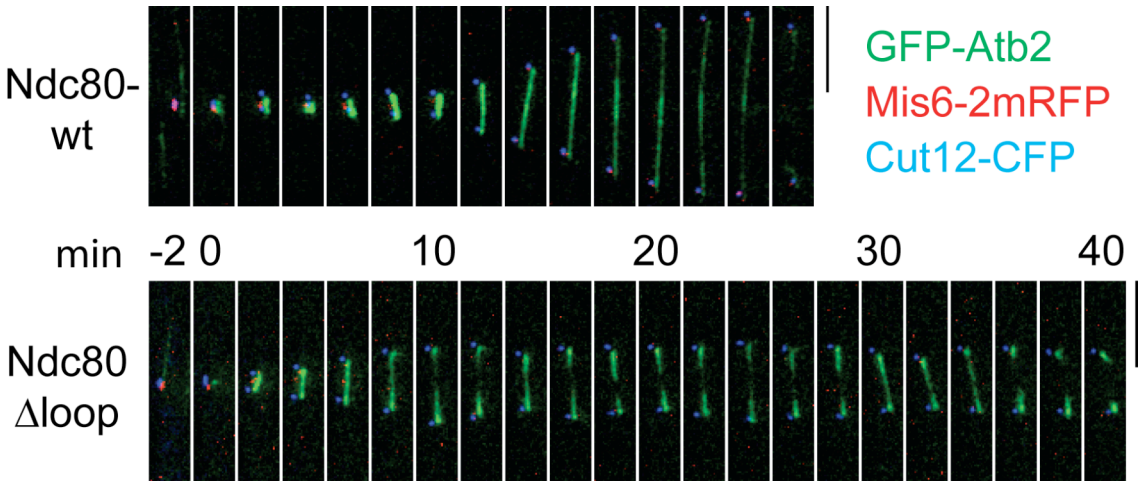

Figure 3.14 Overproducing Ndc80 loop-less mutant proteins phenocopies *ndc80-21* .

Cells were cultured in liquid EMM in the absence of thiamine at 30℃ for 16 hr. While overproducing wild type Ndc80 had no effects on chromosome segregation (upper panel), cells containing overexpressing Ndc80Δloop mutant proteins exhibited mitotic arrest, which was accompanied with unstable preanaphase spindle microtubules. Scale bars, 5 μm.

congresssion to the metaphase plate. Although the mutant cells appear to try hard to separate sister chromatids, proper bipolar attachments are rarely established, resulting in the activation of Mad2-dependent checkpoint, which is dependent on Aurora B kinase activity. When the SAC is disengaged by conditionally inactivating Aurora B, the anaphase spindles form and elongate normally, suggesting Ndc80 is only involved in the maintenance of preanaphase kinetochore microtubules, but may not play a direct role in interpolar spindle interdigitation. Plasmid complementation analysis demonstrates the mutation in the internal loop (L405P) is responsible for the defective phenotype of *ndc80-21*. It thus links the unstable kinetochore microtubule phenotype to the malfunction of the Ndc80 internal loop. The internal loop and N-tail of Ndc80 are both essential for cell viability, but they are functionally distinct from each other. Overexpressing Ndc80 loop-less mutant proteins in a wild type strain acts in a dominant-negative fashion, of which the defective phenotypes recapitulate *ndc80-21*.

3.10 Discussion

3.10.1 Defects in kinetochore microtubules of KMN mutants

In accordance with many other works done in vertebrate Ndc80, fission yeast Ndc80 is absolutely required for the chromosome congression to the metaphase plate (DeLuca et al., 2002, Hori et al., 2003, McCleland et al., 2003, De Wulf et al., 2003, Westermann et al., 2003, Desai et al., 2003, Bharadwaj et al., 2004, McCleland et al., 2004, Cheeseman et al., 2004, DeLuca et al., 2006, Cheeseman et al., 2006, Williams et al., 2007). The unstable spindle microtubule is one of the most characteristic features of *ndc80-21*. Upon Aurora kinase inactivation, *ndc80-21* exhibited nearly normal morphologies of elongated anaphase B spindles. For this reason I argue that Ndc80 is not involved in a global organization of mitotic spindle microtubules, but instead it is required exclusively for proper kinetochore microtubule assembly. Consistent with this argument, in a classic EM study in fission yeast, the spindles are found

to prominently consist of kinetochore microtubules and microtubules emanating from each pole in early mitosis (Ding et al., 1993). The amounts of pole-to-pole microtubules are relatively low at this stage, only 3~4 out of 22 microtubules interdigitating between two poles. This report has an important implication such that the *S. pombe* cells utilise most of the emanating microtubules to "search and capture" all kinetochores in early mitosis, the most important task during this period, and few pole-to-pole microtubules may be sufficient to maintain the bipolar geometry. Therefore it explains why the spindles appear very faint in the middle while only kinetochore microtubules are extremely unstable in *ndc80-21*, which leads to spindle collapse.

Since the KMN network is the major interface of the kinetochore and microtubules, and kinetochore localisation of the Ndc80 complex is dependent on the Mis12 complex, one should expect to see similar spindle defects in other components of KMN. However, such severe spindle phenotypes are not described in previous work done in the *mis12* mutants (Goshima et al., 1999). It is conceivable that when the function of Mis12 complex is completely disrupted, SAC is no longer constitutively activated, and as a result the duration of pre-anaphase becomes very transient (Saitoh et al., 2005). Accordingly the appearance of unstable pre-anaphase spindles would have been overlooked (Goshima et al., 1999).

In terms of the Ndc80 complex, four ts *nuf2* mutants have been isolated and characterised (Nabetani et al., 2001). Although the authors described SAC activation in two of these mutants (*nuf2-2* and *nuf2-3*) and the presence of long anaphase B spindles, unstable pre-anaphase spindle phenotypes were not reported. I suspect that the usage of immunofluorescence microscopy with anti-tubulin antibodies without synchronisation might have contributed to the differences from our observations. Alternatively, it is formally possible that in these *nuf2* mutants, pre-anaphase spindle microtubules are not destabilised, as there is no corresponding loop in the middle of Nuf2.

Intriguingly, similar unstable pre-anaphase spindles are observed in the *spc7* mutants, another kinetochore component that constitutes KMN (Kerres et al., 2007). This is consistent with the view that both Ndc80 and KNL1/Spc7 proteins are involved in microtubule binding (Cheeseman et al., 2006). Interestingly, Spc7 has been shown to coordinate with Mal3/EB1, a plus-end tracking microtubule associated protein (Kerres et al., 2004), which in turn has been linked to prevention of monopolar attachment by cooperation with Bub1/Bub3/Mad3/Mph1 checkpoints in fission yeast (Asakawa et al., 2005b). Intriguingly, the human homologue of Spc7, KNL1/Blinkin, is recently reported to be required for the kinetochore recruitment of Bub1 and BubR1 (Kiyomitsu et al., 2007), as well as the PPI phosphatase in human and yeasts (Liu et al., 2010, Meadows et al., 2011, Rosenberg et al., 2011). Since the *spc7* mutant characterised by Fleig's group is completely loss-of-function, in which most of the Spc7 mutant proteins are dissociated from kinetochores upon heat treatment, the interpretation of a direct role of Spc7 in regulating microtubule dynamics/stability may not be straightforward. Furthermore, the percentage of *spc7* mutant cells with aberrant spindles seems much lower than that of *ndc80-21*. In synchronous cultures, only 6% of the *spc7-23* mutant cells display aberrant spindle morphologies in the first mitosis (Kerres et al., 2007); in sharp contrast, more than 90% of the *ndc80-21* cells exhibit spindle defects under a synchronous condition (not shown). This difference leads me to propose that the role of Ndc80 in regulation of microtubule dynamics and KT-MT attachment is more prominent than that of Spc7.

3.10.2 Aurora B-dependent SAC activation in *ndc80-21*

As the spindle microtubules are extremely unstable in *ndc80-21*, it is not surprising that the spindle assembly checkpoint is activated in this mutant. In higher eukaryotes, the Ndc80 proteins have been implicated in kinetochore recruitment of the spindle assembly checkpoints Mad1, Mad2 and Mps1, as complete depletion of Ndc80 by RNA interference in human cells resulted in SAC deficiency (Martin-Lluesma et al., 2002, DeLuca et al., 2003, Meraldi et al., 2004). Physical interaction between these checkpoint proteins and Ndc80 has

been demonstrated by yeast two-hybrid experiments, implying that Ndc80 at least helps to create a docking site to recruit those SAC proteins onto the unattached/tensionless kinetochores (Martin-Lluesma et al., 2002). In fission yeast, it has also been shown that the kinetochore recruitment of Mad2 requires the Mis6 complex and the Ndc80 complex (Saitoh et al., 2005). In the *ndc80-21* mutant, Mad2 can still be activated to delay the mitotic progress, indicating that although the mutations in Ndc80 mutant proteins influence microtubule dynamics, they may not disrupt the function in respect of recruiting spindle assembly checkpoint components. Mutation sites identified in the *ndc80-21* allele (T307A, E379G, and L405P) agree with the view that the N terminal region of Ndc80 is not only responsible for microtubule binding (aa1-207), but also important for SAC recruitment (aa 81-207) (Guimaraes et al., 2008). Whether or not fission yeast Ndc80 directly recruits the SAC components remains to be determined.

It has been a long debate what the SAC exactly senses during mitosis, either the kinetochore attachment *per se* or the tension status between sister kinetochores (Nezi and Musacchio, 2009, Maresca and Salmon, 2010). Due to the unstable spindle defects, I envision the kinetochore-microtubule attachments in *ndc80-21* are extremely weak and the kinetochores often lose the attachment from microtubules. Therefore the monotelically or syntelically attached or unattached kinetochores all possibly exist in this mutant, and in any case the tension is not satisfied. Consequently it is difficult for me to stand on a side as to what triggers the SAC in *ndc80-21*.

Aurora B is regarded as a tension sensor to detect and destabilise the wrongly attachment by phosphorylating kinetochore substrates at the KT-MT interface, such as the KMN network, the Dam1 complex or MCAK (a kinesin-13 family protein in vertebrates) (Cheeseman et al., 2002, Shang et al., 2003, Andrews et al., 2004, Lan et al., 2004, Ohi et al., 2004, DeLuca et al., 2006, Cheeseman et al., 2006, Welburn et al., 2009). Consequently the corrected kinetochore becomes unattached, being able to recruit the Mad1-Mad2 checkpoint proteins (Tanaka et al., 2002, Ditchfield et al., 2003, Pinsky et al., 2006). In line with this

view, Aurora B kinase activity is required for the prolonged mitotic arrest by retaining Mad2 at the unattached/tensionless kinetochores in *ndc80-21*. While the Aurora kinase activity is inhibited, some of the cells still keep arrested in prometaphase regardless the undetectable level of Mad2 at the kinetochores (Figure 3.8 and 3.10). However, one Mad1 dimer binding to two Mad2 molecules at just one unattached kinetochore is proposed to be sufficient for amplifying the checkpoint signal (De Antoni et al., 2005, Nasmyth, 2005, Musacchio and Salmon, 2007, Kulukian et al., 2009). It is thus possible that residual amounts of Mad2 at the kinetochore, which are below the fluorescently detectable level, might still act to arrest these cells. Alternatively, the function of Aurora B activity and the Mad2 checkpoint pathway may not entirely overlap in *ndc80-21*.

3.10.3 The N-terminal tail and the internal loop of Ndc80

In vertebrate cells, the N-terminal flexible tail of Ndc80 has been shown to be a target of Aurora B (Cheeseman et al., 2002, DeLuca et al., 2006, Cheeseman et al., 2006, Ciferri et al., 2008), and definitely required for direct microtubule binding, especially binding laterally toward the microtubule lattice (Miller et al., 2008, Guimaraes et al., 2008, Alushin et al., 2010, Tooley et al., 2011). In sharp contrast, although the N-tail of budding yeast Ndc80 contributes to chromosome segregation and SAC signalling, it is dispensable for protein's essential function, nor is it needed for cell viability (Kemmler et al., 2009, Akiyoshi et al., 2009a). In my study, I clearly show that the N-tail of Ndc80 in fission yeast is indispensable *in vivo*, imposing a similarity between human and fission yeast Ndc80, in both of which the N-tail is necessary for the protein function. On the other hand, it provides a differentiation in the molecular mechanism of Ndc80's involvement in the establishment of robust kinetochore-microtubule attachment between fission yeast and budding yeast.

The most surprising finding in this chapter is the identification of the internal loop as the crucial part responsible for the unstable spindle phenotypes. It unexpectedly links this internal loop to the proper kinetochore-microtubule

attachment. Both EM study and fluorescence-based length measurement of the Ndc80 complex suggest the existence of the internal loop, which is structurally distinct from adjacent coiled-coil regions (Wei et al., 2005, Ciferri et al., 2008, Wang et al., 2008, Wan et al., 2009). The molecular functions for this loop remain elusive, though two hypotheses have been proposed. The first proposal suggests that this internal loop acts as a flexible kink to fine-tune the binding angle of the N-terminus of Ndc80-Nuf2 toward microtubule lattices (the "fine-tuning" model) (Wang et al., 2008); the other assumes that an unknown linker from inner kinetochore directly binds to the loop that transduces forces generated upon spindle-kinetochore attachment and forms part of the tension-sensing machinery (the "tension sensing/transducing" model) (Wan et al., 2009).

However, so far no *in vivo* data have been presented to support these ideas. Furthermore, The N-tail and the internal loop of Ndc80 can be functionally distinct, as deletion of the former could compensate for *ndc80-21* while deletion of the later could not. The differentiation between the N-tail and the internal loop makes the fine-tuning model less likely, at least not the only explanation for the loop function (section 3.7). In addition, it would be sequence-independent if the loop simply acts as a mechanical fine-tuner. On the contrary, sequence alignment shows that the internal loops are relatively conserved (Figure 3.9), although the length of the loop slightly varies among species.

The "tension sensing/transducing" model lies in the identification of the unknown linker from inner kinetochore. Perhaps the most promising candidate to fit this model is CENP-T, of which the length can be flexibly extended to reach the outer kinetochore (Suzuki et al., 2011). However, a recent report shows that CENP-T indeed interacts with the Ndc80 complex via interaction with Spc24-Spc25, but not through the internal loop of Ndc80 (Gascoigne et al., 2011). It thus downplays the significance of the "tension sensing/transducing model" mediated by the internal loop since no other inner kinetochore components have been identified so far that are more promising than CENP-T.

Here, for the first time, I have demonstrated the essentiality of the Ndc80 internal loop for cell viability. Overexpression of the Ndc80 loop-less mutant proteins destabilises the spindle microtubules and results in the abolishment of the proper KT-MT attachment. These dominant-negative effects imply a more active role for the internal loop in kinetochore microtubule stability upon attachment. Furthermore, a secondary structure is predicted within the internal loop (Wang et al., 2008). I posit that this internal loop may exert its function(s) through protein-protein interaction, which may be directly or indirectly required for microtubule stability.

Chapter 4. Ndc80 loop recruits Dis1 to the kinetochore

4.1 Genetic interaction between MAPs deletion mutants and *ndc80-21*

Results so far predict a critical role of the internal loop in regulating microtubule dynamics and proper kinetochore-spindle attachments. Given that many microtubule associated proteins (MAPs) also alter microtubule dynamics and exhibit aberrant chromosome segregation when deleted or mutated, it is not unreasonable to postulate that the Ndc80 loop function may coordinate some microtubule associated proteins' activity at the microtubule-kinetochore interface. I thus examined possible genetic interaction(s) between those MAP mutants and the *ndc80-21* allele.

A complicated, yet comprehensive, genetic interaction network has been depicted between different MAP mutants (Figure 4.1). Main players involved in the network are Alp14, Dis1, Klp5/Kpl6 and Dam1. All these proteins have been implicated in microtubule dynamics regulation and are crucial for the kinetochore-microtubule attachment. Although none of these MAPs is essential for viability in fission yeast on its own, their protein functions are all mutually interdependent and delicately coordinated, as the double deletions of each combination all exhibit synthetic lethality (Garcia et al., 2001#871, Garcia et al., 2002a, Sanchez-Perez et al., 2005). I crossed *ndc80-21* with these deletion mutants: *Δdis1*, *Δalp14*, *Δdam1*, and *Δklp5*. Tetrad analysis was performed and at least 20 tetrads from each crossing were scored. Surprisingly, I found that the *ndc80-21* strain was synthetically lethal with all the deletion mutants tested (Figure 4.1). These data therefore strongly indicate that Ndc80 is indeed part of the microtubule-associated proteins network, and all the proteins examined

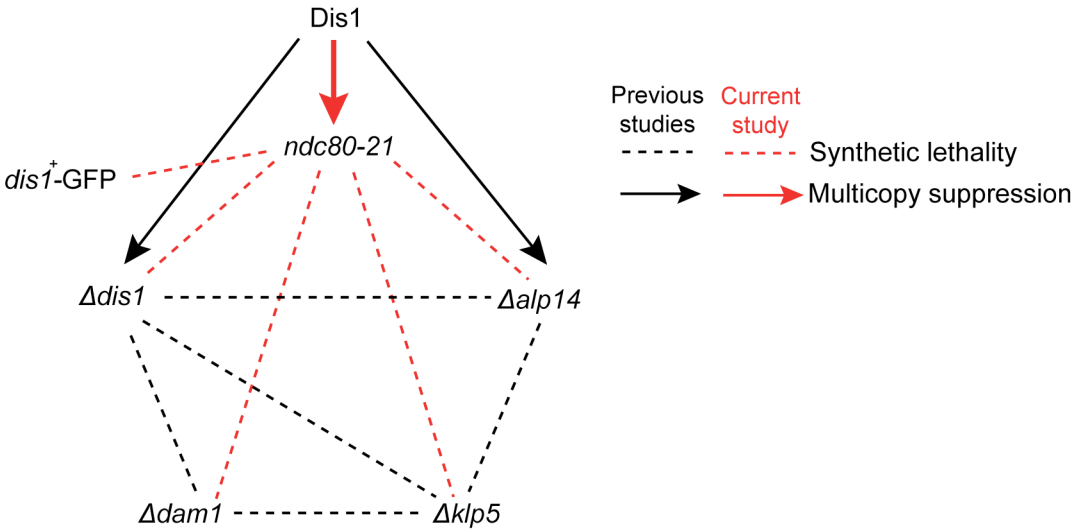

Figure 4.1 Genetic interaction between the MAP mutants and *ndc80-21*.
The dashed lines represent synthetic lethality between two alleles; the arrow indicates multicopy suppression (see section 4.2). Lines in black were depicted from previous research (Garcia et al., 2002a, Sanchez-Perez et al., 2005), whereas lines in red were done in this thesis work. Note that the C-terminal tagging of wild type Dis1 also caught the lethality with *ndc80-21* (see section 4.4).

here may together share a correlatively essential function, thereby coordinating Ndc80-depedent spindle microtubule dynamics.

4.2 Dis1 is a multicopy suppressor of *ndc80-21* mutant

Having seen the extreme unstable spindle phenotype in *ndc80-21*, and the perplexing genetic interactions between several microtubule-associated proteins and *ndc80-21*, I postulated that certain microtubule-associated proteins, which are known to be crucial for microtubule stability, might compensate for the unstable spindle defect in *ndc80-21* when overproduced. Accordingly multicopy plasmids containing the MAP genes were transformed into the mutant strain and spot tests were performed on YE5S plates. Among those MAPs tested were Alp14, Dis1, Ase1, Dam1, Mal3, and Cls1, which are known for their roles in microtubule stabilisation, bundling, plus end tracking, and the establishment of robust kinetochore-microtubule attachment. Klp5 was not on my tested list as it had been shown to function as the microtubule destabiliser, rather than a stabilising factor, despite that it does have a clear genetic interaction with *ndc80-21*. All the tested microtubule-related proteins have been found functionally conserved among different species except Dam1.

Only high dosage of Dis1 rescued the ts phenotype of *ndc80-21* at the semi-permissive temperature (Figure 4.2A and B). Overexpressing other MAP proteins, including a stronger expression of Ase1 (under the *nmt41* promoter) and an activated version of Dam1 (Dam1-1-127) (Sanchez-Perez et al., 2005), seemed to have barely little affect on the temperature sensitivity of *ndc80-21*. The *dis1*$^{+}$ gene was originally identified by the mutant isolation that is defective in sister chromatid disjoining (Ohkura et al., 1988). Following studies established that this gene product closely associates with the kinetochore in mitosis and its function is required for faithful chromosome segregation (Nabeshima et al., 1995, Nabeshima et al., 1998, Nakaseko et al., 2001). Importantly, one member of the Dis1/TOG protein family, XMAP215, has been

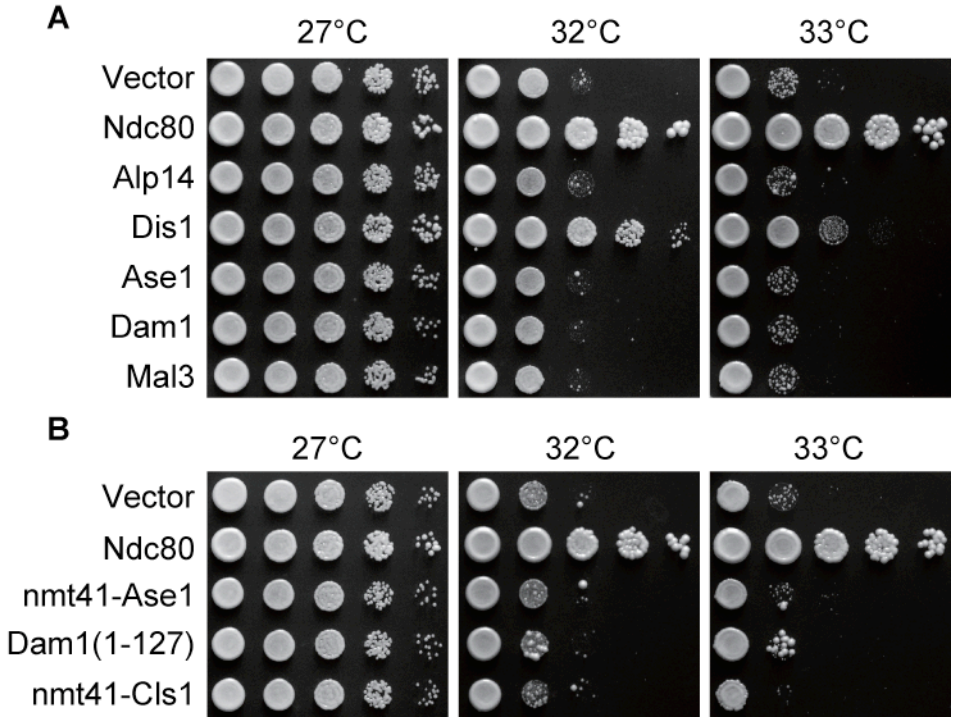

Figure 4.2 High dosage of Dis1 partially suppresses *ndc80-21*.

Multicopy plasmids containing the indicated genes were transformed into an *ndc80-21* strain and spot tests were performed at the indicated temperatures.

recently demonstrated to act as a microtubule polymerase, by which it processively brings the tubulin heterodimer (or arguably oligomers) and adds onto the microtubule dynamic end to stabilise microtubules (Kerssemakers et al., 2006, Brouhard et al., 2008). Considering the unstable spindles observed in *ndc80-21*, it seems logically coherent to identify Dis1 as a multicopy suppressor of this mutant.

Unlike other organisms containing only one Dis1/TOG protein, fission yeast has evolved to have two TOG family proteins, Dis1 and Alp14. However, Alp14 did not rescue *ndc80-21* when overproduced. This observation led me to suspect that an intrinsic difference between these two TOGs might contribute to this discrepancy. One plausible reason is that, while Dis1 may intrinsically be able to dock at the outer kinetochores in the close proximity of microtubule plus ends, Alp14 may require its binding partner Alp7, a protein belonging to the transforming acidic coiled-coil (TACC) family, to translocate from SPB through spindles to the kinetochores (Sato et al., 2004). As a result, expressing Alp14 alone might not be sufficient to suppress the *ndc80* mutant. I tested this possibility by co-overexpressing Alp14 and Alp7 in *ndc80-21*; nevertheless, no signs of significant suppression were observed (not shown). Collectively, these data indicate that overproducing Dis1, but not Alp14 or other MAPs tested here, reverses the unstable spindles in *ndc80-21*, and thus highlight Dis1 as the major MAP, if not the sole, to help Ndc80 establish proper kinetochore-microtubule attachment.

4.3 Dis1 physically interacts with Ndc80 via the internal loop

The genetic interaction and the multicopy suppression results establish that Dis1 is closely and functionally linked to the Ndc80 loop activity. However, it can be argued that suppression of *ndc80-21* by multicopy Dis1 may simply be the consequence of the global stabilisation of spindle microtubules in a non-specific manner independent of Ndc80 internal loop. Nevertheless, a secondary

structure (β-sheet) predicted in this internal loop implies a potential protein-protein interaction activity (Wang et al., 2008). Furthermore, structural studies and super-resolution imaging from several groups have demonstrated the elongated shape of the Ndc80 complex binds spindle microtubules laterally with certain angles away from the spindle axis, and the spatial arrangement allows the dynamic plus end of microtubules to extend averagely about 50 nm further toward inner kinetochores (Ciferri et al., 2008, Wilson-Kubalek et al., 2008, Wan et al., 2009, Alushin et al., 2010). In this configuration, the internal loop of Ndc80 may situate in a position where the space is big enough to recruit other proteins close to microtubule dynamic ends. It is thus possible that Dis1 and Ndc80 may physically interact through the internal loop. To address this point, I tested the possible interaction by using several distinct approaches as described below.

4.3.1 Recombinant Dis1 proteins pull down Ndc80 from cell extracts

Firstly, the pull down assay was conducted to examine the interaction. To do so, I set up to purify the recombinant Dis1 proteins from bacteria. The *dis1*$^{+}$ gene is 2916 bp in length with an intron in close proximity to N-terminus before the first TOG motif (note that Dis1 protein has two TOG domains in its N-terminus). To make the cloning easier, I deleted the first 17 amino acids to get rid of the intron without disturbing the following TOG domains. The PCR amplified *dis1* fragments were cloned into the pGEX-KG vector (Clonetech), and sequencing was performed to confirm the construct accuracy. The recombinant Dis1 proteins were N-terminally tagged with glutathione-s-transferase (GST) and expressed in *E. coli* (Rosetta p*Lys*S, Merck) under IPTG induction. The protein lysates were purified with glutathione-sepharose beads, followed by gel filtration (Figure 4.3A). The gel filtration steps were kindly helped by Dr. Martin Singleton's lab (Cancer Research UK London Research Institute, Macromolecular Structure and Function Laboratory) using their high performance liquid chromatography system (HPLC).

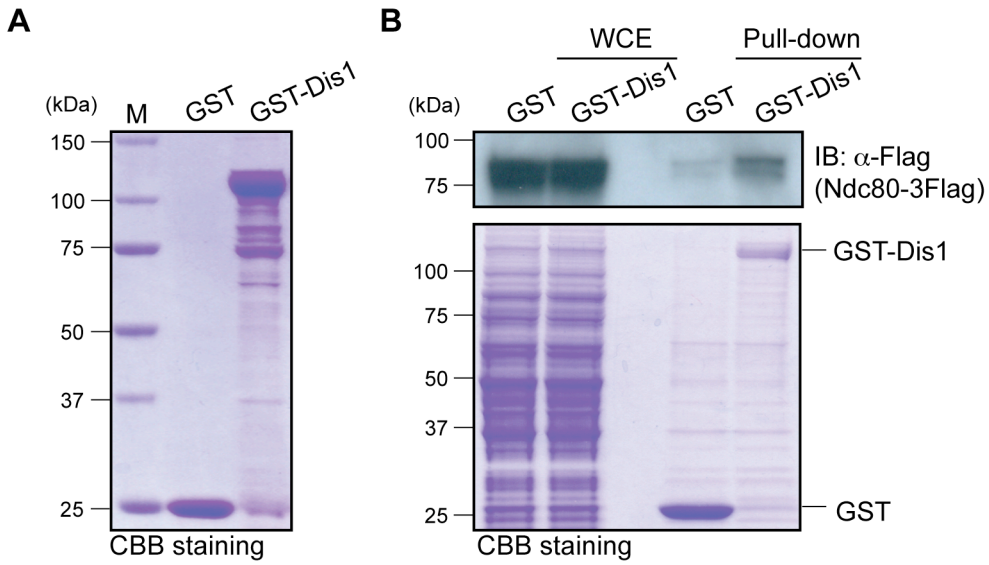

Figure 4.3 GST-Dis1 pulls down Ndc80 from cell extracts.

(A) The pGEX-KG-Dis1 construct was expressed under IPTG induction in *E. coli* (Rosetta p*Lys*S). The recombinant proteins were purified by using the GSH beads and a gel filtration column. (B) Bacterial GST-Dis1 bound on GSH beads was passed through fission yeast cell extracts (2.7 mg) containing Ndc80-3Flag. Eluted fractions were immunoblotted with FLAG antibody (top) or stained with coomassie brilliant blue (bottom). WCE (whole cell extract), 50 μg.

Using GST alone as a control, I coupled GST-Dis1 proteins onto the glutathione-sepharose beads, and passed through cell extracts harvested from liquid cultures of a wild type strain tagged with Ndc80-3Flag. To mimic the condition of the time when Dis1 and Ndc80 are supposed to interact, the hydroxyurea arrest-release method was applied to accumulate the mitotic cell population. I found that the recombinant GST-Dis1 proteins pulled down Ndc80 from fission yeast cell extracts, while GST control pulled down merely little under the same condition (Figure 4.3B). These data render the first piece of evidence that these two proteins interact with each other, either directly or indirectly.

4.3.2 Ndc80 co-immunoprecipitates with Dis1 *in vivo*

Since Ndc80 forms a four-subunits complex with Nuf2, Spc24 and Spc25, purification of the recombinant Ndc80 protein alone has been proved difficult without co-purifying its binding partners together (Section 2.11 and personal communication with Dr. Martin Singleton). To confirm the interaction data in the reverse fashion, I then used co-immunoprecipitation (co-IP) to examine the binding. Boosting the mitotic population in this experiment, a wild type strain tagged with Ndc80-3Flag and Dis1-8Myc was crossed with *cut9-665*, a ts mutant allele defective in the APC/C (anaphase promoting complex/cyclosome) and thus blocking the cell cycle at metaphase (Samejima and Yanagida, 1994). Cells were incubated at 36℃ for 3.5 hr to accumulate the mitotic population before lysis. The anti-Flag antibody was coupled to magnetic beads, and then used to immunoprecipitate Ndc80-3Flag from the cell extracts. Dis1-8Myc proteins co-immunoprecipitated with Ndc80-3Flag in the double tagging cells, whereas this co-IP band could not be seen in cells tagged either only Ndc80-3Flag or Dis1-8Myc alone (Figure 4.4). This reverse binding experiment thus strengthens my previous result that Ndc80 interacts with Dis1 *in vivo*.

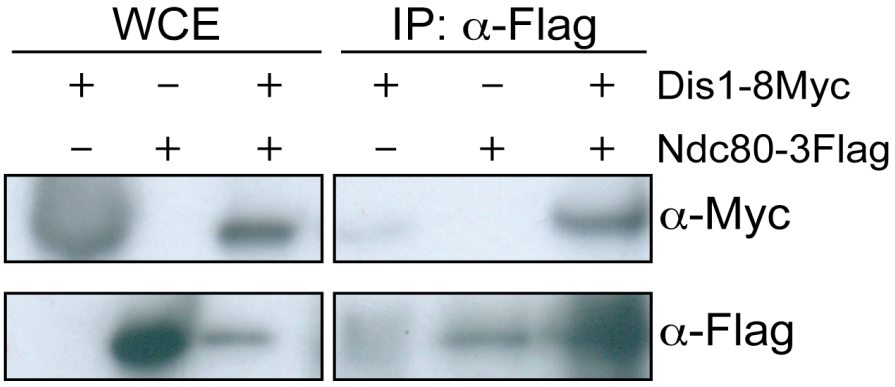

Figure 4.4 Ndc80 immunoprecipitates Dis1 *in vivo*.

Protein extracts (1.5 mg) were prepared from indicated cells with a *cut9-665* background, followed by immunoprecipitation. WCE, 50 μg.

4.3.3 Deletion of Ndc80 internal loop reduces Dis1's binding

To get insight into how these two proteins interact, I asked whether the internal loop of Ndc80 is responsible for the interaction observed above. Since the internal loop is essential for viability, deletion of this loop in endogenous Ndc80 seems unfeasible for the biochemical study. Nevertheless, my previous results demonstrate a dominant negative effect of overproducing Ndc80 loop-less mutant proteins in the wild type cells, of which the defects phenocopy *ndc80-21* (Section 3.8). I thus applied overexpression to investigate the role of the internal loop in Ndc80-Dis1 interaction. I overproduced either wild type Ndc80 or Ndc80Δ371-476 proteins in a strain containing integrated *nmt41*-GFP-Dis1. Immunoprecipitation was performed using the cell extracts collected from thiamine-free cultures. While IgG-coated magnet beads alone (as a negative control) absorbed no Ndc80 mutant proteins nor GFP-Dis1 under the experimental condition, apparent co-immunoprecipitation of GFP-Dis1 was observed with the immunoprecipitation of wild type Ndc80 by the anti-Ndc80 antibody (Figure 4.5). Compared to wild type, the co-immunoprecipitation was drastically reduced when the internal loop of Ndc80 was deleted. These data thus strongly argue that the internal loop is required for Dis1-Ndc80 binding.

4.3.4 *In vitro* peptide array suggests that binding between Dis1 and Ndc80 is direct

From those assessments above, one can likely draw the conclusion that Dis1 directly binds the internal loop of Ndc80 *in vivo*. However, all the above experiments were done with whole cell extracts, which contain a myriad of proteins from the entire cell, including tubulins and possibly short tubulin oligomers. Considering the fact that Dis1 is an authentic microtubule-associated protein, and that Ndc80 directly interacts with microtubules as well, it is formally arguable that the binding might be through potential intermediates, the short microtubules for example or other unknown proteins in the cell lysates.

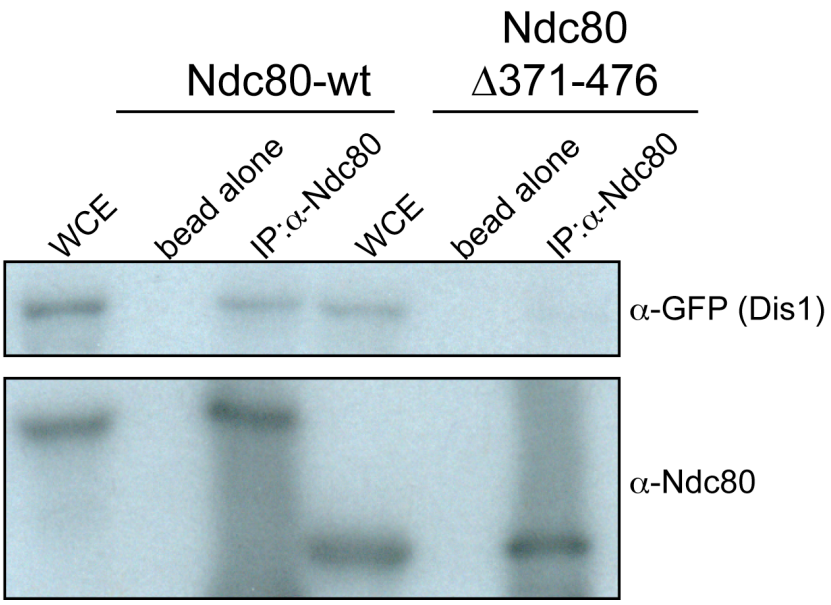

Figure 4.5 Reduced binding of loop-less Ndc80 to Dis1.

Protein extracts (1 mg) were prepared from indicated cells and immunoprecipitation was performed. WCE, 30 μg.

To resolve this uncertainty, I turned to analyse the interaction via a pure *in vitro* system, the peptide array assay. By doing so, the possible intermediates linking Dis1 and Ndc80 can be ruled out, and the direct interaction can thus be confirmed. In this assay, a peptide array was synthesised to cover the whole loop region of Ndc80, from amino acid residue 365 to 502 (note that the loop starts from residue 400 and ends at residue 476). Each 20-residue peptide was spotted onto cellulose membrane with a 2-residue shift between the neighboring spots. Membranes were incubated with recombinant GST-Dis1 or GST alone at 4℃, followed by the extensive washing to remove the unbound proteins. The bound fraction of GST-Dis1 on the membrane array was then detected with an anti-GST antibody. As shown in Figure 4.6, there were three main regions exhibiting the positive interaction in the loop: ^{395}LRKEVFDTDLLIQA^{408}, ^{431}PIAAIR^{436}, and ^{473}ITLEFHEEQNKS^{484}. These positive sites may represent specific binding of Dis1 to the loop, because the same membrane showed no signals on the first several spots corresponding to the coiled-coil shafts (aa 365 to 395) before the internal loop. It also showed extremely low background in the negative control experiment (GST alone) under the same condition. These array data therefore reinforce the notion that Dis1 directly binds to the internal loop of Ndc80. Interestingly, when the same experiment was performed against a peptide array that covered the whole Ndc80 protein sequence, the binding pattern within this loop region was almost the same as the one shown in Figure 4.6, indicating that this array data is reproducible. However, there were several other sites showing positive interaction, including regions within the CH domain of Ndc80, suggesting other regions may also help Dis1 binding. The full-length array data are shown in Appendix 1.

4.3.5 The L405P mutation reduces Dis1 binding *in vitro*

Very interestingly, the crucial mutation (L405P) identified in *ndc80-21* is within the first binding peptide ^{395}LRKEVFDTDLLIQA^{408}. The coincidence implies that in *ndc80-21*, the L405P mutation may reduce the binding affinity of the loop to Dis1. As a result, the initial lateral attachment between kinetochores and

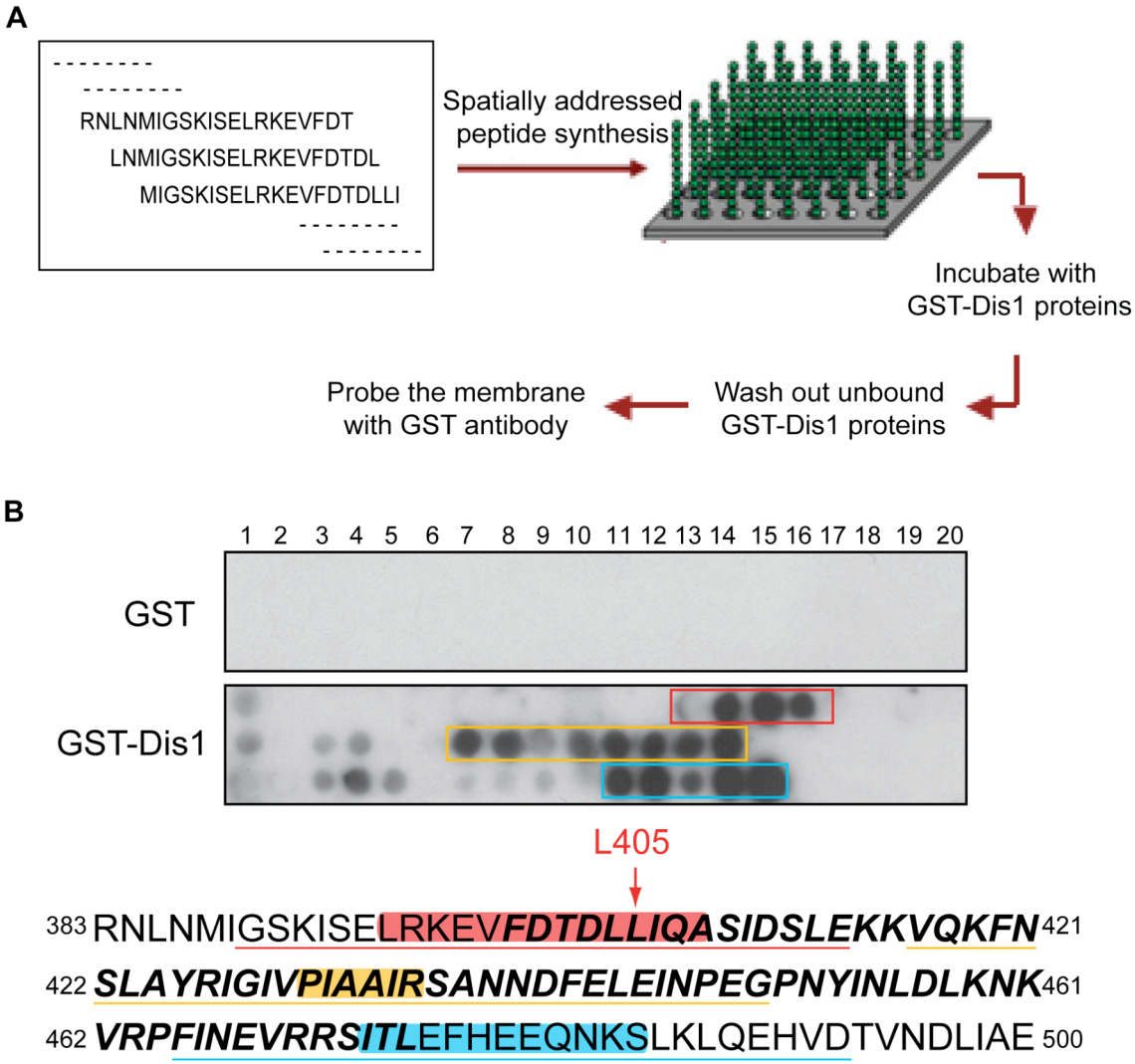

Figure 4.6 *In vitro* peptide binding assay between Ndc80 loop and Dis1.
(A) The illustrative procedure of peptide binding assay. Each peptide containing 20 amino acids was spotted onto a cellulose membrane with a 2-residue shift between the neighbouring spots. 1 μg/ml proteins (GST or GST-Dis1) were incubated with the array membrane at 4℃ overnight. The unbound proteins were washed out, and the membrane was blocked by 3% skim milk, followed by immuno-detection with the anti-GST antibody. (B) The result. Peptides that showed positive interactions with Dis1 are boxed or underlined (395–408, red; 431–436, yellow; and 473–484, blue). Amino acid residues inside the loop are shown in bold and italics (400-475). The key mutation in *ndc80-21*, L405, is pointed out with an arrow.

spindle microtubules might still occur but not strongly enough to congress all chromosomes to the metaphase plate. Tension is therefore never satisfied in this mutant and the SAC is consequently activated.

To verify this notion, the peptides ^{392}ISELRKEVFDTDLLIQASID^{408} with a serious of mutations were synthesised, in which each residue among ^{403}DLLIQ^{407} was individually mutated into all other 19 amino acids. As expected, peptides without changing any amino acid retained the capability to bind GST-Dis1 (Figure 4.7, marked by dashed yellow circles); in contrast, several mutations in this area caused a significant reduction of GST-Dis1's binding. Most importantly, the peptide containing L405P mutation clearly did not bind GST-Dis1 (marked by a red circle), where mutated peptides that retained their binding capability were those containing conservative hydrophobic residues like isoleucine, phenylalanine, tryptophan, tyrosine, and valine (marked in blue text). This mutation array therefore not only underpins my previous pull-down and co-IP data, but also indicates the mutation in the loop disrupts the interaction between Ndc80 and Dis1.

4.4 Dis1 is lost from the kinetochores in the *ndc80-21* cells

The mutation peptide array predicts the signal reduction of the Dis1 proteins at the kinetochores *in vivo*. Back to the cells, I attempted to quantify the fluorescent signals of Dis1-GFP proteins in the *ndc80-21* mutant. During the process of strain constructions, I found that the strain with the C-terminal tagging of Dis1 by GFP was synthetic lethal with *ndc80-21* (Figure 4.8). This lethality suggests that the Dis1-GFP function in this mutant might be somehow compromised. Although *ndc80-21* was isolated as a heat-sensitive mutant, the mutation in *ndc80-21* might also mildly compromise the protein function even at the permissive temperature, as the mutant cells present a slightly pink colour on Phloxin B plates at 27℃ (Figure 2.5). Despite the mild defect, *ndc80-21* cells

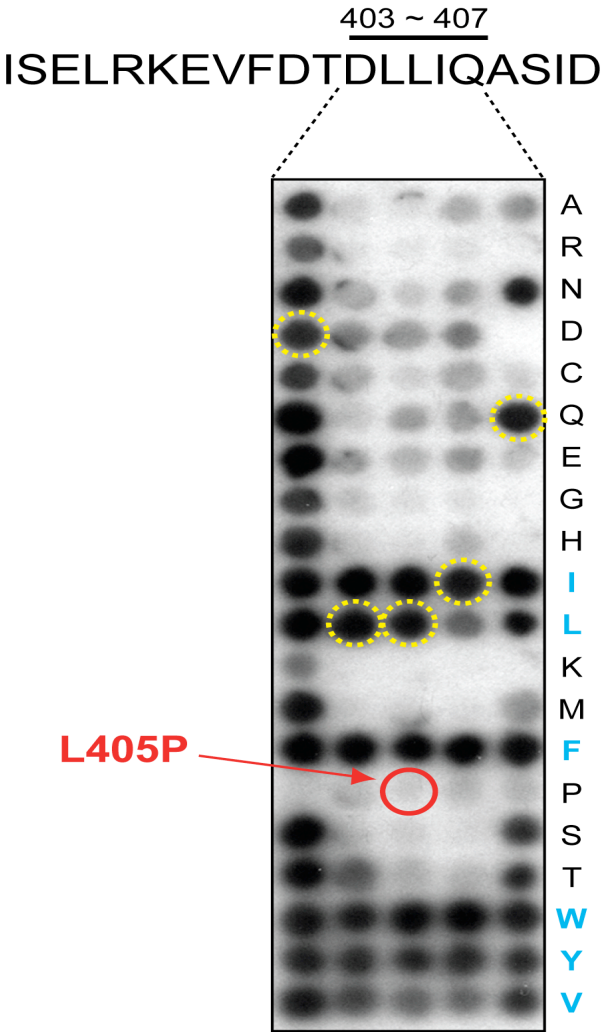

Figure 4.7 Analysis of residues in the loop essential for interaction with Dis1.

20 amino acid-length peptides (shown on the top) each containing a single mutation in one of the DLLIQ region were spotted on a membrane, which was then incubated with GST-Dis1, followed by immunoblotting with anti-GST antibody. Each peptide has one residue replaced with one of the 20 amino acids. Peptides without any amino acid change were marked in a yellow circle; the peptide with the L405P single mutation is pointed out with a red circle. Note that the amino acids labeled in blue were those mutated peptides that retained their binding capability.

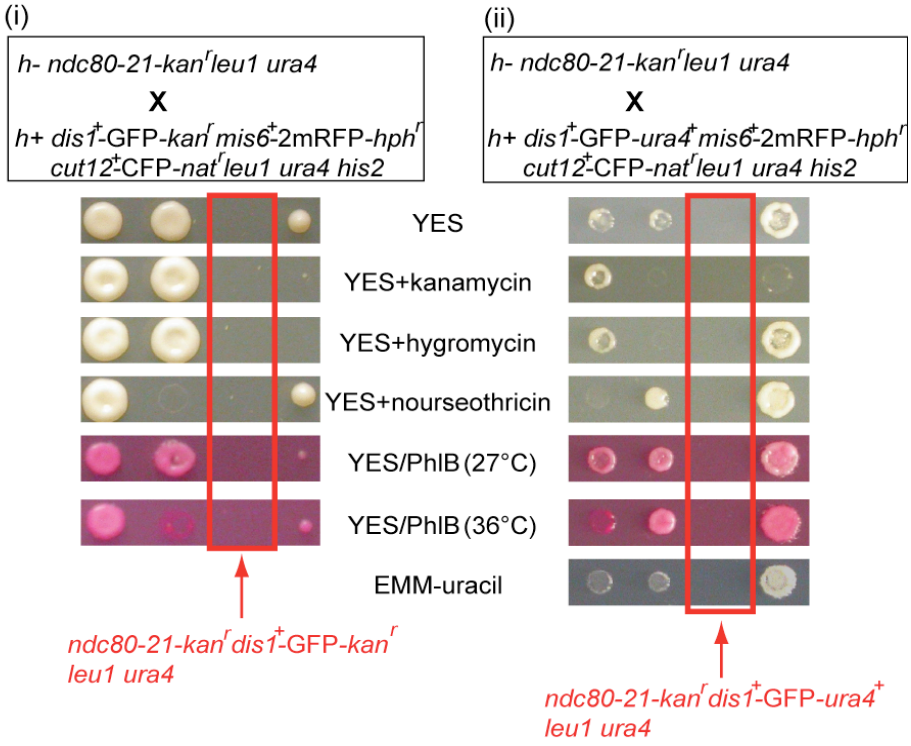

Figure 4.8 C-terminal tagging of Dis1 is lethal with *ndc80-21*.

Two different *dis1*$^+$-GFP strains were individually crossed with an *ndc80-21* strain (i) and (ii). In both cases, the crossing was found to be lethal.

still manage to proliferate, suggesting that at the permissive temperature, the degree of misfolding of the dynamic internal loop is in a tolerable range. However, when one of the key factors of the Ndc80 loop-dependent proliferation machinery is disturbed, like C-terminal tagging of Dis1 in this case, cells may become inviable. From this finding I postulate the C-terminal region of Dis1 may be important for the interaction with Ndc80 (see section 4.8.1).

Changing the strategy, I then tried the N-terminal tagging of Dis1 by GFP under the *nmt1*, *nmt41* and *nmt81* promoter. The *nmt1* promoter turns out to be too strong because it induced toxicity when the cells incubated at the low temperature even under the thiamine-repressive condition (note that a *Δdis1* strain is also cold-sensitive) (Figure 4.9A). Furthermore, the *nmt81*-GFP-Dis1 signals were somehow too weak in the rich media (thiamine-repressed) at 36℃ in my hands. I then decided to integrate *nmt41*-GFP-Dis1 into the endogenous locus in *ndc80-21*. Since the *nmt41* promoter is generally stronger than the average endogenous promoter even under the thiamine-repressed condition, I accordingly checked whether the integrated *nmt41*-GFP-Dis1 can rescue *ndc80-21*. Very similar to episomally overproducing Dis1, the integrated *nmt41*-GFP-Dis1 was able to rescue the mutant's ts phenotype even under the thiamine-repressed condition, but only at semi-permissive temperatures and importantly, not at 36℃(Figure 4.9B and not shown). This result echoes my previous multicopy suppressor experiment (see Figure 4.2), and at the same time allowed me to find a proper condition (36℃) where the N-terminal tagging of Dis1 by *nmt41*-GFP may have relatively little effect on the fluorescent quantification in *ndc80-21*.

Cut12-CFP and Mis6-2mRFP were also introduced into the same strain as an SPB and a kinetochore marker, respectively. Cells were incubated at 36℃ for 2 hr, followed by immediate fixation with chilled methanol at -80℃ for 30 min. Mitotic cells were imaged and the GFP intensity was quantified. In the wild type cells, Dis1 signals were perfectly colocalised with the kinetochore dots in early

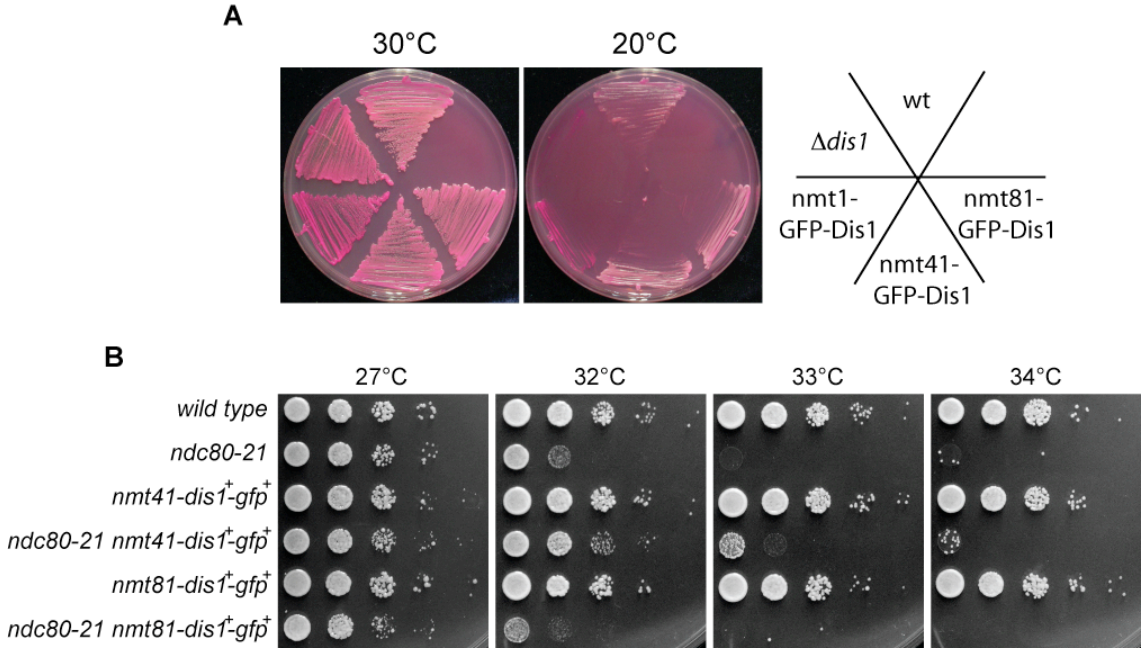

Figure 4.9 Effects of *nmt*-GFP-Dis1 expression in wild type and *ndc80-21*. (A) *nmt1*-GFP-Dis1 confers a cold-sensitive phenotype in wild type cells in the thiamine-repressive condition (YE5S/Phloxin B plate). (B) *nmt41*-GFP-Dis1 partially rescued *ndc80-21* in the thiamine-repressive condition (YE5S plate).

mitosis as reported (Nakaseko et al., 2001, Aoki et al., 2006) (Figure 4.10); in sharp contrast, signals of GFP-Dis1 were largely reduced from the kinetochores in *ndc80-21* (~70% reduction compared to wild type). The kinetochore GFP-Dis1 signals were also decreased when overproducing mutant Ndc80 loop-less proteins in a wild type strain (not shown). Collectively, I conclude the internal loop malfunction caused by L405P mutation results in the delocalisation of Dis1 from the kinetochores, consistent with my mutation array data indicating that L405P drastically weakens the binding of Dis1 to the Ndc80 loop.

4.5 Δ*dis1* mutant exhibits the same spindle phenotype as *ndc80-21*

Results so far pointed towards the idea that Dis1 is a critical microtubule/kinetochore factor that determines kinetochore microtubule stability in an Ndc80 loop-dependent manner. If this argument is correct, one should expect to see similar unstable spindle phenotypes in the *dis1* mutants. However, morphologies of unstable preanaphase spindles in *dis1* mutants have not been described in previous studies (Ohkura et al., 1988, Nabeshima et al., 1995, Nabeshima et al., 1998). To scrutinise this inconsistency, I revisited the *dis1* deletion mutant. I tagged Δ*dis1* with a tubulin, kinetochore, and SPB marker by GFP-Atb2, Mis6-2mRFP, and Cut12-CFP, respectively. Δ*dis1*, a cold-sensitive mutant, was subjected to live imaging after incubation at 20℃ for 4 hr. Under this condition, Δ*dis1* clearly exhibited extremely unstable phase II spindle morphologies (Figure 4.11), indistinguishable from those observed in the *ndc80-21* mutant and cells overproducing Ndc80 loop-less mutant proteins. Similarly, kinetochores were also close to the spindle poles without congressing to the metaphase plate. This was accompanied with the prolonged mitotic delay, presumably due to the SAC activation like in *ndc80-21*. These data thus strengthen my conclusion that Dis1 delocalisation from the kinetochores is responsible for the spindle instability and the fragile kinetochore-microtubule attachment when the Ndc80 loop is malfunctioned. Why were the defective

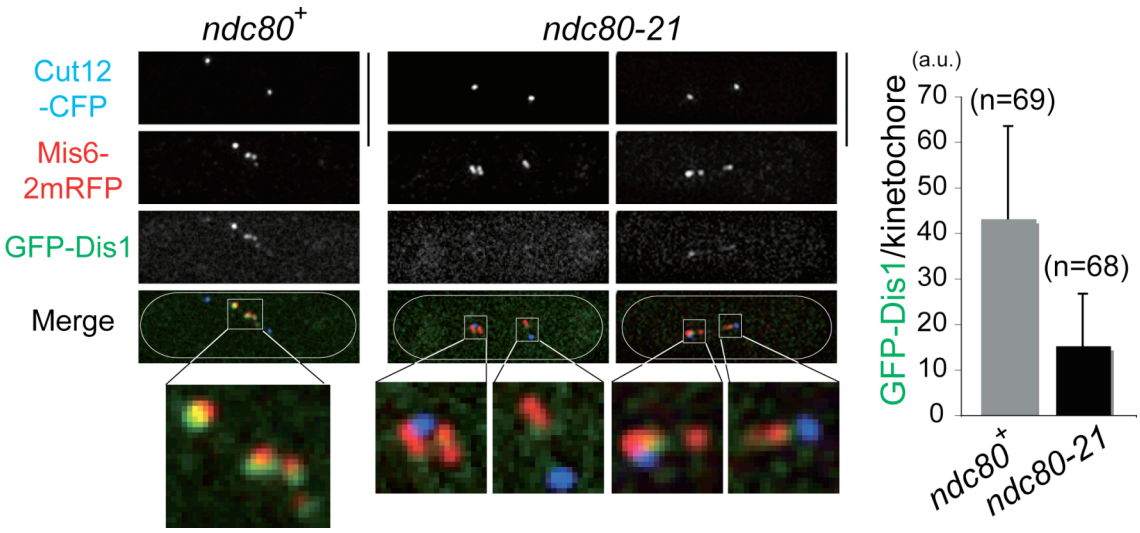

Figure 4.10 The kinetochore localisation of Dis1 is impaired in *ndc80-21*.
Cells were cultured at 36℃ for 2 hr before fixation. The mitotic cells were pictured and the signal intensity was quantified. Quantification is shown on the right. Error bars represent the standard deviation. Sample numbers are indicated in parentheses. Scale bars, 5 μm.

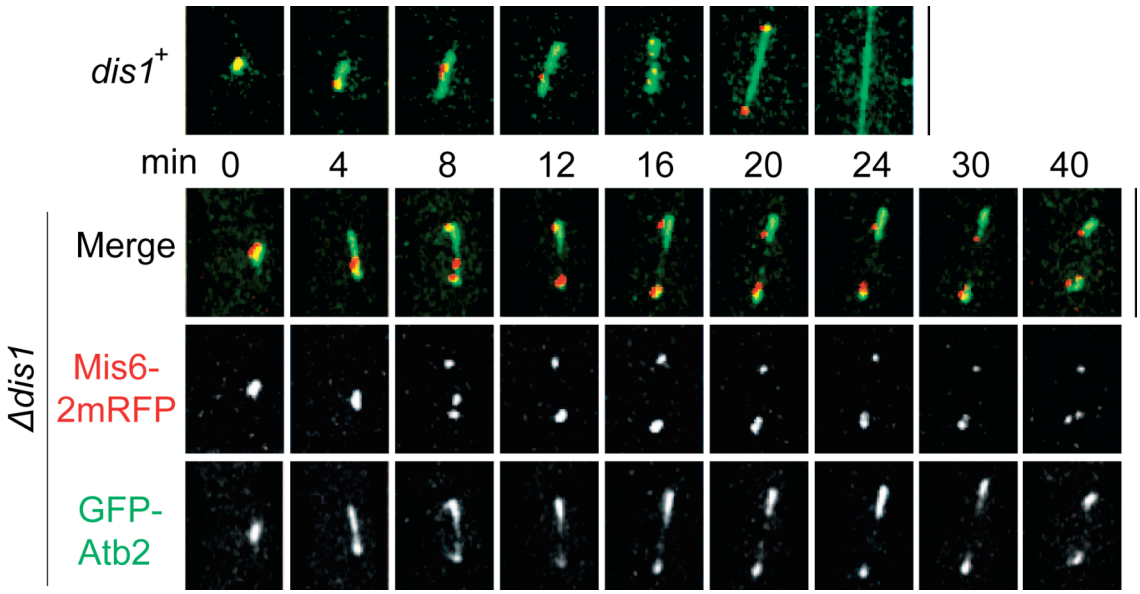

Figure 4.11 Unstable spindle phenotypes in the dis1 deletion mutant.
Cells were grown in YE5S liquid culture at 20℃ for 4 hr and time-lapse imaging was performed. Scale bars, 5 μm.

phenotypes overlooked in previous studies? One possible reason could be that in previous work, microtubules were observed either at the non-restrictive temperatures or in fixed cells with conventional immunostaining with anti-tubulin antibodies. I suspect that without the combined usage of the strict restrictive temperature (20°C) and time-lapse live imaging of microtubules (GFP-Atb2), unstable pre-anaphase microtubules would not have been noticed nor would they be properly interpreted. In fact these unstable microtubules (two blobs without inter-SPB microtubules) were previously reported as anaphase B spindles in which the central part was depolymerised (Ohkura et al., 1988, Nabeshima et al., 1995).

4.6 Tethering Dis1 to endogenous Nuf2 rescues *ndc80-21*

My data have collectively built up an interpretation that the delocalisation of Dis1 is the primary defect of malfunction of the internal loop in *ndc80-21*. A logical prediction extended from this concept is: adding Dis1 back to the Ndc80 complex would suppress the *ndc80-21* mutant phenotype at the physiological level of Dis1 without the need for overexpression. To test this hypothesis, I constructed a strain containing a *nuf2*$^{+}$-*dis1*$^{+}$ fusion gene, which is under control of the endogenous *nuf2*$^{+}$ promoter at the original *nuf2*$^{+}$ locus. At the same time, to learn more about the domain contribution of the *dis1*$^{+}$ gene, constructs that contain only the N-terminal or C-terminal half of *dis1*$^{+}$ fused to *nuf2*$^{+}$ were also made. The former represented the tandem TOG motifs, whilst the latter contained the serine-rich/basic linker plus the coiled-coil domain in the C-terminal end (Ohkura et al., 2001). These strains were then crossed with an *ndc80-21* allele. Strikingly, full length Dis1 fused to Nuf2 indeed partially suppressed the temperature and TBZ sensitivity of *ndc80-21* (Figure 4.12). However, fusing only Dis1 N-terminus or C-terminus to Nuf2 did not have the same complementary activity, rather slightly enhanced the heat and TBZ hypersensitivity, suggesting that both domains are required for the full function of Dis1 at the kinetochores. Alternatively, it is possible that the Nuf2 function

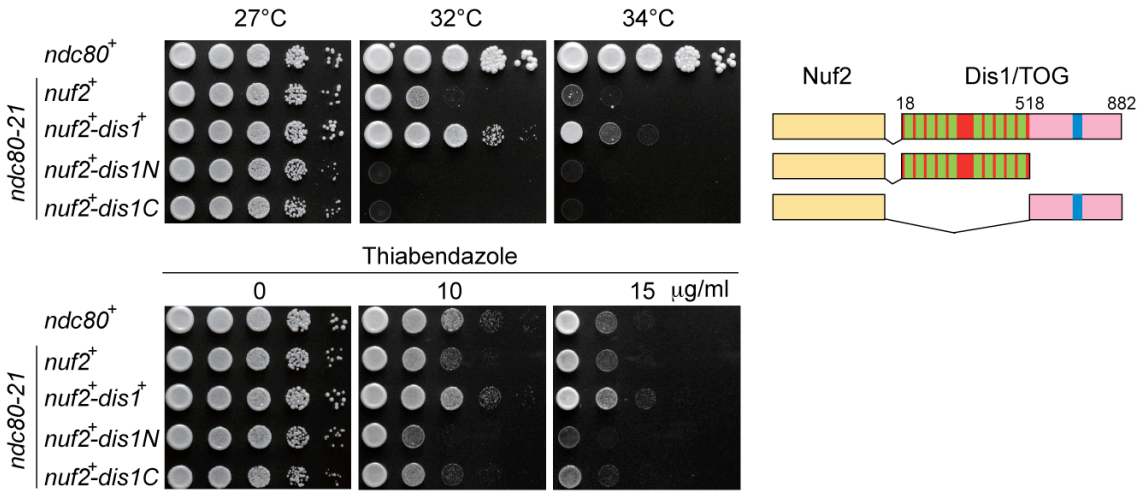

Figure 4.12 Tethering Dis1 to the Ndc80 complex rescues *ndc80-21*.
Full-length (18-882), N-terminal (18-518), or C-terminal (518-882) Dis1 was fused to Nuf2 and produced in the *ndc80-21* mutant. The N-terminal part of Dis1 contains two TOG repeats, each consisting of five HEAT repeats (green boxes), and the C-terminal domain contains a coiled coil domain (blue boxes) (see section 4.8 for more details).

might be somehow compromised by protein fusion in these two cases.

To confirm the Nuf2-Dis1 fusion protein indeed locates to the right place (i.e. the kinetochores), I attempted to observe the fusion protein signals by constructing a new strain containing *nuf2p-nuf2*$^{+}$*-dis1*$^{+}$*-gfp*$^{+}$. However, despite several efforts, strain construction was not successful. A possible reason for the difficulty might be the large size of Dis1-GFP (over 130 kDa), which is likely to interfere with Nuf2 function *in vivo*. I then tried to visualise the Nuf2-Dis1 fusion protein by using indirect immunofluorescence staining. But the only available anti-Dis1 polyclonal antibody, a generous gift from Dr. Mitsuhiro Yanagida's lab which I sincerely appreciated, was regrettably not working well in immunoblotting, immunoprecipitation or immunofluorescence imaging (previously warned by the sender that this antibody might be too old to use). However, as the *nuf2*$^{+}$ gene is essential for Ndc80 complex function, I assume the only copy of Nuf2, which is fused to Dis1, should incorporate into the Ndc80 complex at the outer kinetochores. To gain more insight into how Dis1 fused with Nuf2 functions in the cells, I measured several parameters in the condition where Nuf2-Dis1 fusion rescues *ndc80-21*, including cell number in liquid cultures (a readout of ts suppression), percentage of mitotic cells (a readout of SAC activation) and that of cells exhibiting chromosome mis-segregation (a readout of kinetochore malfunction). Indeed, cell number was increased at 32℃ in the *nuf2*$^{+}$*-dis1*$^{+}$ *ndc80-21* strain (Figure 4.13), which was accompanied by a substantial reduction of both mitotic and missegregating cells. This shows that stable spindle-kinetochore attachment and Ndc80-kinetochore function are at least in part restored by introduction of Nuf2-Dis1 to *ndc80-21*.

The nature of the way in which Dis1 is targeted by the Ndc80 complex is extremely interesting to me. Since tethering Dis1 to the C-terminus of Nuf2, from which the internal loop is about 20 nm away (Wan et al., 2009), successfully suppresses the defect of *ndc80-21*, I then asked whether the precise location of Dis1 is necessary for the suppression to happen. To this end, I targeted Dis1 to Mis12, another KMN component situates toward further the inner kinetochores. Mis12-Dis1, unlike Nuf2-Dis1, did not rescue *ndc80-21*

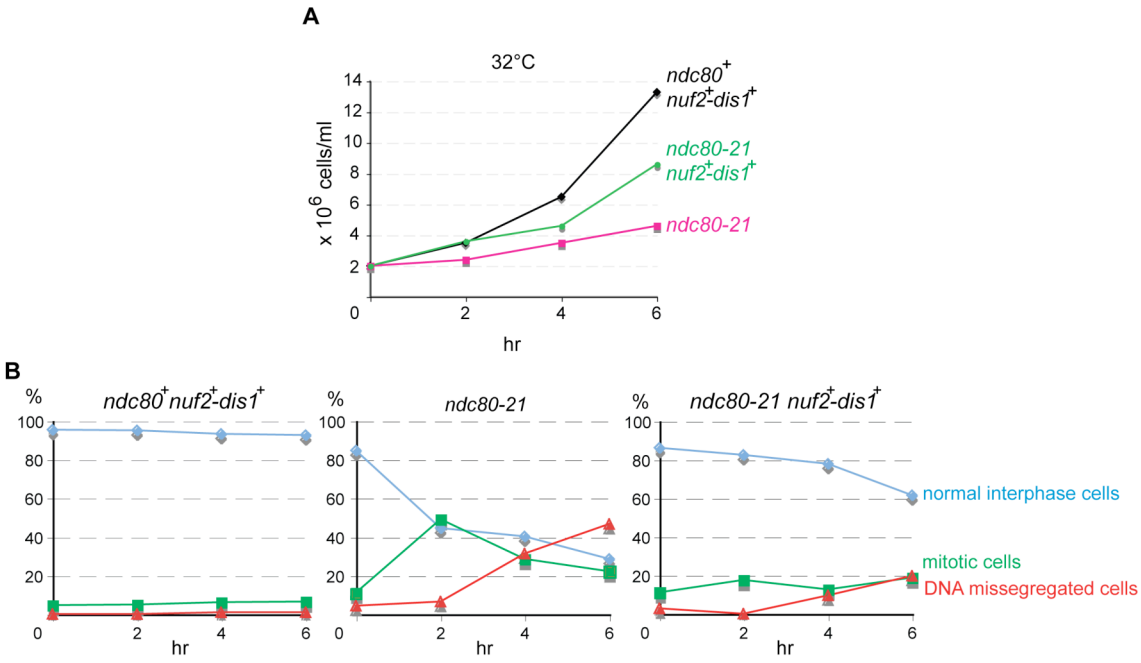

Figure 4.13 Liquid culture analysis of *ndc80-21* containing Nuf2-Dis1.

Indicated strains were grown in rich liquid media (YE5S) and incubated at 32℃. At each time point, cell number (A) and percentages of mitotic cells (a readout of SAC activation) and cells displaying chromosome mis-segregation (an indicator for kinetochore malfunction, stained with DAPI and Calcofluor) were counted (B, n > 100 at each time point).

(Figure 4.14). This intriguing observation suggests that the closer geometrical proximity of Dis1 to the internal loop is required for suppression of *ndc80-21.* Taken together, I conclude that *in vivo*, Dis1 is the major factor to coordinate with Ndc80 via direct interaction. These two proteins at outer kinetochores co-regulate microtubule dynamics and coordinate the function of each other for robust kinetochore-microtubule attachment.

4.7 Dam1 is not directly involved in Ndc80 loop-dependent microtubule dynamics in fission yeast

About the time when I discovered a direct link between Dis1 and Ndc80 internal loop in fission yeast, Dr. Tomoyuki Tanaka's group from Dundee claimed that in budding yeast, the internal loop of ScNdc80 is also crucial for establishing proper end-on KT-MT attachment, which is in accordance with my finding. But based on yeast two hybrid assay, they found it was the Dam1 complex that interacted with ScNdc80 internal loop in budding yeast (personal communication). Interestingly, two independent groups recently reported that *in vitro*, the Dam1 complex enhances the microtubule binding activity of the Ndc80 complex, demonstrating by the microtubule co-sedimentation assay and/or using the total internal reflection fluorescence (TIRF) microscope system (Tien et al., 2010, Lampert et al., 2010). However, this cooperation may require the existing microtubules, as these authors failed to show the biochemical evidence for the direct interaction between budding yeast Ndc80 complex and the Dam1 complex by analytical ultracentrifugation or gel filtration.

This information (from Dr. Tanaka) is extremely intriguing, as in fission yeast Dam1 has been reported to be important for faithful chromosome segregation (Sanchez-Perez et al., 2005), and I also found the genetic interaction between the *dam1* deletion mutant and *ndc80-21* (Figure 4.1). However, unlike budding yeast, in which *dam1*$^{+}$ is an essential gene, fission yeast *dam1*$^{+}$ is non-essential, suggesting the mechanism by which Dam1 is involved in establishing

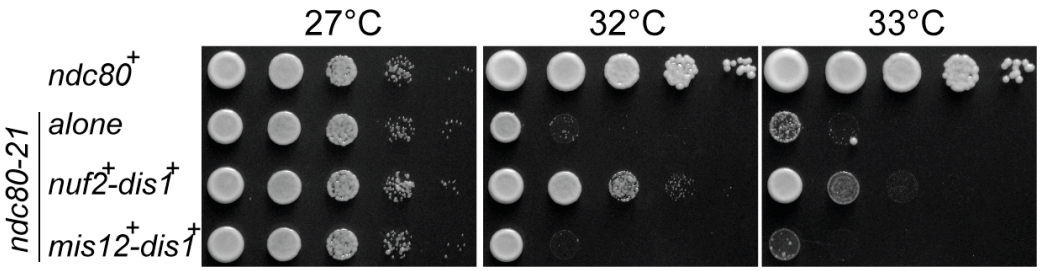

Figure 4.14 Fusion of Dis1 with Mis12 does not rescue *ndc80-21*.

An *ndc80-21* strain containing the Mis12-Dis1 fusion protein was constructed and spot tests were performed at indicated temperatures. Pictures were taken after 3 d incubation.

proper kinetochore-microtubule attachments may differ in two yeasts.

4.7.1 Dam1 does not physically interact with Ndc80

To scrutinise the potential difference between two yeasts, I examined whether or not the interaction between Ndc80 and Dam1 is conserved in fission yeast. It has been reported that the Dam1 complex component, Hos2, remains associated with the core centromeric regions (*cnt* and *imr*) in the *cut9-665* mutant (Kobayashi et al., 2007). I thus conducted immunoprecipitation using a *cut9-665* strain tagged with Ndc80-3Flag and Dam1-GFP. As shown in Figure 4.15, no clear sign of interaction between these two proteins was observed in my hands. These IP data, albeit negative, suggest that Ndc80 may not be the direct interacting point of Dam1 at the kinetochores. In agreement with this result, previous work done in fission yeast indicates that Dam1 localisation is dependent on Dad1 (Sanchez-Perez et al., 2005), another Dam1 complex component whose kinetochore localisation in turn requires Mis6 (a homologue of budding yeast Ctf3 and human CENP-I), but not Mis12, the KMN network component essential for kinetochore loading of the Ndc80 complex (Maskell et al., 2010, Petrovic et al., 2010, Hornung et al., 2011). Thus my data and results from other groups all suggest that Dam1 and Ndc80 may not directly interact with each other in fission yeast.

4.7.2 Localisation dependency

Probing further into how Dam1 could possibly be involved in Ndc80 loop function, I quantified the Dam1 signals at the kinetochore in *ndc80-21*. Unlike Dis1-GFP, in which the C-terminal tagging is synthetic lethal with the loop mutant, Dam1-GFP can be successfully introduced into *ndc80-21*. Upon shifting up to 36℃ for 2 hr, wild type cells and *ndc80-21* cells were fixed with methanol at -80℃ for 30 min. The GFP signals were measured in cells at the mitotic stage, judged by the patterns of an SPB (Cut12-CFP) and a kinetochore (Mis6-2mRFP marker). Compared to wild type, Dam1-GFP signals at the kinetochore were reduced by ~30% in *ndc80-21* (Figure 4.16A).

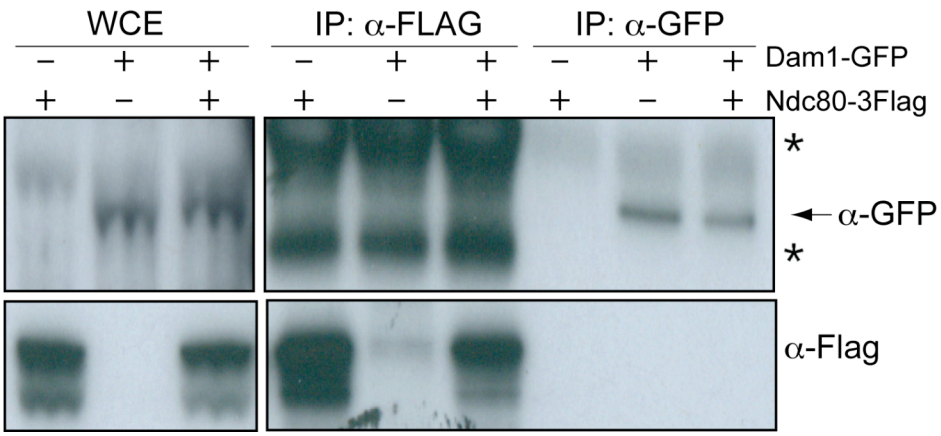

Figure 4.15 Ndc80 and Dam1 do not co-immunoprecipitate *in vivo*.
Cell extracts were prepared from three metaphase arrested *cut9-665* strains that contained Dam1-GFP only, Ndc80-3Flag only or Dam1-GFP and Ndc80-3Flag together, followed by a reciprocal immunoprecipitation using anti-Flag or anti-GFP antibody as a primary antibody. No coimmunoprecipitation was seen in either case. Asterisks indicate IgG bands. 1.67 mg extracts were used for immunoprecipitation. WCE, 50 µg.

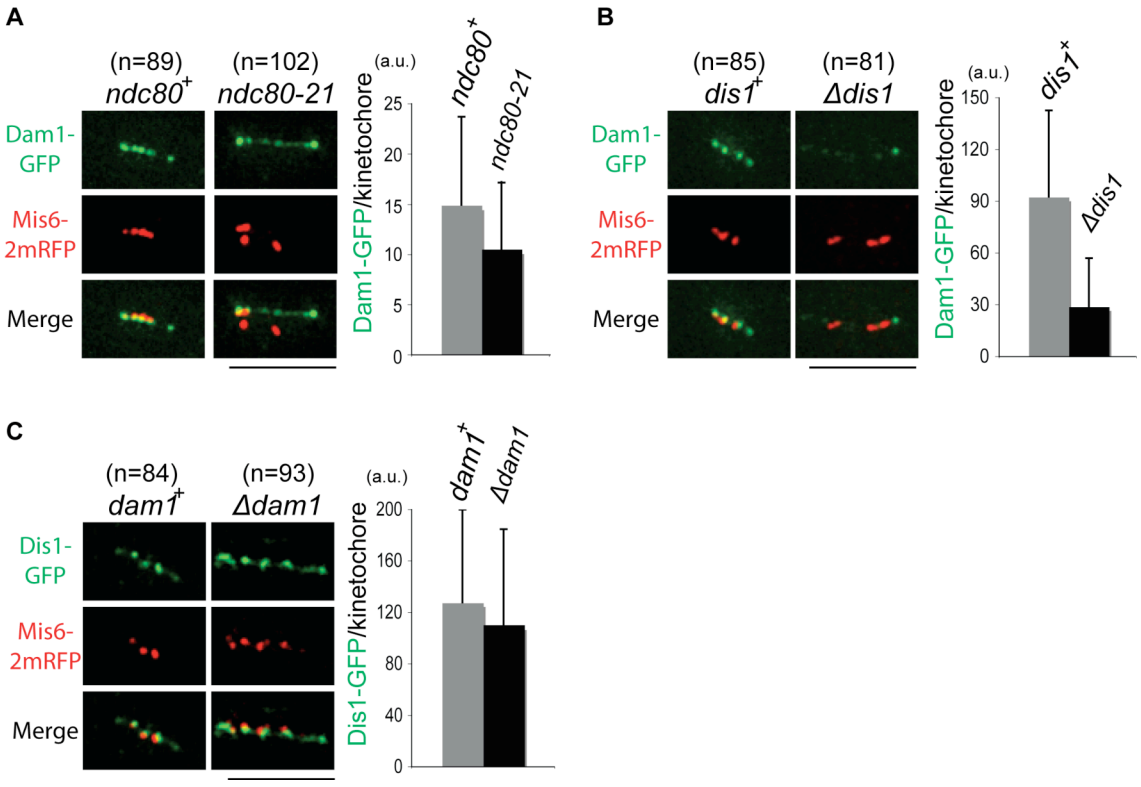

Figure 4.16 Dependency of kinetochore localisation.

Kinetochore localisation of Dam1-GFP signal intensities were reduced to ~70% in the *ndc80-21* mutant incubated at 36℃ for 2 h (A), whereas they dropped down to ~30% in the *dis1* deletion mutant incubated at 20℃ for 4 h (B). In striking contrast, intensities of Dis1-GFP signals were in large not significantly altered in the *dam1* deletion mutant (C) incubated at 20℃ for 6 h. Error bars represent the standard deviation. Sample numbers were indicated in parentheses. Scale bars, 5 μm.

Since no interaction has been detected between Dam1 and Ndc80, and microtubules are reportedly required for Dam1 loading onto kinetochores (Tien et al., 2010, Lampert et al., 2010), I postulate the signal reduction here may simply reflect the fact that spindle microtubules were extremely unstable in the *ndc80-21* mutant.

Given that Dis1 is identified as a major factor directly linked to Ndc80 loop function in fission yeast, I wondered whether Dam1 is indirectly linked through Dis1. Therefore I measured the signals of Dam1-GFP in the Δ*dis1* mutant, as well as the signals of Dis1-GFP in Δ*dam1*. Like Δ*dis1*, the Δ*dam1* strain is also cold sensitive (Kobayashi et al., 2007) (Takashi Toda, unpublished data), thus I incubated these mutants at 20°C for 4 to 6 hr for the appearance of the defective phenotypes. Strikingly, compared to wild type, Dam1-GFP signals were dramatically reduced from the kinetochores (up to ~ 70% reduction) in the Δ*dis1* mutant (Figure 4.16B). In contrast, the signals of Dis1-GFP did not display significant change in the Δ*dam1* mutant (Figure 4.16C). Together with the above data, it is possible that as in *ndc80-21*, the signal reduction in Δ*dis1* is due to the extremely unstable spindle microtubules, on which Dam1 relies for the kinetochore localisation. Alternatively, Dam1 may hierarchically act downstream of Dis1, which in turn depends on the interaction with Ndc80 loop to dock at the kinetochore. Intriguingly, when Tanaka's group evaluated the microtubule binding ability of the Ndc80 loop-less mutant proteins, they found no difference in the degree of enhancement by the Dam1 complex, in constrast with their *in vivo* observation (Maure et al., 2011). This apparent inconsistency suggests two possibilities: (1) in budding yeast Dam1 interacts with another region of Ndc80, not the internal loop (Alushin et al., 2010, Alushin and Nogales, 2011), or (2) a missing factor that acts as an intermediate between Ndc80 loop and the Dam1 complex *in vivo*. Consistent with the second assumption, the interaction between budding yeast Dam1 and Stu2 (the Dis1/TOG ortholog) has been reported (Wong et al., 2007). Furthermore, similar unstable preanaphase spindles were also observed in the *stu2* mutant (Kosco et al., 2001), and the coordination between Stu2 and the Ndc80 complex has been implicated to promote spindle integrity in budding yeast (Ma et al., 2007).

It is thus not impossible that Stu2 may be the missing link between ScNdc80 and ScDam1.

Taken together, I argue that the mechanism of establishing chromosome biorientation might not be identical and rather could be different between budding yeast and fission yeast. In budding yeast, the Ndc80 loop might mediate the interaction with Dam1, most likely indirectly and need help from microtubules and/or other factors, to establish the robust end-on kinetochore-microtubule attachment; In contrast, the fission yeast Ndc80 loop directly recruits Dis1, a microtubule polymerase, to the outer kinetochore, the purpose of which is to regulate microtubule dynamics and thus ensure proper kinetochore-microtubule attachment.

4.8 Domain analysis of Dis1 protein

Thanks to many elegant structural, biochemical, high-resolution microscopic studies, our knowledge of how the Dis1/TOG/XMAP215 protein family functions toward the microtubules are remarkably advanced. Identifying Dis1 linked to Ndc80 function motivates me to explore further the mechanism underlying the coordination between these two proteins.

4.8.1 Region of Dis1 responsible for Ndc80 loop binding

Having established that the crucial function of Ndc80 internal loop is to recruit Dis1, one of the outstanding questions is which part of Dis1 is responsible for the Ndc80 loop binding. I continued this project to dissect the domains on Dis1 for Ndc80 interaction. Dis1 contains 882 amino acids, with two HEAT-repeats-containing TOG domains near the N-terminus, followed by a serine-rich/basic residue rich linker in the middle, and a coiled-coil motif near the C-terminus, arrangement of which is relatively similar to other TOG proteins among species (Figure 4.17). Studies using analytical biochemistry and structural approaches

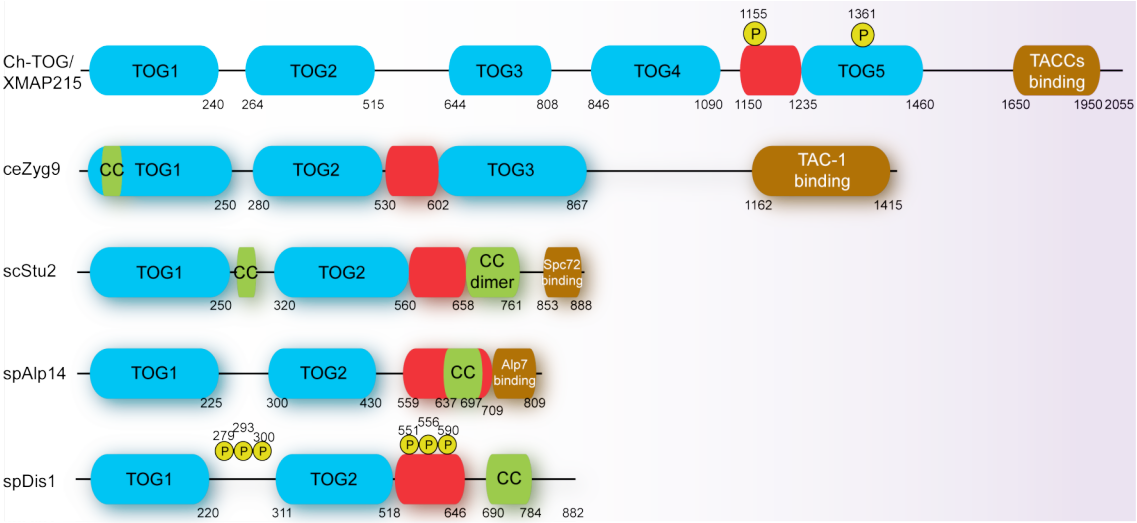

Figure 4.17 Structural summary of Dis1/TOG family proteins.

There are five TOG domains in Dis1/TOG homologues of higher eukaryotes, including human, frog, fly and plant; in *C. elegans*, there are three; in yeasts, there are only two in the N-terminal half of the protein. The red region marks the serine/basic residue-rich motif; the brown region indicates the site for binding to other proteins. CC, the coiled-coil domain. Note that the CDK phosphorylations have been demonstrated in XMAP215 and Dis1. This figure is adapted from (Widlund et al., 2011) and modified up-to-date.

have established the role of the N-terminal TOG domains of this protein family in tubulin heterodimer binding (Al-Bassam et al., 2006, Al-Bassam et al., 2007, Slep and Vale, 2007, Brouhard et al., 2008, Widlund et al., 2011). In line with this, so far all the identified binding partners of this protein family bind to their C-terminal regions (Lee et al., 2001, Cullen and Ohkura, 2001, Lauffart et al., 2002, Usui et al., 2003, Gergely et al., 2003, Srayko et al., 2003, Sato et al., 2004) (see summary in Figure 4.17). Furthermore, the corresponding N-terminal TOG motifs in Dis1 are reportedly diffused in cells and not sufficient to bind microtubules or other organelle structures when overproduced (Nakaseko et al., 1996). All together it suggests the C-terminus may predominantly determine the cellular localisation of Dis1/XMAP215 by anchoring other proteins. I thus assume the C-terminus of Dis1 may be important for its kinetochore loading through the interaction with Ndc80 loop.

To examine this, I set up to construct the GST-tagging expression plasmids that contain the C-terminal half of Dis1 including the Ser/basic linker and the coiled-coil motif (Dis1(520-882)), the basic linker alone (Dis1(520-645)), or the C-terminal region alone including the coiled-coil motif (Dis1(646-882)). Proteins were expressed in *E. coli* (strain FB810), and purified with glutathione-sepharose beads and a size exclusion column (Figure 4.18A). The gel filtration was done again with kind help from Dr. Martin Singleton's lab. Purification of these truncated proteins might not be performed under the optimised condition, as some protein degradation occurred during the purification processes. The peptide-binding assay was performed with these truncated Dis1 proteins. As predicted (Figure 4.18B), the binding pattern of Dis1(520-882) was relatively similar to that of the full length Dis1, whereas Dis1(646-882) exhibited the same binding pattern as full length Dis1. In addition, Dis1(520-645) clearly did not bind to any region on the Ndc80 loop, indicating the corresponding binding motif resides within the C-terminal region. It is of note that, when I applied the purified Dis1 N-terminal half (Dis1(18-518)) to the peptide membrane, the binding pattern was also similar to that of the C-terminal half (Dis1(520-882)). I currently have no reasonable interpretation of this result. Nevertheless, among those newly purified fragments peptide binding

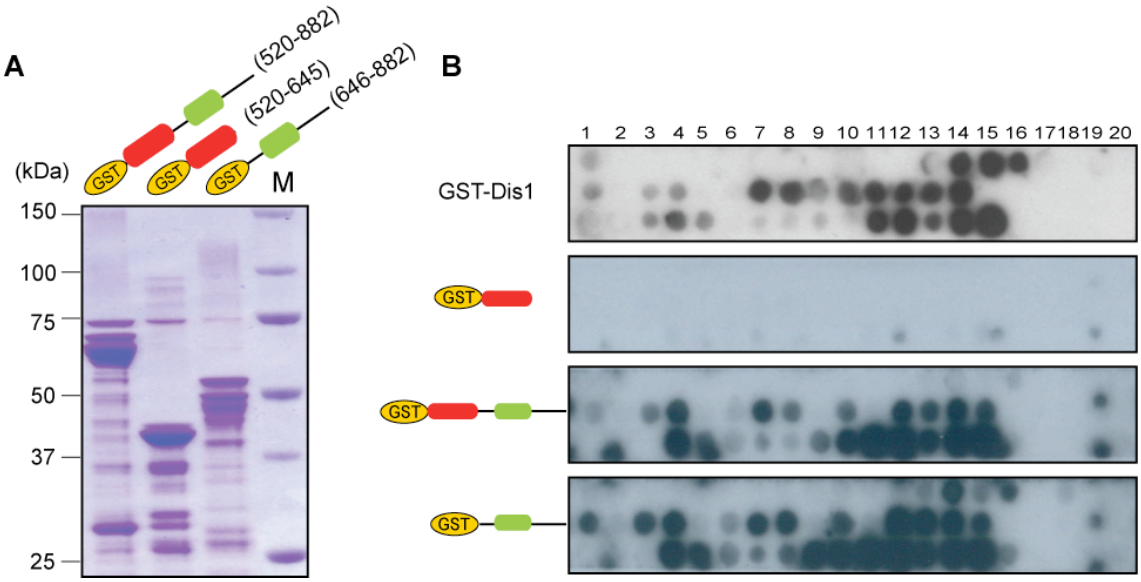

Figure 4.18 Ndc80 loop binds the C-terminus of Dis1.

(A) The truncated recombinant proteins were expressed and purified from *E. coli*. (B) The peptide array was conducted to dissect the domain responsible for Ndc80 binding. Note that the binding pattern of C-terminus alone was similar to that of full length Dis1 (from Figure 4.6), whereas the serine/basic linker showed no interaction.

peptide binding patterns of Dis1(646-882) whose is most similar to that of the full-length Dis1 (the whole data set is presented in Appendix 2).

These *in vitro* binding data might be correlated with the puzzling synthetic lethality between the Dis1 C-terminal tagging strain and the *ndc80-21* mutant (Figure 4.8). Perhaps the C-terminal tagging of Dis1 compromises the binding between Ndc80 and Dis1. Consistent with this, a previous report shows that *in vivo*, episomally overexpressing the C-terminus of Dis1 (from amino acid 658 to 882) tagged with YFP is sufficient to localise at the kinetochore during mitosis and at the kinetochore/SPB in interphase (Nakaseko et al., 2001).

4.8.2 The serine-rich/basic linker of Dis1 interacts with polymerised microtubules

While the molecular function of the middle serine-rich/basic linker (amino acids 520-645) in Dis1 remains uncertain, the corresponding domain in budding yeast Stu2 and *Xenopus* XMAP215 has been implicated in direct binding onto the polymerised microtubular lattice (Wang and Huffaker, 1997, Widlund et al., 2011). Accordingly I performed the microtubule co-sedimentation assays to ask whether this microtubule binding activity of the basic linker is conserved in Dis1. Paclitaxel (commonly named as taxol), a microtubule stabilising drug, was used to promote polymerisation of the purified bovine brain tubulins, a generous gift from Dr. Thomas Surrey's lab (Cancer Research UK London Research Institute, Microtubule Cytoskeleton Laboratory). The polymerised microtubules were serially diluted, and incubated with GST-Dis1 or GST-Dis1(520-645) in the presence of bovine serum albumin (BSA) at room temperature. After ultracentrifugation, the supernatant and pellet fractions were collected and analysed by SDS-PAGE and the proteins were visualised by coomassie brilliant blue staining. As shown in Figure 4.19A, while the BSA proteins were always found in the supernatant fraction, GST-Dis1 was clearly pelleted with the polymerised microtubules. Although a certain amount of GST-Dis1 proteins precipitated in the pellet fraction even without microtubules, which might be due to the low salt experimental condition (BRB80 buffer) and the room temperature

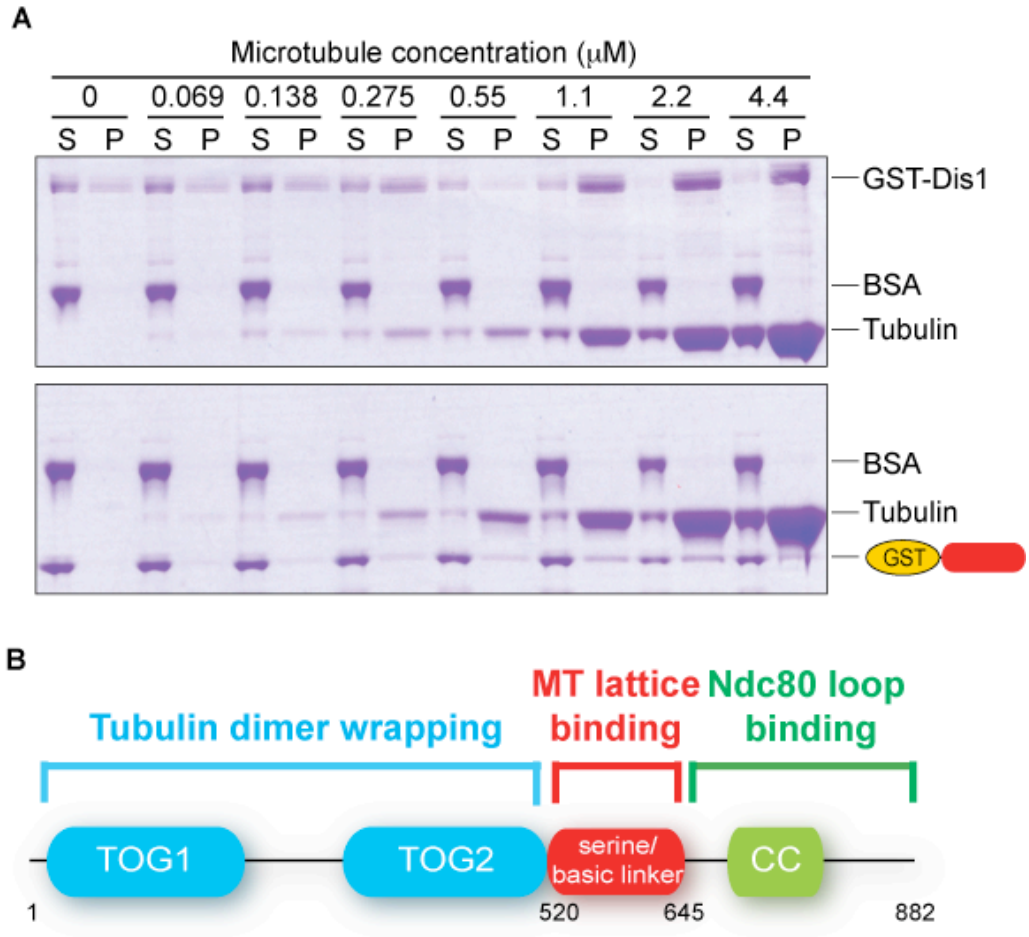

Figure 4.19 The serine/basic linker is capable of MT lattice binding.

(A) Microtubule cosedimentation assay. Taxol-polymerised MT were incubated with BSA and GST-Dis1 or GST-Dis1(520-645) (6 μg/μl) at the room temperature for 10 min, followed by ultracentrifugation with a TLA-100 rotor (80,000 rpm for 10 min). The supernatant and the pellet fraction were analysed by SDS-PAGE and stained with coomassie brilliant blue. Note that GST-Dis1(520-645) alone was capable of binding to the polymerised MT. (B) Summary of the domain analysis.

that is probably not optimal for Dis1 folding, the co-sedimentation clearly increased in a tubulin concentration-dependent manner, and the maximum binding rate was estimated more than 90% (meaning 90% of the total GST-Dis1 proteins bound to microtubules in the pellet fraction). Interestingly, GST-Dis1(520-645) also co-sedimentated with microtubules, with the maximum roughly half of the total proteins bound to microtubules. This result argues that the microtubule binding activity of the serine-rich/basic linker is functionally conserved at least in two yeasts and *Xenopus*. However, other regions of Dis1 may be required to maximise affinity for the microtubule lattice binding. In agreement with this, Dr. Mitsuhiro Yanagida's group have shown that either Dis1(518-646) or Dis1(645-882) alone is not sufficient to bind microtubules in a far-western binding assay, but when these two regions are merged, a stronger binding signal appeared (Nakaseko et al., 1996). Together with other reports, this domain analysis allows me to posit that the Dis1 protein can be divided into three major domains (Figure 4.19B): the N-terminal TOG repeats are able to embrace the free $\alpha\beta$-tubulin dimer, the middle serine rich/basic linker is to bind the microtubule lattice, and the C-terminus including the coiled-coil motif is likely responsible for Ndc80 loop interaction.

4.9 *dis1* phospho-mimic mutants

Upon live imaging observation, Dis1 shows a dramatic translocation during different cell cycle stages. It localises to cytoplasmic microtubules in interphase, which are outside the nuclear membrane. During G2-M transition, Dis1 drastically moves into the nucleus. In early mitosis, the majority of the proteins localises to the kinetochores through the Ndc80 loop interaction. In anaphase, Dis1 translocates again from kinetochores to anaphase B microtubules (Nakaseko et al., 2001). An interesting question is that since Ndc80 loop is the anchoring point of Dis1, why does Dis1 not always localise to kinetochores throughout the cell cycle?

4.9.1 The translocation of Dis1 between the kinetochores and the microtubules is regulated by phosphorylation

The important clue may lie in the finding that Dis1 is a canonical substrate of the Cdc2 kinase. Six residues in Dis1 have been identified as Cdc2 phosphorylation sites: T279, S293, S300, S551, S556, and S590. The first three residues situate between the two TOG domains; the later three locate within the ser/basic linker (Nabeshima et al., 1995, Aoki et al., 2006). In the *dis1*-6A mutant, in which the six phosphorylation sites are mutated into alanine, cells increase the minichromosome loss rate and exhibit a synthetic growth defect with *mis12-537*, another kinetochore mutant, suggesting Cdc2 phosphorylation affects Dis1's role in chromosome segregation fidelity (Aoki et al., 2006).

Inspired by this study, I sought to ask whether the Dis1 phosphorylation could potentially link to and/or affect the kinetochore Ndc80 function. The *dis1*-6E phospho-mimic and the *dis1*-6A non-phosphorylable mutants were received from NBRP (National BioResource Project, Japan). In these strains, the endogenous *dis1*$^+$ gene was disrupted, where the ectopic *dis1*$^+$, *dis1*-6E, or *dis1*-6A gene was C-terminally tagged with GFP and integrated into the genome at the *lys1*$^+$ locus under control of the *dis1*$^+$ endogenous promoter.

To observe the mitotic movement of these Dis1 phospho-mutant proteins, I additionally tagged these strains with Mis6-2mRFP and Cut12-CFP as the kinetochore and SPB marker, respectively. During interphase, the localisations were not noticeably different in those three strains (not shown). In early mitosis, Dis1-6E-GFP accumulated predominantly at the kinetochore dots, and moved together with the kinetochores toward the spindle pole bodies during anaphase A (Figure 4.20A). When anaphase B started, Dis1-6E-GFP seemed to release from the SPB/kinetochore clusters to the elongating interpolar spindles, but in most cases absent from the overlapping midzone area. This dynamic movement of Dis1-6E-GFP was indistinguishable from that of wild type Dis1-GFP (not shown). However, different from the previous report, I did not observe a significant reduction in terms of the translocation from the kinetochores to

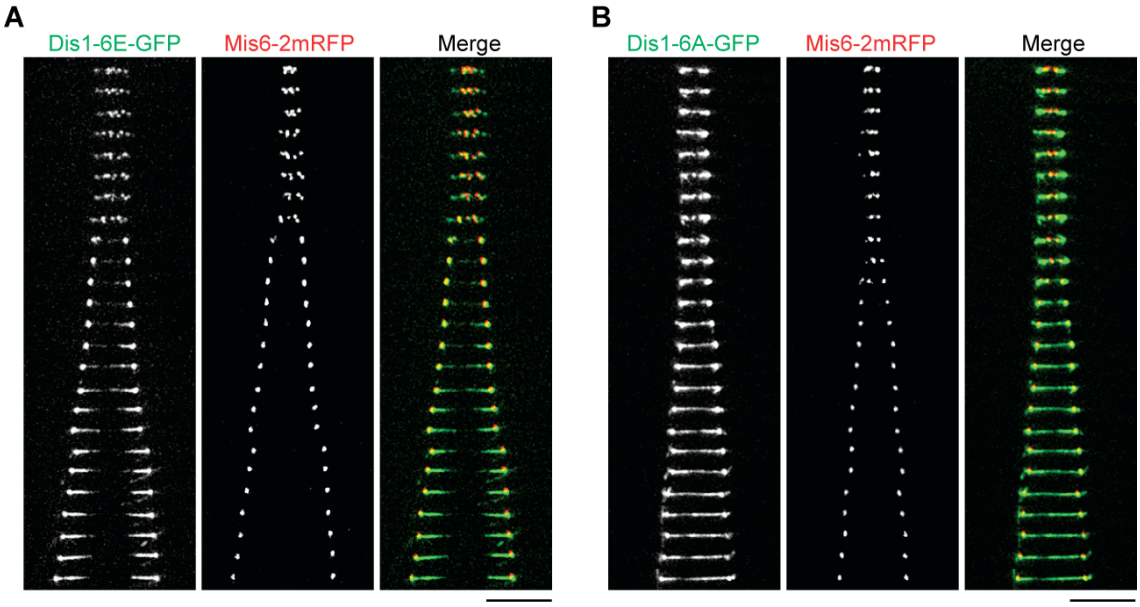

Figure 4.20 Behaviours of *dis1* phospho mutants in mitosis.

Exponentially growing cells at 27℃ were live-imaged for the *dis1*-6E mutant (A) and the *dis1*-6A mutant (B). More than 15 cells were recorded in each strain, and the images of the representative cells were converted into a kymograph here. Bars, 5 μm.

the interpolar microtubules between Dis1-6E-GFP and Dis1-wt-GFP. In sharp contrast, Dis1-6A-GFP predominantly occupied the SPBs and all along the spindle microtubules from the beginning of mitosis. Because of this, it was difficult for me to quantify whether or not the protein intensity at the kinetochore was reduced (Figure 4.20B). Nevertheless, these observations are generally consistent with the previous report (Aoki et al., 2006), and imply that in mitosis, when the Cdc2 kinase activity is high, Dis1 is phosphorylated and tends to deposit at the outer kinetochore, helping Ndc80 to stabilise the bound kinetochore microtubules, thereby ensuring the robust kinetochore-microtubule attachment; upon entry into anaphase A, Cdc2 kinase activity starts to decline and its counterpart phophatase, very likely Cdc14-related phosphatase Clp1 as proposed by Dr. Yanagida (also named Flp1), takes over the control to dephosphorylate Dis1, resulting in the protein translocation from the kinetochore to interpolar microtubules (Aoki et al., 2006).

4.9.2 Keeping the phosphorylated status of Dis1 by deleting phosphatase Clp1 suppresses *ndc80-21*

Since the translocation of Dis1 between spindle microtubules and the kinetochores depends upon Cdc2 phosphorylation and the counterpart phosphatase activity, the genetic manipulation of the Dis1 phosphorylation status may possibly affect *ndc80-21*. I thus crossed the *ndc80-21* mutant with a phosphatase deletion strain, *Δclp1*, and theoretically it would keep the phosphorylation status of the endogenous Dis1 protein as high as in the mitotic stage. Indeed, deletion of Clp1 phosphatase also partially suppressed the growth defect of *ndc80-21* at the semi-permissive temperature (Figure 4.21), suggesting that Ndc80-Dis1 interaction (or function) might be regulated by the phosphorylation control of Dis1. However, I failed to see difference between the recombinant GST-Dis1-6E and GST-Dis1-6A proteins in their binding abilities to Ndc80 loop, which was assessed by the *in vitro* peptide array (see Appendix 2). Further careful examinations are required to understand how Dis1 phosphorylation (and Clp1) affects Ndc80-Dis1 function.

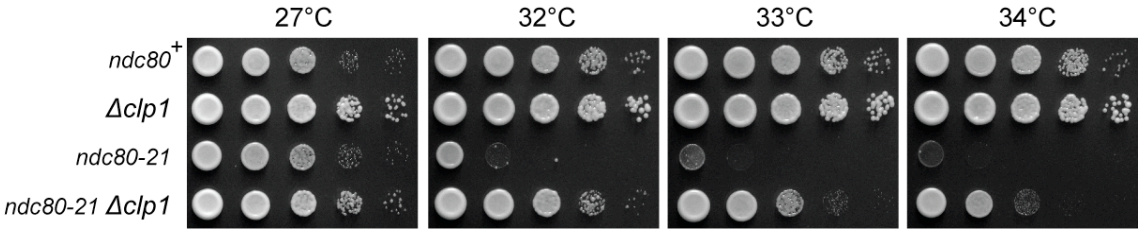

Figure 4.21 Deletion of Clp1 phosphatase partially rescues *ndc80-21*.

The spot assay was performed with the indicated cells and the plates were incubated at various temperatures.

4.10 Summary

Genetic analysis posits the potential yet complicated coordination of several microtubule-associated proteins with Ndc80-depedent microtubule dynamics at the kinetochore-microtubule interface. Episomal expressions of various MAPs reveal that Dis1 is a multicopy suppressor of *ndc80-21*, implying the major role of Dis1 correlated with Ndc80 loop function. Various approaches are used to demonstrate direct interaction between the Dis1 and Ndc80 proteins, including *in vivo* protein pull-down, co-immunoprecipitation, and *in vitro* peptide binding assay. The interaction is abolished upon Ndc80 loop deletion or mutations in the critical residue (L405) in the loop. Consistently, fluorescent quantifications of the Dis1 proteins at the kinetochores are also proved to be drastically reduced in the *ndc80-21* mutant, indicating binding between these two proteins is through the internal loop of Ndc80. Furthermore, the Δ*dis1* mutant indeed exhibits the unstable spindle microtubule phenotypes very similar to those seen in *ndc80-21*. Importantly, artificial tethering Dis1 back to the Ndc80 complex (by fusion with Nuf2), but not to the Mis12 complex, partially suppresses *ndc80-21* without the need of overexpression. Taken together, I conclude that the delocalisation of Dis1 from the kinetochore is the primary defect in *ndc80-21*, which in turn causes microtubule instability and the following improper kinetochore-microtubule attachment. In fission yeast, Dam1 seems not to directly interact with Ndc80, and the Dam1 signal reduction at the kinetochore in *ndc80-21* or Δ*dis1* may be ascribable to the feature of unstable microtubules, as the spindle integrity is required for the Dam1 loading onto the kinetochore. In constrast, no significant change of the Dis1 signals at the kinetochore is observed in the Δ*dam1* mutant, and therefore it is also plausible that Dam1 may hierarchically act downstream of Dis1 in terms of the kinetochore localisation. Preliminary domain analysis reveals that the C-terminus of Dis1 is responsible for Ndc80 loop binding. On the other hand, the middle serine/basic linker region in Dis1 may directly bind to the microtubule lattice, despite the modest MT-binding affinity. Lastly, the translocation of Dis1 between microtubules and kinetochores appear to rely on Cdc2 kinase activity, by which the

phosphorylation status of Dis1 is correlated with the protein's localisation during mitosis. Interestingly, keeping the phosphorylated status of Dis1 by deleting Clp1, a phosphatase counteracting Cdc2, partially suppresses the growth defect of *ndc80-21*, suggesting that the involvement of Clp1 in Ndc80 function is likely through dephosphorylation of Dis1 at the kinetochore.

4.11 Discussion

4.11.1 The two-domain model

The classic "search and capture" model casts the foundation of kinetochore-microtubule field for more than two decades (Kirschner and Mitchison, 1986). But important questions such as how microtubule associated proteins interact with the kinetochore were not considered in the original proposal. Regarding energy consumption, the "search and capture" process should not be random, and rather needs to be accurately efficient in a given time frame. Therefore cells must develop a way to avoid too many futile attempts to properly attach and successfully congress the kinetochore to the metaphase plate. This view is consistent with the fact that *in vivo* the emanating microtubules, once attached by the kinetochore, are much more stable than other spindle microtubules during mitosis (Brinkley and Cartwright, 1975, Salmon et al., 1976, Mitchison and Kirschner, 1985, Mitchison et al., 1986, Hayden et al., 1990). Nevertheless, the underlying mechanism of how the kinetochore stabilises attached microtubules still remains mysterious.

This chapter is the highlight of my study. Identifying Dis1 as a suppressor of the Ndc80 loop mutant prompted me into the close examination of relationship between these two proteins. The first Dis1/TOG family member, XMAP215, was identified as a factor that promotes microtubule assembly and dynamics (Gard and Kirschner, 1987). Later on, a classic *in vitro* study demonstrated that the features of *in vivo* MT dynamics can be reconstituted by mixing just three purified components: tubulins; the microtubule-stabilising protein, XMAP215;

and the KinI-related (currently named Kinesin-13) microtubule-destabilising kinesin, XKCM1, highlighting the prime roles of these two MAPs in MT dynamics regulation (Kinoshita et al., 2001). Most importantly, Dis1/XMAP215 has recently been shown to act as a processive microtubule polymerase at the MT dynamic plus-end (Brouhard et al., 2008). In early mitosis, Dis1 situates at the kinetochore-microtubule interface to accomplish faithful chromosome segregation (Nakaseko et al., 2001). Here I have shown, for the first time, that the fission yeast Dis1/TOG protein is recruited to the outer kinetochore by the interaction with the internal loop of Ndc80, the most important microtubule-binding component of KMN.

Taking all of my results together with previous studies, I propose a model that Ndc80 constitutes two functional microtubule-binding domains, the N-terminal domain and the internal loop, each of which is essential and acts coordinatively to establish proper kinetochore-microtubule attachment (Figure 4.22) (Hsu and Toda, 2011). Ndc80 laterally binds to microtubule lattices with its N-terminal globular domain, perhaps a mode of the initial interaction between the kinetochore and the spindle microtubule in yeasts and vertebrates (Wilson-Kubalek et al., 2008, Alushin et al., 2010); however, this initial binding may not be stable enough and often make the kinetochore detached from microtubules. As a result, the SAC is activated to halt the mitotic progression. The proper kinetochore-microtubule attachment is not established until Ndc80 uses its internal loop to hook Dis1 at the outer kinetochore close to the dynamic end of spindle microtubules. This configuration not only helps Ndc80 indirectly bind to microtubules via Dis1/TOG (as a second hand), but also allows Dis1/TOG to exert its polymerase activity to (1) promote polymerisation of the bound-MT and/or (2) protect the bound-MT from premature shrinkage, either of which promotes chromosome congression. When all the chromosomes are biorientedly attached and aligned at the metaphase plate, tension between sister chromatids is satisfied and the checkpoint is accordingly silenced. According to this two-domain model, Ndc80-Dis1/TOG interaction thus not only helps to secure the physical association between the kinetochore and the spindle microtubule but also could alter microtubule dynamics at the

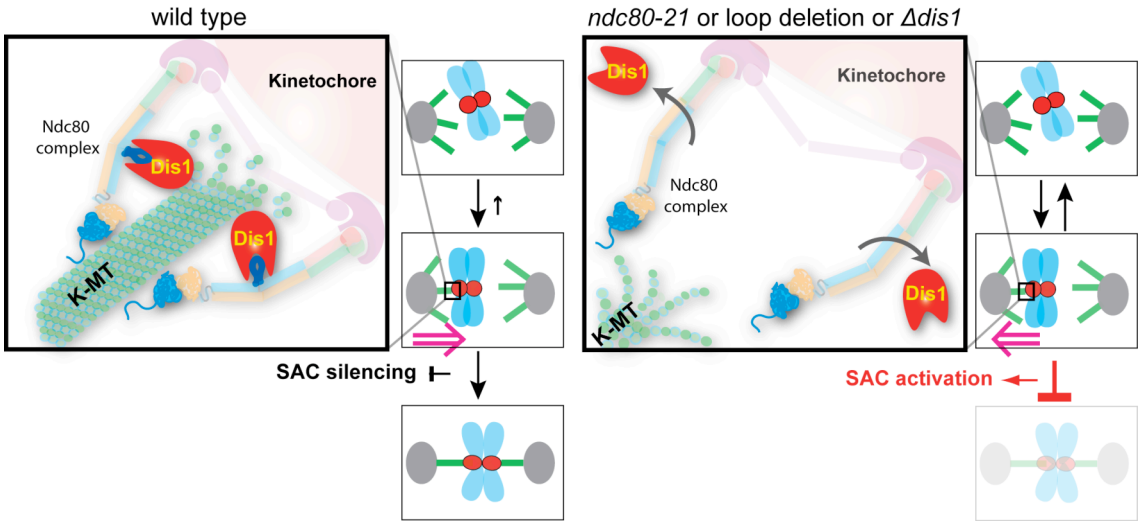

Figure 4.22 A "two-domain" model of the coordination of Ndc80 and Dis1. The N-terminal (CH and the N-tail) of Ndc80 laterally binds to microtubule lattice. The recruitment of Dis1 via Ndc80 loop not only confers the second hand for microtubule binding, but also promotes the stabilisation of the bound microtubule, which is required for the proper microtubule-kinetochore attachment and the following congression in mitosis. When the loop is malfunctional (by mutation or deletion) or dis1 is deleted, the initial binding of Ndc80 N-domains and microtubule lattices may not be stable enough to keep chromosomes aligned properly. As a result, the SAC is activated and the cell cycle is arrested.

kinetochore site.

In line with our finding, a recent report shows that in fly S2 cells, Msps (Dis1/TOG in fly) and γ-tubulin interact with Ndc80 at the kinetochore to promote the kinetochore-driven microtubule formation (Bucciarelli et al., 2009). Furthermore, a *tour de force* reconstitution of almost all the kinetochore components from budding yeast was recently achieved, and the purified kinetochore particles are found to directly stabilise the bound microtubules, which favours polymerisation with tension applied (Akiyoshi et al., 2010). I believe our finding adds an important insight into the longstanding question as to how the kinetochore stabilises microtubules *in vivo*.

4.11.2 Evolutional view of Ndc80 loop-dependent KT-MT attachment

Independent studies from Tanaka's group and our lab have converged to a similar conclusion that the physiological importance of the conserved Ndc80 internal loop relies on protein-protein interaction for integration of multiple MT-binding activities (Maure et al., 2011, Hsu and Toda, 2011). However, the binding partner of Ndc80 loop appears divergent in two yeasts. In fission yeast, the Ndc80 loop directly recruits Dis1 to the kinetochore to regulate spindle dynamics and ensure the proper kinetochore-microtubule attachment, whereas in budding yeast, it is the Dam1 complex recruited by Ndc80 loop to switch the kinetochore-microtubule interaction from weak lateral binding to robust end-on attachment.

It is intriguing to see the conserved loops of Ndc80 having such different binding preference in two yeasts. However, how ScNdc80 loop mediates Dam1 recruitment to the kinetochore is not clear from their report (Maure et al., 2011). Other factors (microtubule and/or Stu2) are likely to intermediate the interaction (Wong et al., 2007). Alternatively, the corresponding region of Ndc80 to interact with Dam1 may not reside at the internal loop, but rather locates near the CH domain, of which the responsible sequences might exist only in budding yeast (Alushin et al., 2010, Alushin and Nogales, 2011)(Stefan Westermann, unpublished data).

Despite some diversification, it is formally possible that these two yeasts evolved to use similar but different mechanisms to accomplish faithful chromosome segregation. Consistent with this view, Dam1 only exists in fungi, being essential in budding yeast but non-essential in fission yeast (Jones et al., 1999, Sanchez-Perez et al., 2005, Liu et al., 2005). In addition, the N-tail of budding yeast Ndc80 is not required for the protein's essential function, whereas the same tails of Ndc80 in *S. pombe* and vertebrate cells are absolutely essential (section 3.7). Those differences lead to an assumption that the Dam1 complex (coordinated with the Ndc80 complex) might play a unique role in chromosome segregation in organisms (e.g. budding yeast) with point centromeres, in which the kinetochore attaches only one microtubule (Kiermaier et al., 2009, Lacefield et al., 2009). On the other hand, when the kinetochores are attached by multiple microtubules in organisms that contain regional centromeres (3~4 MTs/kinetochore in fission yeast and about 20~25 MTs/kinetochore in human) (Ding et al., 1993, McEwen et al., 2001), microtubule dynamics must be tightly regulated for accurate chromosome segregations. I have shown here in fission yeast, the functional coordination of Ndc80 and Dis1 is crucial for the proper microtubule-kinetochore attachment and microtubule dynamics regulation. In the future, more work needs to be done to define how the Ndc80 loop contributes to facilitate the kinetochore-microtubule attachment in other organisms. Especially it will be of great interest to see whether a similar mechanism discovered here exists in higher eukaryotes.

4.11.3 Domain function and phosphorylation control of Dis1/XMAP215

According to the preliminary domain analysis described in this chapter (section 4.8), the serine/basic linker of Dis1 is at least in part involved in the MT lattice binding, whereas the C-terminal region of this protein is likely the site to which the Ndc80 loop binds. Together with several other reports I envision a possible configuration for the Dis1 protein at the outer kinetochore. That is, Dis1 binds to Ndc80 loop with its C-terminus. The C-terminal-hooking to Ndc80 flexible loop leads the middle ser/basic linker to spatially search and attach to the

microtubule lattice that is in the close proximity of microtubule plus ends, allowing the N-terminal TOG domains to bind the tubulin heterodimer and add to the microtubule dynamic end (Brouhard et al., 2008, Widlund et al., 2011).

In higher eukaryotes, XMAP215 and ch-TOG have five TOG repeats (Figure 4.17) (Charrasse et al., 1995, Charrasse et al., 1996, Charrasse et al., 1998). It was originally proposed that these five TOG domains serve as a template to bring up to 6~8 units of short α-β tubulin oligomers at one time adding to the microtubule plus end (Kerssemakers et al., 2006). This so-called “template” model could not explain well the case of yeast TOG proteins, where Stu2 in budding yeast and Dis1 or Alp14 in fission yeast only have 2 TOG repeats. Based on the analytical ultracentrifugation and immunoprecipitation studies, Tony Hyman’s group proposed that Stu2 forms a homodimer by entangling two molecules together through their C-terminal coiled-coil domain. This dimerisation allows Stu2 to form a tetra-TOG entity, which enables to wrap around a single free tubulin heterodimer for its microtubule-stabilising activity (Al-Bassam et al., 2006).

Alp14, the other TOG protein in fission yeast, might also form a dimer through Alp7 dimer tethering (Sato et al., 2004). Whether or not Dis1 forms a dimer *in vivo* is still an open question. Intriguingly, three positive regions in Ndc80 loop identified for Dis1 binding map exactly to the beginning, middle, and the end of the loop (Figure 4.6). The underlying reason(s) for this is unclear. It would be possible that one loop of Ndc80 may recruit more than one Dis1 protein to the kinetochores. Following this assumption, it is tempting to postulate that the loop may behave as the hooking point to gather two Dis1 to form an active homodimer: one by the beginning region and the other by the end region of the loop and glue the dimer together with the middle loop region. However, more careful examination including detailed structural or analytical biochemistry are required in the future for comprehensive understanding of the geometry between Dis1 and Ndc80.

With respect to phosphorylation, XMAP215 was found phosphorylated in a cell

cycle-dependent manner (Gard and Kirschner, 1987). A subsequent study reported that phosphorylation by Cdk1 regulates XMAP215 function *in vitro*, where the stabilisation activity of XMAP215 is affected but not the depolymerisation function, nor the MT lattice binding ability (Vasquez et al., 1999). Intriguingly, Cdk1 phosphorylation sites in XMAP215 reside within the serine/basic linker and the fifth TOG domain (Figure 4.17) (Gard et al., 2004), which are recently shown to be required for MT lattice binding and full enzymatic activity, respectively (Widlund et al., 2011). Why the phosphorylation only affects the polymerisation activity, but not MT lattice binding, is unclear. However, such phosphorylated XMAP215 might still be capable of suppressing XKCM1-induced catastrophes in M-phase extracts (Tournebize et al., 2000), suggesting that the ability of XMAP215 to regulate MT dynamics is more potent than that of XKCM1, or alternatively, phosphorylation might moderately affect the enzymatic activity of XMAP215 in *Xenopus*.

Cdc2 phosphorylation of Dis1 in fission yeast appears to regulate protein translocation during mitosis (Aoki et al., 2006). My observation basically agrees with Dr. Yanagida's group that the non-phosphorylable mutant proteins (Dis1-6A) prematurely and predominantly occupy along the whole spindles, despite that I still see the kinetochore-dot-like signals; in contrast, the phospho-mimic mutant proteins (Dis1-6E) behave similarly to the wild type Dis1, in which the proteins localise predominantly at the kinetochore in early mitosis, though they are still able to translocate to the interpolar microtubule later on (Aoki et al., 2006). Regarding the positions of the phosphorylation sites, three authentic Cdc2 sites of Dis1 have been mapped to the connecting region between two TOG domains, and another three sites are in the serine-rich/basic linker (Figure 4.17) (Nabeshima et al., 1995). It remains unclear why/how Cdc2 phosphorylation could influence the kinetochore localisation of Dis1. It is possible that all the domains of Dis1 are functionally, mutually interdependent, as this class of protein likely encounters a dramatic conformational change when exerting its enzymatic activity at the MT plus end (Al-Bassam et al., 2006, Brouhard et al., 2008). Alternatively, it is not impossible that in addition to localisation control, the phosphorylation might also affect other aspect of Dis1 at

the kinetochore, for example, its enzymatic activity. In line with this, I do not observe the affinity reduction between the Dis1-6E and Dis1-6A proteins to the Ndc80 loop on the *in vitro* peptide-binding assay (Appendix 2). Further domain analysis in greater detail will help us get closer to the underlying mechanism as to how these two proteins coordinate functions at the kinetochore-microtubule interface.

The fact that deletion of Clp1 partially suppresses *ndc80-21* makes the mechanism even more complicated (Figure 4.21). Although the role of Clp1 phosphatase has been linked to the Aurora kinase function at the kinetochores (Trautmann et al., 2004), which makes the interpretation currently difficult, the simplest explanation would be that the suppression by *clp1* deletion is primarily through Dis1's retention, and/or regulation of Dis1's activity at the kinetochore. In either case, it influences functional coordination between Dis1 and Ndc80, though the detailed mechanism is still unclear. Lastly, whether or not the dephosphorylation of Dis1 is through Clp1 phosphatase remains to be confirmed.

4.11.4 The role of Dis1 in Anaphase A

I noticed that Dis1 is still retained at the kinetochore during anaphase A, the transition when microtubule net depolymerisation overpowers polymerisation (see Figure 4.20 and Appendix 3). What Dis1 does at the depolymerising kinetochore-microtubule interface is currently unclear, but this observation implies an unusual characteristic of Dis1 that is reminiscent of the Dam1 complex in budding yeast. This is extremely interesting because so far only the Ndc80 complex, the Dam1 complex and Dis1/XMAP215 have been characterised as the kinetochore components whose movements are able to couple MT depolymerisation in the *in vitro* bead-coupling system (Westermann et al., 2006, Asbury et al., 2006, Brouhard et al., 2008, Powers et al., 2009).

Until chromosomes reach two opposite poles, the Dis1 proteins gradually release from the kinetochore and translocate to interpolar spindle microtubules. It is possible that Dis1 still manages to polymerise MT during anaphase A, but

MT-destabilising proteins such as Klp5 and Klp6 might override the control of MT dynamics at the kinetochores, which would override Dis1-dependent MT polymerisation. Alternatively, as under certain conditions Dis1 would instead promote the disassembly of a microtubule from its plus end (Vasquez et al., 1994, Shirasu-Hiza et al., 2003, van Breugel et al., 2003, Brouhard et al., 2008), Dis1 function and/or activity would be reversed at this stage, though the exact mechanism is currently unknown. Phosphorylation might somehow contribute to this aspect (Vasquez et al., 1999), while the local concentration of free tubulins might be another crucial determinant to trigger the functional switch of Dis1/XMAP215 (Brouhard et al., 2008, Widlund et al., 2011).

I presume that more complex regulatory networks/mechanisms might operate in accordance with the Ndc80 complex at the kinetochore to couple the end-on attachment during prometaphase/metaphase and subsequent chromosome poleward movement during anaphase A.

Chapter 5. The function of Ndc80 beyond mitosis

In vertebrate cells, it is generally believed that the Ndc80 complex starts to assemble onto the kinetochores upon mitotic entries, and disassembles from the outer kinetochores after chromosomal segregation in late anaphase (Wigge and Kilmartin, 2001, Nabetani et al., 2001, McCleland et al., 2003, Maiato et al., 2004, Cheeseman and Desai, 2008). However, studies in chicken DT40 cells reveal a dynamic association of the Ndc80 complex with the centrosome during interphase (late G2), though the molecular significance is unclear (Hori et al., 2003, Mikami et al., 2005). In contrast, the Ndc80 complex locates at the kinetochores throughout the whole mitotic cell cycle in both fission yeast and budding yeast (Rout and Kilmartin, 1990, Osborne et al., 1994, Wigge et al., 1998, Wigge and Kilmartin, 2001, Nabetani et al., 2001, Kniola et al., 2001). Despite its important role in mitosis, the function of Ndc80 in interphase is poorly understood. In this chapter, I describe the interphase roles of fission yeast Ndc80.

5.1 Distinct interphase phenotype in *ndc80-26*

One of the mutants I isolated is *ndc80-26* (Table 2.1). When the spindle morphology and kinetochore localisation were examined in this mutant after 4 hr incubation at 36℃, I found that many cells exhibited an unusual interphase abnormality: the kinetochore dots dissociated from the spindle pole body; furthermore and unexpectedly, these declustered kinetochores were found to colocalise with interphase microtubules (Figure 5.1). This extremely peculiar phenotype motivated me to look in more detail into this mutant.

The aberrance is intriguing in several aspects. Firstly, this unusual phenomenon has never been observed in wild type cells, in which three pairs of sister

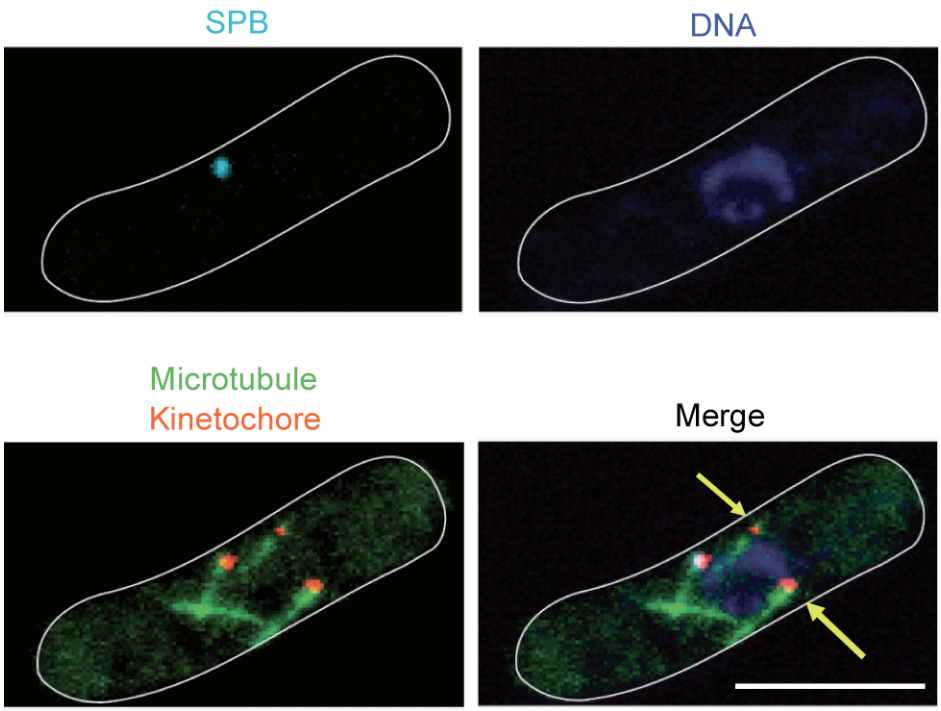

Figure 5.1 Abnormal interphase phenotype in *ndc80-26*.

The *ndc80-26* mutant was tagged with GFP-Atb2 (α2-tubulin), Mis6-2mRFP (a kinetochore marker) and Cut12-CFP (an SPB marker). Cells were incubated at 36℃ for 4 hr before fixation with 3.2% paraformaldehyde plus 0.3% glutaldehyde. DNA was stained by DAPI. Kinetochores declustered from the SPB are marked with yellow arrows. Scale bar, 5 μm.

centromeres/kinetochores are always tightly clustered as a single dot in the vicinity of the spindle pole body during interphase (Uzawa and Yanagida, 1992, Funabiki et al., 1993). Secondly, although similar kinetochore-declustering phenotypes have been described in the *mis6-302* and *nuf2-1* kinetochore mutants (Saitoh et al., 1997, Appelgren et al., 2003), the underlying reason is still unclear and importantly, colocalisation of the declustered kinetochores with the interphase microtubules is not noticed or does not occur in these mutants. Thirdly, given that the nuclear envelope (NE) retains intact throughout the cell cycle in fission yeast, the kinetochore dots should be in the nucleoplasmic site. In contrast, the interphase SPB and other iMTOCs, which are able to nucleate, anchor, and emanate cytoplasmic microtubules, are situated on the cytoplasmic site of the NE (Ding et al., 1993, Ding et al., 1997, Kniola et al., 2001). It is thus a tantalising puzzle as to how the declustered kinetochores could possibly colocalise with cytoplasmic microtubules?

5.2 The Ndc80 complex is involved in the kinetochore clustering at the SPB and the nuclear envelope integrity

Studies on two nuclear transmembrane protein families, the KASH and SUN families, which embed in the double layer nuclear envelope, shed light on the linkage between the cytoplasmic cytoskeletons and the nuclear chromosomes (Bornens, 2008, King et al., 2008, Starr, 2009, Hiraoka and Dernburg, 2009). In fission yeast, tethering SPB to the outer nuclear membrane (ONM) is achieved by the Kms1 and/or Kms2 transmembrane proteins (KASH proteins), which in turn connect Sad1 (a SUN protein) that spans throughout the inner nuclear membrane (INM) and bridges the nuclear chromosomes with an unknown linker (Figure 5.2). Another newly identified inner nuclear transmembrane protein, Ima1, has also been proposed to play a direct role in this process (Miki et al., 2004, King et al., 2008). However, the view that Ima1 contributes to centromere-SPB anchoring is currently challenged (Hiraoka et al., 2011).

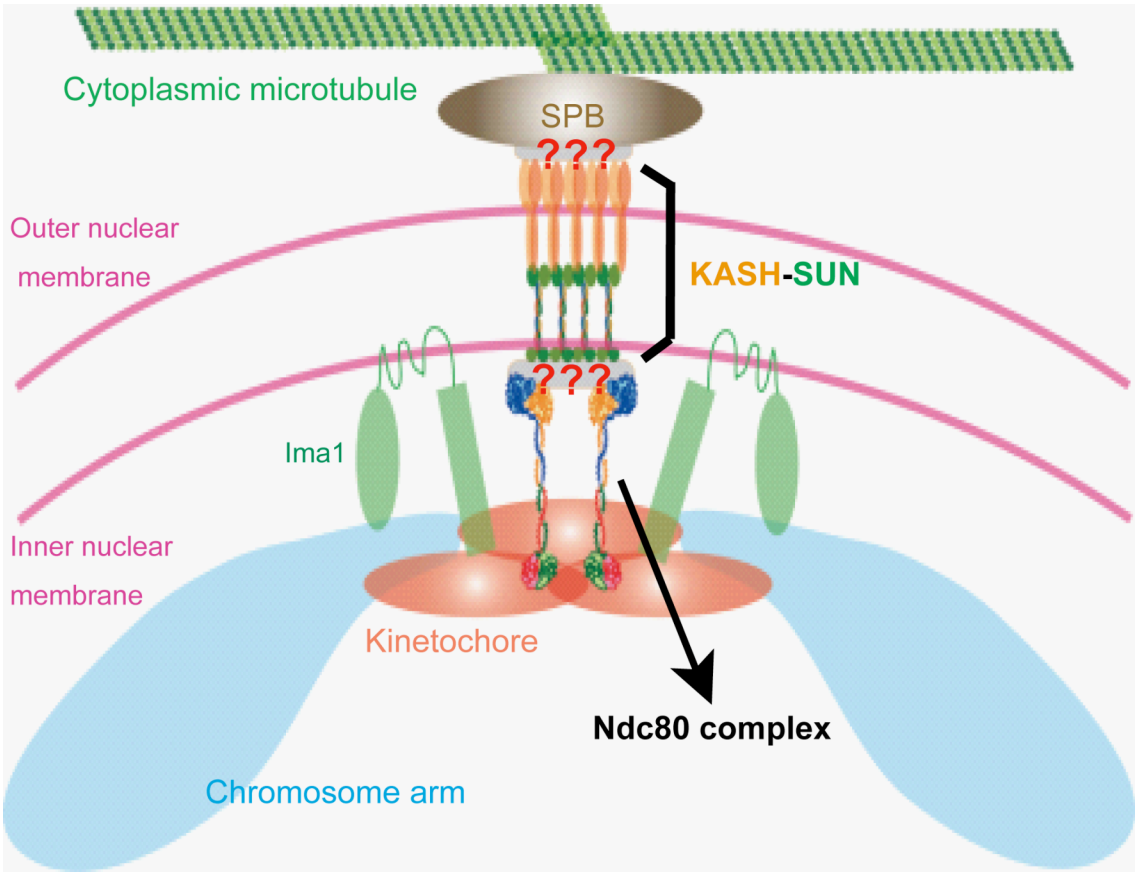

Figure 5.2 An illustration of the KASH-SUN linkage through the nuclear envelope.

The KASH protein family directly or indirectly (labelled by the question mark) connects MTOC, the SPB, to the outer nuclear membrane (ONM); the SUN protein family is recruited to the inner nuclear membrane (INM) and interacts with KASH protein in the lumen between ONM and INM. The SUN proteins then link with the kinetochore in the nucleoplasm through an unknown entity (labelled by the question mark) that possibly in turn interacts with the Ndc80 complex. Ima1 is arguably proposed to participate in the SPB-KASH-SUN-centromere anchorage. The cartoon figure is adapted and modified from (King et al., 2008).

The nuclear envelope, especially the region near the SPB, is constantly pushed by force generated from the cytoplasmic microtubules when reaching the cell tip (Tran et al., 2001, Masuda et al., 2006, Hoog et al., 2007). Uncoupling chromosomes from the SPB site may result in force imbalance and consequently cause a deformation of the nuclear envelope (Figure 5.3A) (King et al., 2008). Therefore the anchorage between the SPB and the nucleoplasm DNA through KASH-SUN may act as an important buffering source to counteract the strong pushing force from the cytoplasmic microtubules exerted on the nuclear membrane.

To explore the potential involvement of the Ndc80 complex in the SPB-chromosome anchoring, I measured the nuclear shape of the *ndc80-26* mutant at 27°C. In the wild type cells, the nuclear shape (visualised by the nuclear membrane marker Cut11-CFP) was spherically round and the ratio between the long and short axis was <1.2 (Figure 5.3B). In contrast, in both the *nuf2-1* and the *ndc80-26* mutant, the nuclear envelope seemed to be locally ruffled and the aspect ratio significantly increased into an oval shape. This result is consistent with a previous study (King et al., 2008) and implies that as the kinetochores decluster from the SPB site, the remaining attached chromosomes may not be “heavy” enough to buffer the microtubule forces exerted on SPB-chromosomes. As a result, the nuclear envelope is often dynamically deformed. From this observation, I postulate that the Ndc80 complex may be involved in the nuclear envelope integrity by clustering kinetochores to the nuclear interior close to the SPB.

5.3 The kinetochore declustering results from a previous mitotic defect

In the *mis6-302* mutant, a similar kinetochore-declustering phenotype appears in interphase only after the passage of previous G1/S phase at the restrictive temperature (Saitoh et al., 1997). To get more insight into the defective nature

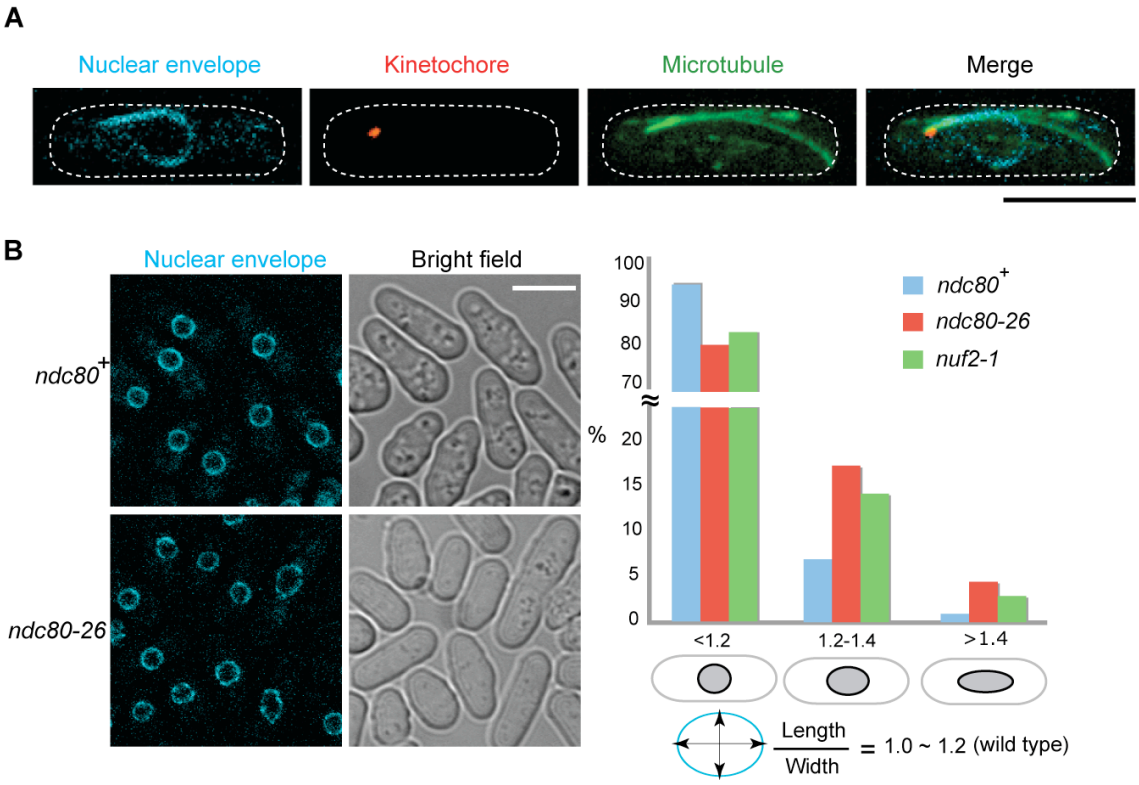

Figure 5.3 The *ndc80-26* mutant uncouples the microtubule force and deforms the nuclear envelope.

(A) The example of the force from the cytoplasmic microtubule exerted on the nucleus. Cells were labelled with Cut11-CFP (a nuclear envelope marker), Mis6-2mRFP (a kinetochore marker), and the GFP-Atb2 (α2-tubulin). (B) Cells tagged with Cut11-CFP (the nuclear envelope marker) were observed under 27°C. The aspect ratio of the nuclear envelope was the division of the length by the width. In wild type, the ratio felt into 1.0~1.2. More than 200 cells were counted in each strain. Scale bars in (A) and (B), 5 μm.

of *ndc80-26*, I synchronised the mutant cells by centrifugal elutriation, and monitored the spindle morphology and the kinetochore distribution over individual cell cycle stages. I found that the viability did not alter in the first G2 interphase (0~60 min), but it dropped dramatically when cells entered mitosis, concomitant with a sharp increase of abnormal chromosome segregation (Figure 5.4A). When cells passed through the first mitosis, they became inviable and could not enter the second mitosis (note that only one septation peak emerged). This analysis indicates that similar to *ndc80-21*, the primarily lethal defect appeared in mitosis in *ndc80-26*.

But unlike *ndc80-21*, mitotic progression seemed not to be delayed, and the mitotic spindles in *ndc80-26* were able to form and elongate normally (Figure 5.4B, 120min). Despite the normal spindle formation, in many cells the chromosomal DNA and the kinetochore dots remained in the cell centre and did not separate to two poles. This pattern differs from the *top2* mutant, in which the ϕ-shaped nuclear chromatin remained in the cell centre but only the centromeric DNA was pulled by the spindle microtubules to the poles (Uemura and Yanagida, 1986). Instead, the pattern is reminiscent of the so-called "kinetochore-null" phenotype found in *C. elegans* embryos, where the kinetochores are unable to interact with the spindle microtubules (Desai et al., 2003, Oegema et al., 2001). This similarity suggests the kinetochore-microtubule attachment was extremely vulnerable or even no microtubule pulling force was coupled onto the kinetochores. As a result, the kinetochores/chromosomes detached from the microtubules and scattered in the nuclear centre (Figure 5.4B, 120min). Furthermore, the declustered kinetochores were not observed in the first interphase, but only after mitosis (Figure 5.4C), suggesting the declustering phenotype is a consequence of the previous mitotic failure.

Since others have reported similar phenotype in *nuf2-1* (Appelgren et al., 2003), I thus re-examined *nuf2-1* using synchronous cultures. I found that timing of the kinetochore declustering phenotype in *nuf2-1* also occurred after the first mitosis (not shown), thereby confirming the above conclusion.

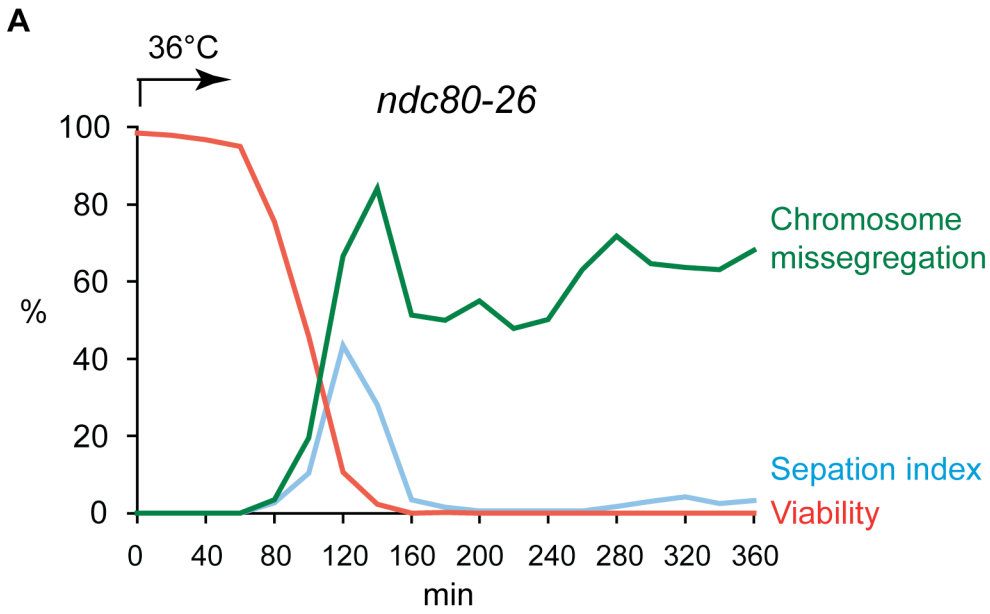

Figure 5.4A Synchronous culture analysis of *ndc80-26*.

(A) Centrifugal elutriation was used to synchronise the *ndc80-26* mutant cells, which were tagged with GFP-Atb2 (α2-tubulin), Mis6-2mRFP (a kinetochore marker) and Cut12-CFP (an SPB marker). Small early G2 cells were collected and shifted-up to 36°C immediately. Cell cycle progression was monitored by the septation index. Viability and the chromosome segregation were recorded in the same way as in Figure 3.1. n>200 at each time point.

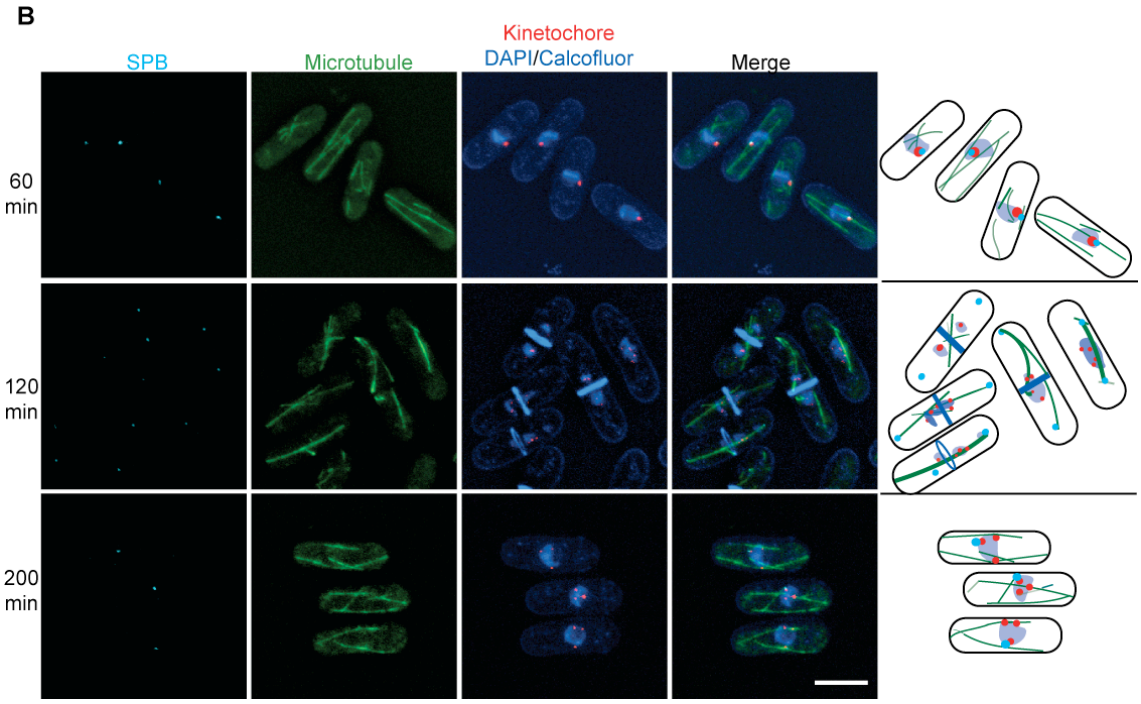

Figure 5.4B Synchronous culture analysis of *ndc80-26* (continued).

(B) Cells from three different time points of the synchronous cultures were imaged after fixation with 3.2% paraformaldehyde plus 0.3% glutaldehyde. For clarity, a cartoon illustration of the cells is presented in the right. Scale bar, 5 μm.

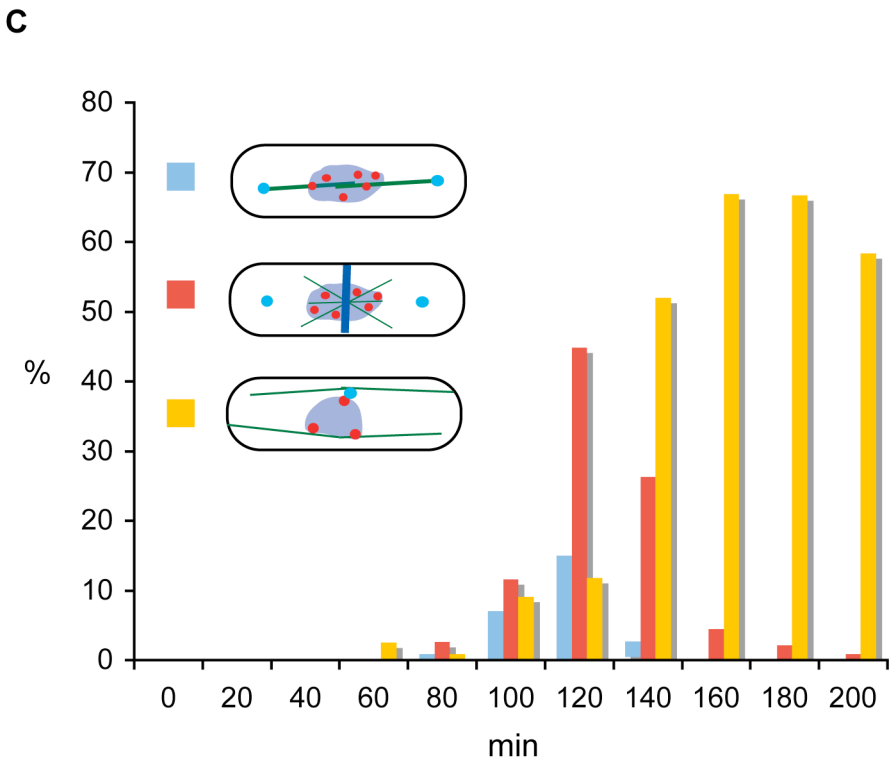

Figure 5.4C Synchronous culture analysis of *ndc80-26* (continued).

(C) Quantification of the different types of cells. Mitotic cells that exhibited the "kinetochore-null" like chromosome segregation pattern with normal elongated spindles are in blue columns; post-mitotic cells that left most of the chromosome/kinetochores in the centre with the septum formation are in red columns; interphase cells that had more than one declustered kinetochores are presented in the yellow columns. n>200 at each time point.

5.4 The Ndc80 complex disassembles in *ndc80-26* in mitosis

The fact that only ~60% of the *ndc80-26* cells retained Nuf2-YFP signals at the kinetochores (Table 2.1), and that the kinetochore-declustering phenotype appears only after the previous mitosis led me to assume the integrity of the Ndc80 complex is not abolished until cells enter mitosis. To address this point, I first observed the *ndc80-26* cells tagged with Nuf2-YFP after HU arrest-release synchronisation. As shown in Figure 5.5A, mitotic cells that exhibited condensed chromosomes drastically reduced their YFP signals (marked by a coloured-dash line). In contrast, interphase cells retained the Nuf2 signals as a clear dot under the same imaging field (Figure 5.5A, marked by a white line). Next, I observed a strain tagged with Spc25-YFP, and Cut11-CFP. The *ndc80-26* mutant exhibited a ϕ-shaped NE with most DNA stuck in the middle bulging area, but no detectable YFP signals were found (Figure 5.5B). This is consistent with my previous description of the kinetochore-null phentype, where the NE protrusion is due to the interpolar spindle elongation. From these data I envisage that loss of the Ndc80 complex at the kinetochores triggers the kinetochore-null phenotype in mitosis, followed by kinetochore declustering during the subsequent interphase.

5.5 The declustered kinetochores colocalise with cytoplasmic microtubules, rather than remnants of mitotic spindle microtubules

Results so far explain how the declustered kinetochores may emerge, but the underlying reason for apparent colocalisation of the declustered kinetochores with the cytoplasmic microtubules is still mysterious. To get further insight, I tagged the mutant cells with markers for the nuclear envelope, kinetochore, and microtubules, and examined the positions of these markers under the fluorescence microscopy. Judging from the images shown in Figure 5.6, the microtubules seemed to locate outside the nuclear envelope because these

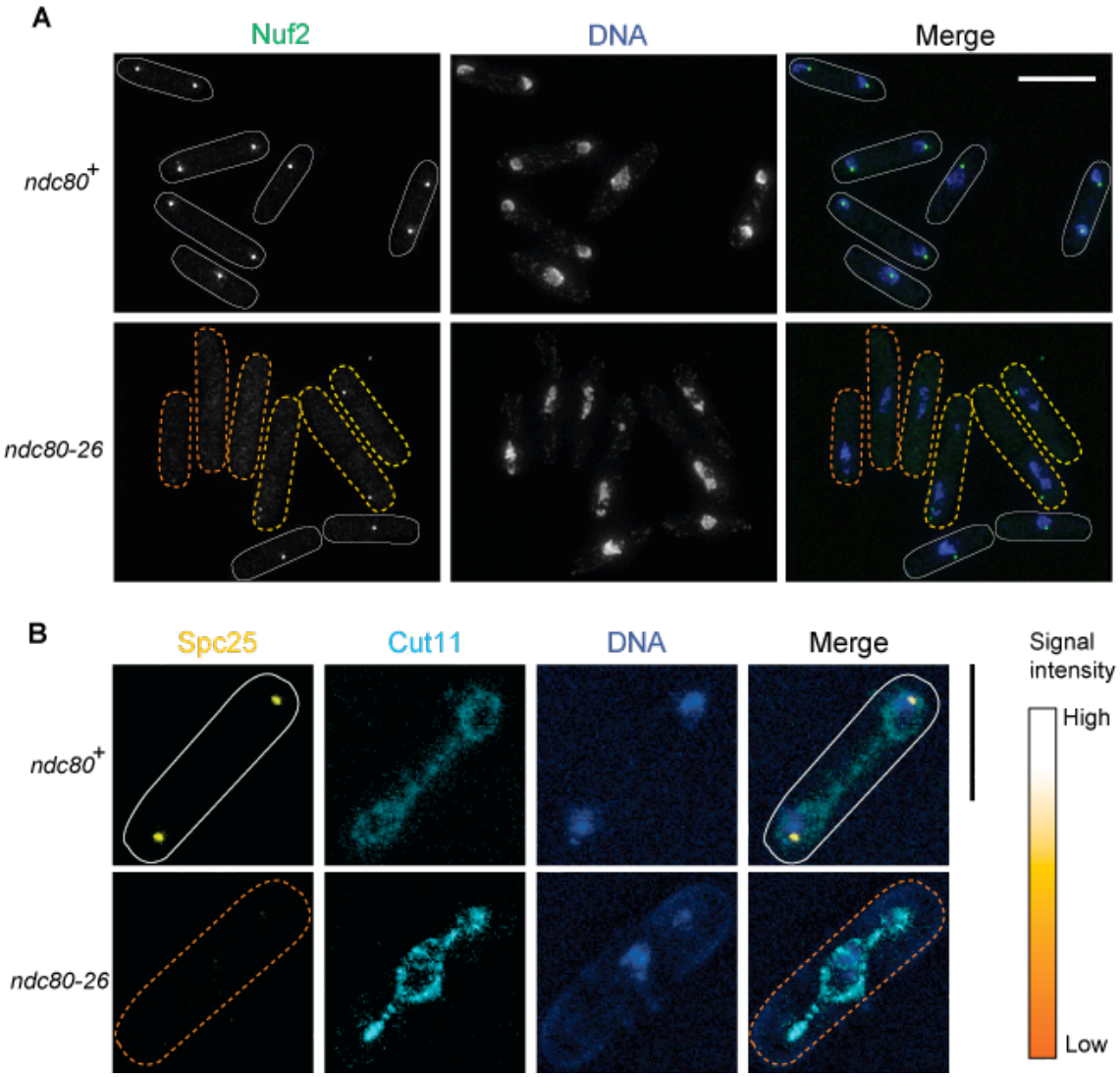

Figure 5.5 The Ndc80 complex disassembles during mitosis in *ndc80-26*. Cells were tagged with Nuf2-YFP in (A) and Spc25-YFP/Cut11-CFP in (B). 12 mM hydroxyurea was used to arrest the cell cycle at the S phase. After 4 hr incubation at 25°C, the cultures were filter-washed and released into fresh HU-free YE5S media at 36°C for 90 min. Note that based on the signal intensity of the Ndc80 complex, cells were marked with different colours, where the white colour represents the strongest intensity and the dark orange colour indicates the complete loss of the signals. Scale bars, 5 μm.

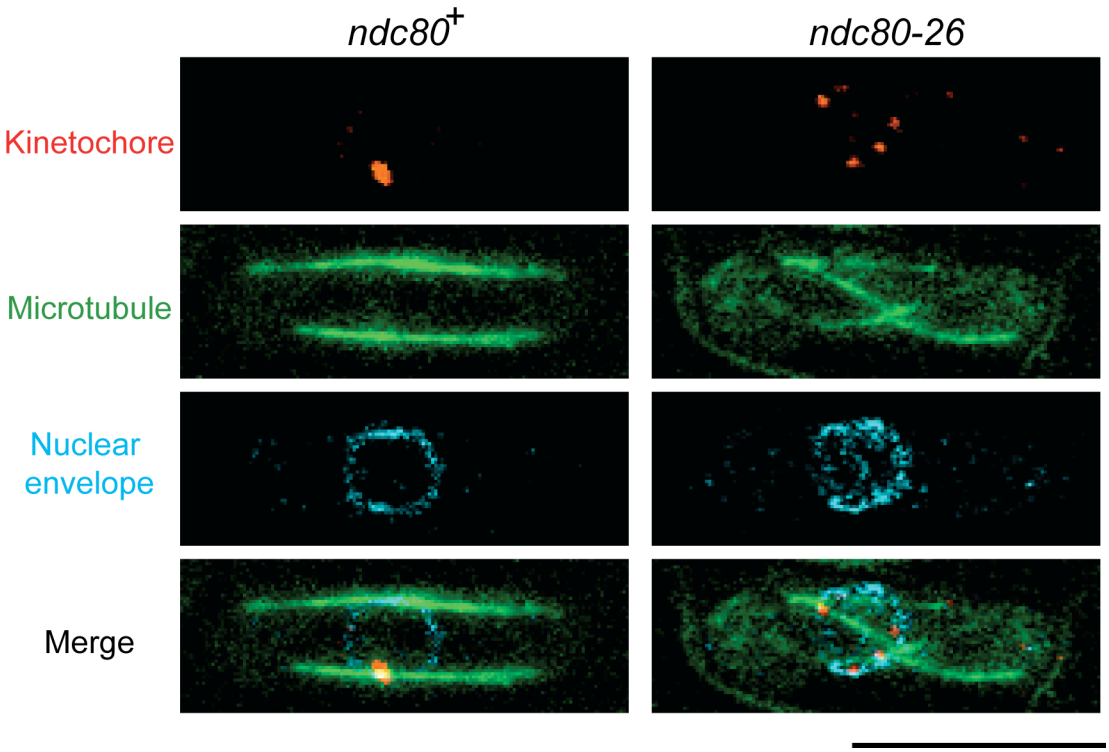

Figure 5.6 The colocalised microtubule is in the cytoplasm.

Cells were tagged with GFP-Atb2 (a2-tubulin), Mis6-2mRFP (a kinetochore marker) and Cut11-CFP (a NE marker). HU arrest-release synchronisation was applied before the temperature shift-up. The images were taken after 2.5 hr incubation at 36°C. Scale bar, 5 μm.

microtubules were longer than the nuclear envelope and many of them could reach the cell tip (also see Figure 5.4B, the images of 200 min). Morphologies of these microtubules were similar to the normal interphase microtubules. Furthermore, if it were the spindle microtubules extending to protrude through the nuclear membrane, as in the *msd1* deletion mutant, one would see an obvious protrusion of the nuclear envelope (Toya et al., 2007). However, such NE protrusion only happened in mitosis in *ndc80-26* (see Figure 5.5B), not in the following interphase. Therefore I postulate that the colocalised microtubules are cytoplasmic interphase microtubules, not intranuclear spindle remnants from the previous mitosis.

5.6 The declustered kinetochores colocalise with the γ-tubulin complex

In addition to the SPB, cytoplasmic microtubules can nucleate from iMTOC that can be near the nuclear surface, on the existing microtubules, or in the cytoplasm (Janson et al., 2005) (see Figure 1.3). These iMTOCs, together with the SPB, all contain the γ-tubulin complex (γ-TuC), an indispensable factor for microtubule nucleation (Sato and Toda, 2004, Janson et al., 2005, Sawin and Tran, 2006). I wondered whether these scattered kinetochores could possibly colocalise with the γ-TuC (as the SPB/iMTOC marker) near the nuclear periphery. Surprisingly, certain declustered kinetochores indeed colocalised with the γ-TuC marker Alp4-GFP, albeit at low frequency (Figure 5.7), suggesting that these declustered kinetochores may somehow colocalise with iMTOCs in *ndc80-26*. It is worth pointing out that in wild type interphase cells, most of the γ-TuC locate to/near the SPB site and only some portions of them locate to other iMTOC sites (like the pattern in Figure 5.7, upper left), but it seems the distribution of γ-TuC is affected in *ndc80-26*. Thus it is possible that Ndc80 might play a role in γ-TuC reorganisation during the mitosis/interphase transition (see discussion).

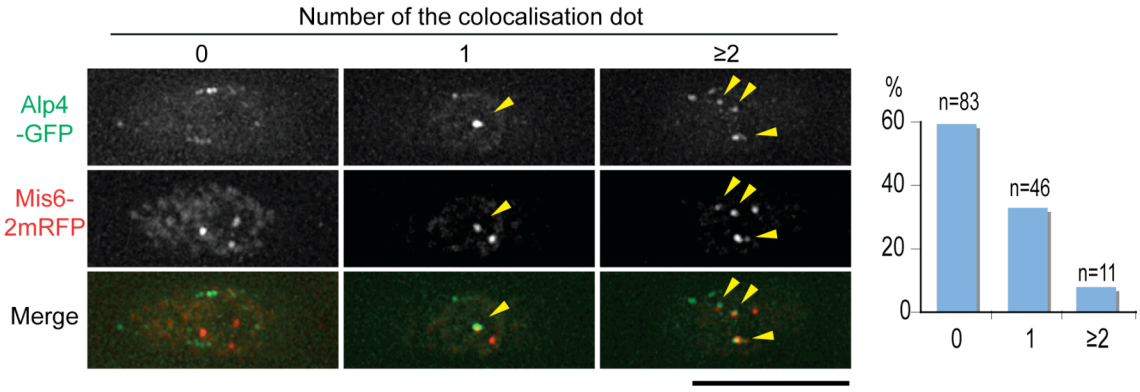

Figure 5.7 The declustered kinetochores colocalise with the γ-tubulin complex.

ndc80-26 mutant cells were tagged with Alp4-GFP (a γ-TuC marker) and Mis6-2mRFP (a kinetochore marker). HU arrest-release synchronisation was used before the temperature shift-up. The images were taken after 2.5 hr incubation at 36°C. The cells were classified into three categories dependent on the number of colocalising dots between the kinetochore and γ-TuC, marked by arrowheads. Note that the brightest signal of Alp4-GFP is likely the SPB site (Zimmerman and Chang, 2005). 140 cells containing declustered-KT were counted. Scale bar, 5 μm.

Further careful investigation is absolutely required for better understanding of the biological significance of the kinetochore/centromere clustering through the Ndc80 complex.

5.7 Summary

In this chapter, I have described the work done in *ndc80-26*, in which the kinetochore dots dissociate from the spindle pole body in interphase; these declustered kinetochores colocalise with interphase microtubules. At the permissive temperature, *ndc80-26* presents the phenotype of nuclear envelope deformation, likely due to the inability of coupling the SPB-kinetochore linkage through the Ndc80 complex. However, synchronous culture analysis reveals that the primarily lethal defect occurs in mitosis, which is concomitant with the presence of the "kinetochore-null" like chromosome mis-segregation. Kinetochore declustering is ascribable to the disassembly of the Ndc80 complex in the course of chromosome segregation, by which the chromosomes are eventually compartmented into two daughter cells by septum formation. Further characterisation of this mutant confirms that the overlapped microtubule is cytoplasmic microtubule, rather than the spindle remnants from the preceding mitosis. Last and most surprisingly, some of the declustered kinetochores indeed colocalise with a marker for the γ-TuC, the essential complex to nucleate microtubules.

5.8 Discussion

5.8.1 The SPB-kinetochore linkage requires the Ndc80 complex integrity.

The KASH-SUN linkage has been implicated in many biological activities in various model organisms, including the nuclear migration or positioning or anchorage, the meiotic telomere-bouquet formation, and homologous

chromosome pairing and synapsis (Yamamoto and Hiraoka, 2001, Chikashige et al., 2006, Sato et al., 2009, Starr and Fridolfsson, 2010). All the studies converge to the same scenario that major tasks of these nuclear transmembrane proteins are to transfer forces generated from the cytoskeleton that is exerting onto nuclei. In this chapter, I provide evidence that the Ndc80 complex is required for the SPB-KASH-SUN-kinetochore anchorage. Loss of the connection results in the kinetochore declustering inside the nucleus, and likely distorts the nuclear envelope due to the force uncoupling.

Despite the fact that similar kinetochore declustering aberrance has been described in other kinetochore mutants like *mis6-302* and *nuf2-1* (Saitoh et al., 1997, Appelgren et al., 2003), the underlying reason for the declustering is unknown. By synchronous culture analysis, I find that the primary lethal defect appears during the first mitosis in *ndc80-26*, and the kinetochore declustering phenotype is rather a consequence of disassembly of the Ndc80 complex in the preceding mitosis. I envision that during the course of chromosome segregation, most of the kinetochores are lost in the cell centre despite the normal anaphase spindle elongation. The scattered chromosomes/kinetochores are then randomly “cut” by the septum, and are unevenly allocated into two daughter cells. However, the divided cells may not die immediately. After cytokinesis, the SPB moves from the cell tip back to the cell centre. The SPB is unable to “recluster” all the detached kinetochores due to the irreversibility of disassembly of the Ndc80 complex. Some kinetochores are consequently free to scatter in the nucleoplasm in the following interphase. Although it is a secondary defective phenotype, I argue that the maintenance of the Ndc80 complex at kinetochores is the prerequisite for the kinetochore clustering in the following interphase.

5.8.2 Potential role of Ndc80 in the SPB-kinetochore linkage?

Physiologically, it is still not clear why the centromeric DNA needs to be clustered at the inner face of the nuclear envelope near the SPB in interphase fission yeast cells. First of all, one straightforward explanation is to gather

enough weight (the chromosome mass) to buffer the pushing force exerted onto the SPB/nucleus. Secondly, another reasonable benefit from keeping a short distance between SPB and kinetochores is to save the energy and shorten the time for "searching and capturing" the kinetochores that are already not too far from the SPB (within 1 μm) upon mitotic entry.

Thirdly, the KASH-SUN linkage also seems to affect the individual chromosomes, by which the chromatin association with nuclear periphery often coordinates with the transcription machinery (Akhtar and Gasser, 2007). Active gene loci tend to associate with nuclear pore structures at the nuclear periphery, whereas silent chromatin (heterochromatin) is linked to other foci through the interaction with Esc1 (enhancer of silent chromatin 1) and Sir4 (silent information regulator 4) (Heun et al., 2001, Andrulis et al., 2002, Taddei et al., 2004, Gartenberg et al., 2004). In fission yeast, the most studied nuclear envelope-associated DNA, telomeres (Hiraoka and Dernburg, 2009), have been shown to associate with the INM proteins Bqt3 and Bqt4 in vegetative interphase cells (Chikashige et al., 2009). Nevertheless, the functional integrity of telomeres including the genetic silencing within telomeres seems to be independent of their attachment to the nuclear envelope (Chikashige et al., 2010). While both the telomeres and centromeres are heterochromatin-rich, it remains to be established whether centromere/kinetochore clustering plays a role in silencing gene expression of the centromeric heterochromatins in *pombe* interphase cells.

Fourthly, in wild type, the majority of the γ-TuC is gathered to the SPB site in interphase. In *ndc80-26*, however, declustered kinetochores are found to colocalise with γ-TuC, suggesting that the gathering of the γ-TuC to the SPB is somehow interfered in this mutant. Considering the dramatic translocation of γ-TuC from the eMTOC in the cell equator to the SPB/iMTOCs during the cytokinesis/interphase transition (see Figure 1.3), I postulate another possibility that the Ndc80 complex might help to mediate the redistribution of γ-TuC to the SPB after the preceding mitosis. But how could this happen?

Thanks to the dynamic fluid nature of the nuclear envelope, proteins embedded in the nuclear membrane are believed to be mobile to some extent. In line with this, the INM protein Sad1, an essential component of the SPB (Hagan and Yanagida, 1995), has been reported to not only exclusively locate to the SPB during meiosis, but also localise to the sites where telomeres attach on the nuclear periphery (Goto et al., 2001, Chikashige et al., 2007). I notice that those previously reported live images of Sad1 (versus microtubules) look extremely similar to the images of declustered kinetochores and microtubules shown in Figure 5.1, 5.4B, and 5.6. Thus it is tempting to assume that some amounts of the INM protein Sad1 could possibly associate with the scattered kinetochores in the *ndc80-26* post mitotic cells. This association might be achieved through the help from residual Ndc80 complex at the declustered kinetochore, or Ima1 that is proposed to anchor heterochromatin to the nuclear periphery (King et al., 2008). Despite that the association between Sad1 and the declustered kinetochore is not robust enough to merge the scattered kinetochore to the SPB, the attached Sad1 might be able to anchor small amounts of the ONM Kms2 proteins (and/or Kms1). This assumption is consistent with the finding that when the SPB-centromere linkage is interrupted in vegetative interphase cells, Kms2 and Sad1 become disorganised from the SPB and fragmented together into several foci in the nuclear periphery (King et al., 2008). This residual Kms2-Sad1 at the declustered KT in turn possibly connects the iMTOC around the nuclear periphery (γ-TuC as the marker), which is overlapping with the cytoplasmic microtubules outside the nuclear envelope (illustrated in Figure 5.8A). This hypothesis explains why two complex entities in the different site of nuclear envelope could possibly overlap under microscopic observation. This hypothesis is at an early stage and requires further examination.

A classic EM study reveals that γ-TuC accumulates at both sites of the nuclear envelope near the SPB (Ding et al., 1997). The nucleoplasmic γ-TuCs are proposed to be active only in mitosis to nucleate nuclear spindles, but to keep silent during interphase. This then raises another puzzle whether the

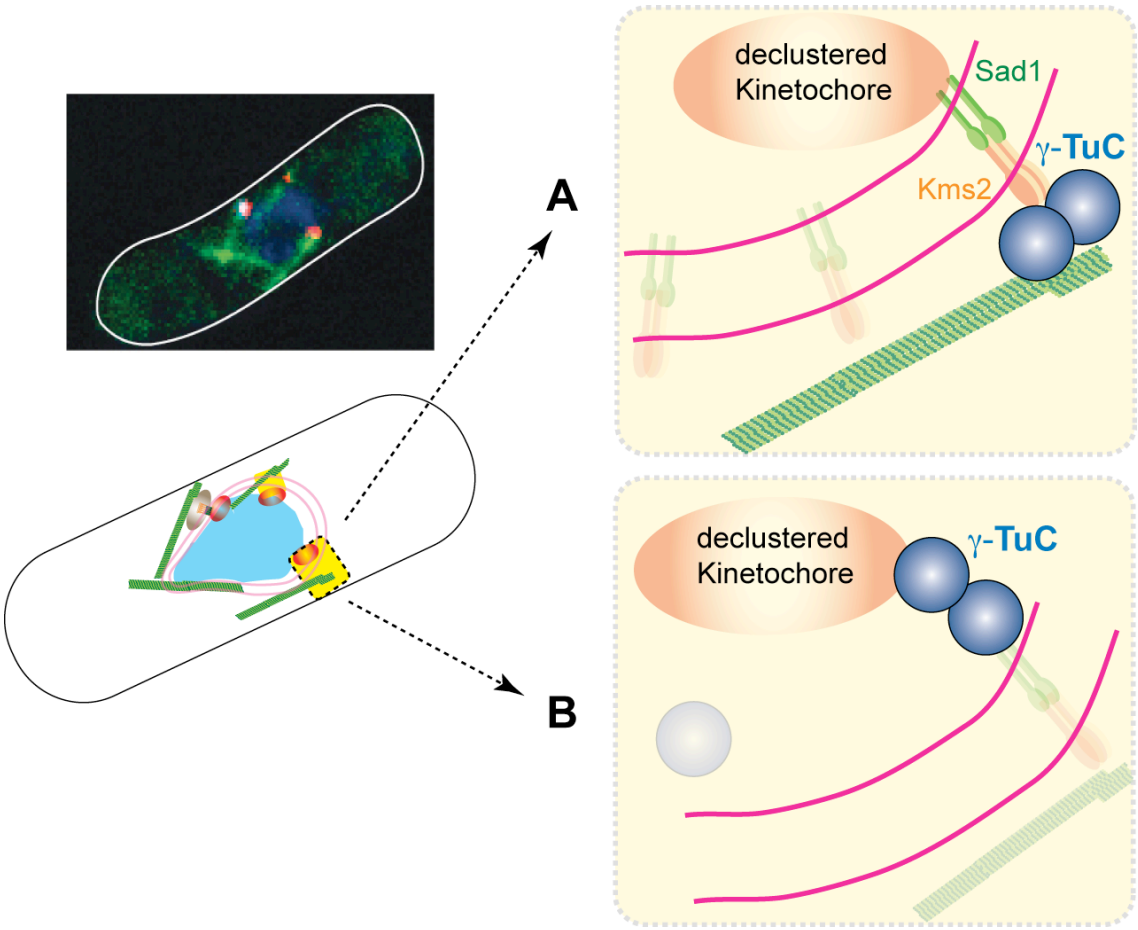

Figure 5.8 Two possible configurations of γ-TuC in the SPB-kinetochore linkage.

(A) The scattered kinetochore might still manage to associate with Sad1-Kms2, which might directly or indirectly link to the iMTOC (containing the γ-TuC) outside the nuclear membrane.

(B) It is also possible that γ-TuC is actually inside the nucleus. In this case, γ-TuC might itself be the missing link between Sad1 and the kinetochore.

colocalised γ-TuC is outside or inside the nucleus. If it is outside, the above hypothesis will make more sense as I regard γ-TuC as an iMTOC marker. Nevertheless, since a hypothetical linker between Sad1 and the Ndc80 complex is missing (see Figure 5.2) (King et al., 2008), it will be equally interesting if the colocalised γ-TuC is in fact inside the nucleus. If this is the case, it will be very likely that the γ-TuC may be the missing linker to bridge KASH-SUN and Ndc80 (illustrated in Figure 5.8B). A longstanding question of the physiological meaning of the inactive γ-TuCs underneath the SPB will thus be revealed and be linked to the SPB-kinetochore anchorage.

Overall, I regard the *ndc80-26* allele as a useful tool to study the potential role of Ndc80 beyond mitosis, especially its involvement in SPB-KASH-SUN-centromere anchorage and the underlying regulation of γ-TuC distribution and/or the function of γ-TuC underneath the SPB, which in turn is important for microtubule nucleation and/or spatial organisation in interphase.

Chapter 6. Concluding remarks

6.1 Overall summary

It has been over one hundred years since the word ‘mitosis’ was first coined by Walther Flemming in early 1880 (Mitchison and Salmon, 2001). How the chromosomes congress and align to the metaphase plate in prometa/metaphase, and equally separate to two daughters in anaphase are collectively a complicated process that fascinates the science field and is still under extensive investigation. Two macromolecular structures are responsible for faithful chromosome segregation: dynamic spindle microtubules emanating from the centrosomes/SPBs, and the kinetochore assembled on centromeric chromosomes. In the classic Hill model, the microtubules-kinetochore interaction is accomplished by two distinct attachments: the multiple links between the kinetochore and the microtubule lattice that generate driving forces required for chromosomal movements, and the complexes interacting with the microtubule ends responsible for the regulation of microtubule dynamics (Hill, 1985). The best candidates for the former are the Ndc80 complexes (~8 copies per kinetochore) surrounding the microtubule lattice existing in all eukaryotes, and/or the Dam1 complex that is proposed to form a ring around the microtubule in budding yeast; whereas a number of microtubule associated proteins are known to be required for microtubule dynamics control at the microtubule-kinetochore interface (Maiato et al., 2004, Jiang and Akhmanova, 2011).

Many elegant studies have established that the Ndc80 complexes constitute the major binding sites for spindle microtubules, but how the Ndc80 complex couples robust microtubule-kinetochore attachments to microtubule dynamics regulation remains largely elusive (DeLuca et al., 2006). Another mysterious aspect of Ndc80 function is how this protein complex contributes to the cellular activities in interphase yeast cells, in which the kinetochores are closely associated underneath the SPB.

Using fission yeast as a model, I have studied the role of Ndc80 throughout the cell cycle. I first used a genetic approach to isolate temperature-sensitive *ndc80* mutants, a powerful tool to make possible the separation-of-function of a single gene. Further characterising these mutants in depth, I have focused on two *ndc80* alleles that exhibit different phenotypes: the unstable mitotic spindle defects in *ndc80-21* and the unusual interphase abnormality in *ndc80-26*.

As described in chapters 2, 3, and 4, by studying *ndc80-21*, which combines various approaches including genetics, molecular biology, cell biology, and biochemistry, I have discovered the functional coordination between the Dis1/TOG (Tumour Overexpressed Gene) microtubule-stabilising protein and Ndc80/Hec1 (Highly Expressed in Cancer) at the microtubule-kinetochore interface. Together with all my data and others' work, I have proposed a 'two-domain' model, in which the Ndc80 protein consists of two essential domains, the N-terminal domains required for initial microtubule lattice interaction, and the internal loop crucial for direct recruitment of Dis1/TOG. In this concept, Dis1/TOG acts as a second interacting point toward microtubules close to the dynamic ends, and exerts its microtubule-stabilising activity to secure the initial attachment and helps to promote the chromosome congression. This model explains how Ndc80 couples spindle microtubule dynamics with kinetochore capture in mitosis. We believe our study not only provides an important insight into the molecular mechanism of establishment of proper KT-MT attachments, but also renders an explanation for a longstanding puzzle in the mitosis field as to how the kinetochore regulates microtubule dynamics at the KT-MT interface (Brinkley and Cartwright, 1975, Salmon et al., 1976, Mitchison and Kirschner, 1985, Mitchison et al., 1986).

In chapter 5, I have presented the results for *ndc80-26*. The most striking phenotype in this mutant is the colocalisation of the declustered kinetochores with the cytoplasmic microtubules in the following interphase. Despite being a secondary effect, it is clear that Ndc80 integrity is required for the SPB-kinetochore anchorage, which renders an important buffering source to balance the microtubule pushing force exerted on the nucleus. In addition, colocalisation

of the γ-TuC (the microtubule nucleation factor) with the scattered kinetochores leads me to a preliminary hypothesis that Ndc80 may have a role in the spatial organisation of the γ-TuC during the cytokinesis/interphase transition, or alternatively, the γ-TuC itself serves as the missing link between Sad1 (the SUN protein) and the Ndc80 complex inside the nucleus.

Overall, my thesis work uncovers dual roles for Ndc80/Hec1 in different cell cycle stages in fission yeast. In mitosis, Ndc80 is indispensible for the molecular establishment of proper microtubule-kinetochore attachment and microtubule dynamics regulation. In interphase, Ndc80 is required for SPB-kinetochore clustering and possibly for γ-TuC redistribution/organisation. I wish knowledge about the basics of Ndc80 extended from this thesis work might, someday, and somehow, help to benefit the human health by facilitating the development of better treatments against diseases, especially against cancers.

6.2 Future directions

Back to reality, there are several technical issues, unsolved questions and new puzzles raised from this thesis work that need to be further explored in the future.

Dis1 definitely plays an important role in the Ndc80 loop-dependent microtubule-kinetochore attachment. However, several lines of evidence demonstrate that Dis1 is the major factor, but not the sole determinant, for Ndc80 loop function. First, the *Δdis1 ndc80-21* double mutant is synthetic lethal at the permissive temperature (Figure 4.1); second, overproducing Dis1 or artificial tethering Dis1 to the Ndc80 complex only partially rescues *ndc80-21* (Figure 4.2, 4.9 and 4.12); third, although the defective phenotypes are very similar, *ndc80-21* is heat-sensitive but *Δdis1* is cold-sensitive. It is thus possible that other factors also participate in this process, such as Alp14, Klp5/Klp6 and Dam1, at least genetically (Figure 4.1).

It is intriguing that fission yeast contains two TOG proteins (Dis1 and Alp14), but only Dis1 suppresses the *ndc80-21* mutant allele (Figure 4.2). Since the Ndc80 internal loop in fission yeast is a bit longer than those in other species (about 75 aa, Figure 3.9), it is not impossible that this loop could act as a multiplatform to recruit different proteins to collectively accomplish accurate chromosome segregation. From our analysis, Dam1's involvement is likely indirect and dependent on Dis1 or microtubules (Figure 4.15 and 4.16). But the role of Alp14 and Klp5/Klp6 in the Ndc80 loop-dependent mechanism is still waiting for investigation. In fact, I have tried but failed to conclusively quantify the intensity of Alp14-GFP in the *ndc80-21* mutant, because Alp14 intrinsically localises to the SPBs, all along the spindles and the kinetochores, which makes the selective quantification of the kinetochore signal difficult.

One feasible approach is to check other mutants that we isolated from the beginning, as many of them contain other mutations in the loop. By transforming plasmids with the gene of interest (e.g. Alp14) to these mutant alleles, we can test if overproducing Alp14 suppresses other mutants, and dissect whether or not Alp14 is functionally correlated with Ndc80 in an allele-specific manner. Direct interaction of Alp14 and Ndc80 can also be tested by immunoprecipitation or pull-down (or peptide array).

Isolation of genetic suppressors is another direction to examine the functional correlation between two genes. We have shown that *ndc80-21* is a loss-of-function mutant allele that fails to recruit Dis1/TOG to the outer kinetochore, consequently leading to defects in establishing the proper microtubule-kinetochore attachments. An interesting experiment would be to isolate *dis1* mutants with the gain-of-function mutation that suppresses *ndc80-21*. Isolation of such mutants would not only significantly strengthen our two-domain model at the genetic level, but also gain invaluable insight into the domain of the Dis1 proteins in the Ndc80 loop-dependent mechanism. Not limited to those MAPs, a genome-wide multicopy suppressor screen in *ndc80-21* could also possibly identify more proteins that closely function with Ndc80 via the internal loop.

The domain analysis of the Dis1 protein is not yet completed (Figure 4.18, 4.19 and Appendix 2). So far, the clear message from the microtubule sedimentation assay is that full-length Dis1 indeed strongly binds to microtubules *in vitro*, as does the serine/basic linker, albeit weakly. Dis1/TOG proteins might encounter a huge conformational change (or dimerisation) when they bind to microtubules or tubulin subunits (Al-Bassam et al., 2006, Brouhard et al., 2008), suggesting different domains might spatially influence each other. It will be necessary to compare the microtubule binding affinity of all the purified fragments with different domains, and the potential synergistic effect (if any) will be of great interest to see. In terms of Ndc80 binding, it is difficult to interpret the peptide array data since all the Dis1 fragments (except the serine/basic linker) display a similar binding pattern as the full-length Dis1. Low protein solubility and the non-optimised experimental condition may be ascribable to those binding patterns. In the future, it will be necessary to adjust the peptide array conditions and increase the protein purity and solubility if possible.

It is also unclear which aspect(s) of Dis1 are exactly regulated by Cdc2 phosphorylation, either localisation or microtubule binding and/or the polymerisation activity. In the preliminary peptide assay, I did not see a difference between Dis1-6E and Dis1-6A for their binding to Ndc80 loop (though the conditions might not be optimised). It will be interesting to compare their microtubule binding activity using the cosedimentation assay. Furthermore, an *in vitro* real-time tubulin polymerisation assay (Liou et al., 2007) can be applied to see whether these two mutant proteins have different microtubule polymerising abilities compared to the wild type Dis1 proteins.

The suppression of *ndc80-21* by *clp1* deletion is intriguing, yet another perplexing enigma to us, as we do not really know whether Clp1 is the corresponding phosphatase for Dis1 *in vivo*. It will be necessary to solve this question first by comparing the gel mobility patterns of Dis1 in the wild type and in the *Δclp1* background. To dissect if Dis1 is the important target for Clp1, it can also be tested genetically by deleting Dis1 in the *Δclp1 ndc80-21* double mutant, to see whether Dis1 is required for the suppression.

Whether or not Dis1 forms a homodimer to bind the tubulin subunit is an open question. The analytical centrifugation (e.g. sucrose gradient centrifuge or ultracentrifuge) or size-exclusion chromatography might need to be conducted to get an answer.

The *in vitro* demonstration is an important future goal to comprehend our understanding of how Ndc80 and Dis1/TOG mechanically coordinate to bind to microtubules and affect microtubule dynamics. This is an ongoing project, in collaboration with Dr. Thomas Surrey's lab in our institute. Recombinant Ndc80 heterotetramers (with or without the internal loop) and Dis1 proteins (and Alp14) have been bacterially expressed and purified. Future work will include the usage of the TIRF (total internal reflection fluorescence) system to observe the protein behaviour on the microtubules at the single molecule level. Three major questions will be answered: (1) whether Dis1 (or Alp14) is able to track the microtubule plus end and indeed polymerise microtubules *in vitro*; (2) whether Dis1 (or Alp14) would enhance the binding of the Ndc80 complex to microtubules and whether they mutually affect the processivity of each other to the microtubule tips; (3) whether the enhancement of processivity, if any, is through the internal loop of Ndc80.

Another key issue is whether the functional coordination between Ndc80 and Dis1/TOG is conserved in higher eukaryotes. This is perhaps one of the most interesting questions waiting to be answered. To examine this, before the *in vivo* investigation, the simplest way is to affinity purify the recombinant TOG homologue proteins (for example XMAP215 and Stu2), and synthesise the peptide array covering the Ndc80 sequence (from *Xenopus* or budding yeast, respectively) to see if there is any significant binding between these TOG proteins and Ndc80 in other species (note that since I am in the final year, two of my intelligent colleagues have taken over the Ndc80 project in our lab).

The kinetochore localisation of spindle assembly checkpoint components, such as Mad1 and Mad2, seems to depend on the N-terminal of Ndc80 in metazoans (Martin-Lluesma et al., 2002, Guimaraes et al., 2008). This is also likely the

case in fission yeast, in that the SAC (Mad2 at the kinetochore) is activated in *ndc80-21*, in which the mutated Ndc80 proteins are retained at the kinetochore; on the other hand, when the mutated Ndc80 proteins are delocalised from the kinetochore in *ndc80-26*, the SAC is no longer activated despite the appearance of unattached kinetochores. Surprisingly, there is only one yeast-two-hybrid data set available for the interaction between Mad1 and Ndc80 over the last ten years (Martin-Lluesma et al., 2002). The difficulty to examine the interaction, if any, is understandable since a tiny amount of Mad1 on one unattached kinetochore is sufficient to amplify the 'wait' signal for SAC activation. In addition, it is not impossible that the binding site of Mad1 on Ndc80 somehow overlaps with the sites for microtubule binding, which means these two binding events might compete with each other *in vivo*. To examine the interaction *in vivo*, it might be helpful to treat the cells with microtubule-depolymerising drugs (such as TBZ) to enhance the checkpoint loading onto the kinetochore. Alternatively, the *in vitro* pull-down may be a feasible way to avoid this foreseen problem.

While the mitotic role of Ndc80 (with Dis1) needs to be further explored, its role in interphase is equally fascinating. The intriguing phenotype found in *ndc80-26* leads me to the hypothesis that Ndc80 may actively participate in the redistribution of the tubulin nucleation factor, γ-TuC, during the mitosis/interphase transition. It will be interesting to test whether the KASH and SUN protein, Kms2 and Sad1, respectively, also colocalise with the declustered kinetochores under this condition. One key outstanding question is whether the colocalised γ-TuC is situated inside or outside the nucleus. One possible way to dissect these two is using the *mto1* deletion strain, a non-essential mutant that has no affect on mitotic progression or mitotic spindle assembly, but fails to recruit γ-TuC to the MTOCs outside the nuclear envelope (Sawin and Tran, 2006). Alternatively, a positive interaction between Ndc80 and the γ-TuC, from immunoprecipitation for example, will be an appropriate way to examine the role of the γ-TuC inside the nucleus as the linker between Sad1 and Ndc80.

Chapter 7. Materials and Methods

7.1 Strain growth and maintenance

Standard methods for yeast genetics and molecular biology were used (Moreno et al., 1991). Cells were grown either in liquid culture media or on agar plates (1.6% agar), of which the recipes are listed. Stocks of yeast strains were in YFM media at -80^{o}C. Selective media were made by adding various drugs as indicated below.

Name	Components
EMM	14.7 mM potassium hydrogen phthalate, 15 mM Na_2HPO_4, 93.5 mM NH_4Cl, 2% w/v glucose, salt stock, vitamin stock, mineral stock
EMM- NH_4Cl	EMM but without NH_4Cl
LB	170 mM NaCl, 0.5% w/v yeast extract, 1% w/v bactotryptone, pH7.0
MEA	3% Difco yeast extract, 75 mg/ml uracil, adenine, histidine, lysine, leucine
YE5S	0.5% Difco yeast extract, 3% dextrose, 250 mg/ml uracil, adenine, histidine, lysine, leucine
YFM	YE5S with 15% glycerol

Name	Components
Hygromycin B	YE5S + 300 μg/ml hygromycin B (Roche)
Kanamycin	YE5S + 100 μg /ml Geneticin (G418) (Sigma)
ClonNAT	YE5S + 100 μg /ml nourseothricin (Werner Bio-agents)
Aureobasidin A	YE5S + 0.5 μg /ml aureobasidin (Takara Bio)
Phloxin B	YE5S + 7.5 μg /ml Phloxin B (Sigma)
5-FOA	YE5S + 1 mg/ml 5-fluoroorotic acid

7.2 Yeast transformation

50 ml (5 x 10^6 cells/ml) overnight cultural cells were harvested by brief spinning (2000 rpm) for 1 min. Cells were washed twice with 1 ml LiAc/TE, and then resuspended in 100 μl LiAc/TE. 7.5 μl of 10 mg/ml salmon sperm carrier DNA (Invitrogen, denatured at 95°C for 5 min and immediately on ice for the first time to use) and 10 μl PCR fragments (or 1 μl plasmid DNA, ~200 ng) were added, gently mixed, and incubated on a slow rotating mixer at RT for 10 min. 260 μl LiAc/TE/40% PEG_{3640} was added and the mixture was briefly voxted. The reaction tube was then incubated at 27 °C for 1hr. 43 μl DMSO was added and gently mixed (by flicking the tube). Cells were heat-shocked at 42 °C for 1 to 5 min, followed by washing with YE5S, resuspended in 500 μl YE5S, and incubated at 27 °C for 2hr. Cells were then plated and incubated at 27°C until colonies grew. For DNA integration, cells were first plated onto a YE5S plate and incubated at 27°C for 1 day. The plate was then replica plated onto a selective plate.

7.3 Gene tagging and deletion

It was performed using a one-step PCR-based method (Bahler et al., 1998). Long oligonucleotides (100 bp) carried 80 bp of homology to flanking sequences of the insertion site at the endogenous locus, and 20 bp of homology to the cassette to be amplified from the template plasmids. After PCR amplification, the fragments were transformed into the cells. The integrants were selected on selective plates. Colony PCR or sequencing was used to verify the accuracy. The long oligo PCR was usually carried out in a 50 μl reaction containing: 5 μl of 10x LA Tag buffer, 16 μl of dNTPs (2.5 mM each), 0.5 μl of templated DNA (~200 ng/ μl), 0.5 μl of forward and reverse primer (10 μM) each, 1 μl LA taq polymerase (Takara Bio.), and H_2O. The PCR setting was as followed:

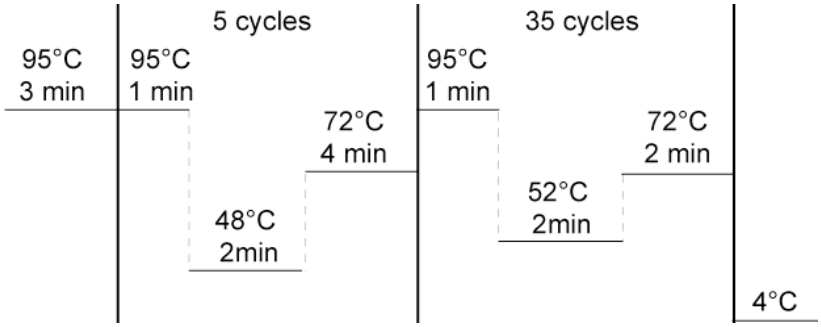

7.4 Isolation of ts *ndc80* mutants

The kanamycin-resistance marker gene cassette (*kan*^{r}) was first inserted in the 3' flanking region of the *ndc80*$^+$ gene (*ndc80*$^+$-*kan*^{r}). After obtaining the right clone (KSH017), genomic DNA was purified from this strain using a commercial kit (Master Pure Yeast DNA Purification Kit, Epicentre Biotect.), and the *ndc80*$^+$-*kan*^{r} fragment was PCR amplified with a primer set that annealed to 500 bp upstream and 330 bp downstream of the *ndc80*$^+$ locus. These PCR fragments were used as the template and amplified again with error-prone PCR using Vent DNA polymerase (New England Biolabs Ltd.) supplemented with 10X deoxyguanosine triphosphate (dGTP). Pools of mutagenised PCR fragments were ethanol precipitated and transformed into a wild type strain tagged with either *nuf2*$^+$-*yfp*$^+$-*ura4*$^+$ or *spc25*$^+$-*yfp*$^+$-*nat*. Approximately 8,000 transformants were screened for temperature sensitivity on the YE5S/Phloxin B replica plates at 27 ^{o}C, 36^{o}C and 22 ^{o}C. 22 ts and 10 cs mutants were initially isolated by comparing the growth of the same colony on different temperatures. These mutants were backcrossed with a wild type strain to make sure the cosegregation of the ts phenotype and kanamycin resistance.

7.5 The mutation sites in *ndc80* mutants

Nucleotide sequencing was done with Cancer Research UK, London Research Institute in-house sequencing facility. The sequencing results were summarised as followed:

ndc80 mutants	ORF mutations*	Amino acid mutations
ts-03	*T1099C, C1157T, T1433C, A1763G*	L336P
ts-20	*C117T, T1015C,*	T23I, M308T
ts-21	*T889C*, *A1011G*, *A1228G*, *T1306C*	T307A, E379G, L405P
ts-24	*C1363A*, *A1771G*	A424D, Q560R
ts-26	*T1546C*, *T1565C*, *T1906C*	L485P, L605S
ts-31	*T359C*, *A449G*, *T486C*, *A933G*, *A1353C*	F132L, N281D, N421H
ts-34	*T1041C*, *A1308G*	S317P, I406V
ts-36	*T328C*, *A501G*, *A1338G*, *T1641C*, *T1853C*	V79A, R137G, K416E, S517P
ts-102	*T1160C*, *A1468G*, *T1864C*	K459R, L591P
cs-01	*T1759C*	L556P
cs-05	*T1888A*	L599Q

*silent mutations were marked in grey colour and the missense mutations were labelled in black.

7.6 Random spore analysis

Cells with opposite mating types, h^- and h^+, were mixed on the MEA plate and incubated at 27°C for normally 2 days. The asci were treated with 100 μl of 0.5% helicase (Biosepra) for 3 hr at 27°C to digest the cell wall. 43 μl ethanol was added and the reaction tube was vortexed for 20 min at RT, to eliminate the non-sporulating cells. The spores were spun down, resuspended in H_2O, and plated onto YE5S plates. After 4 days incubation at 27°C, the grown colonies were then replica plated onto the desired plates for selection.

7.7 Centrifugal elutriation

Before starting, the elutriator needed to be washed by 1.5 L of H_2O, followed by washing and refilling with fresh YE5S liquid. Any bubble should be removed from the whole system, and the chamber temperature was set at 27 ^oC. The rotor speed was set to 3000 rpm before sample loading. 3 litres of overnight YE5S cultures (exponentially grew to $1x10^7$ cells/ml at 27^oC) were run through the elutriator (Avanti J-20 XP equipped with JE-5.0 rotor, Beckman Coulter Inc.). The input of the cells was controlled by the pump (Masterflex 7016-20 pump, Cole Parmer Co.) at a flow rate ~150 ml/min (setting 2.5). The rotor speed was increased to 3500 rpm, and the pump rate was accordingly decreased to 85 ml/min (setting 1.8). When the cells started to appear in the chamber, the pump rate was increased to 120 ml/min (setting 2.3) to speed up the cell accumulation. When the cells were almost up to the boundary in the elutriation chamber, the rotor speed was gradually decreased to 3000 rpm, accompanied by the simultaneous decrease of the pump rate to 60 ml/min (setting 1.5). The process was kept until ~90% of the culture cells were accumulated in the chamber. When collecting the cells, fresh YE5S was pump into the system at a rate of 5 ml/min (setting 0.5). The first ~200 ml of cells were largely dead and stationary population, and the subsequent fraction of flow cells (~100 ml/fraction) were collected and the cell size (and number) was immediately monitored using the KX-21N cell counter (Sysmex Corp.). The fraction of small early G2 cells was typically $1~2x10^6$ cells/ml with a sharp peak on the cell counter. Those cells were quickly filtered and concentrated to ~$4x10^6$ cells/ml for the following experiment.

7.8 Synchronous cultures using HU or *cut9-665* strain

In order to accumulate mitotic cells, HU-induced S phase arrest and release was used (Figure 3.5, 3.6, 3.7, 4.3, 4.5, 5.5, 5.6, and 5.7). Cultures were treated with 12.5 mM hydroxyurea (HU) at 25^oC for 4 hr, filtered and incubated HU-free

media at 36°C for 1-2 hr. For inactivation of Ark1, 5 μM 1NM-PP1 was added to the culture after 30 min incubation at 36°C. Upon further 60 min incubation at 36°C, cells were observed under fluorescent microscope.

In some experiments (Figure 4.4, 4.15), the strain was crossed with *cut9-665*. Cells were grown at 27°C overnight. Adequate amounts of the cultures were then shifted up at 36°C for 3.5 hr to arrest the cell cycle at mid mitosis.

7.9 Construction of plasmids carrying wild type or mutant *ndc80* genes

The whole ORF of the *ndc80*$^+$ gene was PCR-amplified and cloned into *Nde*I/*Bam*HI sites of pREP1 (or pREP41), which carries the thiamine repressible *nmt1* (*nmt41*) promoter, designated pREP-Ndc80 (verified by nucleotide sequencing). Various *ndc80* mutants (T307A, E379G, L405P, T307A/E379G and E379G/L405P) were then constructed using QuikChange kit (Stratagene Co. U. S. A.) according to manufacture's instruction with pREP-Ndc80 as a template. Plasmids producing truncated Ndc80 mutants (Δloop and ΔN tail) were constructed from PCR-amplified corresponding *ndc80* fragments. Ndc80Δloop lacks the internal residues between 400-476 or 371-476, whist Ndc80ΔN tail lacks 2-94 amino acid residues. All the mutations were verified by nucleotide sequencing.

7.10 Construction of strains containing *nuf2-dis1* fusion genes

DNA fragments encoding Nuf2-Dis1 (amino acid 18-882), Nuf2-Dis1N (amino acid 18-518) and Nuf2-Dis1C (amino acid 518-882), flanked by the C-terminal nourseothricin (nat)-resistant marker (Sato et al., 2005), were amplified by using two-step PCR. These fragments were transformed into a *nuf2*$^+$-YFP-*ura4*$^+$ strain (KSH002) and integrants were selected on 5'FOA (5-fluoro-orotic acid)- and

nourseothricin-containing plates. Correct integrations were checked by colony PCR or sequencing. The correct strain was then crossed with *ndc80-21*. Basically the same procedures were followed to construct the *mis12*$^{+}$-*dis1*$^{+}$ fusion gene except that in this case, *mis12*$^{+}$-*dis1*$^{+}$ fragments followed by the *nat*^{r} maker were directly amplified with PCR and transformed into an *ndc80-21* strain

7.11 Fluorescence microscopy and signal quantification

Images were taken using an Olympus IX70 wide-field inverted epifluorescence microscope with an Olympus PlanApo 100×, NA 1.4, oil immersion objective. DeltaVision image acquisition software (softWoRx 3.3.0; Applied Precision) equipped with Coolsnap HQ (Roper Scientific) was used. The sections of images at each time point were compressed into a two-dimensional (2D) projection using the DeltaVision maximum intensity algorithm. Deconvolution was applied before the 2D projection. Kymograph pictures derived from 2D-projected time-lapse images were constructed using softWoRx 3.3.0. Images were taken as 14–18 sections along the *z* axis at 0.25- to 0.3-mm intervals; they were then deconvolved and merged into a single projection. For some experiments, an AxioplanII microscope (Zeiss Lts.) with Volocity software (Improvision Co.) was also used. Captured images were processed with Adobe Photoshop CS3 (version 10.0).

For the signal quantification, cells were fixed by chilled methanol and frozen at -80°C immediately for 30 min. The fixed cells were then washed by PBS twice and observed under the DeltaVision microscopy. Images were merged into a single projection using maximum intensity algorithm in Deltavision-SoftWoRx (Olympus and Applied Precision Ltd.). Fluorescence signals were then quantified using maximum intensity within an area of 6x6 pixel, after subtracting background signals in the vicinity of the fluorescent spot.

7.12 Fast protein extraction

To check the protein expression in the fission yeast cells (Fig 2.10 and 3.13), I used the quick alkaline method developed from our lab. Cells were collected, washed in 1 ml of H_2O, and resuspended in 1 ml of 0.3N NaOH. The tube was incubated at RT for 10 min. Cells were spun down at 4000 rpm for 2 min, and the supernatant was removed. 100 μl of 1x sample buffer was added and the sample was boiled for 5 min. The tube was then briefly spun at 13,000 rpm for 15 sec. The sample was loaded onto a SDS-PAGE for immunoblotting.

7.13 Expressions and purifications of various recombinant Dis1 proteins

Various Dis1 constructs were cloned into the pGEX vector. GST-Dis1 (18-882) fusion proteins were produced in *E. coli* (Rosetta p*Lys*S, Merck) (19°C overnight upon 1 mM IPTG induction), whereas various GST-Dis1 truncated or mutated proteins were expressed in *E. coli* (FB810) (25°C for 6 hr upon 1 mM IPTG induction). Briefly, 1 (or 2) litre of the LB culture was collected, and the *E. coli* was pelleted down. The pellet was incubated with the cold *E. coli* buffer supplied with Roche protease inhibitor cocktail (complete), lysozyme, and DNase I on ice for 30 min. The sample was further sonicated for 6 times (6 sec/time, and 10 sec/interval on ice), and the supernatant was cleared at 14,800 rpm for 20 min, 4°C. The protein extracts were purified with the Glutathione-Sepharose beads as recommended by the manufacturer (Invitrogen, Carlsbad, CA, U. S. A.). The first two or three elution fractions (1 ml/fraction) were merged and concentrated by the Vivaspin column. The concentrated proteins were applied onto the HPLC system equipped with a Superdex 200 10/300GL size exclusion column for further purification. Note that the same buffer was used but degased before the experiment. The gel fitration was kindly helped by Dr. Martin Singleton's lab .

7.14 GST pull down assay

Yeast cell extracts were prepared from a strain containing Ndc80-3Flag upon HU arrest-release. Glutathione-Sepharose beads bound with GST alone or GST-Dis1 were incubated with the cell extracts (10 mg) at 4°C for 2 h. After washing 4 times with IP buffer, the bound proteins were eluted with reduced glutathione, separated by SDS-PAGE and immunoblotted with anti-FLAG antibody (M2, Sigma-Aldrich UK).

7.15 Immunoprecipitation

Cells were harvested, washed by 1 ml of STOP buffer, and resuspended in IP buffer. Proteins were extracted by breaking the cells at 4°C with glass beads (425-600 nm) in a FastPrep FP120 apparatus (setting 5.5, 25 s, 2x) (Savant. Co, MN, USA). The protein extracts were cleared after 15 min of centrifugation at 13,000 x g at 4°C, and the protein concentrations were determined by Braford assay (Bio-Rad). The coimmunoprecipitations were performed by adding 3 mg of protein extracts to protein A dynabeads (Invitrogen Ltd. CA, USA) bound with anti-FLAG antibody (M2, Sigma-Aldrich UK). For immunoblotting, anti-FLAG and anti-Myc (MMS-150R, Covance Inc. CA, USA) antibodies were used at 1:1000 and 1: 2000, respectively. For Dam1-Ndc80 interaction, 1.67 mg extracts were used for immunoprecipitation and 50 µg were run as WCE, and the anti-GFP antibody (1814 460, Roche Diagnostics, Indianapolis, IN) antibodies (1:1000) was used.

7.16 Binding assay between Dis1 and Ndc80-loop mutants

Rabbit polyclonal anti-Ndc80 antibodies were prepared by Eurogenetec Co. (Belgium). Peptides H_2N-CRETASEEKNAFDAE-$CONH_2$ were used to raise sera, which were affinity-purified before usage. *nmt41*-GFP-*dis1*$^+$ cells carrying

episomal pREP1-Ndc80 or pREP1-Ndc80Δ371-476 were grown in the absence of thiamine for 12 h at 30°C, followed by HU arrest for 4 h at 25°C and release at 36°C for 1.5 h. Cell extracts (5 mg) were prepared from these cultures and immunoprecipitation was performed with anti-Ndc80 antibodies, followed by immunoblotting with anti-Ndc80 (1:100) and anti-GFP (1814 460, Roche Diagnostics, Indianapolis, IN) antibodies (1:1000).

7.17 Peptide array assay

The peptide binding experiments described previously (Maskell et al., 2010) were basically followed. Peptides were synthesized and spotted onto a cellulose membrane. The membrane was activated by treatment with 50% ethanol + 10% glacial acetic acid for 1 h and then washed with IP buffer. 1 µg/ml of various GST-Dis1 proteins (full-length or truncated) or GST alone was added to the solution. After overnight incubation at 4°C, the membrane was washed three times using IP buffer to remove the unbound proteins. The membrane was then blocked with 3% skim milk in the same buffer, followed by incubation with anti-GST antibody (27457701V, GE Healthcare Life Science) for 2 hr at room temperature. After further washes, spots with bound GST-Dis1 were detected using bovine anti–goat IgG-HRP–conjugated secondary antibody (sc-2378, Santa Cruz Biotechnology) and visualized by chemiluminescence.

7.18 Microtubule cosedimentation assay

Purified tubulins (from pig brains) were a generous gift from Dr. Thomas Surrey's lab. Tubulins were first polymerised by using paclitaxel in a step-wise manner (adding 1/10 v/v of 1 μM, 10 μM, 100 μM paclitaxel and incubating at 37°C for 10-15 min in each step). Polymerised microtubules were spun down using the TLA-100 rotor at 80,000 rpm, RT, 10 min, and resuspended in BRB80 buffer (with 1 mM DTT and 20 μM taxol). After serial dilution, 10 μl of the

microtubules were incubated with 10 μl of protein mixtures containing 6 μg/μl of BSA and 7 μg/μl of GST-Dis1(18-882) (or GST-Dis1 (520-645)). Reactions were incubated at RT for 10 min, and then 120 μl of BRB80 + 40% glycerol cushions was added. The samples were pelleted for 10 min at 80,000 rpm in a TLA100 rotor at 25°C. For the supernatant sample, 40 μl was removed from the top of the tube. For the pellet fraction, the remaining supernatant was discarded and 40 μl BRB80 + 10 mM $CaCl_2$ was added to the pellet for 10 min on ice. 40 μl of 2x sample buffer was added, and the samples were boiled for 5 min. 15 μl of the samples were loaded and analysed by SDS-PAGE.

7.19 Buffers used in this study

Name	Components
TE	10 mM Tris-HCl, pH7.5, 1 mM EDTA
TAE	0.08 M Tris acetate, pH7.5, 2 mM Na_2EDTA
6x loading dye	30% glycerol, 0.1% bromophenol blue
LiAc/TE	100 mM lithium acetate pH7.4, 10 mM Tris-HCl pH7.4, 1 mM EDTA pH8.0
LiAc/TE/40% PEG3640	LiAc/TE + 40% polyethylene glycol 3640 (Sigma)
Transfer buffer	39 mM glycine, 48 mM Tris-base, 20% methanol
PBS	170 mM NaCl, 3 mM KCl, 10 mM Na_2HPO_4, 2 mM KH_2PO_4
PBST	PBS + 0.1% Tween-20
STOP buffer	150 mM NaCl, 50 mM NaF, 10 mM EDTA, 0.007% v/v NaN_3
IP buffer	50 mM Tris-HCl pH7.4, 1 mM EDTA pH8.0, 500 mM NaCl, 0.05% NP40, 0.1% Triton X-100, 10% glycerol, (plus fresh 1 mM DTT, 15 mM pNPP, 1 x protease cocktail inhibitor (Sigma), 1 mM PMSF)
E.coli buffer	50 mM Tris-HCl pH7.4, 1 mM EDTA pH8.0, 500 mM NaCl, 0.05% NP40, 0.1% Triton X-100, 10% glycerol, 1 mM DTT
2x sample buffer	125 mM Tris-HCl pH6.8, 50% glycerol, 4% SDS, 0.02% bromophenol blue, 100 mM DTT

BRB80 buffer (tubulin)	80 mM PIPES pH6.8, 1 mM $MgCl_2$, 1 mM EGTA, 1 mM DTT, 20 μM taxol

7.20 Plasmids used in fission yeast in this study

Name	Gene	Origin*
pAL-SK-Alp14	*alp14+*	our stock
pREP1-Ase1	*ase1*$^+$	our stock
pREP41-Ase1	*ase1*$^+$	our stock
pSB123	*cls1*$^+$	F. Chang
pUR19-Dam1(full length)	*dam1*$^+$	J. Millar
pUR19-Dam1(1-127)	*dam1*	J. Millar
pSK-Dis1	*dis1*$^+$	our stock
pKZ17	*mal3*$^+$	our stock
pREP1-Ndc80	*ndc80*$^+$	
pREP1-Ndc80-T307A	*ndc80*	
pREP1-Ndc80-E379G	*ndc80*	
pREP1-Ndc80-L405P	*ndc80*	
pREP1-Ndc80-T307A/E379G	*ndc80*	
pREP1-Ndc80-E379G/L405P	*ndc80*	
pREP1-Ndc80Δ371-476	*ndc80*	
pREP1-Ndc80Δ400-476	*ndc80*	
pREP1-Ndc80Δ2-94	*ndc80*	
pREP41-GFP-Ndc80	*ndc80*$^+$	

pREP41-GFP-Ndc80Δ371-476	*ndc80*
pREP41-GFP-Ndc80Δ400-476	*ndc80*

*Plasmids were constructed for this study unless otherwise specified.

7.21 Fission yeast strains used in this study

Strains	Genotypes
513	*h⁻ leu1 ura4*
AR028	*h⁺ klp5⁺::ura4⁺ leu1 ura4 his7 ade6-M216*
CHP428	*h⁺ leu1 ura4 his7 ade6-M210*
CHP429	*h⁻ leu1 ura4 his7 ade6-M216*
KSH002	*h⁻ nuf2⁺-YFP-ura4⁺ leu1 ura4*
KSH003	*h⁻ nuf2⁺-mCherry-ura4⁺ leu1 ura4*
KSH016	*h⁻ ndc80⁺-GFP-kanʳ leu1 ura4*
KSH017	*h⁻ ndc80⁺-TAATAG-kanʳ leu1 ura4*
KSH059	*h⁻ ndc80-21-kanʳ nuf2⁺-YFP-ura4⁺ leu1 ura4*
KSH060	*h⁻ ndc80-21-kanʳ leu1 ura4*
KSH063	*h⁻ ndc80-24-kanʳ nuf2⁺-YFP-ura4⁺ leu1 ura4*
KSH065	*h⁻ ndc80-26-kanʳ nuf2⁺-YFP-ura4⁺ leu1 ura4*
KSH087	*h⁻ ndc80-102-kanʳ nuf2⁺-YFP-ura4⁺ leu1 ura4*
KSH107	*h⁻ spc25⁺-YFP-natʳ leu1 ura4*
KSH139	*h⁻ ndc80-21-kanʳ spc25⁺-YFP-natʳ leu1 ura4*
KSH143	*diploid ndc80⁺/ndc80::kanʳ leu1 ura4 his7 ade6-M210 ade6-M216*
KSH149	*h⁻ ndc80-03-kanʳ kanʳ-GFP-atb2⁺ mis6⁺-2mRFP-hphʳ cut12⁺-CFP-natʳ leu1 ura4*
KSH151	*h⁻ ndc80-20-kanʳ kanʳ-GFP-atb2⁺ mis6⁺-2mRFP-hphʳ cut12⁺-CFP-natʳ leu1 ura4*
KSH153	*h⁻ ndc80-20-kanʳ kanʳ-GFP-atb2⁺ mis6⁺-2mRFP-hphʳ cut12⁺-CFP-natʳ leu1 ura4*
KSH155	*h⁻ ndc80-24-kanʳ kanʳ-GFP-atb2⁺ mis6⁺-2mRFP-hphʳ cut12⁺-CFP-natʳ leu1 ura4*
KSH157	*h⁻ ndc80-31-kanʳ kanʳ-GFP-atb2⁺ mis6⁺-2mRFP-hphʳ cut12⁺-CFP-natʳ leu1 ura4*
KSH161	*h⁻ ndc80-36-kanʳ kanʳ-GFP-atb2⁺ mis6⁺-2mRFP-hphʳ cut12⁺-CFP-natʳ leu1 ura4*
KSH163	*h⁻ kanʳ-GFP-atb2⁺ mis6⁺-2mRFP-hphʳ cut12⁺-CFP-natʳ leu1 ura4*
KSH170	*diploid ndc80⁺/ndc80:: ura4⁺ leu1 ura4 his7 ade6-M210 ade6-M216*
KSH181	*h⁻ ndc80-34-kanʳ aurʳ-mCherry-atb2⁺ nuf2⁺-YFP-ura4⁺ cut12⁺-CFP-natʳ leu1 ura4*

KSH183 *h⁻ ndc80-102-kan^r aur^r-mCherry-atb2$^+$ nuf2$^+$-YFP-ura4$^+$ cut12$^+$-CFP-nat^r leu1 ura4*

KSH189 *h⁻ aur^r-mCherry-atb2$^+$ nuf2$^+$-YFP-ura4$^+$ cut12$^+$-CFP-nat^r leu1 ura4*

KSH193 *h⁻ ndc80-102-kan^r nuf2$^+$-YFP-ura4$^+$ spc25$^+$-YFP-nat^r leu1 ura4*

KSH206 *h⁻ cen2(D107)-kanr-ura4+-lacOp his7$^+$-lacI-GFP-ura4$^+$ sad1$^+$-dsRed-leu2$^+$ leu1 ura4*

KSH221 *h⁻ ndc80-21-kan^r cen2(D107)-kanr-ura4+-lacOp his7$^+$-lacI-GFP-ura4$^+$ sad1$^+$-dsRed-LEU2 leu1 ura4*

KSH224 *h⁻ mad2$^+$-GFP-leu2$^+$ mis6$^+$-2mRFP-hph^r cut12$^+$-CFP- nat^r leu1*

KSH228 *h⁻ ndc80-21-kan^r mad2$^+$-GFP-LEU2 mis6$^+$-2mRFP-hph^r cut12$^+$-CFP- nat^r leu1 ura4*

KSH276 *h⁻ ndc80-26-kan^r kan^r-GFP-atb2$^+$ mis6$^+$-2mRFP-hph^r cut12$^+$-CFP-nat^r leu1 ura4*

KSH308 *h⁻ spc25$^+$-YFP-nat^r cut11$^+$-CFP-kan^r leu1 ura4*

KSH316 *h$^+$ ndc80-26-kan^r spc25$^+$-YFP-nat^r cut11$^+$-CFP-kan^r leu1 ura4 his2*

KSH322 *h⁻ nuf2-1-ura4$^+$ spc25$^+$-YFP-nat^r cut11$^+$-CFP-kan^r leu1 ura4*

KSH397 *h$^+$ ndc80-21-kan^r ark1-as3-hph^r mad2$^+$-GFP-leu2$^+$ cut12$^+$-CFP-nat^r (leu1)*

KSH398 *h⁻ ndc80-21-kan^r mad2$^+$-GFP-leu2$^+$ cut12$^+$-CFP-nat^r (leu1)*

KSH412 *h$^+$ kan^r-GFP-atb2$^+$ mis6$^+$-2mRFP-hph^r cut11$^+$-CFP-kan^r leu1 ura4 his2*

KSH414 *h$^+$ ndc80-26-kan^r kan^r-GFP-atb2$^+$ mis6$^+$-2mRFP-hph^r cut11$^+$-CFP-kan^r leu1 ura4 his2*

KSH446 *h$^+$ dis1-GFP-kan^r mis6$^+$-2mRFP-hph^r cut12$^+$-CFP-nat^r leu1 ura4 his2 (his7)*

KSH450 *h$^+$ dis1-GFP-ura4$^+$ mis6$^+$-2mRFP-hph^r cut12$^+$-CFP-nat^r leu1 ura4 his2 (his7)*

KSH463 *h$^+$ kan^r-nmt1-GFP-dis1$^+$ mis6$^+$-2mRFP-hph^r cut12$^+$-CFP-nat^r leu1 ura4 his7*

KSH466 *h⁻ kan^r-nmt41-GFP-dis1$^+$ mis6$^+$-2mRFP-hph^r cut12$^+$-CFP-nat^r leu1 ura4 his7*

KSH467 *h$^+$ ndc80-21-kan^r kan^r-nmt41-GFP-dis1$^+$ mis6$^+$-2mRFP-hph^r cut12$^+$-CFP-nat^r leu1 ura4 his2 (his7)*

KSH468 *h⁻ kan^r-nmt81-GFP-dis1$^+$ mis6$^+$-2mRFP-hph^r cut12$^+$-CFP-nat^r leu1 ura4 his7*

KSH469 *h$^+$ ndc80-21-kan^r kan^r-nmt81-GFP-dis1$^+$ mis6$^+$-2mRFP-hph^r cut12$^+$-CFP-nat^r leu1 ura4 his2 (his7)*

KSH487 *h⁻ mis6$^+$-2mRFP-hph^r alp4$^+$-GFP-kan^r leu1 ura4*

KSH489 *h⁻ ndc80-26-kan^r mis6$^+$-2mRFP-hph^r alp4$^+$-GFP-kan^r leu1 ura4*

KSH499 *h⁻ cut9-665 dis1$^+$-8Myc-leu2$^+$ (ura4)*

KSH510 *h$^+$ ndc80$^+$-3Flag-kan^r leu1 ura4 his2*

KSH515 *h$^+$ dam1$^+$::hph^r leu1 ura4 his7 ade6*

KSH545 *h⁻ cut9-665 dis1$^+$-8Myc-leu2$^+$ ndc80$^+$-3Flag-kan^r (leu1)*

KSH546 *h⁻ cut9-665 ndc80$^+$-3Flag-kan^r leu1*

KSH550 *h⁻ ndc80-21-kan^r ark1-as3-hph^r kan^r-GFP-atb2$^+$ sid4$^+$-mRFP-nat^r leu1*

KSH552 *h⁻ nuf2$^+$-dis1(18-882)-nat^r leu1 ura4*

KSH555	*h$^+$ ndc80-21-kan^r nuf2$^+$-dis1(18-882)-nat^r leu1 ura4 his2*
KSH556	*h$^-$ ndc80-21-kan^r nuf2$^+$-dis1(18-518)-nat^r leu1 ura4*
KSH557	*h$^-$ ndc80-21-kan^r nuf2$^+$-dis1(518-882)-nat^r leu1 ura4*
KSH576	*h$^-$ dis1::ura4$^+$ kan^r-GFP-atb2$^+$ mis6$^+$-2mRFP-hph^r cut12$^+$-CFP-nat^r leu1 ura4*
KSH582	*h$^-$ ndc80-21-kan^r dam1$^+$-GFP-kan^r mis6$^+$-2mRFP-hph^r cut12$^+$-CFP-nat^r leu1 ura4 his7*
KSH583	*h$^-$ dam1$^+$-GFP-kan^r mis6$^+$-2mRFP-hph^r cut12$^+$-CFP-nat^r leu1 ura4 his7*
KSH589	*h$^-$ dis1::ura4$^+$ dam1$^+$-GFP-kan^r mis6$^+$-2mRFP-hph^r cut12$^+$-CFP-nat^r leu1 ura4 his7*
KSH592	*h$^-$ cut9-665 dam1$^+$-GFP-kan^r leu1*
KSH595	*h$^-$ cut9-665 ndc80$^+$-3Flag-kan^r dam1$^+$-GFP-kan^r leu1*
KSH597	*h$^-$ dis1$^+$-GFP-ura4$^+$ mis6$^+$-2mRFP-hph^r cut12$^+$-CFP-nat^r leu1 ura4*
KSH599	*h$^-$ dam1::kan^r dis1$^+$-GFP-ura4$^+$ mis6$^+$-2mRFP-hph^r cut12$^+$-CFP-nat^r leu1 ura4 ade6*
KSH613	*h$^-$ dis1::ura4$^+$ dis1-6A-GFP-lys1/CN2 mis6$^+$-2mRFP-hph^r cut12$^+$-CFP-nat^r leu1ura4 ade6*
KSH617	*h$^-$ dis1::ura4$^+$ dis1-6E-GFP-lys1/CN2 mis6$^+$-2mRFP-hph^r cut12$^+$-CFP-nat^r leu1ura4 his7 (ade6)*
KSH637	*h$^-$ ndc80-21-kan^r mis12$^+$-dis1(18-882)-nat^r leu1ura4*
KSH640	*h$^+$ flp1::ura4$^+$ leu1ura4 his2*
KSH641	*h$^-$ ndc80-21-kan^r flp1::ura4$^+$ leu1ura4*
TP108-3D	*h$^+$ leu1 ura4 his2*
MS205	*h$^+$ dis1$^+$::ura4$^+$ leu1 ura4 his7 (ade6)*
MS685	*h$^+$ alp14$^+$::ura4$^+$ leu1 ura4 his2*

*Basically strains named by KSH were developed for this study, whereas others were from our lab stock.

7.22 Oligos used in this study

The following figure presents some of the oligos that were designed for sequencing, tagging, and other cloning purposes for (A) Ndc80 and (B) Dis1.

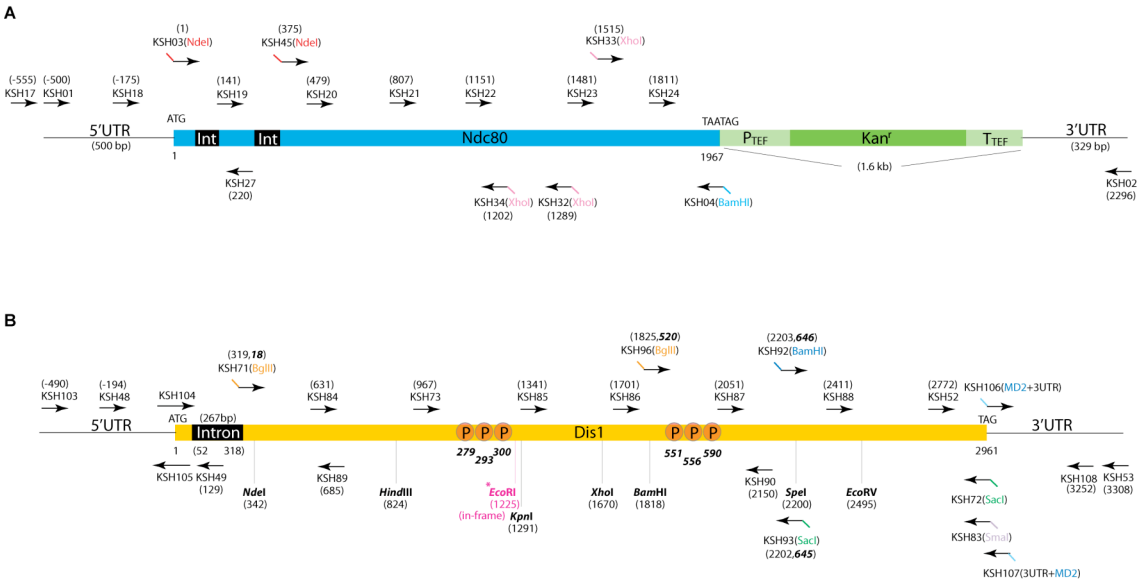

For deletion of *ndc80*$^{+}$:

KSH15 F'-Ndc80 (deletion):
TGTTACTTAGCAAAGTGGTTTTGTTGTTATAACTAACGTCTCCAACGATAAA
AGACAACAATCTGCTTGTATTACTATAACGGATCCCCGGGTTAATTAA

Ndc80-C-tag-3:
AACACAAAAACACCATCGTGATAAAAAAATGTATTCATGAGCCGTGAATATA
GTAGACAGCACAATACGATGAATAGAATGAATTCGAGCTCGTTTAAAC

For mutagenesis of *ndc80*$^{+}$ for ts mutant isolation:

KSH01 F'-Ndc80-Kan^{r}: TCTTATAAATCTTTATGAATTTTG

KSH02 R'-Ndc80-Kan^{r}: TAAATTTTGAACTACTTTCAGC

For C-terminal tagging of *spc25*$^{+}$:

KSH11 F'-Spc25 (C-tag):
CTAGAGACTTTTATCAGTTTCTGAAAGATATGCGGAAGGGATTCCGTGAAC
TTCATAGAAAGGATCTGTCTCAATTGATTCGGATCCCCGGGTTAATTAA

KSH12 R'-Spc25 (C-tag):
TCTGGCGAAATTATTCCTGATACAGTGGAAGCCAACATGGAAGACGAGGA
GGAAGTTTATGTTAAACAAGAAGAAGATCTGAATTCGAGCTCGTTTAAAC

For sequencing of *ndc80* mutants:

KSH17 F'-Ndc80 (-555): AGGATATTTAGAATGCTACAC

KSH18 F'-Ndc80 (-175): AATCCTGCCGTTGTCGATAT

KSH19 F'-Ndc80 (141): GTACTTCAAGAACCAGTTTAG

KSH20 F'-Ndc80 (479): TAATCGTTTCATGCCATCAAC

KSH21 F'-Ndc80 (807): GTTCGCACATATCATTTGTAC

KSH22 F'-Ndc80 (1151): AAGGGACTCTCTGAAGTATC

KSH23 F'-Ndc80 (1481): CCATTTATTAATGAAGTTAGAC

KSH24 F'-Ndc80 (1811): ACATGCTTGCATGGAGTACA

KSH27 R'-Ndc80 (220): AGAAGACAAACCGTCAGGAT

For expression of recombinant Ndc80-Nuf2 subcomplex:

KSH03 F'-Ndc80 (NdeI): CTGCATATGCAAGATTCTTCCTCT

KSH04 R'-Ndc80 (BamHI): TTTGGATCCTTACAGTTCCGAAC

KSH05 F'-Nuf2 (NdeI): ATACATATGGCACGAAAACACAC

KSH06 R'-Nuf2 (BamHI): TTGGGATCCCTAAGAGTTAGAAGAC

KSH25 R'-Ndc80 1-370(BamHI): TTTGGATCCTTATTCGCTTATAGAAATAT

KSH26 R'-Nuf2 1-254(BamHI): TTTGGATCCTTACGATGTGTCTGCTAT

For deletions of Ndc80 N-tail and internal loop:

KSH03 F'-Ndc80 (NdeI): CTGCATATGCAAGATTCTTCCTCT

KSH04 R'-Ndc80 (BamHI): TTTGGATCCTTACAGTTCCGAAC

KSH35 R'-Ndc80(del371-476): TTCTTCATGAAATTCGCTTATAGAAAT

KSH36 F'-Ndc80(del371-476): TCTATAAGCGAATTTCATGAAGAACAA

KSH37 R'-Ndc80(del400-476): TTCTTCATGAAACACTTCTTTCCTTAA

KSH38 F'-Ndc80(del400-476): AGGAAAGAAGTGTTTCATGAAGAACAA

KSH45 F'-Ndc80(del1-94 NdeI): GCAATCCATATGAAAGATCCAAGACCATTG

For site-directed mutagenesis to create mutations of *ndc80-21*:

KSH39 F'-*ndc80-21* T307A:
GAAGAGCGCTATCGAGCTATGCAACGTGATGAAG

KSH40 R'-*ndc80-21* T307A:
CTTCATCACGTTGCATAGCTCGATAGCGCTCTTC

KSH41 F'-*ndc80-21* E379G:
GATGGTCTCAGAGAGGGGGCAATTAGACAG

KSH42 R'-*ndc80-21* E379G:
CTGTCTAATTGCCCCCTCTCTGAGACCATC

KSH43 F'-*ndc80-21* L405P:
GTTTGACACGGACTTGCCCATTCAAGCTAGCATC

KSH44 R'-*ndc80-21* L405P:
GATGCTAGCTTGAATGGGCAAGTCCGTGTCAAAC

For N-terminal tagging of *dis1*$^{+}$:

KSH46 F'-Dis1(N-tag GFP):
AAAATTCATTCTTTTACATAACTATTCATGCTCTGCTGGTTGTAAACATACG
AGTCGTTAATTTATATTTGTTTATGTAAGAATTCGAGCTCGTTTAAAC

KSH47 R'-Dis1(N-tag GFP):
CTATCTCCATTAATTTGTAAAAAGCTTACCTTATCAAAAATTTGACTGAGAAT
GCGGCTATTAAAATCGTCCAACTCCATTTTGTATAGTTCATCCATGC

For various Nuf2-Dis1 fusions or Mis12-Dis1 fusion:

KSH28 F'-Nuf2 (311): ACCTATTGAA ACCAGACAGA

KSH59 F'-Nuf2-Dis1C (518-882):
CTATGGAATTCGAAAAATTGAAATCGCACGTGGAGCTTTATATTGCTGAAC
TTCTCAGAAACTTAAGGTCTTCTAACTCTATGGATCCTAAAAAGTTACCA

KSH62 F'-Nuf2-Dis1 (18aa):
TTAAGGTCTTCTAACTCTTCTTGGAAAGTTCGATTT

KSH63 R'-Nuf2-Dis1 (18aa):
AAATCGAACTTTCCAAGAAGAGTTAGAAGACCTTAA

KSH64 F'-Dis1-MD1:
CAAAGGATGAAGAAGGCGTAGTCCCCGGGTTAATTAAGGCG

KSH65 R'-MD1-Dis1:
CGCCTTAATTAACCCGGGGACTACGCCTTCTTCATCCTTTG

KSH66 F'-MD2-Nuf2 (3UTR):
CGATACTAACGCCGCCATCCTATCTTCATTTTGAAAAATC

KSH67 R'-Nuf2(3UTR)-MD2:
GATTTTTCAAAATGAAGATAGGATGGCGGCGTTAGTATCG

KSH68 R'-MD1-Dis1N(1-518)**:**
CGCCTTAATTAACCCGGGGACTAATCCAATCCCACAATATA

KSH69 R'-Nuf2-Dis1(518-882):
TGGTAACTTTTTAGGATCCATAGAGTTAGAAGACCTTAA

KSH70 R'-Nuf2 (3UTR820): ATGCTGCATGTAAAGCTTCA

KSH76 F'-Mis12 (91): AGGTGTAAATGGTGTGGATA

KSH77 F'-Mis12-Dis1 (18aa):

GGACATACTGACGAGCCTTCTTGGAAAGTTCGATTT

KSH78 R'-Mis12-Dis1 (18aa):

AAATCGAACTTTCCAAGAAGGCTCGTCAGTATGTCC

KSH79 F'-MD2-Mis12(3UTR):

CGATACTAACGCCGCCATCCTACTAATCAACTAGCTAA

KSH80 R'-Mis12(3UTR)-MD2:

TTAGCTAGTTGATTAGTAGGATGGCGGCGTTAGTATCG

KSH81 R'-Mis12(3UTR733): TCACACATCATTGCTTCATT

For expression of various recombinant Dis1 proteins:

KSH71 F'-GST-Dis1 (BglII): ACATCAGATCTTGGAAAGTTCGA

KSH72 R'-GST-Dis1 (SacI): TATTGGAGCTCCTACGCCTTCTTCAT

KSH92 F'-Dis1 646-882 (BamHI): ATAAGGATCCAGTCGACTTTCCACGAAG

KSH93 R'-Dis1 520-645 (SacI): TATTGGAGCTCAGTCTCTAACTTTTTCGA

KSH96 F'-Dis1 520-882 (BglII): ACATCAGATCTAAAAAGTTACCAAAAATA

Appendix

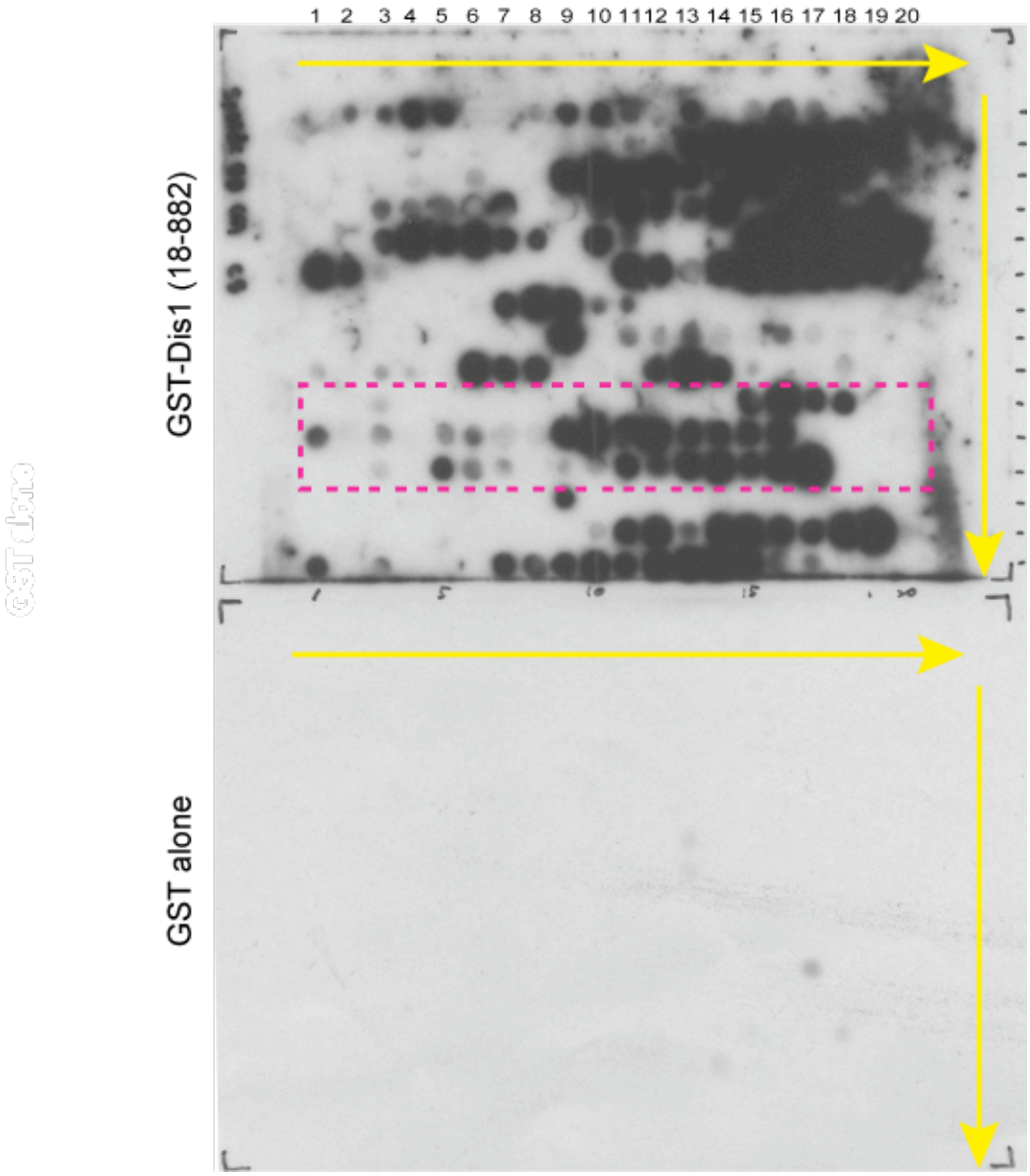

Appendix 0.1 The peptide binding assay of full-length Ndc80.

The peptide array was synthesised to cover the full-length Ndc80 sequence. The array binding was performed as described in Material and Method. Note that the binding pattern of the internal loop region (red-dash square) was the same as that shown in Figure 4.6. However, there were also positive interaction regions near the N-terminal CH domain.

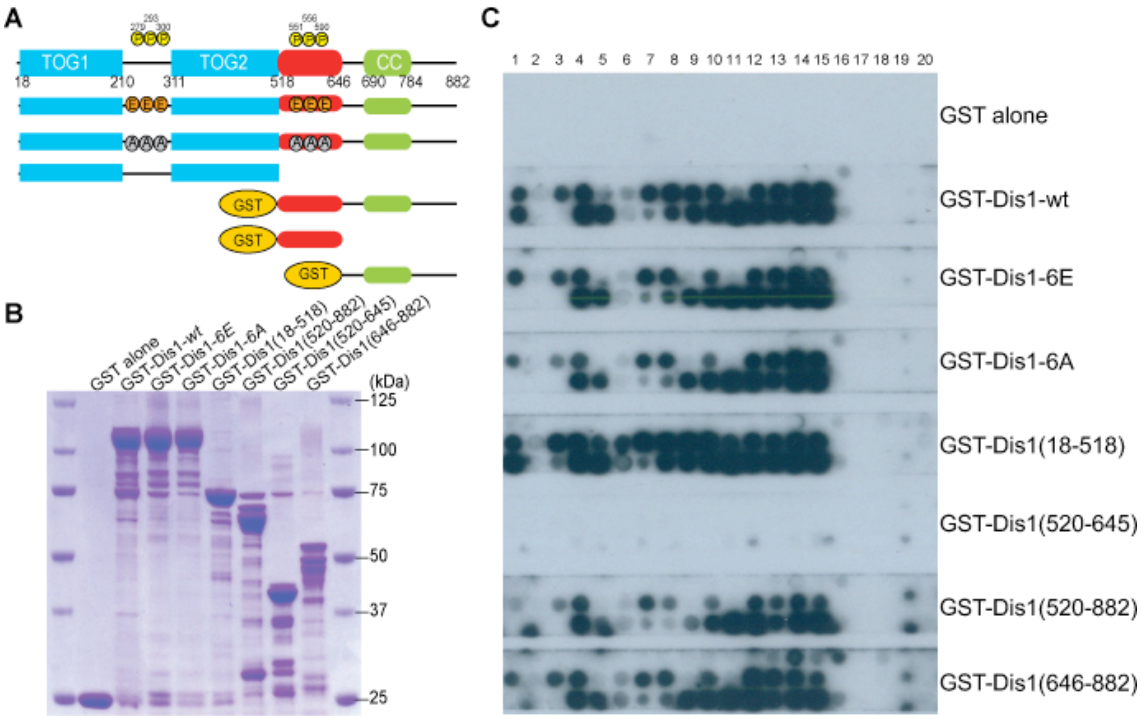

Appendix 0.2 Full set data for Dis1 domain analysis using the peptide assay.

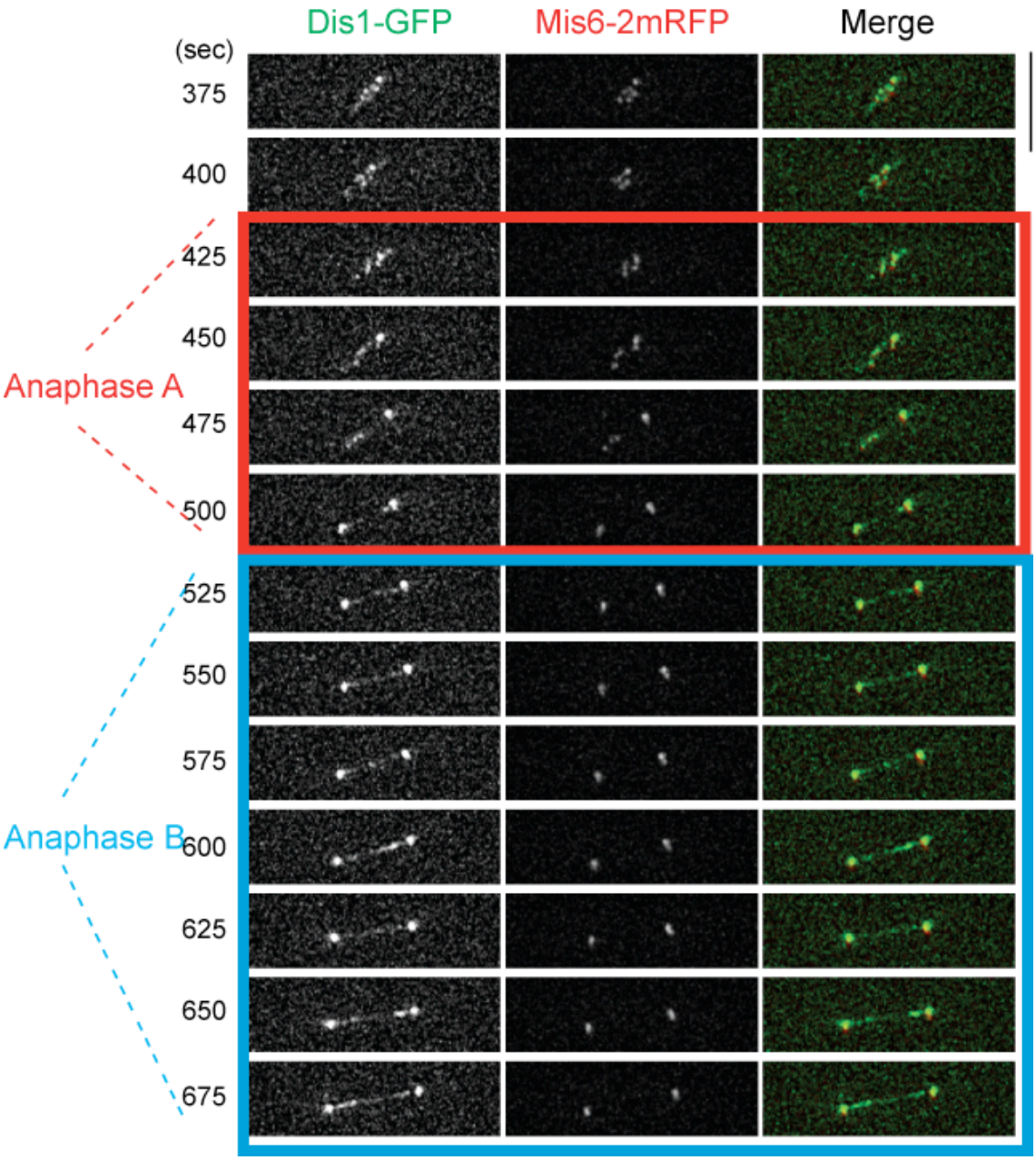

Appendix 0.3 Dis1-GFP still localises to the kinetochore during anaphase A.

Reference

ABRIEU, A., MAGNAGHI-JAULIN, L., KAHANA, J. A., PETER, M., CASTRO, A., VIGNERON, S., LORCA, T., CLEVELAND, D. W. & LABBE, J. C. (2001) Mps1 is a kinetochore-associated kinase essential for the vertebrate mitotic checkpoint. *Cell,* 106**,** 83-93.

AKHMANOVA, A. & STEINMETZ, M. O. (2008) Tracking the ends: a dynamic protein network controls the fate of microtubule tips. *Nat Rev Mol Cell Biol,* 9**,** 309-22.

AKHMANOVA, A. & STEINMETZ, M. O. (2010) Microtubule +TIPs at a glance. *J Cell Sci,* 123**,** 3415-9.

AKHTAR, A. & GASSER, S. M. (2007) The nuclear envelope and transcriptional control. *Nat Rev Genet,* 8**,** 507-17.

AKIYOSHI, B., NELSON, C. R., RANISH, J. A. & BIGGINS, S. (2009a) Analysis of Ipl1-mediated phosphorylation of the Ndc80 kinetochore protein in Saccharomyces cerevisiae. *Genetics,* 183**,** 1591-5.

AKIYOSHI, B., NELSON, C. R., RANISH, J. A. & BIGGINS, S. (2009b) Quantitative proteomic analysis of purified yeast kinetochores identifies a PP1 regulatory subunit. *Genes Dev,* 23**,** 2887-99.

AKIYOSHI, B., SARANGAPANI, K. K., POWERS, A. F., NELSON, C. R., REICHOW, S. L., ARELLANO-SANTOYO, H., GONEN, T., RANISH, J. A., ASBURY, C. L. & BIGGINS, S. (2010) Tension directly stabilizes reconstituted kinetochore-microtubule attachments. *Nature,* 468**,** 576-9.

AL-BASSAM, J., KIM, H., BROUHARD, G., VAN OIJEN, A., HARRISON, S. C. & CHANG, F. (2010) CLASP promotes microtubule rescue by recruiting tubulin dimers to the microtubule. *Dev Cell,* 19**,** 245-58.

AL-BASSAM, J., LARSEN, N. A., HYMAN, A. A. & HARRISON, S. C. (2007) Crystal structure of a TOG domain: conserved features of XMAP215/Dis1-family TOG domains and implications for tubulin binding. *Structure,* 15**,** 355-62.

AL-BASSAM, J., VAN BREUGEL, M., HARRISON, S. C. & HYMAN, A. (2006) Stu2p binds tubulin and undergoes an open-to-closed conformational change. *J Cell Biol,* 172**,** 1009-22.

ALEXANDER, S. P. & RIEDER, C. L. (1991) Chromosome motion during attachment to the vertebrate spindle: initial saltatory-like behavior of chromosomes and quantitative analysis of force production by nascent kinetochore fibers. *J Cell Biol,* 113**,** 805-15.

ALUSHIN, G. & NOGALES, E. (2011) Visualizing kinetochore architecture. *Curr Opin Struct Biol*.

ALUSHIN, G. M., RAMEY, V. H., PASQUALATO, S., BALL, D. A., GRIGORIEFF, N., MUSACCHIO, A. & NOGALES, E. (2010) The Ndc80 kinetochore complex forms oligomeric arrays along microtubules. *Nature,* 467**,** 805-10.

AMARO, A. C., SAMORA, C. P., HOLTACKERS, R., WANG, E., KINGSTON, I. J., ALONSO, M., LAMPSON, M., MCAINSH, A. D. & MERALDI, P. (2010) Molecular control of kinetochore-microtubule dynamics and chromosome oscillations. *Nat Cell Biol,* 12**,** 319-29.

AMOR, D. J. & CHOO, K. H. (2002) Neocentromeres: role in human disease, evolution, and centromere study. *Am J Hum Genet,* 71**,** 695-714.

ANDERS, A., LOURENCO, P. C. & SAWIN, K. E. (2006) Noncore components of the fission yeast gamma-tubulin complex. *Mol Biol Cell,* 17**,** 5075-93.

ANDREWS, P. D., OVECHKINA, Y., MORRICE, N., WAGENBACH, M., DUNCAN, K., WORDEMAN, L. & SWEDLOW, J. R. (2004) Aurora B regulates MCAK at the mitotic centromere. *Dev Cell,* 6**,** 253-68.

ANDRULIS, E. D., ZAPPULLA, D. C., ANSARI, A., PERROD, S., LAIOSA, C. V., GARTENBERG, M. R. & STERNGLANZ, R. (2002) Esc1, a nuclear periphery protein required for Sir4-based plasmid anchoring and partitioning. *Mol Cell Biol,* 22**,** 8292-301.

AOKI, K., NAKASEKO, Y., KINOSHITA, K., GOSHIMA, G. & YANAGIDA, M. (2006) CDC2 phosphorylation of the fission yeast dis1 ensures accurate chromosome segregation. *Curr Biol,* 16**,** 1627-35.

APPELGREN, H., KNIOLA, B. & EKWALL, K. (2003) Distinct centromere domain structures with separate functions demonstrated in live fission yeast cells. *J Cell Sci,* 116**,** 4035-42.

ASAKAWA, H., HAYASHI, A., HARAGUCHI, T. & HIRAOKA, Y. (2005a) Dissociation of the Nuf2-Ndc80 complex releases centromeres from the spindle-pole body during meiotic prophase in fission yeast. *Mol Biol Cell,* 16**,** 2325-38.

ASAKAWA, K., KUME, K., KANAI, M., GOSHIMA, T., MIYAHARA, K., DHUT, S., TEE, W. W., HIRATA, D. & TODA, T. (2006) The V260I mutation in fission yeast alpha-tubulin Atb2 affects microtubule dynamics and EB1-Mal3 localization and activates the Bub1 branch of the spindle checkpoint. *Mol Biol Cell,* 17**,** 1421-35.

ASAKAWA, K., TOYA, M., SATO, M., KANAI, M., KUME, K., GOSHIMA, T., GARCIA, M. A., HIRATA, D. & TODA, T. (2005b) Mal3, the fission yeast EB1 homologue, cooperates with Bub1 spindle checkpoint to prevent monopolar attachment. *EMBO Rep,* 6**,** 1194-200.

ASBURY, C. L., GESTAUT, D. R., POWERS, A. F., FRANCK, A. D. & DAVIS, T. N. (2006) The Dam1 kinetochore complex harnesses microtubule dynamics to produce force and movement. *Proc Natl Acad Sci U S A,* 103**,** 9873-8.

BASI, G., SCHMID, E. & MAUNDRELL, K. (1993) TATA box mutations in the Schizosaccharomyces pombe nmt1 promoter affect transcription efficiency but not the transcription start point or thiamine repressibility. *Gene,* 123**,** 131-6.

BEINHAUER, J. D., HAGAN, I. M., HEGEMANN, J. H. & FLEIG, U. (1997) Mal3, the fission yeast homologue of the human APC-interacting protein EB-1 is required for microtubule integrity and the maintenance of cell form. *J Cell Biol,* 139**,** 717-28.

BETTENCOURT-DIAS, M. & GLOVER, D. M. (2007) Centrosome biogenesis and function: centrosomics brings new understanding. *Nat Rev Mol Cell Biol,* 8**,** 451-63.

BHARADWAJ, R., QI, W. & YU, H. (2004) Identification of two novel components of the human NDC80 kinetochore complex. *J Biol Chem,* 279**,** 13076-85.

BIECHE, I., VACHER, S., LALLEMAND, F., TOZLU-KARA, S., BENNANI, H., BEUZELIN, M., DRIOUCH, K., ROULEAU, E., LEREBOURS, F., RIPOCHE, H., CIZERON-CLAIRAC, G., SPYRATOS, F. & LIDEREAU, R. (2011) Expression analysis of mitotic spindle checkpoint genes in breast carcinoma: role of NDC80/HEC1 in early breast tumorigenicity, and a two-gene signature for aneuploidy. *Mol Cancer,* 10**,** 23.

BIELING, P., LAAN, L., SCHEK, H., MUNTEANU, E. L., SANDBLAD, L., DOGTEROM, M., BRUNNER, D. & SURREY, T. (2007) Reconstitution of a microtubule plus-end tracking system in vitro. *Nature,* 450**,** 1100-5.

BIGGINS, S. & MURRAY, A. W. (2001) The budding yeast protein kinase Ipl1/Aurora allows the absence of tension to activate the spindle checkpoint. *Genes Dev,* 15**,** 3118-29.

BISHOP, A. C., UBERSAX, J. A., PETSCH, D. T., MATHEOS, D. P., GRAY, N. S., BLETHROW, J., SHIMIZU, E., TSIEN, J. Z., SCHULTZ, P. G., ROSE, M. D., WOOD, J. L., MORGAN, D. O. & SHOKAT, K. M. (2000) A chemical switch for inhibitor-sensitive alleles of any protein kinase. *Nature,* 407**,** 395-401.

BITTON, D. A., WOOD, V., SCUTT, P. J., GRALLERT, A., YATES, T., SMITH, D. L., HAGAN, I. M. & MILLER, C. J. (2011) Augmented annotation of the Schizosaccharomyces pombe genome reveals additional genes required for growth and viability. *Genetics,* 187**,** 1207-17.

BOHNERT, K. A., CHEN, J. S., CLIFFORD, D. M., VANDER KOOI, C. W. & GOULD, K. L. (2009) A link between aurora kinase and Clp1/Cdc14 regulation uncovered by the identification of a fission yeast borealin-like protein. *Mol Biol Cell,* 20**,** 3646-59.

BORNENS, M. (2008) Organelle positioning and cell polarity. *Nat Rev Mol Cell Biol,* 9**,** 874-86.

BRATMAN, S. V. & CHANG, F. (2007) Stabilization of overlapping microtubules by fission yeast CLASP. *Dev Cell,* 13**,** 812-27.

BRINKLEY, B. R. & CARTWRIGHT, J., JR. (1975) Cold-labile and cold-stable microtubules in the mitotic spindle of mammalian cells. *Ann N Y Acad Sci,* 253**,** 428-39.

BRINKLEY, B. R. & STUBBLEFIELD, E. (1966) The fine structure of the kinetochore of a mammalian cell in vitro. *Chromosoma,* 19**,** 28-43.

BROUHARD, G. J., STEAR, J. H., NOETZEL, T. L., AL-BASSAM, J., KINOSHITA, K., HARRISON, S. C., HOWARD, J. & HYMAN, A. A. (2008) XMAP215 is a processive microtubule polymerase. *Cell,* 132**,** 79-88.

BROWNING, H., HACKNEY, D. D. & NURSE, P. (2003) Targeted movement of cell end factors in fission yeast. *Nat Cell Biol,* 5**,** 812-8.

BUCCIARELLI, E., PELLACANI, C., NAIM, V., PALENA, A., GATTI, M. & SOMMA, M. P. (2009) Drosophila Dgt6 interacts with Ndc80, Msps/XMAP215, and gamma-tubulin to promote kinetochore-driven MT formation. *Curr Biol,* 19**,** 1839-45.

CARAZO-SALAS, R. E., ANTONY, C. & NURSE, P. (2005) The kinesin Klp2 mediates polarization of interphase microtubules in fission yeast. *Science,* 309**,** 297-300.

CARAZO-SALAS, R. E. & NURSE, P. (2006) Self-organization of interphase microtubule arrays in fission yeast. *Nat Cell Biol,* 8**,** 1102-7.

CARROLL, C. W., SILVA, M. C., GODEK, K. M., JANSEN, L. E. & STRAIGHT, A. F. (2009) Centromere assembly requires the direct recognition of CENP-A nucleosomes by CENP-N. *Nat Cell Biol,* 11**,** 896-902.

CHARRASSE, S., COUBES, P., ARRANCIBIA, S. & LARROQUE, C. (1996) Expression of the tumor over-expressed ch-TOG gene in human and baboon brain. *Neurosci Lett,* 212**,** 119-22.

CHARRASSE, S., MAZEL, M., TAVIAUX, S., BERTA, P., CHOW, T. & LARROQUE, C. (1995) Characterization of the cDNA and pattern of expression of a new gene over-expressed in human hepatomas and colonic tumors. *Eur J Biochem,* 234**,** 406-13.

CHARRASSE, S., SCHROEDER, M., GAUTHIER-ROUVIERE, C., ANGO, F., CASSIMERIS, L., GARD, D. L. & LARROQUE, C. (1998) The TOGp protein is a new human microtubule-associated protein homologous to the Xenopus XMAP215. *J Cell Sci,* 111 (Pt 10)**,** 1371-83.

CHEESEMAN, I. M., ANDERSON, S., JWA, M., GREEN, E. M., KANG, J., YATES, J. R., 3RD, CHAN, C. S., DRUBIN, D. G. & BARNES, G. (2002) Phospho-regulation of kinetochore-microtubule attachments by the Aurora kinase Ipl1p. *Cell,* 111**,** 163-72.

CHEESEMAN, I. M., BREW, C., WOLYNIAK, M., DESAI, A., ANDERSON, S., MUSTER, N., YATES, J. R., HUFFAKER, T. C., DRUBIN, D. G. & BARNES, G. (2001a) Implication of a novel multiprotein Dam1p complex in outer kinetochore function. *J Cell Biol,* 155**,** 1137-45.

CHEESEMAN, I. M., CHAPPIE, J. S., WILSON-KUBALEK, E. M. & DESAI, A. (2006) The conserved KMN network constitutes the core microtubule-binding site of the kinetochore. *Cell,* 127**,** 983-97.

CHEESEMAN, I. M. & DESAI, A. (2008) Molecular architecture of the kinetochore-microtubule interface. *Nat Rev Mol Cell Biol,* 9**,** 33-46.

CHEESEMAN, I. M., ENQUIST-NEWMAN, M., MULLER-REICHERT, T., DRUBIN, D. G. & BARNES, G. (2001b) Mitotic spindle integrity and kinetochore function linked by the Duo1p/Dam1p complex. *J Cell Biol,* 152**,** 197-212.

CHEESEMAN, I. M., NIESSEN, S., ANDERSON, S., HYNDMAN, F., YATES, J. R., 3RD, OEGEMA, K. & DESAI, A. (2004) A conserved protein network controls assembly of the outer kinetochore and its ability to sustain tension. *Genes Dev,* 18**,** 2255-68.

CHEN, C. R., CHEN, J. & CHANG, E. C. (2000) A conserved interaction between Moe1 and Mal3 is important for proper spindle formation in Schizosaccharomyces pombe. *Mol Biol Cell,* 11**,** 4067-77.

CHEN, Y., RILEY, D. J., CHEN, P. L. & LEE, W. H. (1997) HEC, a novel nuclear protein rich in leucine heptad repeats specifically involved in mitosis. *Mol Cell Biol,* 17**,** 6049-56.

CHEN, Y., RILEY, D. J., ZHENG, L., CHEN, P. L. & LEE, W. H. (2002) Phosphorylation of the mitotic regulator protein Hec1 by Nek2 kinase is essential for faithful chromosome segregation. *J Biol Chem,* 277**,** 49408-16.

CHIKASHIGE, Y., HARAGUCHI, T. & HIRAOKA, Y. (2007) Another way to move chromosomes. *Chromosoma,* 116**,** 497-505.

CHIKASHIGE, Y., HARAGUCHI, T. & HIRAOKA, Y. (2010) Nuclear envelope attachment is not necessary for telomere function in fission yeast. *Nucleus,* 1**,** 481-486.

CHIKASHIGE, Y., TSUTSUMI, C., YAMANE, M., OKAMASA, K., HARAGUCHI, T. & HIRAOKA, Y. (2006) Meiotic proteins bqt1 and bqt2 tether telomeres to form the bouquet arrangement of chromosomes. *Cell,* 125**,** 59-69.

CHIKASHIGE, Y., YAMANE, M., OKAMASA, K., TSUTSUMI, C., KOJIDANI, T., SATO, M., HARAGUCHI, T. & HIRAOKA, Y. (2009) Membrane proteins Bqt3 and -4 anchor telomeres to the nuclear envelope to ensure chromosomal bouquet formation. *J Cell Biol,* 187**,** 413-27.

CHIRON, S., BOBKOVA, A., ZHOU, H. & YAFFE, M. P. (2008) CLASP regulates mitochondrial distribution in Schizosaccharomyces pombe. *J Cell Biol,* 182**,** 41-9.

CHUNG, E. & CHEN, R. H. (2003) Phosphorylation of Cdc20 is required for its inhibition by the spindle checkpoint. *Nat Cell Biol,* 5**,** 748-53.

CIFERRI, C., DE LUCA, J., MONZANI, S., FERRARI, K. J., RISTIC, D., WYMAN, C., STARK, H., KILMARTIN, J., SALMON, E. D. & MUSACCHIO, A. (2005) Architecture of the human ndc80-hec1 complex, a critical constituent of the outer kinetochore. *J Biol Chem,* 280**,** 29088-95.

CIFERRI, C., PASQUALATO, S., SCREPANTI, E., VARETTI, G., SANTAGUIDA, S., DOS REIS, G., MAIOLICA, A., POLKA, J., DE LUCA, J. G., DE WULF, P., SALEK, M., RAPPSILBER, J., MOORES, C. A., SALMON, E. D. & MUSACCHIO, A. (2008) Implications for kinetochore-microtubule attachment from the structure of an engineered Ndc80 complex. *Cell,* 133**,** 427-39.

CIMINI, D., WAN, X., HIREL, C. B. & SALMON, E. D. (2006) Aurora kinase promotes turnover of kinetochore microtubules to reduce chromosome segregation errors. *Curr Biol,* 16**,** 1711-8.

CORBETT, K. D., YIP, C. K., EE, L. S., WALZ, T., AMON, A. & HARRISON, S. C. (2010) The monopolin complex crosslinks kinetochore components to regulate chromosome-microtubule attachments. *Cell,* 142**,** 556-67.

CULLEN, C. F. & OHKURA, H. (2001) Msps protein is localized to acentrosomal poles to ensure bipolarity of Drosophila meiotic spindles. *Nat Cell Biol,* 3**,** 637-42.

D'ANGIOLELLA, V., MARI, C., NOCERA, D., RAMETTI, L. & GRIECO, D. (2003) The spindle checkpoint requires cyclin-dependent kinase activity. *Genes Dev,* 17**,** 2520-5.

DAGA, R. R., LEE, K. G., BRATMAN, S., SALAS-PINO, S. & CHANG, F. (2006) Self-organization of microtubule bundles in anucleate fission yeast cells. *Nat Cell Biol,* 8**,** 1108-13.

DAGA, R. R. & NURSE, P. (2008) Interphase microtubule bundles use global cell shape to guide spindle alignment in fission yeast. *J Cell Sci,* 121**,** 1973-80.

DAUM, J. R., WREN, J. D., DANIEL, J. J., SIVAKUMAR, S., MCAVOY, J. N., POTAPOVA, T. A. & GORBSKY, G. J. (2009) Ska3 is required for spindle checkpoint silencing and the maintenance of chromosome cohesion in mitosis. *Curr Biol,* 19**,** 1467-72.

DAVIES, A. E. & KAPLAN, K. B. (2010) Hsp90-Sgt1 and Skp1 target human Mis12 complexes to ensure efficient formation of kinetochore-microtubule binding sites. *J Cell Biol,* 189**,** 261-74.

DE ANTONI, A., PEARSON, C. G., CIMINI, D., CANMAN, J. C., SALA, V., NEZI, L., MAPELLI, M., SIRONI, L., FARETTA, M., SALMON, E. D. & MUSACCHIO, A. (2005) The Mad1/Mad2 complex as a template for Mad2 activation in the spindle assembly checkpoint. *Curr Biol,* 15**,** 214-25.

DE WULF, P., MCAINSH, A. D. & SORGER, P. K. (2003) Hierarchical assembly of the budding yeast kinetochore from multiple subcomplexes. *Genes Dev,* 17**,** 2902-21.
DELUCA, J. G., GALL, W. E., CIFERRI, C., CIMINI, D., MUSACCHIO, A. & SALMON, E. D. (2006) Kinetochore microtubule dynamics and attachment stability are regulated by Hec1. *Cell,* 127**,** 969-82.
DELUCA, J. G., HOWELL, B. J., CANMAN, J. C., HICKEY, J. M., FANG, G. & SALMON, E. D. (2003) Nuf2 and Hec1 are required for retention of the checkpoint proteins Mad1 and Mad2 to kinetochores. *Curr Biol,* 13**,** 2103-9.
DELUCA, J. G., MOREE, B., HICKEY, J. M., KILMARTIN, J. V. & SALMON, E. D. (2002) hNuf2 inhibition blocks stable kinetochore-microtubule attachment and induces mitotic cell death in HeLa cells. *J Cell Biol,* 159**,** 549-55.
DES GEORGES, A., KATSUKI, M., DRUMMOND, D. R., OSEI, M., CROSS, R. A. & AMOS, L. A. (2008) Mal3, the Schizosaccharomyces pombe homolog of EB1, changes the microtubule lattice. *Nat Struct Mol Biol,* 15**,** 1102-8.
DESAI, A., RYBINA, S., MULLER-REICHERT, T., SHEVCHENKO, A., HYMAN, A. & OEGEMA, K. (2003) KNL-1 directs assembly of the microtubule-binding interface of the kinetochore in C. elegans. *Genes Dev,* 17**,** 2421-35.
DIAZ-RODRIGUEZ, E., SOTILLO, R., SCHVARTZMAN, J. M. & BENEZRA, R. (2008) Hec1 overexpression hyperactivates the mitotic checkpoint and induces tumor formation in vivo. *Proc Natl Acad Sci U S A,* 105**,** 16719-24.
DING, R., MCDONALD, K. L. & MCINTOSH, J. R. (1993) Three-dimensional reconstruction and analysis of mitotic spindles from the yeast, Schizosaccharomyces pombe. *J Cell Biol,* 120**,** 141-51.
DING, R., WEST, R. R., MORPHEW, D. M., OAKLEY, B. R. & MCINTOSH, J. R. (1997) The spindle pole body of Schizosaccharomyces pombe enters and leaves the nuclear envelope as the cell cycle proceeds. *Mol Biol Cell,* 8**,** 1461-79.
DITCHFIELD, C., JOHNSON, V. L., TIGHE, A., ELLSTON, R., HAWORTH, C., JOHNSON, T., MORTLOCK, A., KEEN, N. & TAYLOR, S. S. (2003) Aurora B couples chromosome alignment with anaphase by targeting BubR1, Mad2, and Cenp-E to kinetochores. *J Cell Biol,* 161**,** 267-80.
DONG, Y., VANDEN BELDT, K. J., MENG, X., KHODJAKOV, A. & MCEWEN, B. F. (2007) The outer plate in vertebrate kinetochores is a flexible network with multiple microtubule interactions. *Nat Cell Biol,* 9**,** 516-22.
DRECHSEL, D. N. & KIRSCHNER, M. W. (1994) The minimum GTP cap required to stabilize microtubules. *Curr Biol,* 4**,** 1053-61.
DRUMMOND, D. R. & CROSS, R. A. (2000) Dynamics of interphase microtubules in Schizosaccharomyces pombe. *Curr Biol,* 10**,** 766-75.
DU, J., CAI, X., YAO, J., DING, X., WU, Q., PEI, S., JIANG, K., ZHANG, Y., WANG, W., SHI, Y., LAI, Y., SHEN, J., TENG, M., HUANG, H., FEI, Q., REDDY, E. S., ZHU, J., JIN, C. & YAO, X. (2008) The mitotic checkpoint kinase NEK2A regulates kinetochore microtubule attachment stability. *Oncogene,* 27**,** 4107-14.
EARNSHAW, W. C. & ROTHFIELD, N. (1985) Identification of a family of human centromere proteins using autoimmune sera from patients with scleroderma. *Chromosoma,* 91**,** 313-21.
EMANUELE, M. J., LAN, W., JWA, M., MILLER, S. A., CHAN, C. S. & STUKENBERG, P. T. (2008) Aurora B kinase and protein phosphatase 1 have opposing roles in modulating kinetochore assembly. *J Cell Biol,* 181**,** 241-54.
ENQUIST-NEWMAN, M., CHEESEMAN, I. M., VAN GOOR, D., DRUBIN, D. G., MELUH, P. B. & BARNES, G. (2001) Dad1p, third component of the Duo1p/Dam1p complex involved in kinetochore function and mitotic spindle integrity. *Mol Biol Cell,* 12**,** 2601-13.
EUSKIRCHEN, G. M. (2002) Nnf1p, Dsn1p, Mtw1p, and Nsl1p: a new group of proteins important for chromosome segregation in Saccharomyces cerevisiae. *Eukaryot Cell,* 1**,** 229-40.
FOLTZ, D. R., JANSEN, L. E., BLACK, B. E., BAILEY, A. O., YATES, J. R., 3RD & CLEVELAND, D. W. (2006) The human CENP-A centromeric nucleosome-associated complex. *Nat Cell Biol,* 8**,** 458-69.
FONG, C. S., SATO, M. & TODA, T. (2010) Fission yeast Pcp1 links polo kinase-mediated mitotic entry to gamma-tubulin-dependent spindle formation. *EMBO J,* 29**,** 120-30.
FRANCO, A., MEADOWS, J. C. & MILLAR, J. B. (2007) The Dam1/DASH complex is required for the retrieval of unclustered kinetochores in fission yeast. *J Cell Sci,* 120**,** 3345-51.
FRASCHINI, R., BERETTA, A., SIRONI, L., MUSACCHIO, A., LUCCHINI, G. & PIATTI, S. (2001) Bub3 interaction with Mad2, Mad3 and Cdc20 is mediated by WD40 repeats and does not require intact kinetochores. *EMBO J,* 20**,** 6648-59.
FU, C., JAIN, D., COSTA, J., VELVE-CASQUILLAS, G. & TRAN, P. T. (2011) mmb1p Binds Mitochondria to Dynamic Microtubules. *Curr Biol*.
FU, C., WARD, J. J., LOIODICE, I., VELVE-CASQUILLAS, G., NEDELEC, F. J. & TRAN, P. T. (2009) Phospho-regulated interaction between kinesin-6 Klp9p and microtubule bundler Ase1p promotes spindle elongation. *Dev Cell,* 17**,** 257-67.

FUJITA, A., VARDY, L., GARCIA, M. A. & TODA, T. (2002) A fourth component of the fission yeast gamma-tubulin complex, Alp16, is required for cytoplasmic microtubule integrity and becomes indispensable when gamma-tubulin function is compromised. *Mol Biol Cell,* 13**,** 2360-73.

FUNABIKI, H., HAGAN, I., UZAWA, S. & YANAGIDA, M. (1993) Cell cycle-dependent specific positioning and clustering of centromeres and telomeres in fission yeast. *J Cell Biol,* 121**,** 961-76.

GACHET, Y., REYES, C., COURTHEOUX, T., GOLDSTONE, S., GAY, G., SERRURIER, C. & TOURNIER, S. (2008) Sister kinetochore recapture in fission yeast occurs by two distinct mechanisms, both requiring Dam1 and Klp2. *Mol Biol Cell,* 19**,** 1646-62.

GACHET, Y., TOURNIER, S., MILLAR, J. B. & HYAMS, J. S. (2001) A MAP kinase-dependent actin checkpoint ensures proper spindle orientation in fission yeast. *Nature,* 412**,** 352-5.

GACHET, Y., TOURNIER, S., MILLAR, J. B. & HYAMS, J. S. (2004) Mechanism controlling perpendicular alignment of the spindle to the axis of cell division in fission yeast. *EMBO J,* 23**,** 1289-300.

GAITANOS, T. N., SANTAMARIA, A., JEYAPRAKASH, A. A., WANG, B., CONTI, E. & NIGG, E. A. (2009) Stable kinetochore-microtubule interactions depend on the Ska complex and its new component Ska3/C13Orf3. *EMBO J,* 28**,** 1442-52.

GAO, Q., COURTHEOUX, T., GACHET, Y., TOURNIER, S. & HE, X. (2010) A non-ring-like form of the Dam1 complex modulates microtubule dynamics in fission yeast. *Proc Natl Acad Sci U S A,* 107**,** 13330-5.

GARCIA, M. A., KOONRUGSA, N. & TODA, T. (2002a) Spindle-kinetochore attachment requires the combined action of Kin I-like Klp5/6 and Alp14/Dis1-MAPs in fission yeast. *EMBO J,* 21**,** 6015-24.

GARCIA, M. A., KOONRUGSA, N. & TODA, T. (2002b) Two kinesin-like Kin I family proteins in fission yeast regulate the establishment of metaphase and the onset of anaphase A. *Curr Biol,* 12**,** 610-21.

GARCIA, M. A., VARDY, L., KOONRUGSA, N. & TODA, T. (2001) Fission yeast ch-TOG/XMAP215 homologue Alp14 connects mitotic spindles with the kinetochore and is a component of the Mad2-dependent spindle checkpoint. *EMBO J,* 20**,** 3389-401.

GARD, D. L., BECKER, B. E. & JOSH ROMNEY, S. (2004) MAPping the eukaryotic tree of life: structure, function, and evolution of the MAP215/Dis1 family of microtubule-associated proteins. *Int Rev Cytol,* 239**,** 179-272.

GARD, D. L. & KIRSCHNER, M. W. (1987) A microtubule-associated protein from Xenopus eggs that specifically promotes assembly at the plus-end. *J Cell Biol,* 105**,** 2203-15.

GARTENBERG, M. R., NEUMANN, F. R., LAROCHE, T., BLASZCZYK, M. & GASSER, S. M. (2004) Sir-mediated repression can occur independently of chromosomal and subnuclear contexts. *Cell,* 119**,** 955-67.

GASCOIGNE, K. E., TAKEUCHI, K., SUZUKI, A., HORI, T., FUKAGAWA, T. & CHEESEMAN, I. M. (2011) Induced ectopic kinetochore assembly bypasses the requirement for CENP-A nucleosomes. *Cell,* 145**,** 410-22.

GERGELY, F., DRAVIAM, V. M. & RAFF, J. W. (2003) The ch-TOG/XMAP215 protein is essential for spindle pole organization in human somatic cells. *Genes Dev,* 17**,** 336-41.

GESTAUT, D. R., GRACZYK, B., COOPER, J., WIDLUND, P. O., ZELTER, A., WORDEMAN, L., ASBURY, C. L. & DAVIS, T. N. (2008) Phosphoregulation and depolymerization-driven movement of the Dam1 complex do not require ring formation. *Nat Cell Biol,* 10**,** 407-14.

GOSHIMA, G., IWASAKI, O., OBUSE, C. & YANAGIDA, M. (2003) The role of Ppe1/PP6 phosphatase for equal chromosome segregation in fission yeast kinetochore. *EMBO J,* 22**,** 2752-63.

GOSHIMA, G., SAITOH, S. & YANAGIDA, M. (1999) Proper metaphase spindle length is determined by centromere proteins Mis12 and Mis6 required for faithful chromosome segregation. *Genes Dev,* 13**,** 1664-77.

GOSHIMA, G., WOLLMAN, R., STUURMAN, N., SCHOLEY, J. M. & VALE, R. D. (2005) Length control of the metaphase spindle. *Curr Biol,* 15**,** 1979-88.

GOTO, B., OKAZAKI, K. & NIWA, O. (2001) Cytoplasmic microtubular system implicated in de novo formation of a Rabl-like orientation of chromosomes in fission yeast. *J Cell Sci,* 114**,** 2427-35.

GRALLERT, A., BEUTER, C., CRAVEN, R. A., BAGLEY, S., WILKS, D., FLEIG, U. & HAGAN, I. M. (2006) S. pombe CLASP needs dynein, not EB1 or CLIP170, to induce microtubule instability and slows polymerization rates at cell tips in a dynein-dependent manner. *Genes Dev,* 20**,** 2421-36.

GRIFFITHS, K., MASUDA, H., DHUT, S. & TODA, T. (2008) Fission yeast dam1-A8 mutant is resistant to and rescued by an anti-microtubule agent. *Biochem Biophys Res Commun,* 368**,** 670-6.

GRISHCHUK, E. L., EFREMOV, A. K., VOLKOV, V. A., SPIRIDONOV, I. S., GUDIMCHUK, N., WESTERMANN, S., DRUBIN, D., BARNES, G., MCINTOSH, J. R. & ATAULLAKHANOV, F. I. (2008a) The Dam1 ring binds microtubules strongly enough to be a processive as well as energy-efficient coupler for chromosome motion. *Proc Natl Acad Sci U S A,* 105**,** 15423-8.

GRISHCHUK, E. L., SPIRIDONOV, I. S., VOLKOV, V. A., EFREMOV, A., WESTERMANN, S., DRUBIN, D., BARNES, G., ATAULLAKHANOV, F. I. & MCINTOSH, J. R. (2008b) Different assemblies of the DAM1 complex follow shortening microtubules by distinct mechanisms. *Proc Natl Acad Sci U S A,* 105**,** 6918-23.

GRUNEBERG, U., NEEF, R., HONDA, R., NIGG, E. A. & BARR, F. A. (2004) Relocation of Aurora B from centromeres to the central spindle at the metaphase to anaphase transition requires MKlp2. *J Cell Biol,* 166**,** 167-72.

GUIMARAES, G. J., DONG, Y., MCEWEN, B. F. & DELUCA, J. G. (2008) Kinetochore-microtubule attachment relies on the disordered N-terminal tail domain of Hec1. *Curr Biol,* 18**,** 1778-84.

GURZOV, E. N. & IZQUIERDO, M. (2006) RNA interference against Hec1 inhibits tumor growth in vivo. *Gene Ther,* 13**,** 1-7.

HABU, T., KIM, S. H., WEINSTEIN, J. & MATSUMOTO, T. (2002) Identification of a MAD2-binding protein, CMT2, and its role in mitosis. *EMBO J,* 21**,** 6419-28.

HAGAN, I. & YANAGIDA, M. (1992) Kinesin-related cut7 protein associates with mitotic and meiotic spindles in fission yeast. *Nature,* 356**,** 74-6.

HAGAN, I. & YANAGIDA, M. (1995) The product of the spindle formation gene sad1+ associates with the fission yeast spindle pole body and is essential for viability. *J Cell Biol,* 129**,** 1033-47.

HAGAN, I. M. & HYAMS, J. S. (1988) The use of cell division cycle mutants to investigate the control of microtubule distribution in the fission yeast Schizosaccharomyces pombe. *J Cell Sci,* 89 (Pt 3)**,** 343-57.

HAGAN, I. M. & HYAMS, J. S. (1996) Forces acting on the fission yeast anaphase spindle. *Cell Motil Cytoskeleton,* 34**,** 69-75.

HANAHAN, D. & WEINBERG, R. A. (2011) Hallmarks of cancer: the next generation. *Cell,* 144**,** 646-74.

HANISCH, A., SILLJE, H. H. & NIGG, E. A. (2006) Timely anaphase onset requires a novel spindle and kinetochore complex comprising Ska1 and Ska2. *EMBO J,* 25**,** 5504-15.

HARDWICK, K. G., WEISS, E., LUCA, F. C., WINEY, M. & MURRAY, A. W. (1996) Activation of the budding yeast spindle assembly checkpoint without mitotic spindle disruption. *Science,* 273**,** 953-6.

HAUF, S., BISWAS, A., LANGEGGER, M., KAWASHIMA, S. A., TSUKAHARA, T. & WATANABE, Y. (2007) Aurora controls sister kinetochore mono-orientation and homolog bi-orientation in meiosis-I. *EMBO J,* 26**,** 4475-86.

HAUF, S., COLE, R. W., LATERRA, S., ZIMMER, C., SCHNAPP, G., WALTER, R., HECKEL, A., VAN MEEL, J., RIEDER, C. L. & PETERS, J. M. (2003) The small molecule Hesperadin reveals a role for Aurora B in correcting kinetochore-microtubule attachment and in maintaining the spindle assembly checkpoint. *J Cell Biol,* 161**,** 281-94.

HAYAMA, S., DAIGO, Y., KATO, T., ISHIKAWA, N., YAMABUKI, T., MIYAMOTO, M., ITO, T., TSUCHIYA, E., KONDO, S. & NAKAMURA, Y. (2006) Activation of CDCA1-KNTC2, members of centromere protein complex, involved in pulmonary carcinogenesis. *Cancer Res,* 66**,** 10339-48.

HAYASHI, A., ASAKAWA, H., HARAGUCHI, T. & HIRAOKA, Y. (2006) Reconstruction of the kinetochore during meiosis in fission yeast Schizosaccharomyces pombe. *Mol Biol Cell,* 17**,** 5173-84.

HAYASHI, A., DING, D. Q., TSUTSUMI, C., CHIKASHIGE, Y., MASUDA, H., HARAGUCHI, T. & HIRAOKA, Y. (2009) Localization of gene products using a chromosomally tagged GFP-fusion library in the fission yeast Schizosaccharomyces pombe. *Genes Cells,* 14**,** 217-25.

HAYASHI, T., FUJITA, Y., IWASAKI, O., ADACHI, Y., TAKAHASHI, K. & YANAGIDA, M. (2004) Mis16 and Mis18 are required for CENP-A loading and histone deacetylation at centromeres. *Cell,* 118**,** 715-29.

HAYDEN, J. H., BOWSER, S. S. & RIEDER, C. L. (1990) Kinetochores capture astral microtubules during chromosome attachment to the mitotic spindle: direct visualization in live newt lung cells. *J Cell Biol,* 111**,** 1039-45.

HE, X., RINES, D. R., ESPELIN, C. W. & SORGER, P. K. (2001) Molecular analysis of kinetochore-microtubule attachment in budding yeast. *Cell,* 106**,** 195-206.

HERZOG, F., PRIMORAC, I., DUBE, P., LENART, P., SANDER, B., MECHTLER, K., STARK, H. & PETERS, J. M. (2009) Structure of the anaphase-promoting complex/cyclosome interacting with a mitotic checkpoint complex. *Science,* 323**,** 1477-81.

HEUN, P., LAROCHE, T., SHIMADA, K., FURRER, P. & GASSER, S. M. (2001) Chromosome dynamics in the yeast interphase nucleus. *Science,* 294**,** 2181-6.

HILL, T. L. (1985) Theoretical problems related to the attachment of microtubules to kinetochores. *Proc Natl Acad Sci U S A,* 82**,** 4404-8.

HIRAOKA, Y. & DERNBURG, A. F. (2009) The SUN rises on meiotic chromosome dynamics. *Dev Cell,* 17**,** 598-605.

HIRAOKA, Y., MAEKAWA, H., ASAKAWA, H., CHIKASHIGE, Y., KOJIDANI, T., OSAKADA, H., MATSUDA, A. & HARAGUCHI, T. (2011) Inner nuclear membrane protein Ima1 is dispensable for intranuclear positioning of centromeres. *Genes Cells*.

HOFMANN, C., CHEESEMAN, I. M., GOODE, B. L., MCDONALD, K. L., BARNES, G. & DRUBIN, D. G. (1998) Saccharomyces cerevisiae Duo1p and Dam1p, novel proteins involved in mitotic spindle function. *J Cell Biol,* 143**,** 1029-40.

HOLLAND, S., IOANNOU, D., HAINES, S. & BROWN, W. R. (2005) Comparison of Dam tagging and chromatin immunoprecipitation as tools for the identification of the binding sites for S. pombe CENP-C. *Chromosome Res,* 13**,** 73-83.

HOOG, J. L. & ANTONY, C. (2007) Whole-cell investigation of microtubule cytoskeleton architecture by electron tomography. *Methods Cell Biol,* 79**,** 145-67.

HOOG, J. L., SCHWARTZ, C., NOON, A. T., O'TOOLE, E. T., MASTRONARDE, D. N., MCINTOSH, J. R. & ANTONY, C. (2007) Organization of interphase microtubules in fission yeast analyzed by electron tomography. *Dev Cell,* 12**,** 349-61.

HORI, T., AMANO, M., SUZUKI, A., BACKER, C. B., WELBURN, J. P., DONG, Y., MCEWEN, B. F., SHANG, W. H., SUZUKI, E., OKAWA, K., CHEESEMAN, I. M. & FUKAGAWA, T. (2008) CCAN makes multiple contacts with centromeric DNA to provide distinct pathways to the outer kinetochore. *Cell,* 135**,** 1039-52.

HORI, T., HARAGUCHI, T., HIRAOKA, Y., KIMURA, H. & FUKAGAWA, T. (2003) Dynamic behavior of Nuf2-Hec1 complex that localizes to the centrosome and centromere and is essential for mitotic progression in vertebrate cells. *J Cell Sci,* 116**,** 3347-62.

HORNUNG, P., MAIER, M., ALUSHIN, G. M., LANDER, G. C., NOGALES, E. & WESTERMANN, S. (2011) Molecular architecture and connectivity of the budding yeast Mtw1 kinetochore complex. *J Mol Biol,* 405**,** 548-59.

HOWE, M., MCDONALD, K. L., ALBERTSON, D. G. & MEYER, B. J. (2001) HIM-10 is required for kinetochore structure and function on Caenorhabditis elegans holocentric chromosomes. *J Cell Biol,* 153**,** 1227-38.

HOWELL, B. J., MCEWEN, B. F., CANMAN, J. C., HOFFMAN, D. B., FARRAR, E. M., RIEDER, C. L. & SALMON, E. D. (2001) Cytoplasmic dynein/dynactin drives kinetochore protein transport to the spindle poles and has a role in mitotic spindle checkpoint inactivation. *J Cell Biol,* 155**,** 1159-72.

HOYT, M. A., TOTIS, L. & ROBERTS, B. T. (1991) S. cerevisiae genes required for cell cycle arrest in response to loss of microtubule function. *Cell,* 66**,** 507-17.

HSU, K. S. & TODA, T. (2011) Ndc80 internal loop interacts with Dis1/TOG to ensure proper kinetochore-spindle attachment in fission yeast. *Curr Biol,* 21**,** 214-20.

HWANG, L. H., LAU, L. F., SMITH, D. L., MISTROT, C. A., HARDWICK, K. G., HWANG, E. S., AMON, A. & MURRAY, A. W. (1998) Budding yeast Cdc20: a target of the spindle checkpoint. *Science,* 279**,** 1041-4.

IZUTA, H., IKENO, M., SUZUKI, N., TOMONAGA, T., NOZAKI, N., OBUSE, C., KISU, Y., GOSHIMA, N., NOMURA, F., NOMURA, N. & YODA, K. (2006) Comprehensive analysis of the ICEN (Interphase Centromere Complex) components enriched in the CENP-A chromatin of human cells. *Genes Cells,* 11**,** 673-84.

JANKE, C., ORTIZ, J., LECHNER, J., SHEVCHENKO, A., MAGIERA, M. M., SCHRAMM, C. & SCHIEBEL, E. (2001) The budding yeast proteins Spc24p and Spc25p interact with Ndc80p and Nuf2p at the kinetochore and are important for kinetochore clustering and checkpoint control. *EMBO J,* 20**,** 777-91.

JANKE, C., ORTIZ, J., TANAKA, T. U., LECHNER, J. & SCHIEBEL, E. (2002) Four new subunits of the Dam1-Duo1 complex reveal novel functions in sister kinetochore biorientation. *EMBO J,* 21**,** 181-93.

JANSON, M. E., LOUGHLIN, R., LOIODICE, I., FU, C., BRUNNER, D., NEDELEC, F. J. & TRAN, P. T. (2007) Crosslinkers and motors organize dynamic microtubules to form stable bipolar arrays in fission yeast. *Cell,* 128**,** 357-68.

JANSON, M. E., SETTY, T. G., PAOLETTI, A. & TRAN, P. T. (2005) Efficient formation of bipolar microtubule bundles requires microtubule-bound gamma-tubulin complexes. *J Cell Biol,* 169**,** 297-308.

JELLUMA, N., DANSEN, T. B., SLIEDRECHT, T., KWIATKOWSKI, N. P. & KOPS, G. J. (2010) Release of Mps1 from kinetochores is crucial for timely anaphase onset. *J Cell Biol,* 191**,** 281-90.

JIANG, K. & AKHMANOVA, A. (2011) Microtubule tip-interacting proteins: a view from both ends. *Curr Opin Cell Biol,* 23**,** 94-101.

JOGLEKAR, A. P., BOUCK, D., FINLEY, K., LIU, X., WAN, Y., BERMAN, J., HE, X., SALMON, E. D. & BLOOM, K. S. (2008) Molecular architecture of the kinetochore-microtubule attachment site is conserved between point and regional centromeres. *J Cell Biol,* 181**,** 587-94.

JOGLEKAR, A. P., BOUCK, D. C., MOLK, J. N., BLOOM, K. S. & SALMON, E. D. (2006) Molecular architecture of a kinetochore-microtubule attachment site. *Nat Cell Biol,* 8**,** 581-5.

JOGLEKAR, A. P. & DELUCA, J. G. (2009) Chromosome segregation: Ndc80 can carry the load. *Curr Biol,* 19**,** R404-7.

JOKELAINEN, P. T. (1967) The ultrastructure and spatial organization of the metaphase kinetochore in mitotic rat cells. *J Ultrastruct Res,* 19**,** 19-44.

JONES, M. H., BACHANT, J. B., CASTILLO, A. R., GIDDINGS, T. H., JR. & WINEY, M. (1999) Yeast Dam1p is required to maintain spindle integrity during mitosis and interacts with the Mps1p kinase. *Mol Biol Cell,* 10**,** 2377-91.

JOSEPH, J., LIU, S. T., JABLONSKI, S. A., YEN, T. J. & DASSO, M. (2004) The RanGAP1-RanBP2 complex is essential for microtubule-kinetochore interactions in vivo. *Curr Biol,* 14**,** 611-7.

KALLIO, M. J., MCCLELAND, M. L., STUKENBERG, P. T. & GORBSKY, G. J. (2002) Inhibition of aurora B kinase blocks chromosome segregation, overrides the spindle checkpoint, and perturbs microtubule dynamics in mitosis. *Curr Biol,* 12**,** 900-5.

KANG, J., CHEESEMAN, I. M., KALLSTROM, G., VELMURUGAN, S., BARNES, G. & CHAN, C. S. (2001) Functional cooperation of Dam1, Ipl1, and the inner centromere protein (INCENP)-related protein Sli15 during chromosome segregation. *J Cell Biol,* 155**,** 763-74.

KAPOOR, T. M., MAYER, T. U., COUGHLIN, M. L. & MITCHISON, T. J. (2000) Probing spindle assembly mechanisms with monastrol, a small molecule inhibitor of the mitotic kinesin, Eg5. *J Cell Biol,* 150**,** 975-88.

KEATING, T. J. & BORISY, G. G. (2000) Immunostructural evidence for the template mechanism of microtubule nucleation. *Nat Cell Biol,* 2**,** 352-7.

KEMMLER, S., STACH, M., KNAPP, M., ORTIZ, J., PFANNSTIEL, J., RUPPERT, T. & LECHNER, J. (2009) Mimicking Ndc80 phosphorylation triggers spindle assembly checkpoint signalling. *EMBO J,* 28**,** 1099-110.

KERRES, A., JAKOPEC, V., BEUTER, C., KARIG, I., POHLMANN, J., PIDOUX, A., ALLSHIRE, R. & FLEIG, U. (2006) Fta2, an essential fission yeast kinetochore component, interacts closely with the conserved Mal2 protein. *Mol Biol Cell,* 17**,** 4167-78.

KERRES, A., JAKOPEC, V. & FLEIG, U. (2007) The conserved Spc7 protein is required for spindle integrity and links kinetochore complexes in fission yeast. *Mol Biol Cell,* 18**,** 2441-54.

KERRES, A., VIETMEIER-DECKER, C., ORTIZ, J., KARIG, I., BEUTER, C., HEGEMANN, J., LECHNER, J. & FLEIG, U. (2004) The fission yeast kinetochore component Spc7 associates with the EB1 family member Mal3 and is required for kinetochore-spindle association. *Mol Biol Cell,* 15**,** 5255-67.

KERSSEMAKERS, J. W., MUNTEANU, E. L., LAAN, L., NOETZEL, T. L., JANSON, M. E. & DOGTEROM, M. (2006) Assembly dynamics of microtubules at molecular resolution. *Nature,* 442**,** 709-12.

KIERMAIER, E., WOEHRER, S., PENG, Y., MECHTLER, K. & WESTERMANN, S. (2009) A Dam1-based artificial kinetochore is sufficient to promote chromosome segregation in budding yeast. *Nat Cell Biol,* 11**,** 1109-15.

KIM, D. U., HAYLES, J., KIM, D., WOOD, V., PARK, H. O., WON, M., YOO, H. S., DUHIG, T., NAM, M., PALMER, G., HAN, S., JEFFERY, L., BAEK, S. T., LEE, H., SHIM, Y. S., LEE, M., KIM, L., HEO, K. S., NOH, E. J., LEE, A. R., JANG, Y. J., CHUNG, K. S., CHOI, S. J., PARK, J. Y., PARK, Y., KIM, H. M., PARK, S. K., PARK, H. J., KANG, E. J., KIM, H. B., KANG, H. S., PARK, H. M., KIM, K., SONG, K., SONG, K. B., NURSE, P. & HOE, K. L. (2010a) Analysis of a genome-wide set of gene deletions in the fission yeast Schizosaccharomyces pombe. *Nat Biotechnol,* 28**,** 617-23.

KIM, S., SUN, H., BALL, H. L., WASSMANN, K., LUO, X. & YU, H. (2010b) Phosphorylation of the spindle checkpoint protein Mad2 regulates its conformational transition. *Proc Natl Acad Sci U S A,* 107**,** 19772-7.

KIM, S. H., LIN, D. P., MATSUMOTO, S., KITAZONO, A. & MATSUMOTO, T. (1998) Fission yeast Slp1: an effector of the Mad2-dependent spindle checkpoint. *Science,* 279**,** 1045-7.

KING, M. C., DRIVAS, T. G. & BLOBEL, G. (2008) A network of nuclear envelope membrane proteins linking centromeres to microtubules. *Cell,* 134**,** 427-38.

KINOSHITA, K., ARNAL, I., DESAI, A., DRECHSEL, D. N. & HYMAN, A. A. (2001) Reconstitution of physiological microtubule dynamics using purified components. *Science,* 294**,** 1340-3.

KIRSCHNER, M. & MITCHISON, T. (1986) Beyond self-assembly: from microtubules to morphogenesis. *Cell,* 45**,** 329-42.

KIYOMITSU, T., IWASAKI, O., OBUSE, C. & YANAGIDA, M. (2010) Inner centromere formation requires hMis14, a trident kinetochore protein that specifically recruits HP1 to human chromosomes. *J Cell Biol,* 188**,** 791-807.

KIYOMITSU, T., MURAKAMI, H. & YANAGIDA, M. (2011) Protein interaction domain mapping of human kinetochore protein Blinkin reveals a consensus motif for binding of spindle assembly checkpoint proteins Bub1 and BubR1. *Mol Cell Biol,* 31**,** 998-1011.

KIYOMITSU, T., OBUSE, C. & YANAGIDA, M. (2007) Human Blinkin/AF15q14 is required for chromosome alignment and the mitotic checkpoint through direct interaction with Bub1 and BubR1. *Dev Cell,* 13**,** 663-76.

KLINE, S. L., CHEESEMAN, I. M., HORI, T., FUKAGAWA, T. & DESAI, A. (2006) The human Mis12 complex is required for kinetochore assembly and proper chromosome segregation. *J Cell Biol,* 173**,** 9-17.

KNIOLA, B., O'TOOLE, E., MCINTOSH, J. R., MELLONE, B., ALLSHIRE, R., MENGARELLI, S., HULTENBY, K. & EKWALL, K. (2001) The domain structure of centromeres is conserved from fission yeast to humans. *Mol Biol Cell,* 12**,** 2767-75.

KNOWLTON, A. L., LAN, W. & STUKENBERG, P. T. (2006) Aurora B is enriched at merotelic attachment sites, where it regulates MCAK. *Curr Biol,* 16**,** 1705-10.

KOBAYASHI, Y., SAITOH, S., OGIYAMA, Y., SOEJIMA, S. & TAKAHASHI, K. (2007) The fission yeast DASH complex is essential for satisfying the spindle assembly checkpoint induced by defects in the inner-kinetochore proteins. *Genes Cells,* 12**,** 311-28.

KOLLMAN, J. M., POLKA, J. K., ZELTER, A., DAVIS, T. N. & AGARD, D. A. (2010) Microtubule nucleating gamma-TuSC assembles structures with 13-fold microtubule-like symmetry. *Nature,* 466**,** 879-82.

KOPS, G. J., WEAVER, B. A. & CLEVELAND, D. W. (2005) On the road to cancer: aneuploidy and the mitotic checkpoint. *Nat Rev Cancer,* 5**,** 773-85.

KOSCO, K. A., PEARSON, C. G., MADDOX, P. S., WANG, P. J., ADAMS, I. R., SALMON, E. D., BLOOM, K. & HUFFAKER, T. C. (2001) Control of microtubule dynamics by Stu2p is essential for spindle orientation and metaphase chromosome alignment in yeast. *Mol Biol Cell,* 12**,** 2870-80.

KULUKIAN, A., HAN, J. S. & CLEVELAND, D. W. (2009) Unattached kinetochores catalyze production of an anaphase inhibitor that requires a Mad2 template to prime Cdc20 for BubR1 binding. *Dev Cell,* 16**,** 105-17.

LA CARBONA, S., LE GOFF, C. & LE GOFF, X. (2006) Fission yeast cytoskeletons and cell polarity factors: connecting at the cortex. *Biol Cell,* 98**,** 619-31.

LACEFIELD, S., LAU, D. T. & MURRAY, A. W. (2009) Recruiting a microtubule-binding complex to DNA directs chromosome segregation in budding yeast. *Nat Cell Biol,* 11**,** 1116-20.

LAMPERT, F., HORNUNG, P. & WESTERMANN, S. (2010) The Dam1 complex confers microtubule plus end-tracking activity to the Ndc80 kinetochore complex. *J Cell Biol,* 189**,** 641-9.

LAMPSON, M. A. & CHEESEMAN, I. M. (2011) Sensing centromere tension: Aurora B and the regulation of kinetochore function. *Trends Cell Biol,* 21**,** 133-40.

LAMPSON, M. A., RENDUCHITALA, K., KHODJAKOV, A. & KAPOOR, T. M. (2004) Correcting improper chromosome-spindle attachments during cell division. *Nat Cell Biol,* 6**,** 232-7.

LAN, W., ZHANG, X., KLINE-SMITH, S. L., ROSASCO, S. E., BARRETT-WILT, G. A., SHABANOWITZ, J., HUNT, D. F., WALCZAK, C. E. & STUKENBERG, P. T. (2004) Aurora B phosphorylates centromeric MCAK and regulates its localization and microtubule depolymerization activity. *Curr Biol,* 14**,** 273-86.

LAUFFART, B., HOWELL, S. J., TASCH, J. E., COWELL, J. K. & STILL, I. H. (2002) Interaction of the transforming acidic coiled-coil 1 (TACC1) protein with ch-TOG and GAS41/NuBI1 suggests multiple TACC1-containing protein complexes in human cells. *Biochem J,* 363**,** 195-200.

LAWRENCE, C. J., DAWE, R. K., CHRISTIE, K. R., CLEVELAND, D. W., DAWSON, S. C., ENDOW, S. A., GOLDSTEIN, L. S., GOODSON, H. V., HIROKAWA, N., HOWARD, J., MALMBERG, R. L., MCINTOSH, J. R., MIKI, H., MITCHISON, T. J., OKADA, Y., REDDY, A. S., SAXTON, W. M., SCHLIWA, M., SCHOLEY, J. M., VALE, R. D., WALCZAK, C. E. & WORDEMAN, L. (2004) A standardized kinesin nomenclature. *J Cell Biol,* 167**,** 19-22.

LE MASSON, I., SAVEANU, C., CHEVALIER, A., NAMANE, A., GOBIN, R., FROMONT-RACINE, M., JACQUIER, A. & MANN, C. (2002) Spc24 interacts with Mps2 and is required for chromosome segregation, but is not implicated in spindle pole body duplication. *Mol Microbiol,* 43**,** 1431-43.

LEE, M. J., GERGELY, F., JEFFERS, K., PEAK-CHEW, S. Y. & RAFF, J. W. (2001) Msps/XMAP215 interacts with the centrosomal protein D-TACC to regulate microtubule behaviour. *Nat Cell Biol,* 3**,** 643-9.

LI, L., YANG, L., SCUDIERO, D. A., MILLER, S. A., YU, Z. X., STUKENBERG, P. T., SHOEMAKER, R. H. & KOTIN, R. M. (2007) Development of recombinant adeno-associated virus vectors carrying small interfering RNA (shHec1)-mediated depletion of kinetochore Hec1 protein in tumor cells. *Gene Ther,* 14**,** 814-27.

LI, R. & MURRAY, A. W. (1991) Feedback control of mitosis in budding yeast. *Cell,* 66**,** 519-31.

LI, X. & NICKLAS, R. B. (1995) Mitotic forces control a cell-cycle checkpoint. *Nature,* 373**,** 630-2.

LI, Y. & CHANG, E. C. (2003) Schizosaccharomyces pombe Ras1 effector, Scd1, interacts with Klp5 and Klp6 kinesins to mediate cytokinesis. *Genetics,* 165**,** 477-88.

LIAO, H., WINKFEIN, R. J., MACK, G., RATTNER, J. B. & YEN, T. J. (1995) CENP-F is a protein of the nuclear matrix that assembles onto kinetochores at late G2 and is rapidly degraded after mitosis. *J Cell Biol,* 130**,** 507-18.

LIOU, J. P., HSU, K. S., KUO, C. C., CHANG, C. Y. & CHANG, J. Y. (2007) A novel oral indoline-sulfonamide agent, N-[1-(4-methoxybenzenesulfonyl)-2,3-dihydro-1H-indol-7-yl]-isonicotinamide (J30), exhibits potent activity against human cancer cells in vitro and in vivo through the disruption of microtubule. *J Pharmacol Exp Ther,* 323**,** 398-405.

LIU, D., VADER, G., VROMANS, M. J., LAMPSON, M. A. & LENS, S. M. (2009) Sensing chromosome bi-orientation by spatial separation of aurora B kinase from kinetochore substrates. *Science,* 323**,** 1350-3.

LIU, D., VLEUGEL, M., BACKER, C. B., HORI, T., FUKAGAWA, T., CHEESEMAN, I. M. & LAMPSON, M. A. (2010) Regulated targeting of protein phosphatase 1 to the outer kinetochore by KNL1 opposes Aurora B kinase. *J Cell Biol,* 188**,** 809-20.

LIU, X., MCLEOD, I., ANDERSON, S., YATES, J. R., 3RD & HE, X. (2005) Molecular analysis of kinetochore architecture in fission yeast. *EMBO J,* 24**,** 2919-30.

LUO, X., TANG, Z., RIZO, J. & YU, H. (2002) The Mad2 spindle checkpoint protein undergoes similar major conformational changes upon binding to either Mad1 or Cdc20. *Mol Cell,* 9**,** 59-71.
LUO, X., TANG, Z., XIA, G., WASSMANN, K., MATSUMOTO, T., RIZO, J. & YU, H. (2004) The Mad2 spindle checkpoint protein has two distinct natively folded states. *Nat Struct Mol Biol,* 11**,** 338-45.
MA, L., MCQUEEN, J., CUSCHIERI, L., VOGEL, J. & MEASDAY, V. (2007) Spc24 and Stu2 promote spindle integrity when DNA replication is stalled. *Mol Biol Cell,* 18**,** 2805-16.
MAIATO, H., DELUCA, J., SALMON, E. D. & EARNSHAW, W. C. (2004) The dynamic kinetochore-microtubule interface. *J Cell Sci,* 117**,** 5461-77.
MAIOLICA, A., CITTARO, D., BORSOTTI, D., SENNELS, L., CIFERRI, C., TARRICONE, C., MUSACCHIO, A. & RAPPSILBER, J. (2007) Structural analysis of multiprotein complexes by cross-linking, mass spectrometry, and database searching. *Mol Cell Proteomics,* 6**,** 2200-11.
MALDONADO, M. & KAPOOR, T. M. (2011) Constitutive Mad1 targeting to kinetochores uncouples checkpoint signalling from chromosome biorientation. *Nat Cell Biol,* 13**,** 475-82.
MAO, Y., DESAI, A. & CLEVELAND, D. W. (2005) Microtubule capture by CENP-E silences BubR1-dependent mitotic checkpoint signaling. *J Cell Biol,* 170**,** 873-80.
MAPELLI, M., MASSIMILIANO, L., SANTAGUIDA, S. & MUSACCHIO, A. (2007) The Mad2 conformational dimer: structure and implications for the spindle assembly checkpoint. *Cell,* 131**,** 730-43.
MARESCA, T. J. & SALMON, E. D. (2009) Intrakinetochore stretch is associated with changes in kinetochore phosphorylation and spindle assembly checkpoint activity. *J Cell Biol,* 184**,** 373-81.
MARESCA, T. J. & SALMON, E. D. (2010) Welcome to a new kind of tension: translating kinetochore mechanics into a wait-anaphase signal. *J Cell Sci,* 123**,** 825-35.
MARTIN-LLUESMA, S., STUCKE, V. M. & NIGG, E. A. (2002) Role of Hec1 in spindle checkpoint signaling and kinetochore recruitment of Mad1/Mad2. *Science,* 297**,** 2267-70.
MASKELL, D. P., HU, X. W. & SINGLETON, M. R. (2010) Molecular architecture and assembly of the yeast kinetochore MIND complex. *J Cell Biol,* 190**,** 823-34.
MASUDA, H., TODA, T., MIYAMOTO, R., HARAGUCHI, T. & HIRAOKA, Y. (2006) Modulation of Alp4 function in Schizosaccharomyces pombe induces novel phenotypes that imply distinct functions for nuclear and cytoplasmic gamma-tubulin complexes. *Genes Cells,* 11**,** 319-36.
MASUMOTO, H., MASUKATA, H., MURO, Y., NOZAKI, N. & OKAZAKI, T. (1989) A human centromere antigen (CENP-B) interacts with a short specific sequence in alphoid DNA, a human centromeric satellite. *J Cell Biol,* 109**,** 1963-73.
MATSUYAMA, A., ARAI, R., YASHIRODA, Y., SHIRAI, A., KAMATA, A., SEKIDO, S., KOBAYASHI, Y., HASHIMOTO, A., HAMAMOTO, M., HIRAOKA, Y., HORINOUCHI, S. & YOSHIDA, M. (2006) ORFeome cloning and global analysis of protein localization in the fission yeast Schizosaccharomyces pombe. *Nat Biotechnol,* 24**,** 841-7.
MAUNDRELL, K. (1993) Thiamine-repressible expression vectors pREP and pRIP for fission yeast. *Gene,* 123**,** 127-30.
MAURE, J. F., KOMOTO, S., OKU, Y., MINO, A., PASQUALATO, S., NATSUME, K., CLAYTON, L., MUSACCHIO, A. & TANAKA, T. U. (2011) The Ndc80 loop region facilitates formation of kinetochore attachment to the dynamic microtubule plus end. *Curr Biol,* 21**,** 207-13.
MAURER, S. P., BIELING, P., COPE, J., HOENGER, A. & SURREY, T. (2011) GTPgammaS microtubules mimic the growing microtubule end structure recognized by end-binding proteins (EBs). *Proc Natl Acad Sci U S A,* 108**,** 3988-93.
MCCLELAND, M. L., GARDNER, R. D., KALLIO, M. J., DAUM, J. R., GORBSKY, G. J., BURKE, D. J. & STUKENBERG, P. T. (2003) The highly conserved Ndc80 complex is required for kinetochore assembly, chromosome congression, and spindle checkpoint activity. *Genes Dev,* 17**,** 101-14.
MCCLELAND, M. L., KALLIO, M. J., BARRETT-WILT, G. A., KESTNER, C. A., SHABANOWITZ, J., HUNT, D. F., GORBSKY, G. J. & STUKENBERG, P. T. (2004) The vertebrate Ndc80 complex contains Spc24 and Spc25 homologs, which are required to establish and maintain kinetochore-microtubule attachment. *Curr Biol,* 14**,** 131-7.
MCEWEN, B. F., CHAN, G. K., ZUBROWSKI, B., SAVOIAN, M. S., SAUER, M. T. & YEN, T. J. (2001) CENP-E is essential for reliable bioriented spindle attachment, but chromosome alignment can be achieved via redundant mechanisms in mammalian cells. *Mol Biol Cell,* 12**,** 2776-89.
MCEWEN, B. F. & DONG, Y. (2010) Contrasting models for kinetochore microtubule attachment in mammalian cells. *Cell Mol Life Sci,* 67**,** 2163-72.
MCINTOSH, J. R., GRISHCHUK, E. L., MORPHEW, M. K., EFREMOV, A. K., ZHUDENKOV, K., VOLKOV, V. A., CHEESEMAN, I. M., DESAI, A., MASTRONARDE, D. N. & ATAULLAKHANOV, F. I. (2008) Fibrils connect microtubule tips with kinetochores: a mechanism to couple tubulin dynamics to chromosome motion. *Cell,* 135**,** 322-33.
MEADOWS, J. C. & MILLAR, J. (2008) Latrunculin A delays anaphase onset in fission yeast by disrupting an Ase1-independent pathway controlling mitotic spindle stability. *Mol Biol Cell,* 19**,** 3713-23.

MEADOWS, J. C., SHEPPERD, L. A., VANOOSTHUYSE, V., LANCASTER, T. C., SOCHAJ, A. M., BUTTRICK, G. J., HARDWICK, K. G. & MILLAR, J. B. (2011) Spindle checkpoint silencing requires association of PP1 to both Spc7 and kinesin-8 motors. *Dev Cell,* 20**,** 739-50.

MEASDAY, V., HAILEY, D. W., POT, I., GIVAN, S. A., HYLAND, K. M., CAGNEY, G., FIELDS, S., DAVIS, T. N. & HIETER, P. (2002) Ctf3p, the Mis6 budding yeast homolog, interacts with Mcm22p and Mcm16p at the yeast outer kinetochore. *Genes Dev,* 16**,** 101-13.

MERALDI, P., DRAVIAM, V. M. & SORGER, P. K. (2004) Timing and checkpoints in the regulation of mitotic progression. *Dev Cell,* 7**,** 45-60.

MERALDI, P., MCAINSH, A. D., RHEINBAY, E. & SORGER, P. K. (2006) Phylogenetic and structural analysis of centromeric DNA and kinetochore proteins. *Genome Biol,* 7**,** R23.

MIKAMI, Y., HORI, T., KIMURA, H. & FUKAGAWA, T. (2005) The functional region of CENP-H interacts with the Nuf2 complex that localizes to centromere during mitosis. *Mol Cell Biol,* 25**,** 1958-70.

MIKI, F., KURABAYASHI, A., TANGE, Y., OKAZAKI, K., SHIMANUKI, M. & NIWA, O. (2004) Two-hybrid search for proteins that interact with Sad1 and Kms1, two membrane-bound components of the spindle pole body in fission yeast. *Mol Genet Genomics,* 270**,** 449-61.

MILLBAND, D. N., CAMPBELL, L. & HARDWICK, K. G. (2002) The awesome power of multiple model systems: interpreting the complex nature of spindle checkpoint signaling. *Trends Cell Biol,* 12**,** 205-9.

MILLER, S. A., JOHNSON, M. L. & STUKENBERG, P. T. (2008) Kinetochore attachments require an interaction between unstructured tails on microtubules and Ndc80(Hec1). *Curr Biol,* 18**,** 1785-91.

MIRANDA, J. J., DE WULF, P., SORGER, P. K. & HARRISON, S. C. (2005) The yeast DASH complex forms closed rings on microtubules. *Nat Struct Mol Biol,* 12**,** 138-43.

MIRCHENKO, L. & UHLMANN, F. (2010) Sli15(INCENP) dephosphorylation prevents mitotic checkpoint reengagement due to loss of tension at anaphase onset. *Curr Biol,* 20**,** 1396-401.

MITCHISON, T., EVANS, L., SCHULZE, E. & KIRSCHNER, M. (1986) Sites of microtubule assembly and disassembly in the mitotic spindle. *Cell,* 45**,** 515-27.

MITCHISON, T. & KIRSCHNER, M. (1984) Dynamic instability of microtubule growth. *Nature,* 312**,** 237-42.

MITCHISON, T. J. (1993) Localization of an exchangeable GTP binding site at the plus end of microtubules. *Science,* 261**,** 1044-7.

MITCHISON, T. J. & KIRSCHNER, M. W. (1985) Properties of the kinetochore in vitro. II. Microtubule capture and ATP-dependent translocation. *J Cell Biol,* 101**,** 766-77.

MITCHISON, T. J. & SALMON, E. D. (2001) Mitosis: a history of division. *Nat Cell Biol,* 3**,** E17-21.

MOMENY, M., KHORRAMIZADEH, M. R., GHAFFARI, S. H., YOUSEFI, M., YEKANINEJAD, M. S., ESMAEILI, R., JAHANSHIRI, Z. & NOORIDALOII, M. R. (2008) Effects of silibinin on cell growth and invasive properties of a human hepatocellular carcinoma cell line, HepG-2, through inhibition of extracellular signal-regulated kinase 1/2 phosphorylation. *Eur J Pharmacol,* 591**,** 13-20.

MONTPETIT, B., THORNE, K., BARRETT, I., ANDREWS, K., JADUSINGH, R., HIETER, P. & MEASDAY, V. (2005) Genome-wide synthetic lethal screens identify an interaction between the nuclear envelope protein, Apq12p, and the kinetochore in Saccharomyces cerevisiae. *Genetics,* 171**,** 489-501.

MORENO, S., KLAR, A. & NURSE, P. (1991) Molecular genetic analysis of fission yeast Schizosaccharomyces pombe. *Methods Enzymol,* 194**,** 795-823.

MORITZ, M., BRAUNFELD, M. B., GUENEBAUT, V., HEUSER, J. & AGARD, D. A. (2000) Structure of the gamma-tubulin ring complex: a template for microtubule nucleation. *Nat Cell Biol,* 2**,** 365-70.

MORROW, C. J., TIGHE, A., JOHNSON, V. L., SCOTT, M. I., DITCHFIELD, C. & TAYLOR, S. S. (2005) Bub1 and aurora B cooperate to maintain BubR1-mediated inhibition of APC/CCdc20. *J Cell Sci,* 118**,** 3639-52.

MUSACCHIO, A. & SALMON, E. D. (2007) The spindle-assembly checkpoint in space and time. *Nat Rev Mol Cell Biol,* 8**,** 379-93.

NABESHIMA, K., KUROOKA, H., TAKEUCHI, M., KINOSHITA, K., NAKASEKO, Y. & YANAGIDA, M. (1995) p93dis1, which is required for sister chromatid separation, is a novel microtubule and spindle pole body-associating protein phosphorylated at the Cdc2 target sites. *Genes Dev,* 9**,** 1572-85.

NABESHIMA, K., NAKAGAWA, T., STRAIGHT, A. F., MURRAY, A., CHIKASHIGE, Y., YAMASHITA, Y. M., HIRAOKA, Y. & YANAGIDA, M. (1998) Dynamics of centromeres during metaphase-anaphase transition in fission yeast: Dis1 is implicated in force balance in metaphase bipolar spindle. *Mol Biol Cell,* 9**,** 3211-25.

NABETANI, A., KOUJIN, T., TSUTSUMI, C., HARAGUCHI, T. & HIRAOKA, Y. (2001) A conserved protein, Nuf2, is implicated in connecting the centromere to the spindle during chromosome segregation: a link between the kinetochore function and the spindle checkpoint. *Chromosoma,* 110**,** 322-34.

NAKAJIMA, Y., TYERS, R. G., WONG, C. C., YATES, J. R., 3RD, DRUBIN, D. G. & BARNES, G. (2009) Nbl1p: a Borealin/Dasra/CSC-1-like protein essential for Aurora/Ipl1 complex function and integrity in Saccharomyces cerevisiae. *Mol Biol Cell,* 20**,** 1772-84.

NAKASEKO, Y., GOSHIMA, G., MORISHITA, J. & YANAGIDA, M. (2001) M phase-specific kinetochore proteins in fission yeast: microtubule-associating Dis1 and Mtc1 display rapid separation and segregation during anaphase. *Curr Biol,* 11**,** 537-49.

NAKASEKO, Y., NABESHIMA, K., KINOSHITA, K. & YANAGIDA, M. (1996) Dissection of fission yeast microtubule associating protein p93Dis1: regions implicated in regulated localization and microtubule interaction. *Genes Cells,* 1**,** 633-44.

NASMYTH, K. (2005) How do so few control so many? *Cell,* 120**,** 739-46.

NEKRASOV, V. S., SMITH, M. A., PEAK-CHEW, S. & KILMARTIN, J. V. (2003) Interactions between centromere complexes in Saccharomyces cerevisiae. *Mol Biol Cell,* 14**,** 4931-46.

NEZI, L. & MUSACCHIO, A. (2009) Sister chromatid tension and the spindle assembly checkpoint. *Curr Opin Cell Biol,* 21**,** 785-95.

NICKLAS, R. B. & KOCH, C. A. (1969) Chromosome micromanipulation. 3. Spindle fiber tension and the reorientation of mal-oriented chromosomes. *J Cell Biol,* 43**,** 40-50.

NISHIHASHI, A., HARAGUCHI, T., HIRAOKA, Y., IKEMURA, T., REGNIER, V., DODSON, H., EARNSHAW, W. C. & FUKAGAWA, T. (2002) CENP-I is essential for centromere function in vertebrate cells. *Dev Cell,* 2**,** 463-76.

NOGALES, E., WHITTAKER, M., MILLIGAN, R. A. & DOWNING, K. H. (1999) High-resolution model of the microtubule. *Cell,* 96**,** 79-88.

NOGALES, E., WOLF, S. G. & DOWNING, K. H. (1998) Structure of the alpha beta tubulin dimer by electron crystallography. *Nature,* 391**,** 199-203.

NUMNUM, T. M., MAKHIJA, S., LU, B., WANG, M., RIVERA, A., STOFF-KHALILI, M., ALVAREZ, R. D., ZHU, Z. B. & CURIEL, D. T. (2008) Improved anti-tumor therapy based upon infectivity-enhanced adenoviral delivery of RNA interference in ovarian carcinoma cell lines. *Gynecol Oncol,* 108**,** 34-41.

O'CONNELL, C. B., LONCAREK, J., HERGERT, P., KOURTIDIS, A., CONKLIN, D. S. & KHODJAKOV, A. (2008) The spindle assembly checkpoint is satisfied in the absence of interkinetochore tension during mitosis with unreplicated genomes. *J Cell Biol,* 183**,** 29-36.

O'TOOLE, E. T., MCDONALD, K. L., MANTLER, J., MCINTOSH, J. R., HYMAN, A. A. & MULLER-REICHERT, T. (2003) Morphologically distinct microtubule ends in the mitotic centrosome of Caenorhabditis elegans. *J Cell Biol,* 163**,** 451-6.

OBUSE, C., IWASAKI, O., KIYOMITSU, T., GOSHIMA, G., TOYODA, Y. & YANAGIDA, M. (2004a) A conserved Mis12 centromere complex is linked to heterochromatic HP1 and outer kinetochore protein Zwint-1. *Nat Cell Biol,* 6**,** 1135-41.

OBUSE, C., YANG, H., NOZAKI, N., GOTO, S., OKAZAKI, T. & YODA, K. (2004b) Proteomics analysis of the centromere complex from HeLa interphase cells: UV-damaged DNA binding protein 1 (DDB-1) is a component of the CEN-complex, while BMI-1 is transiently co-localized with the centromeric region in interphase. *Genes Cells,* 9**,** 105-20.

OEGEMA, K., DESAI, A., RYBINA, S., KIRKHAM, M. & HYMAN, A. A. (2001) Functional analysis of kinetochore assembly in Caenorhabditis elegans. *J Cell Biol,* 153**,** 1209-26.

OHI, R., SAPRA, T., HOWARD, J. & MITCHISON, T. J. (2004) Differentiation of cytoplasmic and meiotic spindle assembly MCAK functions by Aurora B-dependent phosphorylation. *Mol Biol Cell,* 15**,** 2895-906.

OHKURA, H., ADACHI, Y., KINOSHITA, N., NIWA, O., TODA, T. & YANAGIDA, M. (1988) Cold-sensitive and caffeine-supersensitive mutants of the Schizosaccharomyces pombe dis genes implicated in sister chromatid separation during mitosis. *EMBO J,* 7**,** 1465-73.

OHKURA, H., GARCIA, M. A. & TODA, T. (2001) Dis1/TOG universal microtubule adaptors - one MAP for all? *J Cell Sci,* 114**,** 3805-12.

OHTA, S., BUKOWSKI-WILLS, J. C., SANCHEZ-PULIDO, L., ALVES FDE, L., WOOD, L., CHEN, Z. A., PLATANI, M., FISCHER, L., HUDSON, D. F., PONTING, C. P., FUKAGAWA, T., EARNSHAW, W. C. & RAPPSILBER, J. (2010) The protein composition of mitotic chromosomes determined using multiclassifier combinatorial proteomics. *Cell,* 142**,** 810-21.

OKADA, M., CHEESEMAN, I. M., HORI, T., OKAWA, K., MCLEOD, I. X., YATES, J. R., 3RD, DESAI, A. & FUKAGAWA, T. (2006) The CENP-H-I complex is required for the efficient incorporation of newly synthesized CENP-A into centromeres. *Nat Cell Biol,* 8**,** 446-57.

OLIFERENKO, S. & BALASUBRAMANIAN, M. K. (2002) Astral microtubules monitor metaphase spindle alignment in fission yeast. *Nat Cell Biol,* 4**,** 816-20.

OSBORNE, M. A., SCHLENSTEDT, G., JINKS, T. & SILVER, P. A. (1994) Nuf2, a spindle pole body-associated protein required for nuclear division in yeast. *J Cell Biol,* 125**,** 853-66.

PAGLIUCA, C., DRAVIAM, V. M., MARCO, E., SORGER, P. K. & DE WULF, P. (2009) Roles for the conserved spc105p/kre28p complex in kinetochore-microtubule binding and the spindle assembly checkpoint. *PLoS One,* 4**,** e7640.

PALFRAMAN, W. J., MEEHL, J. B., JASPERSEN, S. L., WINEY, M. & MURRAY, A. W. (2006) Anaphase inactivation of the spindle checkpoint. *Science,* 313**,** 680-4.

PEREIRA, G. & SCHIEBEL, E. (2003) Separase regulates INCENP-Aurora B anaphase spindle function through Cdc14. *Science,* 302**,** 2120-4.

PERPELESCU, M. & FUKAGAWA, T. (2011) The ABCs of CENPs. *Chromosoma*.

PETERS, J. M. (2006) The anaphase promoting complex/cyclosome: a machine designed to destroy. *Nat Rev Mol Cell Biol,* 7**,** 644-56.

PETERSEN, J. & HAGAN, I. M. (2003) S. pombe aurora kinase/survivin is required for chromosome condensation and the spindle checkpoint attachment response. *Curr Biol,* 13**,** 590-7.

PETROVIC, A., PASQUALATO, S., DUBE, P., KRENN, V., SANTAGUIDA, S., CITTARO, D., MONZANI, S., MASSIMILIANO, L., KELLER, J., TARRICONE, A., MAIOLICA, A., STARK, H. & MUSACCHIO, A. (2010) The MIS12 complex is a protein interaction hub for outer kinetochore assembly. *J Cell Biol,* 190**,** 835-52.

PINSKY, B. A., KUNG, C., SHOKAT, K. M. & BIGGINS, S. (2006) The Ipl1-Aurora protein kinase activates the spindle checkpoint by creating unattached kinetochores. *Nat Cell Biol,* 8**,** 78-83.

PINSKY, B. A., NELSON, C. R. & BIGGINS, S. (2009) Protein phosphatase 1 regulates exit from the spindle checkpoint in budding yeast. *Curr Biol,* 19**,** 1182-7.

PINSKY, B. A., TATSUTANI, S. Y., COLLINS, K. A. & BIGGINS, S. (2003) An Mtw1 complex promotes kinetochore biorientation that is monitored by the Ipl1/Aurora protein kinase. *Dev Cell,* 5**,** 735-45.

POTAPOVA, T. A., DAUM, J. R., PITTMAN, B. D., HUDSON, J. R., JONES, T. N., SATINOVER, D. L., STUKENBERG, P. T. & GORBSKY, G. J. (2006) The reversibility of mitotic exit in vertebrate cells. *Nature,* 440**,** 954-8.

POWERS, A. F., FRANCK, A. D., GESTAUT, D. R., COOPER, J., GRACYZK, B., WEI, R. R., WORDEMAN, L., DAVIS, T. N. & ASBURY, C. L. (2009) The Ndc80 kinetochore complex forms load-bearing attachments to dynamic microtubule tips via biased diffusion. *Cell,* 136**,** 865-75.

PRZEWLOKA, M. R., VENKEI, Z., BOLANOS-GARCIA, V. M., DEBSKI, J., DADLEZ, M. & GLOVER, D. M. (2011) CENP-C is a structural platform for kinetochore assembly. *Curr Biol,* 21**,** 399-405.

PRZEWLOKA, M. R., VENKEI, Z. & GLOVER, D. M. (2009) Searching for Drosophila Dsn1 kinetochore protein. *Cell Cycle,* 8**,** 1292-3.

RAAIJMAKERS, J. A., TANENBAUM, M. E., MAIA, A. F. & MEDEMA, R. H. (2009) RAMA1 is a novel kinetochore protein involved in kinetochore-microtubule attachment. *J Cell Sci,* 122**,** 2436-45.

RADCLIFFE, P., HIRATA, D., CHILDS, D., VARDY, L. & TODA, T. (1998) Identification of novel temperature-sensitive lethal alleles in essential beta-tubulin and nonessential alpha 2-tubulin genes as fission yeast polarity mutants. *Mol Biol Cell,* 9**,** 1757-71.

RATTNER, J. B., RAO, A., FRITZLER, M. J., VALENCIA, D. W. & YEN, T. J. (1993) CENP-F is a .ca 400 kDa kinetochore protein that exhibits a cell-cycle dependent localization. *Cell Motil Cytoskeleton,* 26**,** 214-26.

REDDY, S. K., RAPE, M., MARGANSKY, W. A. & KIRSCHNER, M. W. (2007) Ubiquitination by the anaphase-promoting complex drives spindle checkpoint inactivation. *Nature,* 446**,** 921-5.

RHIND, N., CHEN, Z., YASSOUR, M., THOMPSON, D. A., HAAS, B. J., HABIB, N., WAPINSKI, I., ROY, S., LIN, M. F., HEIMAN, D. I., YOUNG, S. K., FURUYA, K., GUO, Y., PIDOUX, A., CHEN, H. M., ROBBERTSE, B., GOLDBERG, J. M., AOKI, K., BAYNE, E. H., BERLIN, A. M., DESJARDINS, C. A., DOBBS, E., DUKAJ, L., FAN, L., FITZGERALD, M. G., FRENCH, C., GUJJA, S., HANSEN, K., KEIFENHEIM, D., LEVIN, J. Z., MOSHER, R. A., MULLER, C. A., PFIFFNER, J., PRIEST, M., RUSS, C., SMIALOWSKA, A., SWOBODA, P., SYKES, S. M., VAUGHN, M., VENGROVA, S., YODER, R., ZENG, Q., ALLSHIRE, R., BAULCOMBE, D., BIRREN, B. W., BROWN, W., EKWALL, K., KELLIS, M., LEATHERWOOD, J., LEVIN, H., MARGALIT, H., MARTIENSSEN, R., NIEDUSZYNSKI, C. A., SPATAFORA, J. W., FRIEDMAN, N., DALGAARD, J. Z., BAUMANN, P., NIKI, H., REGEV, A. & NUSBAUM, C. (2011) Comparative functional genomics of the fission yeasts. *Science,* 332**,** 930-6.

RIBEIRO, S. A., VAGNARELLI, P., DONG, Y., HORI, T., MCEWEN, B. F., FUKAGAWA, T., FLORS, C. & EARNSHAW, W. C. (2010) A super-resolution map of the vertebrate kinetochore. *Proc Natl Acad Sci U S A,* 107**,** 10484-9.

RIEDER, C. L., COLE, R. W., KHODJAKOV, A. & SLUDER, G. (1995) The checkpoint delaying anaphase in response to chromosome monoorientation is mediated by an inhibitory signal produced by unattached kinetochores. *J Cell Biol,* 130**,** 941-8.

RIEDER, C. L. & SALMON, E. D. (1998) The vertebrate cell kinetochore and its roles during mitosis. *Trends Cell Biol,* 8**,** 310-8.

ROBINETT, C. C., STRAIGHT, A., LI, G., WILLHELM, C., SUDLOW, G., MURRAY, A. & BELMONT, A. S. (1996) In vivo localization of DNA sequences and visualization of large-scale chromatin organization using lac operator/repressor recognition. *J Cell Biol,* 135**,** 1685-700.

ROGUEV, A., BANDYOPADHYAY, S., ZOFALL, M., ZHANG, K., FISCHER, T., COLLINS, S. R., QU, H., SHALES, M., PARK, H. O., HAYLES, J., HOE, K. L., KIM, D. U., IDEKER, T., GREWAL, S. I., WEISSMAN, J. S. & KROGAN, N. J. (2008) Conservation and rewiring of functional modules revealed by an epistasis map in fission yeast. *Science,* 322**,** 405-10.

ROSENBERG, J. S., CROSS, F. R. & FUNABIKI, H. (2011) KNL1/Spc105 recruits PP1 to silence the spindle assembly checkpoint. *Curr Biol,* 21**,** 942-7.

ROUT, M. P. & KILMARTIN, J. V. (1990) Components of the yeast spindle and spindle pole body. *J Cell Biol,* 111**,** 1913-27.

RUCHAUD, S., CARMENA, M. & EARNSHAW, W. C. (2007) Chromosomal passengers: conducting cell division. *Nat Rev Mol Cell Biol,* 8**,** 798-812.

SAGOLLA, M. J., UZAWA, S. & CANDE, W. Z. (2003) Individual microtubule dynamics contribute to the function of mitotic and cytoplasmic arrays in fission yeast. *J Cell Sci,* 116**,** 4891-903.

SAITOH, S., ISHII, K., KOBAYASHI, Y. & TAKAHASHI, K. (2005) Spindle checkpoint signaling requires the mis6 kinetochore subcomplex, which interacts with mad2 and mitotic spindles. *Mol Biol Cell,* 16**,** 3666-77.

SAITOH, S., TAKAHASHI, K. & YANAGIDA, M. (1997) Mis6, a fission yeast inner centromere protein, acts during G1/S and forms specialized chromatin required for equal segregation. *Cell,* 90**,** 131-43.

SALMON, E. D., GOODE, D., MAUGEL, T. K. & BONAR, D. B. (1976) Pressure-induced depolymerization of spindle microtubules. III. Differential stability in HeLa cells. *J Cell Biol,* 69**,** 443-54.

SAMEJIMA, I., LOURENCO, P. C., SNAITH, H. A. & SAWIN, K. E. (2005) Fission yeast mto2p regulates microtubule nucleation by the centrosomin-related protein mto1p. *Mol Biol Cell,* 16**,** 3040-51.

SAMEJIMA, I. & YANAGIDA, M. (1994) Bypassing anaphase by fission yeast cut9 mutation: requirement of cut9+ to initiate anaphase. *J Cell Biol,* 127**,** 1655-70.

SANCHEZ-PEREZ, I., RENWICK, S. J., CRAWLEY, K., KARIG, I., BUCK, V., MEADOWS, J. C., FRANCO-SANCHEZ, A., FLEIG, U., TODA, T. & MILLAR, J. B. (2005) The DASH complex and Klp5/Klp6 kinesin coordinate bipolar chromosome attachment in fission yeast. *EMBO J,* 24**,** 2931-43.

SANDALL, S., SEVERIN, F., MCLEOD, I. X., YATES, J. R., 3RD, OEGEMA, K., HYMAN, A. & DESAI, A. (2006) A Bir1-Sli15 complex connects centromeres to microtubules and is required to sense kinetochore tension. *Cell,* 127**,** 1179-91.

SANDBLAD, L., BUSCH, K. E., TITTMANN, P., GROSS, H., BRUNNER, D. & HOENGER, A. (2006) The Schizosaccharomyces pombe EB1 homolog Mal3p binds and stabilizes the microtubule lattice seam. *Cell,* 127**,** 1415-24.

SANTAGUIDA, S. & MUSACCHIO, A. (2009) The life and miracles of kinetochores. *EMBO J,* 28**,** 2511-31.

SATO, A., ISAAC, B., PHILLIPS, C. M., RILLO, R., CARLTON, P. M., WYNNE, D. J., KASAD, R. A. & DERNBURG, A. F. (2009) Cytoskeletal forces span the nuclear envelope to coordinate meiotic chromosome pairing and synapsis. *Cell,* 139**,** 907-19.

SATO, M., DHUT, S. & TODA, T. (2005) New drug-resistant cassettes for gene disruption and epitope tagging in Schizosaccharomyces pombe. *Yeast,* 22**,** 583-91.

SATO, M. & TODA, T. (2004) Reconstruction of microtubules; entry into interphase. *Dev Cell,* 6**,** 456-8.

SATO, M., VARDY, L., ANGEL GARCIA, M., KOONRUGSA, N. & TODA, T. (2004) Interdependency of fission yeast Alp14/TOG and coiled coil protein Alp7 in microtubule localization and bipolar spindle formation. *Mol Biol Cell,* 15**,** 1609-22.

SAWIN, K. E., LOURENCO, P. C. & SNAITH, H. A. (2004) Microtubule nucleation at non-spindle pole body microtubule-organizing centers requires fission yeast centrosomin-related protein mod20p. *Curr Biol,* 14**,** 763-75.

SAWIN, K. E. & TRAN, P. T. (2006) Cytoplasmic microtubule organization in fission yeast. *Yeast,* 23**,** 1001-14.

SCHAAR, B. T., CHAN, G. K., MADDOX, P., SALMON, E. D. & YEN, T. J. (1997) CENP-E function at kinetochores is essential for chromosome alignment. *J Cell Biol,* 139**,** 1373-82.

SCHITTENHELM, R. B., CHALECKIS, R. & LEHNER, C. F. (2009) Intrakinetochore localization and essential functional domains of Drosophila Spc105. *EMBO J,* 28**,** 2374-86.

SCHITTENHELM, R. B., HEEGER, S., ALTHOFF, F., WALTER, A., HEIDMANN, S., MECHTLER, K. & LEHNER, C. F. (2007) Spatial organization of a ubiquitous eukaryotic kinetochore protein network in Drosophila chromosomes. *Chromosoma,* 116**,** 385-402.

SCREPANTI, E., DE ANTONI, A., ALUSHIN, G. M., PETROVIC, A., MELIS, T., NOGALES, E. & MUSACCHIO, A. (2011) Direct binding of Cenp-C to the Mis12 complex joins the inner and outer kinetochore. *Curr Biol,* 21**,** 391-8.

SHAH, J. V., BOTVINICK, E., BONDAY, Z., FURNARI, F., BERNS, M. & CLEVELAND, D. W. (2004) Dynamics of centromere and kinetochore proteins; implications for checkpoint signaling and silencing. *Curr Biol,* 14**,** 942-52.

SHANG, C., HAZBUN, T. R., CHEESEMAN, I. M., ARANDA, J., FIELDS, S., DRUBIN, D. G. & BARNES, G. (2003) Kinetochore protein interactions and their regulation by the Aurora kinase Ipl1p. *Mol Biol Cell,* 14**,** 3342-55.

SHIMOGAWA, M. M., GRACZYK, B., GARDNER, M. K., FRANCIS, S. E., WHITE, E. A., ESS, M., MOLK, J. N., RUSE, C., NIESSEN, S., YATES, J. R., 3RD, MULLER, E. G., BLOOM, K., ODDE, D. J. & DAVIS, T. N. (2006) Mps1 phosphorylation of Dam1 couples kinetochores to microtubule plus ends at metaphase. *Curr Biol,* 16**,** 1489-501.

SHIRASU-HIZA, M., COUGHLIN, P. & MITCHISON, T. (2003) Identification of XMAP215 as a microtubule-destabilizing factor in Xenopus egg extract by biochemical purification. *J Cell Biol,* 161**,** 349-58.

SHIROIWA, Y., HAYASHI, T., FUJITA, Y., VILLAR-BRIONES, A., IKAI, N., TAKEDA, K., EBE, M. & YANAGIDA, M. (2011) Mis17 is a regulatory module of the Mis6-Mal2-Sim4 centromere complex that is required for the recruitment of CenH3/CENP-A in fission yeast. *PLoS One,* 6**,** e17761.

SHONN, M. A., MCCARROLL, R. & MURRAY, A. W. (2000) Requirement of the spindle checkpoint for proper chromosome segregation in budding yeast meiosis. *Science,* 289**,** 300-3.

SIRONI, L., MAPELLI, M., KNAPP, S., DE ANTONI, A., JEANG, K. T. & MUSACCHIO, A. (2002) Crystal structure of the tetrameric Mad1-Mad2 core complex: implications of a 'safety belt' binding mechanism for the spindle checkpoint. *EMBO J,* 21**,** 2496-506.

SIRONI, L., MELIXETIAN, M., FARETTA, M., PROSPERINI, E., HELIN, K. & MUSACCHIO, A. (2001) Mad2 binding to Mad1 and Cdc20, rather than oligomerization, is required for the spindle checkpoint. *EMBO J,* 20**,** 6371-82.

SKOUFIAS, D. A., ANDREASSEN, P. R., LACROIX, F. B., WILSON, L. & MARGOLIS, R. L. (2001) Mammalian mad2 and bub1/bubR1 recognize distinct spindle-attachment and kinetochore-tension checkpoints. *Proc Natl Acad Sci U S A,* 98**,** 4492-7.

SLEP, K. C. & VALE, R. D. (2007) Structural basis of microtubule plus end tracking by XMAP215, CLIP-170, and EB1. *Mol Cell,* 27**,** 976-91.

SPIREK, M., BENKO, Z., CARNECKA, M., RUMPF, C., CIPAK, L., BATOVA, M., MAROVA, I., NAM, M., KIM, D. U., PARK, H. O., HAYLES, J., HOE, K. L., NURSE, P. & GREGAN, J. (2010) S. pombe genome deletion project: an update. *Cell Cycle,* 9**,** 2399-402.

SRAYKO, M., QUINTIN, S., SCHWAGER, A. & HYMAN, A. A. (2003) Caenorhabditis elegans TAC-1 and ZYG-9 form a complex that is essential for long astral and spindle microtubules. *Curr Biol,* 13**,** 1506-11.

STARR, D. A. (2009) A nuclear-envelope bridge positions nuclei and moves chromosomes. *J Cell Sci,* 122**,** 577-86.

STARR, D. A. & FRIDOLFSSON, H. N. (2010) Interactions between nuclei and the cytoskeleton are mediated by SUN-KASH nuclear-envelope bridges. *Annu Rev Cell Dev Biol,* 26**,** 421-44.

STEARNS, T., EVANS, L. & KIRSCHNER, M. (1991) Gamma-tubulin is a highly conserved component of the centrosome. *Cell,* 65**,** 825-36.

STERN, B. M. & MURRAY, A. W. (2001) Lack of tension at kinetochores activates the spindle checkpoint in budding yeast. *Curr Biol,* 11**,** 1462-7.

SUDAKIN, V., CHAN, G. K. & YEN, T. J. (2001) Checkpoint inhibition of the APC/C in HeLa cells is mediated by a complex of BUBR1, BUB3, CDC20, and MAD2. *J Cell Biol,* 154**,** 925-36.

SUGATA, N., MUNEKATA, E. & TODOKORO, K. (1999) Characterization of a novel kinetochore protein, CENP-H. *J Biol Chem,* 274**,** 27343-6.

SUNDIN, L. J., GUIMARAES, G. J. & DELUCA, J. G. (2011) The NDC80 complex proteins Nuf2 and Hec1 make distinct contributions to kinetochore-microtubule attachment in mitosis. *Mol Biol Cell,* 22**,** 759-68.

SUZUKI, A., HORI, T., NISHINO, T., USUKURA, J., MIYAGI, A., MORIKAWA, K. & FUKAGAWA, T. (2011) Spindle microtubules generate tension-dependent changes in the distribution of inner kinetochore proteins. *J Cell Biol,* 193**,** 125-40.

TADDEI, A., HEDIGER, F., NEUMANN, F. R., BAUER, C. & GASSER, S. M. (2004) Separation of silencing from perinuclear anchoring functions in yeast Ku80, Sir4 and Esc1 proteins. *EMBO J,* 23**,** 1301-12.

TADEU, A. M., RIBEIRO, S., JOHNSTON, J., GOLDBERG, I., GERLOFF, D. & EARNSHAW, W. C. (2008) CENP-V is required for centromere organization, chromosome alignment and cytokinesis. *EMBO J,* 27**,** 2510-22.

TAKAHASHI, K., CHEN, E. S. & YANAGIDA, M. (2000) Requirement of Mis6 centromere connector for localizing a CENP-A-like protein in fission yeast. *Science,* 288**,** 2215-9.

TAKAHASHI, K., YAMADA, H. & YANAGIDA, M. (1994) Fission yeast minichromosome loss mutants mis cause lethal aneuploidy and replication abnormality. *Mol Biol Cell,* 5**,** 1145-58.

TALLADA, V. A., TANAKA, K., YANAGIDA, M. & HAGAN, I. M. (2009) The S. pombe mitotic regulator Cut12 promotes spindle pole body activation and integration into the nuclear envelope. *J Cell Biol,* 185**,** 875-88.

TANAKA, K., CHANG, H. L., KAGAMI, A. & WATANABE, Y. (2009) CENP-C functions as a scaffold for effectors with essential kinetochore functions in mitosis and meiosis. *Dev Cell,* 17**,** 334-43.

TANAKA, K., KITAMURA, E., KITAMURA, Y. & TANAKA, T. U. (2007) Molecular mechanisms of microtubule-dependent kinetochore transport toward spindle poles. *J Cell Biol,* 178**,** 269-81.

TANAKA, T. U., RACHIDI, N., JANKE, C., PEREIRA, G., GALOVA, M., SCHIEBEL, E., STARK, M. J. & NASMYTH, K. (2002) Evidence that the Ipl1-Sli15 (Aurora kinase-INCENP) complex promotes chromosome bi-orientation by altering kinetochore-spindle pole connections. *Cell,* 108**,** 317-29.

THEIS, M., SLABICKI, M., JUNQUEIRA, M., PASZKOWSKI-ROGACZ, M., SONTHEIMER, J., KITTLER, R., HENINGER, A. K., GLATTER, T., KRUUSMAA, K., POSER, I., HYMAN, A. A., PISABARRO, M. T., GSTAIGER, M., AEBERSOLD, R., SHEVCHENKO, A. & BUCHHOLZ, F. (2009) Comparative profiling identifies C13orf3 as a component of the Ska complex required for mammalian cell division. *EMBO J,* 28**,** 1453-65.

TIEN, J. F., UMBREIT, N. T., GESTAUT, D. R., FRANCK, A. D., COOPER, J., WORDEMAN, L., GONEN, T., ASBURY, C. L. & DAVIS, T. N. (2010) Cooperation of the Dam1 and Ndc80 kinetochore complexes enhances microtubule coupling and is regulated by aurora B. *J Cell Biol,* 189**,** 713-23.

TOOLEY, J. G., MILLER, S. A. & STUKENBERG, P. T. (2011) The Ndc80 complex uses a tripartite attachment point to couple microtubule depolymerization to chromosome movement. *Mol Biol Cell,* 22**,** 1217-26.

TOURNEBIZE, R., POPOV, A., KINOSHITA, K., ASHFORD, A. J., RYBINA, S., POZNIAKOVSKY, A., MAYER, T. U., WALCZAK, C. E., KARSENTI, E. & HYMAN, A. A. (2000) Control of microtubule dynamics by the antagonistic activities of XMAP215 and XKCM1 in Xenopus egg extracts. *Nat Cell Biol,* 2**,** 13-9.

TOURNIER, S., GACHET, Y., BUCK, V., HYAMS, J. S. & MILLAR, J. B. (2004) Disruption of astral microtubule contact with the cell cortex activates a Bub1, Bub3, and Mad3-dependent checkpoint in fission yeast. *Mol Biol Cell,* 15**,** 3345-56.

TOYA, M., SATO, M., HASELMANN, U., ASAKAWA, K., BRUNNER, D., ANTONY, C. & TODA, T. (2007) Gamma-tubulin complex-mediated anchoring of spindle microtubules to spindle-pole bodies requires Msd1 in fission yeast. *Nat Cell Biol,* 9**,** 646-53.

TRAN, P. T., MARSH, L., DOYE, V., INOUE, S. & CHANG, F. (2001) A mechanism for nuclear positioning in fission yeast based on microtubule pushing. *J Cell Biol,* 153**,** 397-411.

TRAUTMANN, S., RAJAGOPALAN, S. & MCCOLLUM, D. (2004) The S. pombe Cdc14-like phosphatase Clp1p regulates chromosome biorientation and interacts with Aurora kinase. *Dev Cell,* 7**,** 755-62.

TYTELL, J. D. & SORGER, P. K. (2006) Analysis of kinesin motor function at budding yeast kinetochores. *J Cell Biol,* 172**,** 861-74.

UCHIDA, K. S., TAKAGAKI, K., KUMADA, K., HIRAYAMA, Y., NODA, T. & HIROTA, T. (2009) Kinetochore stretching inactivates the spindle assembly checkpoint. *J Cell Biol,* 184**,** 383-90.

UEMURA, T. & TANAGIDA, M. (1986) Mitotic spindle pulls but fails to separate chromosomes in type II DNA topoisomerase mutants: uncoordinated mitosis. *EMBO J,* 5**,** 1003-10.

UNSWORTH, A., MASUDA, H., DHUT, S. & TODA, T. (2008) Fission yeast kinesin-8 Klp5 and Klp6 are interdependent for mitotic nuclear retention and required for proper microtubule dynamics. *Mol Biol Cell,* 19**,** 5104-15.

USUI, T., MAEKAWA, H., PEREIRA, G. & SCHIEBEL, E. (2003) The XMAP215 homologue Stu2 at yeast spindle pole bodies regulates microtubule dynamics and anchorage. *EMBO J,* 22**,** 4779-93.

UZAWA, S. & YANAGIDA, M. (1992) Visualization of centromeric and nucleolar DNA in fission yeast by fluorescence in situ hybridization. *J Cell Sci,* 101 (Pt 2)**,** 267-75.

VAN BREUGEL, M., DRECHSEL, D. & HYMAN, A. (2003) Stu2p, the budding yeast member of the conserved Dis1/XMAP215 family of microtubule-associated proteins is a plus end-binding microtubule destabilizer. *J Cell Biol,* 161**,** 359-69.

VANOOSTHUYSE, V. & HARDWICK, K. G. (2009a) A novel protein phosphatase 1-dependent spindle checkpoint silencing mechanism. *Curr Biol,* 19**,** 1176-81.

VANOOSTHUYSE, V. & HARDWICK, K. G. (2009b) Overcoming inhibition in the spindle checkpoint. *Genes Dev,* 23**,** 2799-805.

VARDY, L. & TODA, T. (2000) The fission yeast gamma-tubulin complex is required in G(1) phase and is a component of the spindle assembly checkpoint. *EMBO J,* 19**,** 6098-111.

VASQUEZ, R. J., GARD, D. L. & CASSIMERIS, L. (1994) XMAP from Xenopus eggs promotes rapid plus end assembly of microtubules and rapid microtubule polymer turnover. *J Cell Biol,* 127**,** 985-93.

VASQUEZ, R. J., GARD, D. L. & CASSIMERIS, L. (1999) Phosphorylation by CDK1 regulates XMAP215 function in vitro. *Cell Motil Cytoskeleton,* 43**,** 310-21.

VAZQUEZ-NOVELLE, M. D. & PETRONCZKI, M. (2010) Relocation of the chromosomal passenger complex prevents mitotic checkpoint engagement at anaphase. *Curr Biol,* 20**,** 1402-7.

VENKATRAM, S., JENNINGS, J. L., LINK, A. & GOULD, K. L. (2005) Mto2p, a novel fission yeast protein required for cytoplasmic microtubule organization and anchoring of the cytokinetic actin ring. *Mol Biol Cell,* 16**,** 3052-63.

VENKATRAM, S., TASTO, J. J., FEOKTISTOVA, A., JENNINGS, J. L., LINK, A. J. & GOULD, K. L. (2004) Identification and characterization of two novel proteins affecting fission yeast gamma-tubulin complex function. *Mol Biol Cell,* 15**,** 2287-301.

VENKEI, Z., PRZEWLOKA, M. R. & GLOVER, D. M. (2011) Drosophila Mis12 complex acts as a single functional unit essential for anaphase chromosome movement and a robust spindle assembly checkpoint. *Genetics,* 187**,** 131-40.

VOGEL, S. K., RAABE, I., DERELI, A., MAGHELLI, N. & TOLIC-NORRELYKKE, I. (2007) Interphase microtubules determine the initial alignment of the mitotic spindle. *Curr Biol,* 17**,** 438-44.

WAN, X., O'QUINN, R. P., PIERCE, H. L., JOGLEKAR, A. P., GALL, W. E., DELUCA, J. G., CARROLL, C. W., LIU, S. T., YEN, T. J., MCEWEN, B. F., STUKENBERG, P. T., DESAI, A. & SALMON, E. D. (2009) Protein architecture of the human kinetochore microtubule attachment site. *Cell,* 137**,** 672-84.

WANG, E., BALLISTER, E. R. & LAMPSON, M. A. (2011) Aurora B dynamics at centromeres create a diffusion-based phosphorylation gradient. *J Cell Biol,* 194**,** 539-49.

WANG, H. W., LONG, S., CIFERRI, C., WESTERMANN, S., DRUBIN, D., BARNES, G. & NOGALES, E. (2008) Architecture and flexibility of the yeast Ndc80 kinetochore complex. *J Mol Biol,* 383**,** 894-903.

WANG, H. W., RAMEY, V. H., WESTERMANN, S., LESCHZINER, A. E., WELBURN, J. P., NAKAJIMA, Y., DRUBIN, D. G., BARNES, G. & NOGALES, E. (2007) Architecture of the Dam1 kinetochore ring complex and implications for microtubule-driven assembly and force-coupling mechanisms. *Nat Struct Mol Biol,* 14**,** 721-6.

WANG, P. J. & HUFFAKER, T. C. (1997) Stu2p: A microtubule-binding protein that is an essential component of the yeast spindle pole body. *J Cell Biol,* 139**,** 1271-80.

WASSMANN, K., LIBERAL, V. & BENEZRA, R. (2003) Mad2 phosphorylation regulates its association with Mad1 and the APC/C. *EMBO J,* 22**,** 797-806.

WEAVER, B. A., BONDAY, Z. Q., PUTKEY, F. R., KOPS, G. J., SILK, A. D. & CLEVELAND, D. W. (2003) Centromere-associated protein-E is essential for the mammalian mitotic checkpoint to prevent aneuploidy due to single chromosome loss. *J Cell Biol,* 162**,** 551-63.

WEI, R. R., AL-BASSAM, J. & HARRISON, S. C. (2007) The Ndc80/HEC1 complex is a contact point for kinetochore-microtubule attachment. *Nat Struct Mol Biol,* 14**,** 54-9.

WEI, R. R., SCHNELL, J. R., LARSEN, N. A., SORGER, P. K., CHOU, J. J. & HARRISON, S. C. (2006) Structure of a central component of the yeast kinetochore: the Spc24p/Spc25p globular domain. *Structure,* 14**,** 1003-9.

WEI, R. R., SORGER, P. K. & HARRISON, S. C. (2005) Molecular organization of the Ndc80 complex, an essential kinetochore component. *Proc Natl Acad Sci U S A,* 102**,** 5363-7.

WEISS, E. & WINEY, M. (1996) The Saccharomyces cerevisiae spindle pole body duplication gene MPS1 is part of a mitotic checkpoint. *J Cell Biol,* 132**,** 111-23.

WELBURN, J. P., GRISHCHUK, E. L., BACKER, C. B., WILSON-KUBALEK, E. M., YATES, J. R., 3RD & CHEESEMAN, I. M. (2009) The human kinetochore Ska1 complex facilitates microtubule depolymerization-coupled motility. *Dev Cell,* 16**,** 374-85.

WELBURN, J. P., VLEUGEL, M., LIU, D., YATES, J. R., 3RD, LAMPSON, M. A., FUKAGAWA, T. & CHEESEMAN, I. M. (2010) Aurora B phosphorylates spatially distinct targets to differentially regulate the kinetochore-microtubule interface. *Mol Cell,* 38**,** 383-92.

WEST, R. R., MALMSTROM, T. & MCINTOSH, J. R. (2002) Kinesins klp5(+) and klp6(+) are required for normal chromosome movement in mitosis. *J Cell Sci,* 115**,** 931-40.

WEST, R. R., MALMSTROM, T., TROXELL, C. L. & MCINTOSH, J. R. (2001) Two related kinesins, klp5+ and klp6+, foster microtubule disassembly and are required for meiosis in fission yeast. *Mol Biol Cell,* 12**,** 3919-32.

WEST, R. R., VAISBERG, E. V., DING, R., NURSE, P. & MCINTOSH, J. R. (1998) cut11(+): A gene required for cell cycle-dependent spindle pole body anchoring in the nuclear envelope and bipolar spindle formation in Schizosaccharomyces pombe. *Mol Biol Cell,* 9**,** 2839-55.

WESTERMANN, S., AVILA-SAKAR, A., WANG, H. W., NIEDERSTRASSER, H., WONG, J., DRUBIN, D. G., NOGALES, E. & BARNES, G. (2005) Formation of a dynamic kinetochore- microtubule interface through assembly of the Dam1 ring complex. *Mol Cell,* 17**,** 277-90.

WESTERMANN, S., CHEESEMAN, I. M., ANDERSON, S., YATES, J. R., 3RD, DRUBIN, D. G. & BARNES, G. (2003) Architecture of the budding yeast kinetochore reveals a conserved molecular core. *J Cell Biol,* 163**,** 215-22.

WESTERMANN, S., WANG, H. W., AVILA-SAKAR, A., DRUBIN, D. G., NOGALES, E. & BARNES, G. (2006) The Dam1 kinetochore ring complex moves processively on depolymerizing microtubule ends. *Nature,* 440**,** 565-9.

WIDLUND, P. O., STEAR, J. H., POZNIAKOVSKY, A., ZANIC, M., REBER, S., BROUHARD, G. J., HYMAN, A. A. & HOWARD, J. (2011) XMAP215 polymerase activity is built by combining multiple tubulin-binding TOG domains and a basic lattice-binding region. *Proc Natl Acad Sci U S A,* 108**,** 2741-6.

WIGGE, P. A., JENSEN, O. N., HOLMES, S., SOUES, S., MANN, M. & KILMARTIN, J. V. (1998) Analysis of the Saccharomyces spindle pole by matrix-assisted laser desorption/ionization (MALDI) mass spectrometry. *J Cell Biol,* 141**,** 967-77.

WIGGE, P. A. & KILMARTIN, J. V. (2001) The Ndc80p complex from Saccharomyces cerevisiae contains conserved centromere components and has a function in chromosome segregation. *J Cell Biol,* 152**,** 349-60.

WILLIAMS, B., LEUNG, G., MAIATO, H., WONG, A., LI, Z., WILLIAMS, E. V., KIRKPATRICK, C., AQUADRO, C. F., RIEDER, C. L. & GOLDBERG, M. L. (2007) Mitch a rapidly evolving

component of the Ndc80 kinetochore complex required for correct chromosome segregation in Drosophila. *J Cell Sci,* 120**,** 3522-33.

WILSON-KUBALEK, E. M., CHEESEMAN, I. M., YOSHIOKA, C., DESAI, A. & MILLIGAN, R. A. (2008) Orientation and structure of the Ndc80 complex on the microtubule lattice. *J Cell Biol,* 182**,** 1055-61.

WONG, J., NAKAJIMA, Y., WESTERMANN, S., SHANG, C., KANG, J. S., GOODNER, C., HOUSHMAND, P., FIELDS, S., CHAN, C. S., DRUBIN, D., BARNES, G. & HAZBUN, T. (2007) A protein interaction map of the mitotic spindle. *Mol Biol Cell,* 18**,** 3800-9.

WOOD, V., GWILLIAM, R., RAJANDREAM, M. A., LYNE, M., LYNE, R., STEWART, A., SGOUROS, J., PEAT, N., HAYLES, J., BAKER, S., BASHAM, D., BOWMAN, S., BROOKS, K., BROWN, D., BROWN, S., CHILLINGWORTH, T., CHURCHER, C., COLLINS, M., CONNOR, R., CRONIN, A., DAVIS, P., FELTWELL, T., FRASER, A., GENTLES, S., GOBLE, A., HAMLIN, N., HARRIS, D., HIDALGO, J., HODGSON, G., HOLROYD, S., HORNSBY, T., HOWARTH, S., HUCKLE, E. J., HUNT, S., JAGELS, K., JAMES, K., JONES, L., JONES, M., LEATHER, S., MCDONALD, S., MCLEAN, J., MOONEY, P., MOULE, S., MUNGALL, K., MURPHY, L., NIBLETT, D., ODELL, C., OLIVER, K., O'NEIL, S., PEARSON, D., QUAIL, M. A., RABBINOWITSCH, E., RUTHERFORD, K., RUTTER, S., SAUNDERS, D., SEEGER, K., SHARP, S., SKELTON, J., SIMMONDS, M., SQUARES, R., SQUARES, S., STEVENS, K., TAYLOR, K., TAYLOR, R. G., TIVEY, A., WALSH, S., WARREN, T., WHITEHEAD, S., WOODWARD, J., VOLCKAERT, G., AERT, R., ROBBEN, J., GRYMONPREZ, B., WELTJENS, I., VANSTREELS, E., RIEGER, M., SCHAFER, M., MULLER-AUER, S., GABEL, C., FUCHS, M., DUSTERHOFT, A., FRITZC, C., HOLZER, E., MOESTL, D., HILBERT, H., BORZYM, K., LANGER, I., BECK, A., LEHRACH, H., REINHARDT, R., POHL, T. M., EGER, P., ZIMMERMANN, W., WEDLER, H., WAMBUTT, R., PURNELLE, B., GOFFEAU, A., CADIEU, E., DREANO, S., GLOUX, S., et al. (2002) The genome sequence of Schizosaccharomyces pombe. *Nature,* 415**,** 871-80.

WORDEMAN, L. (2010) How kinesin motor proteins drive mitotic spindle function: Lessons from molecular assays. *Semin Cell Dev Biol,* 21**,** 260-8.

WU, G., QIU, X. L., ZHOU, L., ZHU, J., CHAMBERLIN, R., LAU, J., CHEN, P. L. & LEE, W. H. (2008) Small molecule targeting the Hec1/Nek2 mitotic pathway suppresses tumor cell growth in culture and in animal. *Cancer Res,* 68**,** 8393-9.

XIA, G., LUO, X., HABU, T., RIZO, J., MATSUMOTO, T. & YU, H. (2004) Conformation-specific binding of p31(comet) antagonizes the function of Mad2 in the spindle checkpoint. *EMBO J,* 23**,** 3133-43.

YAMAMOTO, A. & HIRAOKA, Y. (2001) How do meiotic chromosomes meet their homologous partners?: lessons from fission yeast. *Bioessays,* 23**,** 526-33.

YAMASHITA, A., SATO, M., FUJITA, A., YAMAMOTO, M. & TODA, T. (2005) The roles of fission yeast ase1 in mitotic cell division, meiotic nuclear oscillation, and cytokinesis checkpoint signaling. *Mol Biol Cell,* 16**,** 1378-95.

YANG, M., LI, B., TOMCHICK, D. R., MACHIUS, M., RIZO, J., YU, H. & LUO, X. (2007) p31comet blocks Mad2 activation through structural mimicry. *Cell,* 131**,** 744-55.

YANG, Y., WU, F., WARD, T., YAN, F., WU, Q., WANG, Z., MCGLOTHEN, T., PENG, W., YOU, T., SUN, M., CUI, T., HU, R., DOU, Z., ZHU, J., XIE, W., RAO, Z., DING, X. & YAO, X. (2008) Phosphorylation of HsMis13 by Aurora B kinase is essential for assembly of functional kinetochore. *J Biol Chem,* 283**,** 26726-36.

YAO, X., ANDERSON, K. L. & CLEVELAND, D. W. (1997) The microtubule-dependent motor centromere-associated protein E (CENP-E) is an integral component of kinetochore corona fibers that link centromeres to spindle microtubules. *J Cell Biol,* 139**,** 435-47.

YEN, T. J., COMPTON, D. A., WISE, D., ZINKOWSKI, R. P., BRINKLEY, B. R., EARNSHAW, W. C. & CLEVELAND, D. W. (1991) CENP-E, a novel human centromere-associated protein required for progression from metaphase to anaphase. *EMBO J,* 10**,** 1245-54.

ZIMMERMAN, S. & CHANG, F. (2005) Effects of {gamma}-tubulin complex proteins on microtubule nucleation and catastrophe in fission yeast. *Mol Biol Cell,* 16**,** 2719-33.

ZIMMERMAN, S., DAGA, R. R. & CHANG, F. (2004) Intra-nuclear microtubules and a mitotic spindle orientation checkpoint. *Nat Cell Biol,* 6**,** 1245-6.

ZOVKO, S., ABRAHAMS, J. P., KOSTER, A. J., GALJART, N. & MOMMAAS, A. M. (2008) Microtubule plus-end conformations and dynamics in the periphery of interphase mouse fibroblasts. *Mol Biol Cell,* 19**,** 3138-46.